The Role of Peroxiredoxin Asp f3 in Redox Homeostasis and Virulence of the Human Fungal Pathogen *Aspergillus fumigatus*

Dissertation

in Partial Fulfilment of the Requirements for the Degree of

"doctor rerum naturalium" (Dr. rer. nat.)

Submitted to the Council of the Faculty of Biological Sciences

of Friedrich Schiller University Jena

by

Master of Science

Jana Marie Boysen

born on February 15th, 1990 in Neumünster, Germany

1. Gutachter/in: Prof. Dr. Axel A. Brakhage (Jena)

2. Gutachter/in: Prof. Dr. Ilse D. Jacobsen (Jena)

3. Gutachter/in: Prof. Dr. Utz Reichard (Göttingen)

Datum der öffentlichen Verteidigung: 21.06.2022

It is a capital mistake to theorize before one has data. Insensibly one begins to twist facts to suit theories, instead of theories to suit facts.

Sherlock Holmes – A Scandal in Bohemia, Sir Arthur Conan Doyle

Table of Contents

1 Introduction

1.1 *Aspergillus fumigatus*

1.1.1 Natural Occurrence and Life cycle

The filamentous fungus *Aspergillus fumigatus* (lat.: fumus = smoke) is a ubiquitous ascomycete with a generally saprophytic lifestyle. It was first described in 1863 by the German physician J. B. Georg W. Fresenius, who studied the species isolated from human lungs (Schmidt, 1998). As a saprophyte *A. fumigatus* can be readily found in soil and compost heaps, organic plant matter, flower soil, food or even on wallpapers (Mullins et al., 1976; Brakhage and Langfelder, 2002). In its natural habitat, *A. fumigatus* is involved in the decomposition of organic matter and has thus a major role in the recycling of both carbon and nitrogen (Brakhage and Langfelder, 2002; Rhodes, 2006). Due to its highly versatile metabolism the fungus is capable to adept successfully to a wide range of stress factors (Paulussen et al., 2017). This versatility includes the biosynthesis of numerous secondary metabolites, which grant the fungus helpful effects in its environment (Bignell et al., 2016; Keller, 2019). It can grow on a variety of complex carbon- and nitrogen sources and cope with nutrient limitations, such as low iron conditions (Brandon et al., 2015; Amich and Bignell, 2016). In addition, it can withstand irradiation, oxygen limitation and adjust to a range of pH-values as low as pH 3.5 to alkaline conditions (Hall and Denning, 1994; Bignell, 2012; Knox et al., 2016; van de Veerdonk et al., 2017). Additionally, *A. fumigatus* has a broad temperature optimum and can grow from 12°C to 55°C, while conidia can survive even temperatures as high as 70°C (Latgé, 1999; Samson, 1999; Rhodes, 2006).

During favourable conditions, the life cycle of *A. fumigatus* starts with the swelling and subsequent germ tube formation of asexual conidia, which takes 3-6 h (van de Veerdonk et al., 2017)(Figure 1). In 6-12 hours they grow into filament-like hyphae, which then form a network. This primary mycelium can already be established after 12-14 hours (McDonagh et al., 2008). When forming a biofilm during a stationary growth phase, the mycelium is embedded in extracellular matrix (ECM) (Loussert et al., 2010). After a few days, hyphae start to grow perpendicular from the mycelium to generate a conidiophore, consisting of a clavate vesicle, which has a layer of elongated phialide cells attached on its apical side. Haploid conidia

are formed by constriction of small portions on the elongated phialides and stay loosely attached as long chains of spores until their dispersal (Brakhage and Langfelder, 2002).

A. fumigatus produces a massive amount of asexual conidia, which are only 2.5-3.0 µm in diameter and of a grey-greenish colour characteristic for this species (Kwon-Chung and Sugui, 2013; Latge and Chamilos, 2019). The colour results from pigmentation with dihydroxynaphthalene (DHN)-melanin that is the melanin most prevalent in fungi (Wheeler and Bell, 1988). The melanin covers the whole spore surface and in turn is covered with a layer of aggregated hydrophobin-proteins – the rodlet layer. Both the rodlet layer and DHN-melanin strongly contribute to the spore surface morphology and play an important role during virulence (Jahn et al., 1997; Langfelder et al., 1998; Aimanianda et al., 2009; Heinekamp et al., 2013). The rodlet layer also confers strong hydrophobicity to *A. fumigatus* conidia, which contributes to their buoyancy in the air (Latge and Chamilos, 2019).

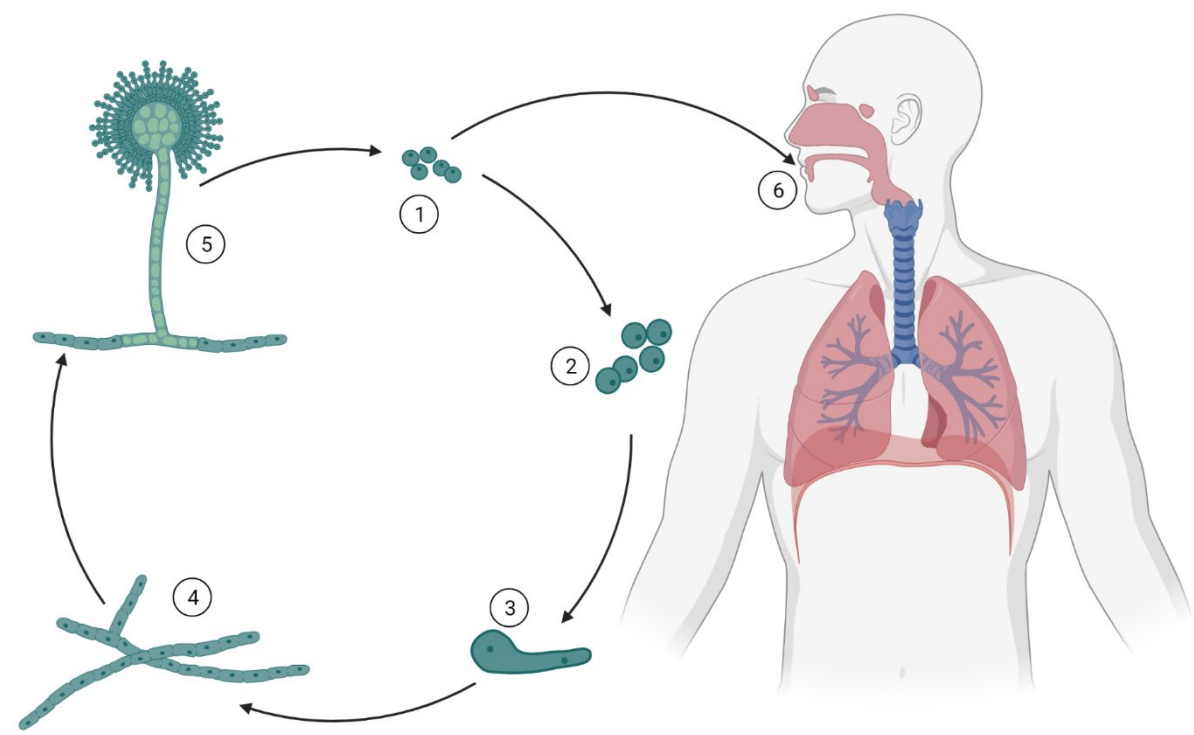

Figure 1 Asexual life cycle of *Aspergillus fumigatus*. 1 Dormant conidia**, 2** Swollen conidia**, 3** Germling, **4,** Fully formed mycelium, **5** Mycelium with conidia forming conidiophores, **6** Conidia as the causative agent of infection after inhalation into the human respiratory system (created with biorender.com).

For a long time, *A. fumigatus* was believed to reproduce exclusively by asexual spore formation or create genetic diversity by a parasexual cycle based on hyphal phusion (Debeaupuis et al., 1997). However, analyses of the sequenced *A. fumigatus* genome revealed a vast number of genes associated with a sexual cycle (Nierman et al., 2005). Further

investigation suggested heterothallism and evidenced the occurrence of two different mating types – MAT1-1 and MAT1-2 (Paoletti et al., 2005; Bain et al., 2007). And indeed, in 2009 O'Gorman and colleagues (2009) were able to induce mating in *A. fumigatus* for the first time, which resulted in light-yellow cleistothecia. The applied conditions were very specific though and its occurrence is unknown in nature (O'Gorman et al., 2009; Dyer and O'Gorman, 2012).

1.1.2 Pathogenicity and virulence determinants

In addition to its saprophytic lifestyle, *A. fumigatus* is also known as an opportunistic pathogen, which can cause severe infections in both immunocompetent and immunocompromised hosts (Latge and Chamilos, 2019). It is responsible for 60 % of all cases of aspergillosis and with over 200,000 annual cases of invasive aspergillosis (IA) worldwide, it is the most prevalent airborne fungal pathogen (Latgé, 1999; Brown et al., 2012; Bandres and Sharma, 2020). The infectious agents of *A. fumigatus* are its conidia, which can float for extended periods of time on liquid as well as being dispersed through the air. Due to their continuous presence in the air, they are frequently inhaled by humans and their small size of 2.5-3 µm allows them to reach the alveoli deep in the lung (Latgé, 2001). Once in the lung, conidia encounter several host defence mechanisms and are generally cleared quickly by mucociliary clearance or the innate immunity, involving phagocytes like alveolar macrophages, neutrophilic granulocytes and the physical barrier of lung epithelia cells (Shepardson et al., 2014; Kerr et al., 2016). However, if a successful clearance of the fungus fails, conidia can start to germinate and proceed growth to establish different kinds of diseases.

Infections can be divided in three categories, namely invasive aspergillosis, chronic pulmonary infections and allergic reactions, which are closely associated with the host's immune status (Paulussen et al., 2017). In an estimation of health care costs of fungal diseases in the USA *A. fumigatus* rated second after *Candida* infections with a total of $1.2 billion per year (Benedict et al., 2019). Depending on the underlying conditions in infected populations mortality rates of *A. fumigatus* infections range from 30-95 %. Reasons for these high mortality rates are not only the severity of the underlying condition and the fungal infection, but also a lack of quick and reliable diagnostic possibilities to identify infections in a timely and reliable manner that allow early and precise treatment (Brown et al., 2012; Winters et al., 2012; Dignani, 2014; Latge and Chamilos, 2019).

In immunocompetent hosts, infections with *A. fumigatus* can for example lead to chronic, non-invasive infections like the development of aspergilloma or chronic pulmonary aspergillosis (CPA). Although these infections take place in an immunocompetent host, they are generally following a primary medical condition, like tuberculosis, which enables the fungus to grow in pre-existing pulmonary cavities (Denning et al., 2016; Patterson et al., 2016; Alastruey-Izquierdo et al., 2018).

In atopic patients *A. fumigatus* can cause allergic bronchopulmonary aspergillosis (ABPA), a hypersensitivity disease of the lung (Agarwal et al., 2013). Risk groups include patients with chronic asthma or cystic fibrosis (CF) (Greenberger, 2002; Knutsen and Slavin, 2011).

Invasive aspergillosis occurs frequently in immunocompromised hosts and is the most common fungal infection in recipients of hematopoietic stem cell transplantation (HSCT) or a solid-organ transplant (SOT) (Latge and Chamilos, 2019). Diseases like acute leukaemia, acquired immunodeficiency syndrome (AIDS) or the Chronic Granulomatous disease (CGD) likewise render humans susceptible to IA (Gregg and Kauffman, 2015). Furthermore, rising numbers of immunocompromised people are also due to environmental pollution and a general increase of longevity as well as being influenced as a result of human behaviours like alcoholism, a sedentary lifestyle and obesity (Maschmeyer et al., 2007; Paulussen et al., 2017).

The same abilities that enable *A. fumigatus* to thrive in harsh conditions and disperse its conidia on a large scale also facilitate its survival in the hostile environment of the human host. To successfully establish an infection, the fungus has to defy a number of challenges (Latge and Chamilos, 2019). Nutrients must be acquired from the host, including carbon and nitrogen as well as divalent cations like copper, iron or zinc. To intentionally starve the fungus of nitrogen is a strategy employed by the host to fight infection (Amich and Bignell, 2016). Simultaneously the fungus has to protect from an overload of nutrients like redox-active copper and iron, which are essential for growth and virulence but are toxic in excess (Hartmann et al., 2011; Blatzer and Latgé, 2017). Further host conditions to adjust to include hypoxia, pH and the challenges of the host immune response, which encompass physical interactions like phagocytosis or chemical immune responses like the production of reactive oxygen species that will be explained in detail later (Tekaia and Latgé, 2005; Canton et al., 2014; Kowalski et al., 2016). The human body temperature of 37°C is an asset for the fungus, though, as it supports fast growth and is even used for standard laboratory cultivations of

A. fumigatus. Also higher temperatures of 40-41°C associated with fever are favoured above lower temperatures like 25°C (Latge and Chamilos, 2019).

A. fumigatus' metabolic versatility allows quick and coordinated adjustments to occurring changes in its environment, in both nature and the human host. These abilities can thus be considered major pathogenic traits and are often strongly interconnected and dependent on one another, the loss of a single one of these abilities may thus lead to a loss of virulence. However, in comparison to primary pathogens, the traits of *A. fumigatus* have not been developed in association with the human host but rather in its natural environment (Askew, 2008). Recent publications even suggest that the mechanisms, which allow the fungus to evade, counteract and survive phagocytosis developed due to their close interaction with protozoan predators in their natural habitat - the soil. High similarities between amoebae and immune cells like macrophages thus allow the fungus to escape amoeba predation and macrophages likewise (Casadevall, 2012; Novohradska et al., 2017). However, in their natural environment secondary metabolites like gliotoxin or fumigaclavine, which exhibit protective mechanisms against other organisms like amoeba or even insects, respectively, seem to play an even more pronounced role than during virulence (**Figure 2**). Nevertheless, several secondary metabolites have been implicated to be involved in virulence as they were shown to help avoid immune recognition (DHN-melanin), diminish function of immune cells (fumagillin, endocrocin, gliotoxin) or are toxic to lung cells *in vitro* (trypadicin). Regulation of secondary metabolite biosynthesis is subject to a complex regulatory network and often depends on the concerted effect of several regulatory layers, which are highly dependent on environmental conditions like nutrient availability or stress (Brakhage, 2013; Tudzynski, 2014; Keller, 2019).

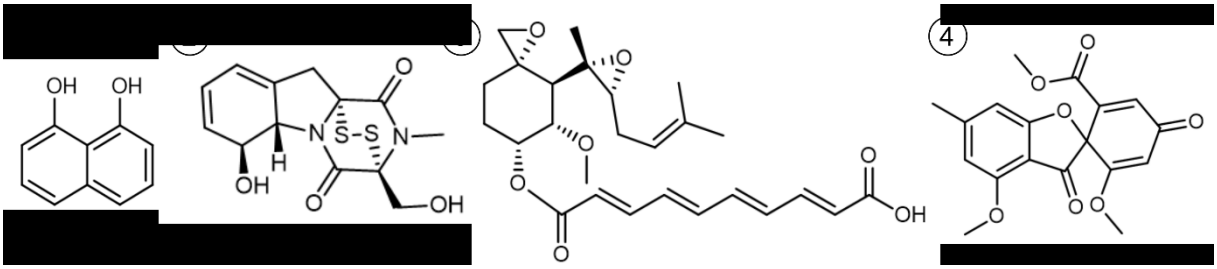

Figure 2 Examples for typical secondary metabolites of *Aspergillus fumigatus*. **1** Dihydroxynaphthalene (DHN)-Melanin (**monomer) 2** Gliotoxin **3** Fumagillin **4** Fumagillin

1.2 Molecular maintenance mechanisms for redox balance in *A. fumigatus*

For the successful establishment of an *A. fumigatus* infection two of the biggest obstacles of hostile host conditions are the challenge with reactive oxygen species and iron deficiency. The importance of ROS for the hosts defence against *A. fumigatus* infections is highlighted by the high susceptibility of CGD-patients with incident rates of 20-40% to develop IA (Henriet et al., 2013). CGD is a hereditary genetic defect in the NADPH oxidase (NOX) complex of their phagocytic cells. In healthy individuals the NOX complex assembles in the membranes of phagolysosomes where it catalyses the oxidative burst, thereby releasing high concentrations (up to 25 µM] of superoxide into the phagolysosome (Winterbourn et al., 2006; Romani, 2011). In CGD mutations impair the ability to produce superoxide radicals ($\cdot O_2^-$), which renders these patients susceptible to microbial (bacterial and fungal) infections (Segal, 2009). The dependency on iron is shown by the fungus itself, which becomes avirulent when it loses its ability to tap the host iron supply (Schrettl et al., 2004; Schrettl et al., 2007). However, here we focus mainly on the redox homeostasis mechanism, which will be addressed in detail.

Molecular oxygen (O_2) is a reactive molecule and of paramount importance for the development of multicellular eukaryotic life since it allows total oxidation of food sources. A respiratory chain enables organisms to gain roughly 18 times more energy than they can derive from glycolysis. However, during this process potentially damaging reactive oxygen species like hydrogen peroxide (H_2O_2), superoxide anion ($\cdot O_2^-$) and hydroxyl radical ($\cdot O_2^-$) are produced (Cadet and Davies, 2017). These two sides of oxygen – its essentiality for aerobic life and the threat it poses to life at the same time - are described as the Oxygen Paradox (Davies, 2016). Due to their destructive potential ROS have to be tightly regulated by the cell. They originate not only from a variety of natural sources like UV radiation, heat shock, inflammation or environmental toxins and oxidants such as heavy metals but also from a number of endogenous cellular sources like the mitochondria in eukaryotes (Ermak and Davies, 2002; Dalle-Donne et al., 2005). In contrast to their hazardous nature ROS also fulfil an important role for the generation of redox microenvironments in different organelles and serve as signal molecules and are thus involved in intracellular signalling pathways and subsequently the modulation of physiological processes like apoptosis (Thannickal and Fanburg, 2000; Winterbourn, 2008; Finkel, 2011).

1.2.1 Endogenous sources of reactive oxygen species

In eukaryotic cells reactive oxygen species are produced as the result of enzymatic and non-enzymatic activity and originate mainly from the mitochondria but also from the endoplasmic reticulum (ER), the cytoplasm, the plasma membranes and peroxi- and lysosomes (Moldovan and Moldovan, 2004; Dalle-Donne et al., 2005). Generation of ROS occurs as a by-product of some enzymatic reactions like in the mitochondria or as a primary product of enzymatic function as in the case of NADPH oxidases. Enzymes typically involved in ROS production (as by-product or primary product) are NADPH oxidases, cytochrome p450 enzymes, Flavin-dependent demethylases, cyclooxygenases, oxidases for xanthine, amino acids and polyamines or glucose oxidase and lipoxygenases (Bedard and Krause, 2007; Wong et al., 2008; Nonell and Flors, 2016).

Proteins tightly associated with the generation of ROS at the plasma membrane are NADPH oxidases (NOXs), which contribute to the formation of the transmembrane potential by the transport of electrons, generating superoxide in the process (Moldovan and Moldovan, 2004; Nathan and Cunningham-Bussel, 2013) (Figure 3, 1). During this process NOX transfers an electron from cytosolic NADPH first to a FAD cofactor and then to a heme group before it is passed on to extracellular O_2 to form $\cdot O_2^-$. The function of NOX complexes is often coupled with receptors, their activation leading to the assembly of proteins needed for a functional NOX complex (Nathan and Cunningham-Bussel, 2013). The number of proteins depends on the organism, the fungal NOX-complex is well studied in filamentous and plant pathogenic fungi like *Botrytis cinerea* and consists of three proteins – Nox, NoxR and Rac (Tudzynski et al., 2012; Warris and Ballou, 2019).

In the ER of eukaryotic cells hydrogen peroxide is generated as a by-product of protein folding. The flavoenzyme ER oxidoredoxin 1 (Ero1) provides oxidizing equivalents and regulates the reductive/oxidizing environment of the ER lumen and further can transfer disulphide bonds to the protein disulphide isomerase 1 (Pdi1) which in turn transfers the disulphide bond to an unfolded protein to guide and accelerate correct folding (Figure 3, 2). To create the disulphide Ero1 uses molecular oxygen as final electron acceptor, thus generating one hydrogen peroxide molecule for each disulphide bond formed (Tu and Weissman, 2002; Sevier and Kaiser, 2008;

Zito, 2015). In *Saccharomyces cerevisiae,* the activity of Ero1 was shown to be regulated by Pdi1, dependent on its own oxidative state (Kim et al., 2012).

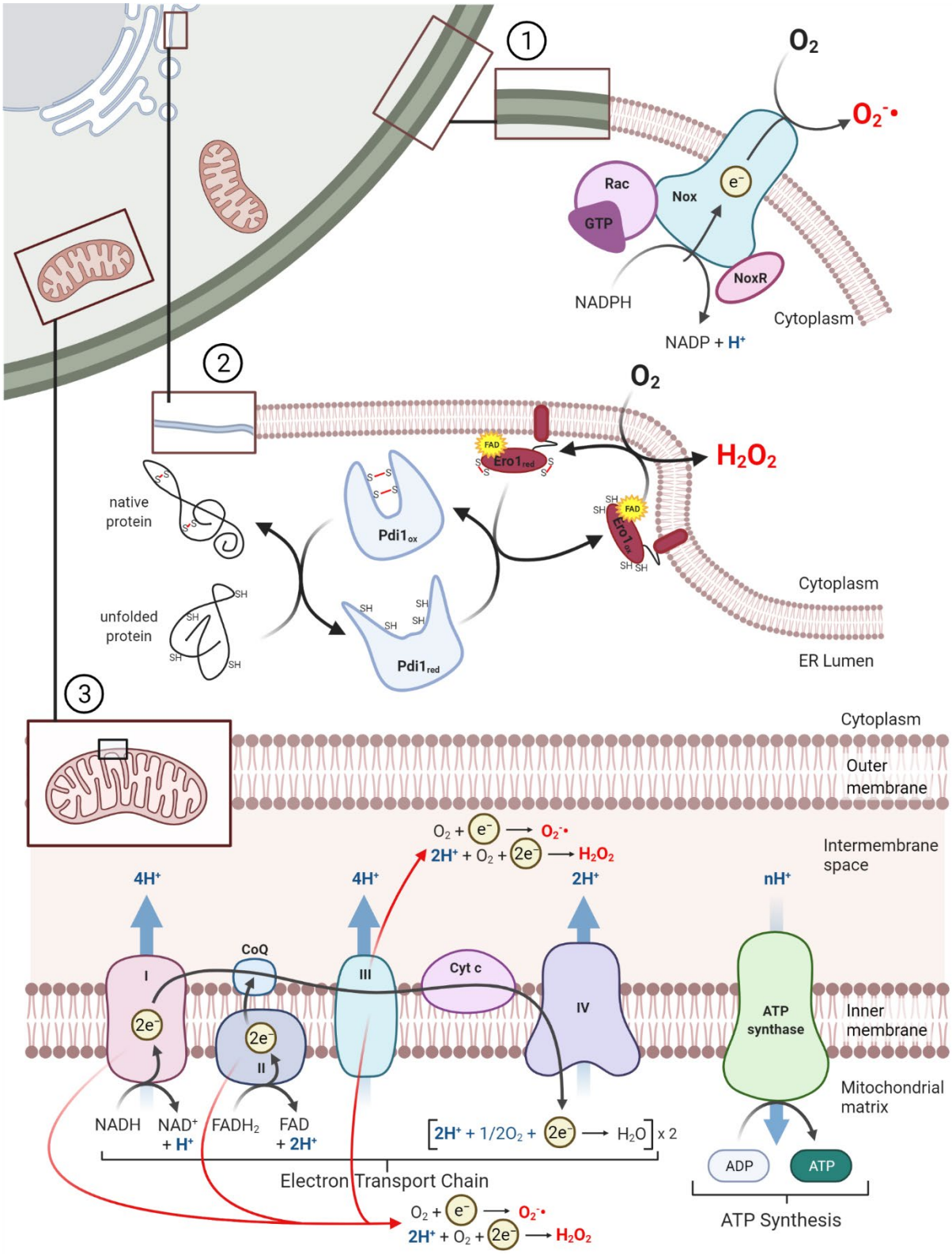

Figure 3 Endogenous sources of reactive oxygen species. 1 NADPH oxidase supports the transmembrane potential by the transport of electrons across the cell membrane. Electrons are transferred from NADPH through the NOX complex to molecular oxygen as final electron acceptor *via* an FAD and a heme group. **2** Protein folding by Pdi1 and Ero1 in the ER. To facilitate protein folding

$Pdi1_{ox}$ transfers oxidizing equivalents to an unfolded protein being reduced in the process. $Pdi1_{red}$ is reoxidized by Ero1, which uses molecular oxygen as final electron acceptor in a FAD-dependent reaction, which serves as cofactor. **3** Formation of reactive oxygen species in the electron transport chain. Electrons, leaking from the complexes of the respiratory chain, react with molecular oxygen to form superoxide and hydrogen peroxide. Depending on the complex leakage occurs toward the mitochondrial matrix (Complex I-III) or the intermembrane space (Complex III). Adapted and extended from "Electron Transport Chain", by BioRender.com (2021). Retrieved from https://app.biorender.com/biorender-templates.

Ero1 was not studied in *A. fumigatus*, but the fungus contains an orthologue of *S. cerevisiae* Ero1 (Cerqueira et al., 2014). The *A. fumigatus* orthologue of yeast Pdi1 is PdiA, which was described as immunoreactive, binding both IgG and IgE (Nigam et al., 2001; Asif et al., 2006). Interestingly, there is evidence that both Ero1 and Pdi1 are also active on the cell surface instead of being restricted to ER localization (Laurindo et al., 2012). In addition to their function in disulphide exchange PDIs are also associated with thiol redox functions and chaperone activity (Wilkinson and Gilbert, 2004; Laurindo et al., 2012; Ali Khan and Mutus, 2014).

Mitochondria are a major source of ROS. Superoxide is formed mainly at two steps in the electron-transport chain: Complex I (NADH-ubiquinone oxidoreductase) and complex III (ubiquinone-cytochrome *c* reductase) due to the leakage of electrons (Figure 3, 3). At Complex I two electrons are transferred from NADH to a flavomononukleotide (FMN) cofactor from which the electrons are transferred to coenzyme Q10 (ubiquinone) *via* Fe-S-clusters (Sazanov, 2015). Fully reduced FMN can also transfer electrons to molecular oxygen reducing it to superoxide which is released into the mitochondrial matrix (Kussmaul and Hirst, 2006; Murphy, 2009). At complex III coenzyme ubiquinone (Q) receives electrons from complex I or II. In a number of sequential reactions called "Q cycle" these electrons are transferred from ubiquinol (QH_2) to cytochrome c thereby moving protons across the lipid bilayer. One of the intermediates of this reaction is the unstable intermediate ubisemiquinone ($Q^{-}\cdot$) which readily reacts with molecular oxygen to form superoxide in a non-enzymatic autoxidation reaction (Turrens, 1997; Finkel and Holbrook, 2000). Superoxide generated at complex III is released in both the mitochondrial matrix and the inner mitochondrial space from which superoxide can access the cytoplasm through voltage-dependent anion channels, while leakage from complex I and II occurs mostly into mitochondrial matrix (Han et al., 2003; Turrens, 2003; Muller et al., 2004).

Additionally, ROS can result from the reaction of molecular oxygen with free ions of copper or iron which derive from heme groups, iron-sulphur-clusters or metal storage proteins – known as Fenton and Haber-Weiss reaction (Haber and Weiss, 1934; Walling, 1998; Nonell and Flors, 2016) (Figure 4).

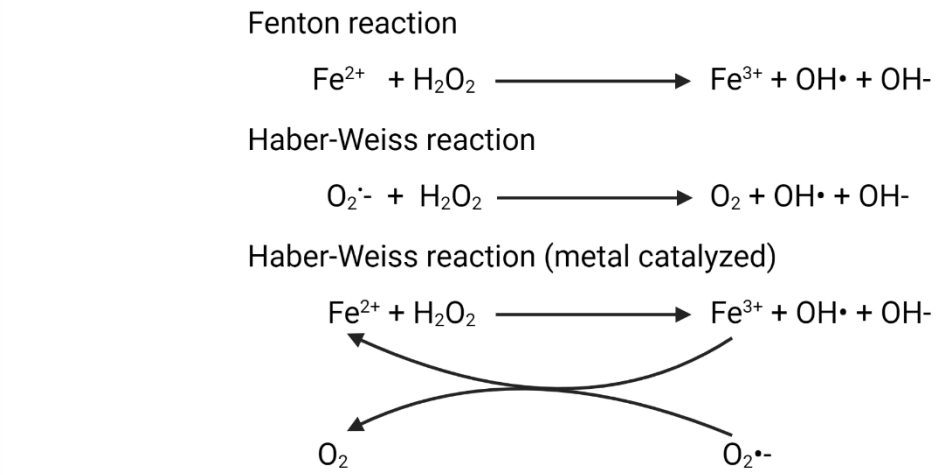

Figure 4 Reaction mechanisms of ROS detoxification. Maintenance of redox homeostasis is facilitated by different ROS detoxification mechanisms like superoxide dismutases (SODs), catalases (Cats), glutathione peroxidases (Gpxs) and peroxiredoxins (Prxs).

1.2.2 Antioxidant strategies in *A. fumigatus*

To maintain redox homeostasis *A. fumigatus* possesses a number of antioxidant mechanisms which include glutathione and thioredoxin systems and antioxidant enzymes such as catalases (Cats), superoxide dismutases (SODs), peroxidases and peroxiredoxins (Prxs) (Fridovich, 1978; Sies, 1994; Aguirre et al., 2005; Halliwell and Gutteridge, 2015) (Figure 5).

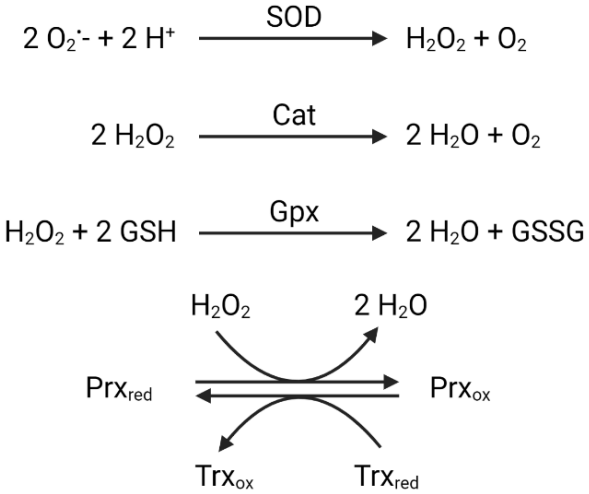

Figure 5 Reaction mechanisms of ROS detoxification. Maintenance of redox homeostasis is facilitated by different ROS detoxification mechanisms like superoxide dismutases (SODs), catalases (Cats), and glutathione peroxidases (Gpxs) converting reduced, monomeric (GSH) to oxidized, dimeric (GSSG) glutathiones and peroxiredoxins (Prxs) depending on thioredoxin (Trx).

Superoxide dismutases catalyse the dismutation of superoxide to hydrogen peroxide and oxygen. The genome of *A. fumigatus* encodes five putative SODS of which four (Sod1-4) were characterized by Lambou and colleagues (2010). Even though expressed weakly at all tested time points, deletion mutants of Af*sod4* appeared to be non-viable. *Sod1-2* were expressed mainly in spores, while *sod3* was mainly expressed in the mycelium at later time points (>20 h)(Cagas et al., 2011). Knock-out mutants of *sod1* and *sod2* both lead to high superoxide sensitivity and growth inhibition under high temperatures. Deletion of *sod3* was unaffected by both superoxide and high temperatures. A triple deletion of *sod1-3* (*sod1/sod2/sod3)* showed higher sensitivity to superoxide and temperature than either of the single deletion mutants and also showed a delay in conidial germination. Although killing by alveolar phagocytes of immunocompetent mice was increased, virulence in an immunocompromised mouse model was not affected. *Sod5* was identified as orthologue to *Candida albicans Sod5* but has not been further characterized until now (Cerqueira et al., 2014).

Hydrogen peroxide can be detoxified by a number of mechanisms including catalases, of which the *A. fumigatus* genome encodes five (Cerqueira et al., 2014). The gene AFUA_2g00200 has orthologues with catalase activity but was not yet further characterized. The catalase fgaCat (easC) is part of the fumigaclavine C (fga) biosynthetic gene cluster and was shown to be involved in the biosynthesis of ergot alkaloids. Its role during oxidative stress was not investigated, but Goetz and colleagues (2011) suggest a specific role as a partner catalase to the hydrogen peroxide producing oxidase EasE during chanoclavine-I biosynthesis. The other catalases are CatA, the conidial catalase and Cat1 and Cat2 which are expressed in the mycelium of *A. fumigatus* (Paris et al., 2003). A knock-out of the conidial catalase CatA showed its protective function against hydrogen peroxide *in vitro* but killing by alveolar macrophages is not affected. Knock-out mutants of the mycelial catalases Cat1 and Cat2 were not more sensitive to hydrogen peroxide than the wild type. However, a double knock-out showed higher sensitivity to hydrogen peroxide and an involvement in virulence, although loss of both Cat1 and Cat2 does not lead to avirulence (Paris et al., 2003).

The glutathione and thioredoxin systems are based on the use of electron donors such as the tripeptide glutathione (GSH). The reaction of hydrogen peroxide and GSH results in water and oxidized glutathione which forms a dimer connected by a disulphide (GSSG) (Mannervik, 1985; Aguirre et al., 2005). GSSG is regenerated by the glutathione reductase and NADPH oxidation

(Couto et al., 2013). The *A. fumigatus* genome contains three genes with a putative glutathione disulphide oxidoreductase activity but neither their impact in ROS detoxification nor on virulence have been studied (Cerqueira et al., 2014).

Peroxiredoxins comprise a ubiquitous family of cysteine-dependent enzymes which based on biochemical and structural traits can be divided in six sub-classes (Prx1-AhpC, BCP-PrxQ, Tpx, Prx5, Prx6, and AhpE) and three types, typical 2-Cys, atypical 2-Cys and 1-Cys Prxs, which differ slightly in their catalytic mechanism (de Oliveira et al., 2021). They are closely connected in a reductive cycle with thiol systems like thioredoxin or glutathione that can be divided in three steps – peroxidation, resolution and recycling (Figure 6). During peroxidation, the universally-conserved redox-active cysteine, also called peroxidatic cysteine (CysP) residue of the peroxiredoxin performs a nucleophilic attack on the peroxide and is in turn oxidized to a sulfenic acid accompanied by the release of a water molecule. In typical and atypical 2-Cys Prxs the second step, which is left out in 1-Cys Prx due to a lack of a second cysteine, is called resolution (Ellis and Poole, 1997; Choi et al., 1998). The second cysteine (resolving cysteine or CysR) attacks the sulfenic acid to form an inter- or intramolecular bond in typical and atypical 2-Cys Prx, respectively and again releases a water-molecule. During recycling the oxidized peroxiredoxins are then reduced in a thiol-dependent reaction by electron donors like thioredoxin and can again enter into the cycle (Perkins et al., 2015; Su et al., 2018). In general peroxiredoxins function as homodimeric units, which is also the smallest functional unit for typical 2-Cys Prx. Dimer formation can occur in two distinct ways; A-type, when binding as globular domains and B-type, by alignment of the central β-sheets of the Prx-monomers. Some peroxiredoxins are also able to assemble in larger functional units like octamers, decamers and dodecamers. However, the ability to form higher-order complexes strongly depends on the kind on dimer assembly (A-type or B-type) (Hall et al., 2011; de Oliveira et al., 2021).

Like most organisms, *A. fumigatus* contains several putative peroxiredoxin-like proteins, indeed six of them were identified, three of them belonging to the 1-Cys peroxiredoxins of the Prx6 subfamily while the other three are atypical 2-Cys Prx, which include allergen and peroxiredoxin Asp f3. So far only Asp f3 and recently the three 1-Cys peroxiredoxins (Prx1, PrxB, PrxC) were further characterized (Hemmann et al., 1999; Hillmann et al., 2016; Rocha et al., 2018). Due to its importance for this study Asp f3 will be introduced in detail later.

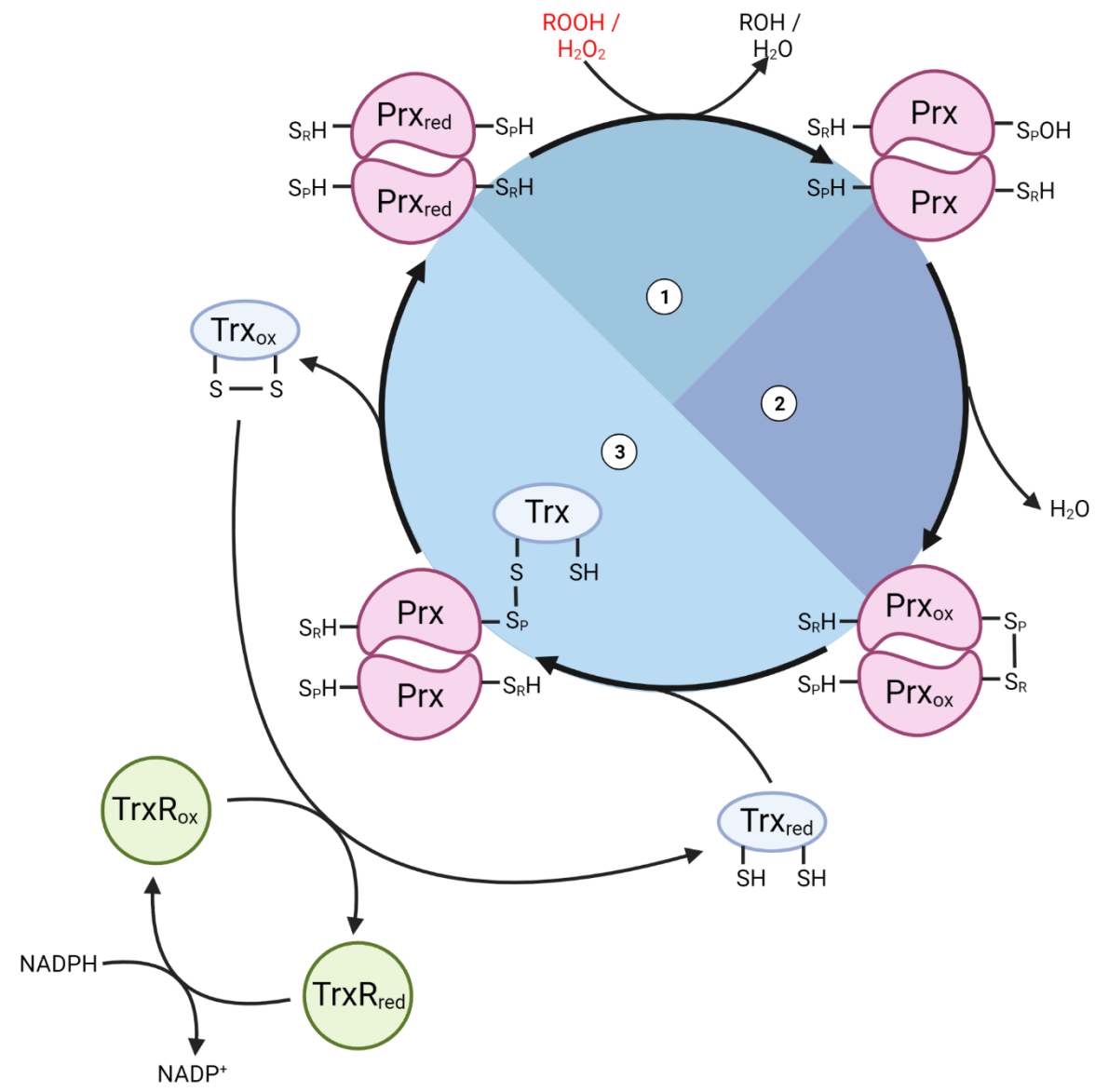

Figure 6 Reaction mechanisms of Prx-dependent ROS detoxification on the example of typical 2-Cys Prx. Prx – peroxiredoxin, Trx – thioredoxin, TrxR thioredoxin reductase **1 Peroxidation**: oxidation of the peroxidatic cysteines thiol group (S_PH) to sulfenic acid (S_POH) by hydroperoxide (ROOH)/hydrogen peroxide (H_2O_2) interaction. The detoxified hydroperoxides/hydrogen peroxide are released as alcohol (ROH)/ water molecule (H_2O). **2 Resolution**: the resolving cysteines thiol group (S_RH) attacks the sulfenic acid group to establish an intermolecular disulphide bond and a water molecule is released in the process. **3 Recycling:** the oxidized Prx is reduced by interaction with thioredoxin. In turn, regeneration of thioredoxin is accomplished by NADPH-dependent reduction catalysed by thioredoxin reductase (TrxR).

1.2.3 Transcriptional regulators of the oxidative stress response on *A. fumigatus*

To initiate a specific, but multi-gene associated transcriptional change in response to a change in environmental circumstances or the challenge with different stress factors, many organisms have broadly acting transcription factors (TFs). These TFs are not responsible for the transcription of a single gene, or even a whole cluster of genes, which are localized in close proximity to one another and belong to the biosynthetic pathway of a single secondary

metabolite. Instead, they govern the transcription of a number of genes that do not have to be in close proximity to one another but are related to specific stress answers of the organism by binding to consecutive motifs in the promoter region of respective genes. In *A. fumigatus* one of these TFs is the bZIP family transcription factor AfYap1, an orthologue of Yap1 in *S. cerevisiae*, a well-studied key regulator of oxidative stress response (Lessing et al., 2007). Regulation of Yap1-dependent genes is ensured by a continuous export of Yap1 out of the nucleus in non-stress conditions, and accumulation of Yap1 in the nucleus upon oxidative challenge. The nuclear export is facilitated by the nuclear protein Crm1 which interacts with the nuclear export sequence (NES) of the inactive form of Yap1 (Yan et al., 1998). Translocation of Yap1 to the nucleus is facilitated by transport receptor Pse1 and independent of oxidative stress (Isoyama et al., 2001). Upon oxidative challenge, Yap1 is oxidized and disulphide bonds are formed in the cysteine-rich domain thus inducing a conformational change and masking of the NES. Indeed, accumulation of Yap1 results from the inability of Crm1 to bind and export oxidized Yap1, thus activating its target genes in the nucleus (Kuge et al., 2001; Wood et al., 2004). Oxidation of Yap1 occurs either by direct oxidation encountering ROS or by interaction with the glutathione peroxidase (GPx)-like enzyme Orp1. Once oxidized Orp1 can form an intermolecular disulphide bond with Yap1, which is then transposed to the cysteine-rich region of Afyap1, thus forming an intramolecular bond. Yap1 is reduced back to its inactive state by thioredoxin (Delaunay et al., 2002). In *A. fumigatus* deletion of AfYap1 renders the fungus susceptible to oxidants like menadione or H_2O_2, virulence however, is not affected (Lessing et al., 2007; Qiao et al., 2008).

Another transcription factor is the two-component response regulator Skn7 that was shown to control several responses including cell wall gene expression and oxidative stress. In *S. cerevisiae* Skn7 regulates the expression of both thioredoxin (Trx2) and thioredoxin reductase (Morgan et al., 1997). Indeed, about half the targets of Yap1 also require Skn7 for their induction. Loss of *skn7* led to a sensitivity against certain oxidizing agents like hydrogen peroxide. Double deletion of *yap1/skn7* did not enhance sensitivity to hydrogen peroxide and diamide compared to *yap1* single deletion (Lee et al., 1999a). In *A. fumigatus* deletion mutants of *skn7* are sensitive to H_2O_2 and *t*-BOOH, but not to other oxidants. Also, virulence was not affected (Lamarre et al., 2007).

In addition to Yap1 and Skn7 there are also some other regulators involved in the oxidative stress response. The TF StuA is involved in *A. fumigatus* development, e.g. conidiation. Loss of StuA has no effect on virulence but hyphae are sensitive to hydrogen peroxide and StuA was shown to be required for catalase expression (Sheppard et al., 2005).

Sho1 is an adaptor protein in the upstream branches of the HOG-MAPK pathway in *S. cerevisiae*. In *A. fumigatus* deletion leads to reduced growth and germination rates. Virulence was not affected but the mutant was more sensitive to hydrogen peroxide and menadione and was shown to be involved in the adaptation to oxidative stress (Ma et al., 2008).

The transcriptional regulator SebA is relevant for tolerance to poor nutrition, heat shock and oxidative stress in *A. fumigatus*. Deletion leads to attenuated virulence in a murine mouse model of IA. *In vitro* growth is reduced by hydrogen peroxide and paraquat amongst others and killing by murine alveolar macrophages *in vitro* was enhanced compared to the WT (Dinamarco et al., 2012).

The modulation of cellular processes is organized in a complex interwoven network that allows for a finely tuned adaptation to a host of different conditions. The redox state of cells is very important for their function and the determination of their cell fate and the examples above suggest a redundancy on the regulatory level where the loss of one player does not necessarily lead to a loss of functionality. This complex answer triggered by different processes allows the fungus to adapt competently to oxidative stress and stay balanced.

1.2.4 Oxidative damage affects DNA, proteins and lipids

As a regular by-product an aerobic lifestyle, ROS are produced constantly and thus cannot be avoided. Hence, they have to be tightly controlled. If homeostasis cannot be maintained and basal levels are exceeded, oxidation of macromolecules such as DNA, proteins or lipids occurs. This oxidation can lead to reversible, but more often to irreversible changes and subsequent damage (Sies, 1986; Sies, 2000).

Oxidative damage of DNA frequently occurs and is associated with aging (Ashok and Ali, 1999). To compensate the occurring damage a number of repair mechanisms like mismatch repair, nucleotide excision repair etc. have evolved and in 1994 the “DNA repair enzyme” was even awarded the title of molecule of the year by *Science* (Koshland Jr, 1994). A less sophisticated

DNA-repair than that of the nucleus and the lack of histones makes mitochondrial DNA a major target of oxidative damage (Richter et al., 1988). Oxidation of the guanine base occurs at the highest frequency due to its reduction potential and leads to 8-oxo-2'-deoxyguanosine (8-oxo-dG) which in turn may lead to strand scissions (Hall et al., 1996; Hemnani and Parihar, 1998).

Due to their cellular abundance, proteins are oftentimes targets for ROS. On one hand oxidation can lead to reversible modifications such as methionine sulfoxidation or S-glutathionylation which protect against irreversible oxidation and are involved in redox regulation (Levine et al., 2000; Dalle-Donne et al., 2005). On the other hand, oxidation may lead to alterations of structural integrity, which may lead to a loss of function. This includes carbonylation, an irreversible oxidative damage. Carbonylation impacts protein folding and activity. Generally, oxidized proteins should be recognized and repaired or degraded by proteolytic enzymes. However, excessive carbonylation leads to the cross-linkage of proteins which form aggregates which resist proteolytic cleavage. Accumulation of these aggregates can lead to cell death and tissue damage and is associated with diseases such as Parkinson (Dalle‐Donne et al., 2006; McNaught and Olanow, 2006).

Lipids are a main component of cell membranes and important for their function. They are easily attacked by ROS and especially the double bonds of polyunsaturated fatty acids are susceptible to react with the hydroxyl radical ($OH^{\cdot}$). This initiates a chain reaction starting with the production of lipid hydroperoxides (LOOH). The variety of resulting secondary compounds are often harmful substances such as the mutagenic malondialdehyde (MDA) or the toxic 4-hydroxyninenal (4-HNE) (Esterbauer et al., 1991; Ayala et al., 2014).

1.2.5 Crosslinks in Iron and ROS homeostasis

Next to oxidative stress, iron is a key factor for growth and virulence in *A. fumigatus*. Indeed, loss of the main mechanism, which enables the fungus to tap the hosts iron sources and the subsequent cut off of iron supply, leads to avirulence in a mouse model of IA (Schrettl et al., 2004; Schrettl et al., 2007). Iron is a vital component of metabolic processes such as respiration, DNA biosynthesis and repair or amino acid metabolism. It is thus not surprising that the iron metabolism is closely interconnected with a number of cellular pathways, including not only the oxidative stress response but also zinc metabolism or pH regulation (Eisendle et al., 2004; Yasmin et al., 2009; Kurucz et al., 2018). Especially the crosslinks

between iron and ROS homeostasis are extensive, as the involvement of iron in both ROS generation (Fenton/Haber-Weiss reactions) and detoxification, for example as an integral part of peroxidases or catalases in form of an iron containing heme, closely links them together (Amir et al., 2010; Galaris et al., 2019).

1.2.6 The peroxiredoxin Asp f3

The protein Asp f3 of *A. fumigatus* is a two-cysteine type peroxiredoxin which was first identified by Crameri and Blaser (1996) as a major fungal allergen from patients with ABPA. It is highly abundant and has a strong affinity to serum immunoglobulin (Ig)E and thus served as a vaccine candidate against *A. fumigatus* infections (Hemmann et al., 1998; Ito et al., 2006). In a mouse model of IA immunization with Asp f3 was shown to protect successfully against invasive infection (Ito et al., 2006). Interestingly, Asp f3 was shown to be localized in the peroxisome in *A. fumigatus* hyphae where it is inaccessible to antibodies until both cell wall and cell membrane are permeabilized, suggesting that the vaccine-effect is independent of antibody formation. Instead protection was mediated by $CD4^+$ T cells, at least for a recombinant version of Asp f3, carrying only the amino acids 15-168 (Diaz-Arevalo et al., 2011).

The crystal structure of the protein and its catalytic mechanism where described recently by Hillmann and colleagues (2016). Asp f3 forms a functional homodimeric structure (Figure 7). When oxidized, the dimer is stabilized by two intermolecular disulphide bonds The cysteines (C31 and C61) are not essential for the structural integrity of the homodimer, but their exchange with different amino acids like serine or alanine leads to a strongly decreased peroxidase activity. The catalytic center of Asp f3 consists of proline, threonine and cysteine, which form a catalytic triad highly conserved in the PxxxTxxC active site motif typical for Prx5 subfamily proteins. Nevertheless, although the catalytic mechanism of Asp f3 is known, the exact cellular function and putative interaction partners remain elusive. However, loss of Asp f3 in a knock-out strain led not only to a phenotype hypersensitive to ROS but also results in avirulence in a mouse model of pulmonary aspergillosis, thus highlighting its importance in the complex process of redox homeostasis

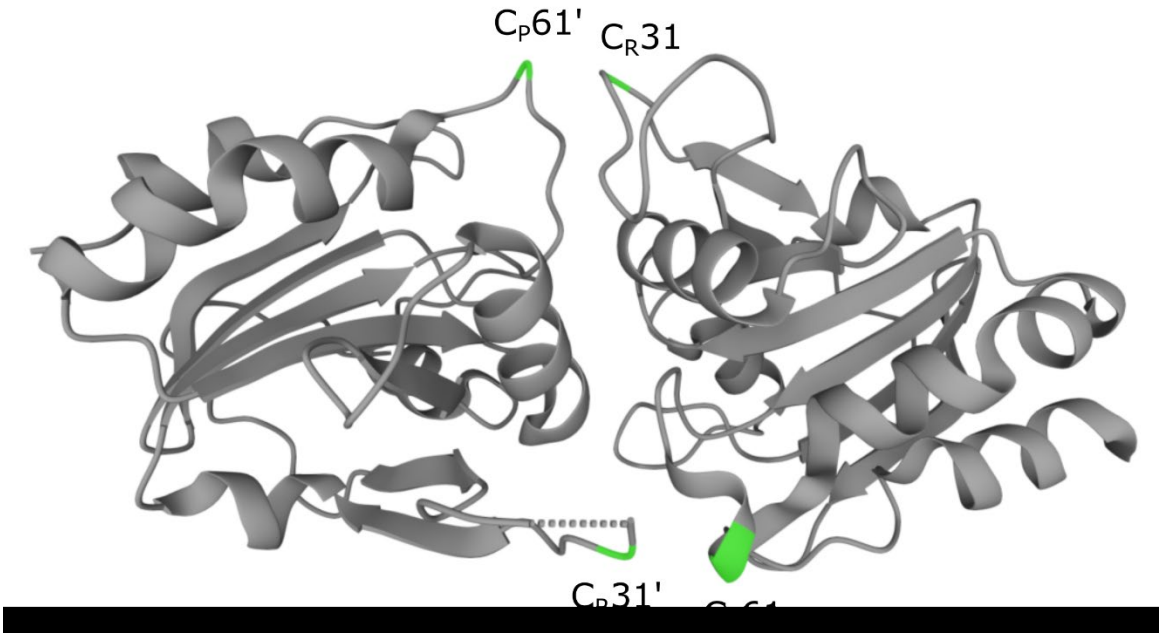

Figure 7 Asp f3 homodimer of *A. fumigatus* as a ribbon cartoon. The atypical 2-Cyx peroxiredoxin Asp f3 functions as a homodimer. Cysteines C31 and C61 are able to form two intermolecular disulphide bonds upon oxidation with C61 being the peroxidatic cysteine (C_P) and C31 the resolving cysteine (C_R). Shown he is the reduced form of Asp f3. (https://www.uniprot.org/uniprot/O43099/protvista; accessed 25.10.2021).

.

2 Aims of the Study

During the last years incident rates of fungal infections rose continually and will rise further as the number of immunocompromised patients is generally increasing. Those infections have a high death toll due to a lack of time efficient identification of the pathogens involved as well as a limited availability of effective treatments, especially of fungal infections. Moreover they are a cost-intensive burden on health care systems worldwide. Therefore, it is crucial that we enhance our efforts to not only improve our diagnostic capabilities but also discover new bioactive compounds with possible therapeutic potential and identify promising biological targets to open the possibility for customised drug design in the future.

The recent description of the Δ*asp f3* mutant of *A. fumigatus*, which lacks the peroxiredoxin Asp f3 and was shown to be highly sensitive to reactive oxygen species and furthermore avirulent in a murine model of pulmonary aspergillosis, represents such a potential target for anti-*A. fumigatus* treatment. In this study I therefore aimed to elucidate the functional role of the protein in vivo and to identify how Asp f3 integrates to the transcriptional and proteomic network in response to oxidative stress. I therefore conducted a transcriptome analysis, which showed fundamental transcriptional differences between the wild type and Δ*asp f3* in response to oxidative stress. The proteomic approach should reveal possible target proteins that may be further candidates for drug design. Finally, in a collaborative effort and murine model of pulmonary aspergillosis I could conclude on possible reasons and a biochemical crosslink that make Asp f3 an essential player during infection.

3 Manuscripts

Manuscript 1

Titel: Yeast two-hybrid screening reveals a dual function for the histone acetyltransferase GcnE by controlling glutamine synthesis and development in *Aspergillus fumigatus*

Authors: Marcel Noßmann, Jana M. Boysen, Thomas Krüger, Claudia C. König, Falk Hillmann, Thomas Munder, Axel A. Brakhage

Status: published manuscript

Bibliographic Information: Nossmann, M., Boysen, J. M., Krüger, T., König, C. C., Hillmann, F., Munder, T., & Brakhage, A. A. (2019). Yeast two-hybrid screening reveals a dual function for the histone acetyltransferase GcnE by controlling glutamine synthesis and development in *Aspergillus fumigatus*. *Current genetics, 65*(2), 523-538. https://doi.org/10.1007/s00294-018-0891-z

Summary: In this article, we describe and verify *in vivo* two new interaction partners for the histone acetyltransferase GcnE of *Aspergillus fumigatus*. We could show that GcnE physically interacts with the uncharacterized protein GbpA (Afu8g00780) as well as with the glutamine synthetase GlnA (Afu4g13120). Further, we could show that GcnE regulates the enzyme activity of GlnA. However, this regulation is due rather to the physical interaction, since no Change in the acetylation pattern could be found. A phenotypical analysis of deletion mutant of *gcnE* shows a deficiency in growth and sporulation. Deletion of *glnA* results in a glutamine auxotrophy, thereby confirming the function of GlnA as the only functional glutamine synthetase of *A. fumigatus.*

Manuscript 2

Titel: The Peroxiredoxin Asp f3 Acts as Redox Sensor in *Aspergillus fumigatus*

Authors: Jana Boysen, Nauman Saeed, Thomas Wolf, Gianni Panagiotou, Falk Hillmann

Status: veröffentlicht

Bibliographic Information: Boysen, J. M., Saeed, N., Wolf, T., Panagiotou, G., & Hillmann, F. (2021). The Peroxiredoxin Asp f3 Acts as Redox Sensor in *Aspergillus fumigatus*. Genes, 12(5), 668. https://doi.org/10.3390/genes12050668

Summary: *Aspergillus fumigatus* is an opportunistic fungal pathogen, which can cause life-threatening infections in immunocompromised patients. For the successful establishment of infection *A. fumigatus* must overcome the bodies defence mechanisms in which protection against reactive oxygen species (ROS) and redox homeostasis are of major importance. The peroxiredoxin Asp f3 was recently shown to be essential for virulence in a mouse model of

pulmonary aspergillosis. Here, we apply a next generation sequencing approach to analyse the transcriptomic changes in an *asp f3* deficient strain of *A. fumigatus* upon challenge with ROS. Global transcription is not affected by the absence of Asp f3 while it is required for the activation of the oxidative stress response when confronted with ROS. Asp f3 deficient hyphae fail to activate redox active genes such as members of the Afyap1 regulon. Indeed, nuclear localization of Afyap1 during ROS exposure was significantly restricted in comparison to the wild type indicating its function as an intracellular redox sensor.

Manuscript 3

Titel: Natural products in the predatory defence of the filamentous fungal pathogen *Aspergillus fumigatus*

Authors: Jana Boysen, Nauman Saeed, Falk Hillmann

Status: veröffentlicht

Bibliographic Information: Boysen, J. M., Saeed, N., & Hillmann, F. (2021). Natural products in the predatory defence of the filamentous fungal pathogen *Aspergillus fumigatus*. Beilstein journal of organic chemistry, 17(1), 1814-1827. https://doi.org/10.3762/bjoc.17.124

Summary: Fungi are ubiquitous and are found in diverse natural habitats where they have to adapt to often harsh living conditions. This includes not only abiotic stress factors and the gain of necessary nutrition but also protection against competition and predators as well as communication with other organisms during symbiotic or parasitic interactions. Therefore, fungi have developed several mechanisms including the production of secondary metabolites, which help scavenging rare nutrients like iron or protect from both competition and predation with antibiotic effects against different types of organisms. This review exemplarily highlights a selection of secondary metabolites in the opportunistic fungal pathogen *Aspergillus fumigatus* and their impact on protection during predatory interactions.

Manuscript 4

Titel: Natural products in the predatory defence of the filamentous fungal pathogen *Aspergillus fumigatus*

Authors: Victor Brantl, Jana M. Boysen, Annie Yap, Evgeny Golubtsov, Dominik Ruf, Thorsten Heinekamp, Maria Straßburger, Karl Dichtl, Hubertus Haas, Falk Hillmann, Johannes Wagener

Status: veröffentlicht

Bibliographic Information: Brantl, V., Boysen, J. M., Yap, A., Golubtsov, E., Ruf, D., Heinekamp, T., Straßburger, M., Dichtl, K., Haas, H., Hillmann, F., Wagener, J. (2021).

Peroxiredoxin Asp f3 Is Essential for *Aspergillus fumigatus* To Overcome Iron Limitation during Infection. *Mbio*, *12*(4), e00976-21. https://doi.org/10.1128/mBio.00976-21

Summary: As a major fungal pathogen *A. fumigatus* is the causative agent of severe and often fatal infections in immunocompromised patients. Loss of peroxiredoxin Asp f3 causes the fungus to loose virulence, which is caused by a significant sensitivity to iron deficient conditions, as replete iron supply is able to restore full virulence. The effect is independent of regulatory changes in iron homeostasis or siderophore biosynthesis.

Manuscript 5

Titel: The protein disulphide isomerase PdiA is involved in low temperature adaptation of *Aspergillus fumigatus*

Authors: Jana M. Boysen, Elena Shekhova, Olaf Kniemeyer, Axel A. Brakhage, Falk Hillmann

Status: in Vorbereitung

Bibliographic Information: -

Summary: In a peroxiredoxin Asp f3 deficient strain of *A. fumigatus* is avirulent and sensitive to oxidative stress. In a proteomics approach we aspire to identify possible protein targets of oxidative stress contributing to Δ*asp f3*'s phenotype. Results identify the protein disulphide isomerase A (PdiA) as a major target of oxidation, however PdiA-deletion contradicts its involvement in Asp f3 dependent redox sensitivity. Instead, PdiA is involved in the adaptation to low temperature conditions.

3.1 Manuscript 1 - Yeast two-hybrid screening reveals a dual function for the histone acetyltransferase GcnE by controlling glutamine synthesis and development in *Aspergillus fumigatus*

FORMULAR 1

Manuskript Nr. 1

Titel des Manuskriptes: Yeast two-hybrid screening reveals a dual function for the histone acetyltransferase GcnE by controlling glutamine synthesis and development in *Aspergillus fumigatus*

Autoren: Marcel Noßmann, Jana M. Boysen, Thomas Krüger, Claudia C. König, Falk Hillmann, Thomas Munder, Axel A. Brakhage

Bibliographische Informationen: Nossmann, M., Boysen, J. M., Krüger, T., König, C. C., Hillmann, F., Munder, T., & Brakhage, A. A. (2019). Yeast two-hybrid screening reveals a dual function for the histone acetyltransferase GcnE by controlling glutamine synthesis and development in *Aspergillus fumigatus*. *Current genetics, 65*(2), 523-538. https://doi.org/10.1007/s00294-018-0891-z

Die Kandidatin ist

☐ Erstautor/-in, ☐ Ko-Erstautor/-in, ☐ Korresp. Autor/-in, ☒ Koautor/-in.

Status: publiziert

Anteile (in %) der Autoren / der Autorinnen an der Publikation (anzugeben ab 20%)

Autor/-in	Konzeptionell	Datenanalyse	Experimentell	Verfassen des Manuskriptes	Bereitstellung von Material
Jana M. Boysen	5%	5%	10 %	15 %	0%
Marcel Noßmann	20%	90%	80%	65%	0%
Thomas Munder	25%	-	-	-	20 %
Axel A. Brakhage	25%	-	-	-	60 %
Falk Hillmann	25%	-	-	-	20 %

Current Genetics (2019) 65:523–538
https://doi.org/10.1007/s00294-018-0891-z

ORIGINAL ARTICLE

Yeast two-hybrid screening reveals a dual function for the histone acetyltransferase GcnE by controlling glutamine synthesis and development in *Aspergillus fumigatus*

Marcel Nossmann[1,2,3] · Jana M. Boysen[3,4] · Thomas Krüger[2] · Claudia C. König[2,3] · Falk Hillmann[4] · Thomas Munder[1] · Axel A. Brakhage[2,3]

Received: 25 June 2018 / Revised: 25 September 2018 / Accepted: 8 October 2018 / Published online: 15 October 2018

Abstract

The acetyltransferase GcnE is part of the SAGA complex which regulates fungal gene expression through acetylation of chromatin. Target genes of the histone acetyltransferase GcnE include those involved in secondary metabolism and asexual development. Here, we show that the absence of GcnE not only abrogated conidiation, but also strongly impeded vegetative growth of hyphae in the human pathogenic fungus *Aspergillus fumigatus*. A yeast two-hybrid screen using a *Saccharomyces cerevisiae* strain whose tRNA molecules were specifically adapted to express *A. fumigatus* proteins identified two unprecedented proteins that directly interact with GcnE. Glutamine synthetase GlnA as well as a hypothetical protein located on chromosome 8 (GbpA) were identified as binding partners of GcnE and their interaction was confirmed in vivo via bimolecular fluorescence complementation. Phenotypic characterization of *gbpA* and *glnA* deletion mutants revealed a role for GbpA during conidiogenesis and confirmed the central role of GlnA in glutamine biosynthesis. The increase of glutamine synthetase activity in the absence of GcnE indicated that GcnE silences GlnA through binding. This finding suggests an expansion of the regulatory role of GcnE in *A. fumigatus*.

Keywords *Aspergillus fumigatus* · Yeast two-hybrid system · Histone acetyltransferase GcnE · Glutamine synthetase GlnA · Bimolecular fluorescence complementation assay

Introduction

The ubiquitous saprophytic fungus *Aspergillus fumigatus* thrives in the soil and decaying organic matter such as fruits or compost (reviewed in Latgé 1999; Brakhage and Langfelder 2002; Brown et al. 2012). The asexual reproduction of *A. fumigatus* is mediated by formation of conidia from conidiophores. Following their dispersal through the air and subsequent inhalation by humans, their small size

Communicated by M. Kupiec.

Electronic supplementary material The online version of this article (https://doi.org/10.1007/s00294-018-0891-z) contains supplementary material, which is available to authorized users.

✉ Falk Hillmann
Falk.Hillmann@leibniz-hki.de

✉ Thomas Munder
Thomas.Munder@eah-jena.de

✉ Axel A. Brakhage
Axel.Brakhage@leibniz-hki.de

[1] Department of Medical Engineering and Biotechnology, Ernst-Abbe-Hochschule Jena, University of Applied Sciences, Carl-Zeiss-Promenade 2, 07745 Jena, Germany

[2] Department of Molecular and Applied Microbiology, Leibniz Institute for Natural Product Research and Infection Biology-Hans Knöll Institute (HKI), Beutenbergstr. 11a, 07745 Jena, Germany

[3] Institute of Microbiology, Friedrich Schiller University Jena, Jena, Germany

[4] Junior Research Group Evolution of Microbial Interactions, Leibniz Institute for Natural Product Research and Infection Biology-Hans Knöll Institute (HKI), Beutenbergstr. 11a, 07745 Jena, Germany

of 2.5–3 µm allows them to reach the lung alveoli, thereby acting as the infectious agent. Depending on the host and its immune status, such an infection may lead to different diseases, e.g., respiratory allergies, obstructive bronchitis, invasive rhinosinusitis, or in the most severe case, to the often fatal invasive aspergillosis (reviewed in Latgé 1999). The latter is one of the most serious diseases among immunosuppressed patients, especially for patients suffering from chronic granulomatous disease (CGD), leukemia, HIV, organ transplant or stem cell recipients. The mortality rate reaches 50–95% depending on the underlying condition (reviewed in Brown et al. 2012).

For understanding pathogenicity and the biology of *A. fumigatus* in general, it is required to analyze the metabolism and the protein repertoire of the fungus on a functional level. Although insight into metabolic pathways of *A. fumigatus* and interaction of proteins has been obtained mainly from bioinformatic analyses, the identification of biochemically defined interactions between two or more proteins is required to support predictions and elucidate unprecedented functions (Altwasser et al. 2015; Linde et al. 2010; Sarikaya Bayram et al. 2018). Experimentally verified interactions allow to identify interactions, prior unknown proteins, and to elucidate the interactome of an organism. The yeast two-hybrid (Y2H) technology enables the detection of protein partners in vivo and represents a pioneering technology for all interaction studies (Fields and Song 1989). This method allows study of protein interactions by a modular construction of transcription factors which are separated from each other. An interaction of bait and prey proteins directly correlates with the reconstitution of this transcription factor which leads to the expression of different reporter genes. Y2H was used to generate interactome maps of different organisms such as human, *Saccharomyces cerevisiae*, and *Schizosaccharomyces pombe* (Yu et al. 2008; Vo et al. 2016). Further, it was used to elucidate the function of proteins that are involved in pathogenicity (reviewed in Munder and Hinnen 1999).

The importance of GcnE as a central hub in development and secondary metabolism (Nützmann et al. 2011) prompted us to characterize its function in *A. fumigatus* and choose GcnE as bait for a protein interaction assay. GcnE is part of the multisubunit SAGA-complex (Spt-Ada-Gcn5-acetyltransferase). It regulates specific subsets of genes through chromatin modification (Daniel and Grant 2007; Sellam et al. 2009; Pray-Grant 2002). GcnE-like acetyltransferases consist of four domains of which domain A is the most conserved. It represents the acetyl-CoA recognition and binding domain, essential for the transfer of acetyl-CoA (Hassan et al. 2002). Domain B spans the bromodomain and mediates the recognition of lysine residues that are already acetylated, while the other domains C–E are less conserved (reviewed in Dyda et al. 2000; Hassan et al. 2002). A GcnE orthologous protein was first isolated from *S. cerevisiae* (GCN5). It is widely conserved throughout eukaryotes (Salah Ud-Din et al. 2016). In *S. cerevisiae*, it was identified as transcriptional regulator due to its interaction and complex formation with ADA2 and ADA3. Mutations within this gene or its loss lead to severe phenotypes. In the filamentous fungus *Aspergillus nidulans*, deletion of the *gcnE* gene led to reduced growth, loss of asexual reproduction as well as a shift in secondary metabolite profile (Nützmann et al. 2011; Cánovas et al. 2014). The same is true for *Fusarium fujikuroi*, where the loss of *gcn5* additionally resulted in a general growth deficiency (Rösler et al. 2016). In HeLa cell lines it was shown that Gcn5 not only acetylates histones but is also responsible for the acetylation of cell-division cycle (CDC6) protein which is involved in mitosis. Here, the acetylation is an important prerequisite for further modifications and thus the function of CDC6 and its stability (Paolinelli et al. 2009).

To our knowledge, the Y2H system has not been applied to screen for interactions of proteins from *A. fumigatus*. One reason might lie in the different codon usage between *S. cerevisiae* and *A. fumigatus* precluding heterologous expression. Recently, we have shown that this limitation can be overcome using a tRNA-adapted *S. cerevisiae* strain (Nossmann et al. 2017). Here, this strain was successfully exploited to screen for GcnE interaction partners using a cDNA library from *A. fumigatus*. The glutamine synthetase GlnA and an unknown protein (GbpA) encoded next to the secondary metabolite fumagillin-pseurotin-fumitremorgin-supercluster (Wiemann et al. 2013) were among the confirmed binding partners of GcnE indicating further unprecedented regulatory functions of GcnE.

Materials and methods

Strains used in this study

All strains used in the study are listed in Table 1.

Preparation of a cDNA library from *A. fumigatus*

The cDNA library based on the total RNA from *A. fumigatus* was generated using a modified protocol of the Make Your Own Mate & Plate™ Library from Takara Bio Company, St Germain en Laye, France. After performing a long-distance PCR using 3.3 µg single-stranded (ss) cDNA as template the generated double-stranded (ds) cDNA molecules were loaded onto a 1% (w/v) agarose gel. All DNA fragments between 500 and 12,000 bps were excised from the gel (Fig. 2a). The DNA fragments were used to transform *S. cerevisiae* strain Y187 together with the linearized plasmids pGADT7-rec to generate the prey plasmids by homologous recombination within the cells.

Table 1 Strains of *S. cerevisiae* and *A. fumigatus*

Strain	Genotype	References
Saccharomyces cerevisiae		
KFY1	MATa, ura3-52, his3-200, ade2-101, lys2-801, trp1-901, leu2-3, -112, gal4Δ, gal80Δ, cyh^r2, LYS2::$GAL1_{UAS}$-$HIS3_{TATA}$-HIS3, URA3::$GAL1_{UAS}$-$GAL1_{TATA}$-lacZ, ADE2::ADE2	Gola et al. (2015)
Y187	MATα, ura3-52, his3-200, ade2-101, trp1-901, leu2-3, 112, gal4Δ, gal80Δ, met-, URA3::$GAL1_{UAS}$-$GAL1_{TATA}$-LacZ, MEL1	Takara, Saint-Germain-en-Laye, France
MNY3	MATa, ura3-52, his3-200, ade2-101, trp1-901, leu2-3, -112, gal4Δ, gal80Δ, LYS2::$GAL1_{UAS}$-$GAL1_{TATA}$-HIS3, $GAL2_{UAS}$-$GAL2_{TATA}$-ADE2, URA3::$MEL1_{UAS}$-$MEL1_{TATA}$-AUR1, MEL1, Δ$tRNA^{Arg}_{UCU}$, KanMx::$tRNA^{Arg}_{CCG}$, KanMx::$tRNA^{Arg}_{GCG}$, KanMx::$tRNA^{Arg}_{UCG}$	Nossmann et al. (2017)
Aspergillus fumigatus		
CEA10 (A1163)	Wild type	Fedorova et al. (2008)
GpdA-GcnE-V	P_{gpdA}-gcnE-$Venus_{Full}$-T_{nos}::hph, Hyg^R	This study
GpdA-GlnA-V	P_{gpdA}-glnA-$Venus_{Full}$-T_{nos}::hph, Hyg^R	This study
GpdA-GbpA-V	P_{gpdA}-gbpA-$Venus_{Full}$-T_{nos}::hph, Hyg^R	This study
GpdA-GcnE-V(C)	P_{gpdA}-gcnE-$Venus_C$-T_{nos}::hph, Hyg^R	This study
GpdA-GlnA-V(N)	P_{gpdA}-glnA-$Venus_N$-T_{nos}::ptrA; PT^R	This study
GpdA-GbpA-V(N)	P_{gpdA}-gbpA-$Venus_N$-T_{nos}::ptrA; PT^R	This study
GpdA-Aspf3-V(N)	P_{gpdA}-aspf3-$Venus_{Full}$-T_{nos}::ptrA; PT^R	This study
GpdA-GcnE-V(C) + GpdA-GlnA-V(N)	P_{gpdA}-gcnE-$Venus_C$-T_{nos}::hph, Hyg^R, P_{gpdA}-glnA-$Venus_N$-T_{nos}::ptrA; PT^R	This study
GpdA-GcnE-V(C) + GpdA-GbpA-V(N)	P_{GpdA}-gcnE-$Venus_C$-T_{nos}::hph, Hyg^R, P_{gpdA}-gbpA-$Venus_N$-T_{nos}::ptrA; PT^R	This study
GpdA-GcnE-V(C) + GpdA-Aspf3-V(N)	P_{GpdA}-gcnE-$Venus_C$-T_{nos}::hph, Hyg^R, P_{gpdA}-aspf3-$Venus_N$-T_{nos}::ptrA; PT^R	This study
CEA17	Δ$akuB^{KU80}$::pyrG; $PyrG^+$	da Silva Ferreira et al. (2006)
ΔgcnE	Δ$akuB^{KU80}$::pyrG; $PyrG^+$, gcnE::ptrA; PT^R	This study
Δ$gcnE^C$	Δ$akuB^{KU80}$::pyrG; $PyrG^+$, gcnE::ptrA, hph::gcnE-hph; Hyg^R	This study
ΔglnA	Δ$akuB^{KU80}$::pyrG; $PyrG^+$, glnA::hph, Hyg^R	This study
Δ$glnA^C$	Δ$akuB^{KU80}$::pyrG; $PyrG^+$, glnA::hph, hph::glnA-ptrA; PT^R	This study
ΔgbpA	Δ$akuB^{KU80}$::pyrG; $PyrG^+$, gbpA::ptrA; PT^R	This study
pGTH-GlnA	P_{gpdA}-glnA-StrepII-T_{nos}::hph, Hyg^R	This study
pGTH-GbpA	P_{gpdA}-gbpA-StrepII-T_{nos}::hph, Hyg^R	This study

Cloning of GcnE as a bait protein and generation of diploid yeast cells

The gene sequence of *gcnE* (Afu4g12650) was obtained from NCBI database and a synthetic codon-optimized *gcnE* gene (GeneArt, Thermo Fisher Scientific, Dreieich, Germany) was cloned into the Y2H plasmid pGBKT7 using *Eco*RI and *Pst*I sites. The changes of the nucleotide sequence did not change the GcnE amino acid sequence. The resulting plasmid pMN5 was transformed into yeast strain MNY3, carrying elevated tRNA levels for arginine ($tRNA^{Arg}_{CCG}$, $tRNA^{Arg}_{GCG}$ and $tRNA^{Arg}_{UCG}$) to increase prey expression after mating the haploid yeast strains (Nossmann et al. 2017).

Yeast cells of the bait-expressing strain MNY3 were cultivated in YPD media (Carl Roth) and harvested during the logarithmic growth phase. MNY3 was then mated with strain Y187 containing the optimized cDNA library for 24–28 h at 30 °C and shaking with 40 rpm. Formation of zygotes was monitored using a microscope. Diploid yeast cells were directly selected by their protein interaction-dependent ability to grow in SD-QDO media [2% (w/v) glucose, 0.67% (w/v) yeast nitrogen base, 1.15 mM arginine, 1.34 mM methionine, 1.65 mM cysteine, 1.66 mM tyrosine, 1.78 mM

uracil, 2.05 mM lysine, 2.29 mM isoleucine, 3.03 mM phenylalanine, 6.8 mM glutamic acid, 7.51 mM aspartic acid, 12.80 mM valine, 16.79 mM threonine and 38.06 mM serine] lacking adenine and histidine. The latter supplements are needed to complement the auxotrophic yeast strains in the absence of protein interactions. Bait- and prey-encoding plasmids were isolated by phenol/chloroform extraction and amplified in *Escherichia coli*. The prey plasmid was transformed into Y187. The generated strain was subsequently mated with the respective bait-containing strain MNY3. Growth was monitored on SD-QDO agar plates. Furthermore, both plasmids were transformed into the yeast strain KFY1 and colonies were analyzed for *lacZ* reporter gene expression by filter lift assays according to Breeden and Nasmyth (1985).

Cultivation of strains and determination of the numbers of conidia from *A. fumigatus*

All *A. fumigatus* strains were cultivated in *Aspergillus* minimal medium (AMM) (Brakhage and Van den Brulle 1995) by inoculation of 10^5 conidia in flasks containing AMM for 24 h at 37 °C and constant shaking at 180 rpm. Due to slower growth the *gcnE* deletion mutant ΔgcnE was cultivated for 48 h at 37 °C. The deletion strain for *glnA* (*ΔglnA*) was cultivated additionally with 20 mM glutamine to complement the respective auxotrophy. The selection of deletion strains was performed by three consecutive transfers on AMM-agar with 250 mM hygromycin B or 100 mM pyrithiamine. To study the overexpression effects of *gcnE, glnA*, and *gbpA*, 10^4 conidia of each mutant strain containing a *gpdA* promoter fused to the YFP fusion proteins were first inoculated on AMM-agar plates. After incubation at 37 °C for 96 h conidia were harvested using 0.1% (v/v) Tween80. The number of conidia for all cultures were determined using CASY® Modell TT (OLS, Bremen, Germany).

Generation of bimolecular fluorescence complementation (BiFC) and acetylation reporter strains of *A. fumigatus*

Genes encoding *gcnE, glnA*, and *gbpA* were cloned into plasmids (see Fig. S1) which contain parts of the yellow fluorescent protein (YFP) gene encoding the N- or C-terminal domain of YFP or the entire YFP (Gsaller et al. 2014). The expression of the various constructs was driven by the constitutive *gpdA* promoter. For details see Fig. 4a, b. *A. fumigatus* CEA10 was transformed with all constructs *via* the generation of protoplasts (Ballance and Turner 1985). The PCR product obtained using primers *Trafo_Fw* and *Trafo_Rv* (Primer see Supplement Table II) were integrated into the genome of CEA10. For an overview of how the plasmids were generated, see Supplement Fig. S1. The selection of transformant strains was carried out using the hygromycin B or pyrithiamine resistance cassette (see Table 1). Integration of DNA constructs into the genomic DNA was verified by PCR. To determine the acetylation of GlnA and GbpA, these proteins were labeled with the StrepII tag (WSHPQFEK) and the corresponding genes cloned by CPEC (Quan and Tian 2009) with *gpdA* promoter and *tef* terminator yielding plasmids pGTH (P_{GpdA}, T_{tef}, Hyp^R)-GlnA and pGTH-GbpA. For selection, a hygromycin B cassette under the control of the *trpC* promoter and terminator was used (Supplement Table II). The construct was integrated into the genome of CEA10. Mutant strains were verified by PCR and Western blot analysis.

Gene deletion and complementation in *A. fumigatus*

Knockout mutants for *gcnE, glnA, gbpA*, and complementation strains for *ΔgcnE* and *ΔglnA* were obtained by homologous recombination. Selection of recombinant strains was carried out using either hygromycin B (*ΔglnA* and $\Delta gcnE^C$) or pyrithiamine (*ΔgcnE, ΔgbpA* and $\Delta glnA^C$) resistance cassettes. Mutant strains were verified by Southern hybridization after three consecutive rounds of selection (Brakhage and Van den Brulle 1995). Isolation of chromosomal DNA, the generation of DIG-labeled DNA probes, blotting, hybridization, and detection steps were all carried out as previously described.

BiFC microscopy

To image BiFC, 10^2 conidia of *A. fumigatus* strains containing different split-YFP constructs were grown on cover slips in 12-well plates for 18 h at 37 °C without shaking, fixed on microscopy slides using Vectashield™ Mounting Media and directly used for microscopy in a Spinning Disk Confocal Microscope (Axio Observer 7, ZEISS, Jena, Germany) equipped with a color camera. Fungal cells were illuminated with 475 nm and emission was detected at 524 nm. Images were analyzed and processed using software ZEN 2.3 lite (ZEISS). All settings were adapted and digitally improved to the signal of the lowest abundant positive control for GcnE except for the positive control for GlnA since in this case the signal displays tenfold higher intensity when compared to all other samples. With these adjustments autofluorescence of hyphae was not observed. Pictures were taken with 630× magnification.

Preparation of protein extracts

For the enzyme assay and the determination of acetylated lysine residues, crude protein extracts were obtained from mycelia of *A. fumigatus* grown for 16 h in AMM and used as a source for StrepII-tagged GlnA and GbpA. The cultures

were harvested through miracloth and the mycelium was thoroughly washed with water, dried, and subsequently frozen with liquid nitrogen. The frozen mycelium was ground to a fine powder which was used for protein isolation. Approximately 100 mg of ground mycelium were resuspended in 500 µl of 100 mM potassium phosphate buffer (pH 7.4), vortexed and sonicated for 10 min. Cell debris was pelleted by centrifugation and the protein concentration of the supernatant was determined spectrophotometrically using the Bradford assay (Bradford 1976).

Glutamine synthetase activity assay

Activity of GlnA was measured indirectly by an enzymatic assay coupling the glutamate to glutamine conversion to the oxidation of pyruvate to L-lactate. Thereby β-NADH is oxidized to β-NAD (Kornberg and Pricer 1951).

$$\text{Glutamate} + NH_4^+ + \text{ATP} \xrightarrow{\text{L–Glutamine Synthetase}} \text{L} - \text{Glutamine} + \text{ADP} + P_i$$

$$\text{ADP} + \text{Phospho(enol)pyruvate} \xrightarrow{\text{Pyruvate Kinase}} \text{ATP} + \text{Pyruvate}$$

$$\text{Pyruvate} + \beta - \text{NADH} \xrightarrow{\text{L-Lactate Dehydrogenase}} \text{L} - \text{Lactate} + \beta - \text{NAD}$$

The decrease in β-NADH absorbance was measured spectrophotometrically at 340 nm and was directly proportional to glutamine formation. The reaction mixture was composed of 34.1 mM imidazole, 60 mM magnesium chloride, 18.9 mM potassium chloride, 45 mM ammonium chloride, 102 mM sodium glutamate, 1.1 mM phosphoenolpyruvate, 8.5 mM adenosine 5′-triphosphate, 0.25 mM β-nicotinamide adenine dinucleotide, 28 units pyruvate kinase and 40 units of L-lactate dehydrogenase. All assays were incubated at room temperature. One unit of GlnA was defined as the amount of protein which catalyzed the conversion of 1 µmol L-glutamate to L-glutamine in 1 min.

LC–MS analysis and identification of acetylated peptides

Harvested mycelia were shock-frozen in liquid N_2, ground and resuspended in 100 mM potassium phosphate buffer (pH 7.4). The GlnA-StrepII-tag® fusion proteins were isolated from the protein extract by Strep-Tactin®XT purification columns (IBA GmbH). Eluates of the enriched fusion protein were reduced for 1 h at 55 °C by addition of 2 µl of 500 mM TCEP (tris(2-carboxyethyl)phosphine) and further carbamidomethylated for 30 min at room temperature in the dark by addition of 2 µl of 625 mM iodoacetamide. Subsequently, the samples were further purified by methanol–chloroform–water precipitation (Wessel and Flügge 1984). Protein precipitates were resolubilized in 100 mM TEAB (Sigma-Aldrich) and digested overnight (18 h) with a trypsin + LysC mixture (Promega) at a protein-to-protease ratio of 25:1. Samples were evaporated in a SpeedVac, resolubilized in 25 µl of 0.05% (w/v) TFA in H_2O/ACN 98/2 (v/v) filtered through Ultrafree-MC 0.2 µm PTFE membrane spin filters (Merck-Millipore). The filtrate was analyzed by LC–MS/MS. Each sample was measured in triplicate (three analytical replicates).

LC–MS/MS analysis was carried out on an Ultimate 3000 nano RSLC system coupled to a QExactive HF mass spectrometer (both Thermo Fisher Scientific, Waltham, MA, USA). Peptides were trapped for 5 min on an Acclaim Pep Map 100 column (2 cm × 75 µm, 3 µm) at 5 µl/min followed by gradient elution separation on an Acclaim Pep Map RSLC column (50 cm × 75 µm, 2 µm). Eluent A (0.1% (v/v) formic acid in water) was mixed with eluent B (0.1% (v/v) formic acid in 90/10 acetonitrile/water) as follows: 0 min at 4% B, 30 min at 12% B, 75 min at 30% B, 85 min at 50% B, 90–95 min at 96% B, 95.1–120 min at 4% B.

Positively charged ions were generated at 2.2 kV using a stainless steel emitter and a Nanospray Flex Ion Source (Thermo Fisher Scientific). The QExactive HF was operated in Full MS / data-dependent MS2 (Top10) mode. Precursor ions were monitored at m/z 300–1500 at a resolution of 60,000 full width at half-maximum (FWHM) using a maximum injection time (ITmax) of 120 ms and an automatic gain control (AGC) target of 1e6. Precursor ions with a charge state of $z = 2$–5 were filtered at an isolation width of m/z 1.6 amu for HCD fragmentation at 30% normalized collision energy (NCE). MS2 ions were scanned at 15,000 FWHM (ITmax = 120 ms, AGC = 2e5). Dynamic exclusion of precursor ions was set to 30 s. The LC–MS/MS instrument was controlled by Chromeleon 7.2, QExactive HF Tune 2.8 and Xcalibur 4.0 software.

Protein database search

Tandem mass spectra were searched against the UniProt reference proteome database (2018/01/18; http://www.uniprot.org/proteomes/UP000002530) of *A. fumigatus* (*Neosartorya fumigata*) Af293, using Proteome Discoverer (PD) 2.2 (Thermo) and the algorithms of Mascot 2.4 (Matrix Science, UK), Sequest HT (version of PD2.2) and MS Amanda 2.0. Two missed cleavages were allowed for the tryptic digestion. The precursor mass tolerance was set to 10 ppm and the fragment mass tolerance was set to 0.02 Da. Modifications were defined as dynamic Met oxidation and acetylation of

Ser, Thr, Tyr, Lys, and the protein N-terminus as well as static Cys carbamidomethylation. At least two peptides per protein and a strict false discovery rate (FDR) < 1% were required for positive protein hits. The Percolator node of PD2.2 and a reverse decoy database was used for *q*-value validation of spectral matches. Only rank 1 proteins and peptides of the top-scored proteins were counted. The Minora algorithm of PD2.2 was applied for relative label-free quantification of the abundance of differentially modified tryptic peptides related to distinct proteoforms.

Results

GcnE controls conidiogenesis, germination and radial growth of *A. fumigatus*

As expected from the important role of GcnE during growth and the asexual development of *A. nidulans* (Nützmann et al. 2011; Canovas et al. 2014), deletion of the *A. fumigatus gcnE* orthologue also abrogated conidiation. Conidia of *A. fumigatus* wild type normally develop into fully grown mycelia after 5 days (Fig. 1a). The typical green color originated from the countless number of dihydroxynaphthalene-melanin containing conidia (Langfelder et al. 1998) growing from single conidiophores (Fig. 1b–d). In contrast, upon deletion of the *gcnE* gene, mycelia remained essentially without any mature conidiophores (Fig. 1e–h). The total amount of conidia produced by Δ*gcnE* was reduced to approximately 2.5% of that observed for the wild type, while overexpression of a GcnE-YFP fusion led a 50% increase in conidia (Fig. 1i), overall confirming a conserved role of GcnE during conidiation in *Aspergillus*. Germination and radial growth of the Δ*gcnE* strain were also severely impeded in comparison to wild type, even when cultivated under replete condition in a complex medium (Fig. 1j, k). This growth defect could not solely be attributed to a germination defect, as the germination of Δ*gcnE* conidia was not delayed by more than two hours (Fig. 1l). Re-integration of a functional *gcnE* gene in the Δ*gcnE* mutant strain complemented the defects in growth and development of the deletion strain, as the phenotype of $\Delta gcnE^{C}$ was not distinguishable from that of the wild-type strain (Fig. 1m).

An improved Y2H screening approach for *A. fumigatus*

The Y2H system represents a powerful tool to tag new protein interactions, but to our knowledge there are no examples of a successful screen in *A. fumigatus*. We found that the quality of the cDNA libraries as well as the diverse codon usage of *A. fumigatus* and *S. cerevisiae* were two major technical drawbacks. In our hands, the standard protocol from Takara generated *A. fumigatus* cDNA libraries with an insert size ranging from 20 to 600 bp with an average size of 400 bp. Despite conducting several Y2H screenings we failed to identify distinct positive clones using GcnE as bait, which might have been due to the relatively small sizes of the inserts of the libraries. Therefore, we generated a library with larger cDNA fragments isolated directly from an agarose gel. As a result, we obtained a library with approximately 700,000 independent yeast colonies. PCR analyses of randomly selected colonies revealed the average insert size to be increased by more than a factor of two, yielding average cDNA fragments of approximately 1000 bp (Fig. 2a). Although this advanced library contained larger fragments and thus represented a higher content of protein-coding genes, novel protein/protein interactions were not identified in any screening experiments using the commercial Y2HGold strain. The use of the tRNA-adapted *S. cerevisiae* strain *MNY3* (Nossmann et al. 2017) overcame this problem and increased the efficiency of Y2H screens (Fig. 2b). This advanced method was successfully exploited for the identification of interaction partners of GcnE.

Identification of protein interactions with GcnE as a bait

Several Y2H screenings using the entire GcnE sequence from *A. fumigatus* as bait were performed identifying putative interaction partners. All prey proteins were analyzed for potential autoactivation to distinguish protein/protein interactions from false-positives. Confirmation by retransformation of prey and bait revealed two proteins potentially interacting with GcnE (Fig. 3). In contrast to the negative control, diploid yeast cells were able to grow on selection media resulting from bait/prey interactions (Fig. 3a, b). In addition, in vivo protein interaction leads to an activation of the enzyme reporter gene *Mel1* which converts the chromogenic substrate X-α-gal. One interaction partner comprised the N-terminal amino acids 1–264 of a hypothetical protein encoded by Afu8g00780 (Fig. 3c). According to the *Fungal and Oomycete Genomics Resource* (FungiDB) database this encodes an uncharacterized ORF (Stajich et al. 2012). A comparison of the amino acid sequence with other *Aspergillus* species using Emboss Needle pairwise alignment tool from EMBL-EBI (Rice et al. 2000) results in a similarity of 64.6% and 63.8% to ORFs of *Aspergillus oryzae* [AO090010000059] and *Aspergillus niger* [An03g01570], respectively. An identification of conserved domains shows three type VII secretion AAA-ATPase EccA domains (Marchler-Bauer et al. 2017) from amino acid 75 to 265, 355 to 587, and 662 to 837 (Fig. S2). Due to its interaction with GcnE, we coined this protein GcnE-binding protein A (GbpA). The second prey protein represented the putative

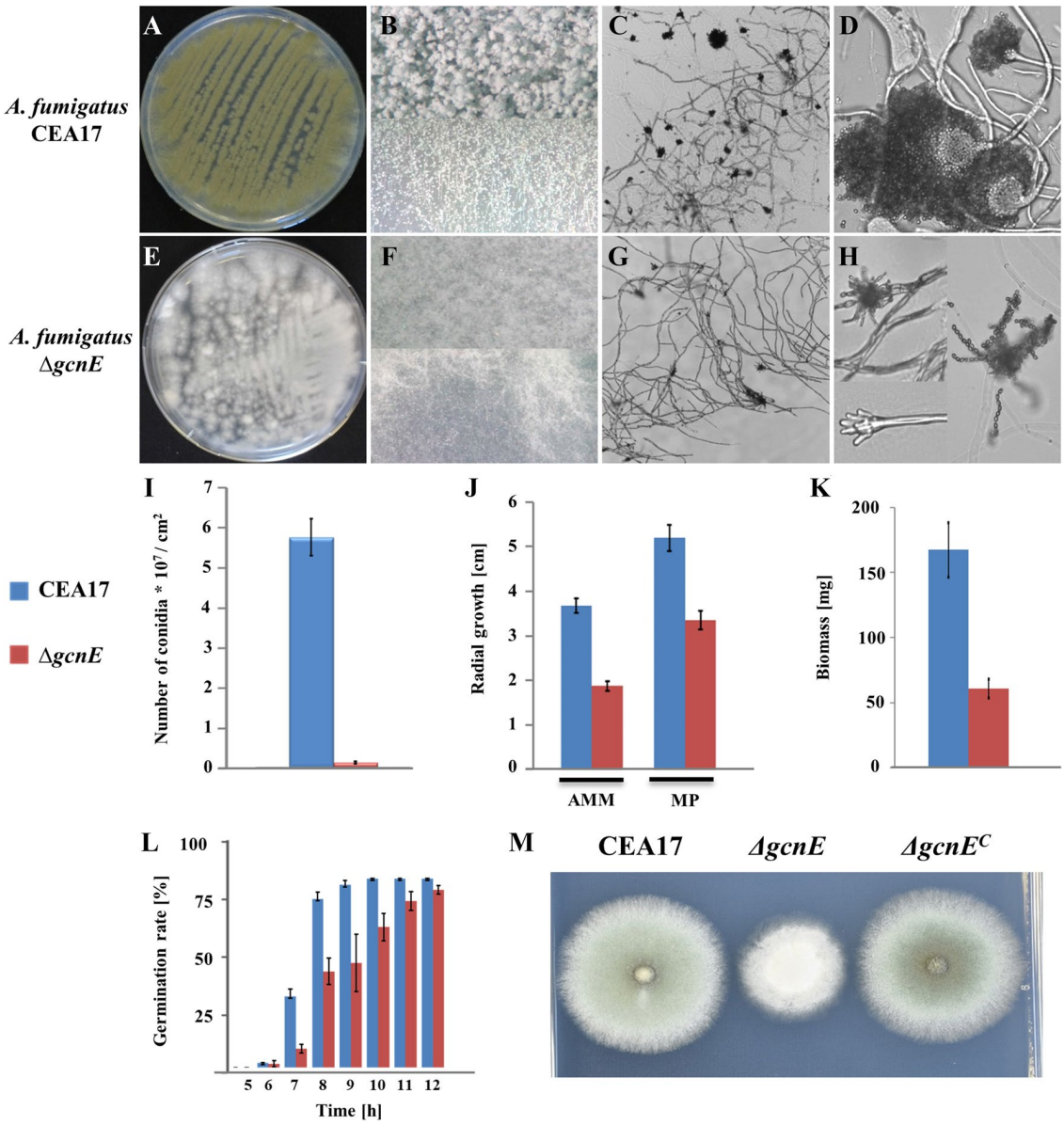

Fig. 1 GcnE contributes to development and hyphal growth in *A. fumigatus*. *A. fumigatus* wild-type (CEA17, **a**–**d**) and knockout strain ΔgcnE (**e**–**h**) were grown on AMM-agar plates (**a**+**e**). Microscopic images display mycelia with conidia-including area (**b**+**f**, top), the border of colonies (**b**+**f**, bottom) and conidiophores (**c**+**g**, 100 × magnification and **d**+**h**, ×400). Both strains differed in the total number of conidia after 96 h (**i**), the radial growth of colonies after 72 h (**j**), biomass formation after 72 h (**k**), and the germination rate (**l**). Transformation of the *gcnE*-deletion strain with a functional copy of *gcnE* restored the defects in growth and development of the *gcnE*-mutant strain (**m**)

glutamine synthetase GlnA (Afu4g13120) which was identified twice in two independent screening experiments. Sequencing of the prey-plasmid revealed that the two clones expressed the C-terminal amino acids 188–358 of GlnA and 197–358, respectively, both being part of the catalytic domain (Fig. 3b, d).

GcnE interacts with GlnA and GbpA in vivo

To verify the results from the Y2H screens, we investigated whether GcnE interacts with either GlnA or GbpA in *A. fumigatus* in vivo using BiFC (Fig. 4). The full-length gene sequences encoding the proteins were fused to either

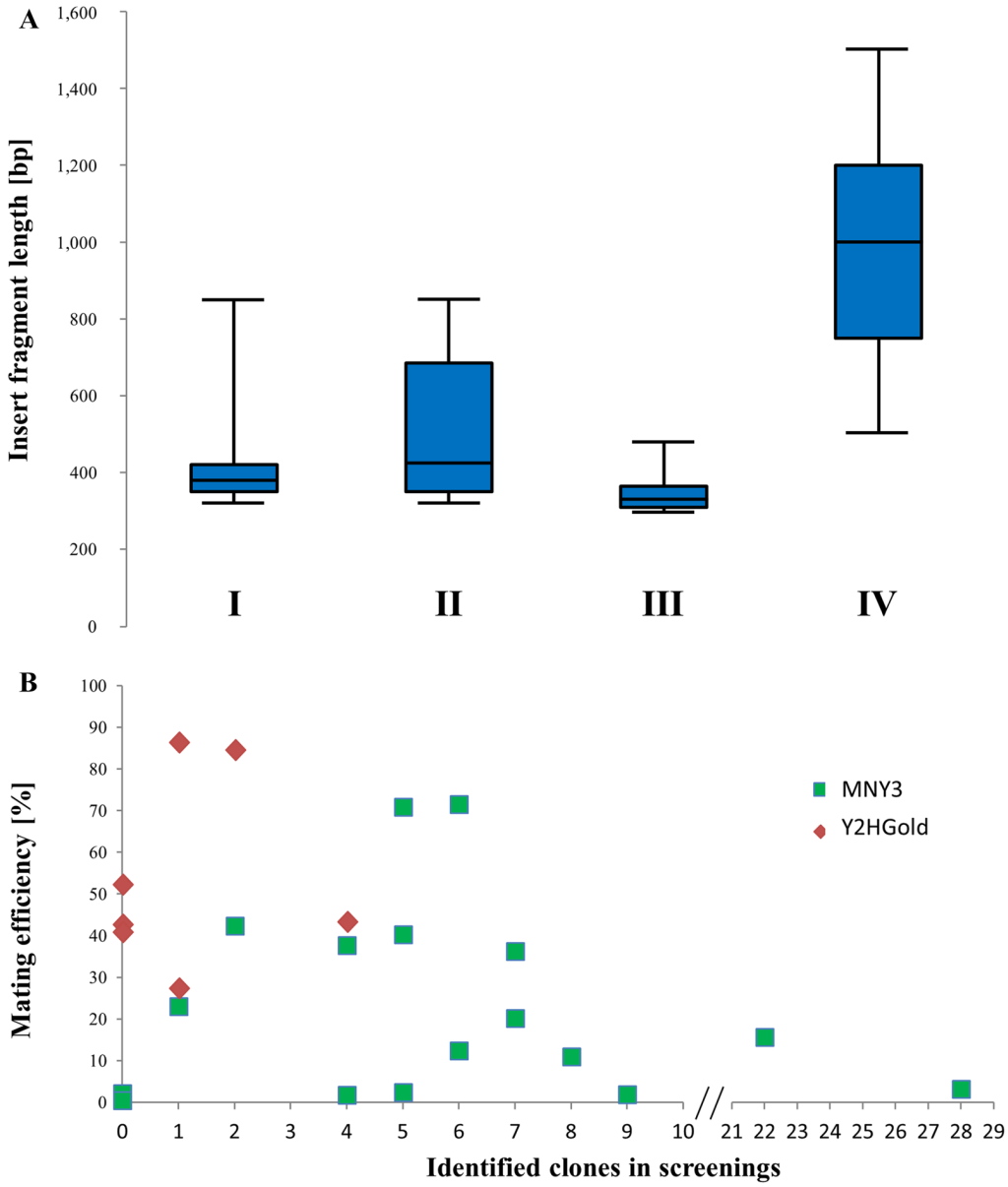

Fig. 2 Y2H screening method adapted to *A. fumigatus*. **a** The Box-and-Whisker-plot displays the average insert length of cDNA libraries generated either by the original protocol Make Your Own Mate & Plate™ library from Takara Bio Company (I–III) or after enrichment for longer RNA fragments (IV). Boxes indicate the first and third quartiles whereas the median is represented by a black line within the box. The bottom whisker in IV indicates that the DNA fragments of all 24 samples were greater than 500 bp (IV). **b** The efficiency for individual screens is displayed as function of mating efficiency and the number of identified clones. Screens using the standard Y2H strain of *S. cerevisiae* Y187 or the codon-optimized yeast strains (Nossmann et al. 2017) are indicated by red diamonds and green squares, respectively

the N- or C-terminus of a split-YFP gene. Both constructs were integrated into the *A. fumigatus* genome. Expression of the fusion proteins was driven by the constitutive *gpdA* promoter. GlnA fused to the entire YFP showed a very strong fluorescence signal and exposure time was reduced by a factor of ten compared to all other samples. GlnA was distributed throughout the mycelium, but was enhanced in spotty structures within hyphae (Fig. 4a). In contrast, hyphae expressing GcnE fused to the entire YFP displayed an evenly distributed fluorescence throughout the cytoplasm, albeit at lower signal intensity than the GlnA positive control (Fig. 4b). The strain containing both GcnE and GlnA with the YFP-C and -N terminal part of the Venus, respectively, showed a fluorescent signal comparable to the GcnE control. When fused to the entire YFP protein,

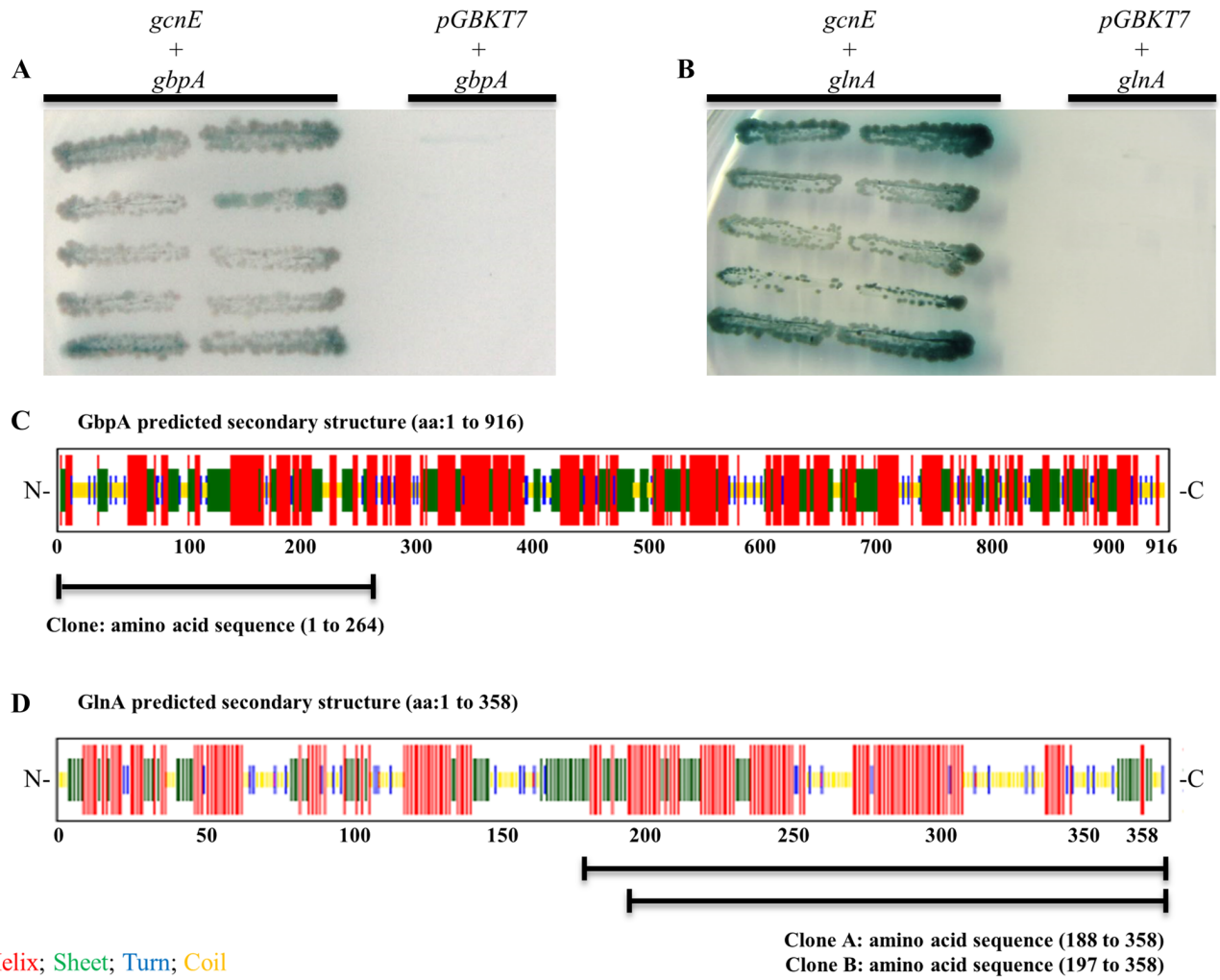

Fig. 3 Prey proteins interacting with GcnE identified by Y2H screens. **a, b** Growth of yeast cells expressing either GcnE or containing the empty plasmid control (pGBKT7) as baits and GbpA (**a**) or GlnA (**b**) as prey proteins. Growth on SD-QDO agar plates lacking adenine, histidine, leucine, and tryptophan occurred only upon protein interactions complementing the respective auxotrophies. **c, d** Schematic display of the secondary structures (Ashok Kumar 2013) and the fished amino terminal fragments of GbpA (**c**) and the carboxy terminal fragment of GlnA (**d**). Clone A and B indicate that the two protein fragments for GlnA were identified in two independent screens

GbpA was evenly distributed throughout the cytoplasm with a slightly stronger signal accumulating in the nuclei (Fig. S3). Again, a regularly distributed fluorescence signal was observed in the BiFC strain containing GcnE-YFP (C) and GbpA-YFP (N). Thus, the BiFC experiments confirmed the interaction of GcnE with GlnA (Fig. 4a) and GbpA (Fig. 4b), as YFP-specific fluorescence was only observed in strains expressing both interaction partners as complementary YFP-fusions. As expected, no BiFC signal occurred when either the N- or C-terminal fusions alone or a combination of GcnE and the highly expressed protein Asp f3 which served as a negative control were analyzed (Bowyer and Denning 2007; Hillmann et al. 2016).

Deletion and overexpression of *glnA* and *gbpA* genes suggest functional crosslinks to development and sporulation

Since it is known from previous studies in other organisms that the absence of GcnE resulted in developmental and sporulation defects, we analyzed whether deletion and overexpression strains for both prey proteins would also display such phenotypes. As the genome of *A. fumigatus* also comprises a second gene encoding a putative glutamine synthetase [Afu6g03530], with an amino acid sequence similarity to GlnA of 21.5% (Fig. S4), it was questionable whether deleting *glnA* (Afu4g13120) would lead to glutamine auxotrophy. This was indeed observed for the corresponding

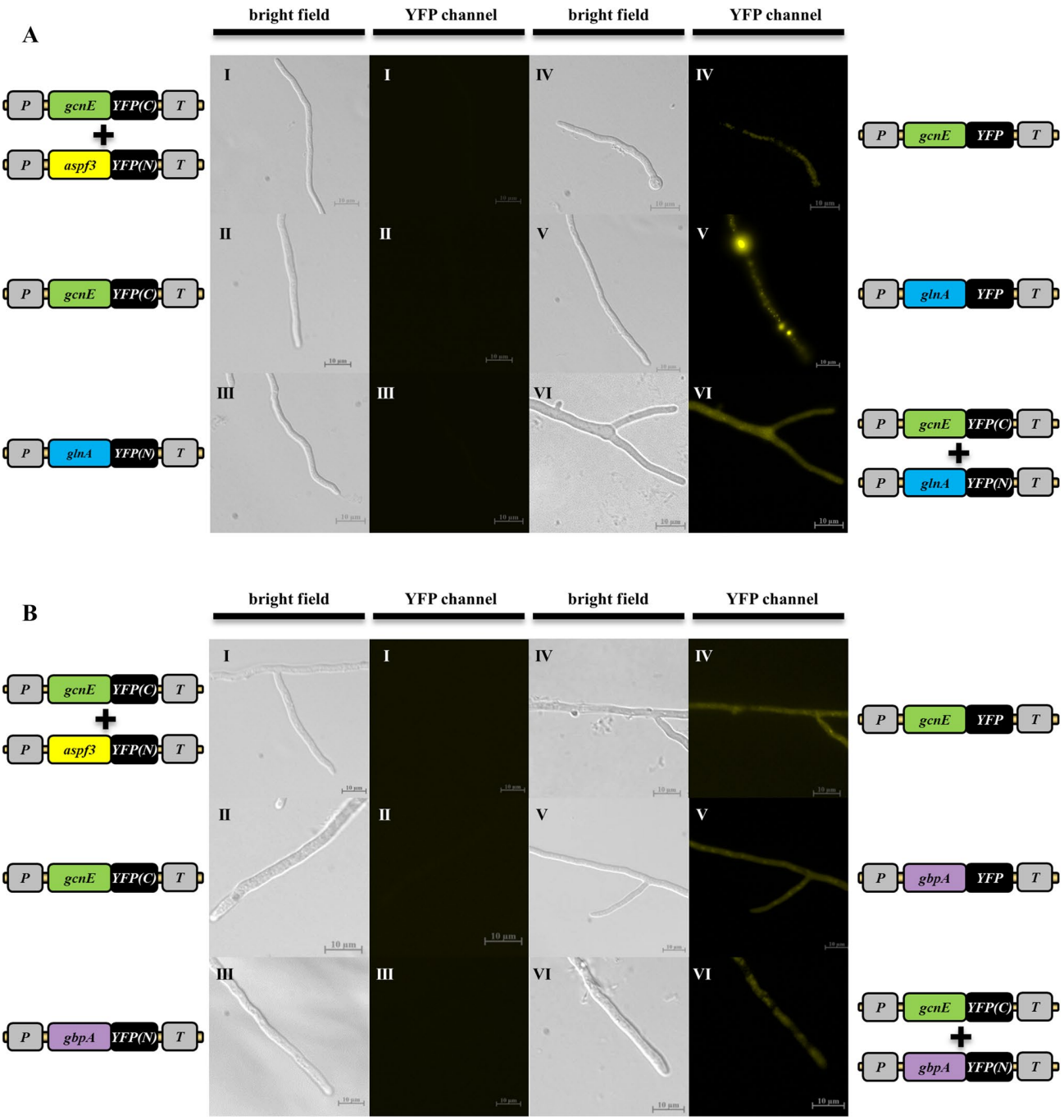

Fig. 4 Bimolecular fluorescence complementation assay to confirm bait/prey interactions in vivo. Images from bright field and YFP channels of *A. fumigatus* strains overexpressing a split-YFP fusions of **a** GcnE (green) and GlnA (blue) and **b** GcnE (green) and GbpA (purple). (I) Strains expressing C-terminal fragment of YFP fused to GcnE and the N-terminal fragment of YFP fused to an abundant, but not interacting protein (Aspf3, yellow); (II + III) N- or C-terminal fragments of YFP alone are negative for YFP fluorescence; (IV + V) Fusions of GcnE and GlnA or GbpA to the full-length YFP display fluorescence; (VI) Strains expressing both proteins containing N- or C-terminal fragments of YFP

deletion mutant, that did not grow on AMM or malt-peptone agar without supplements of glutamine (Fig. 5). This finding demonstrates that *glnA* encodes the only functional glutamine synthetase in *A. fumigatus* under the applied conditions. In comparison to the wild type, the absence of GlnA resulted in a sporulation defect as the total number of conidia in Δ*glnA* mutant strain was reduced to 44% (Fig. 6). When compared to the wild-type strain on different media,

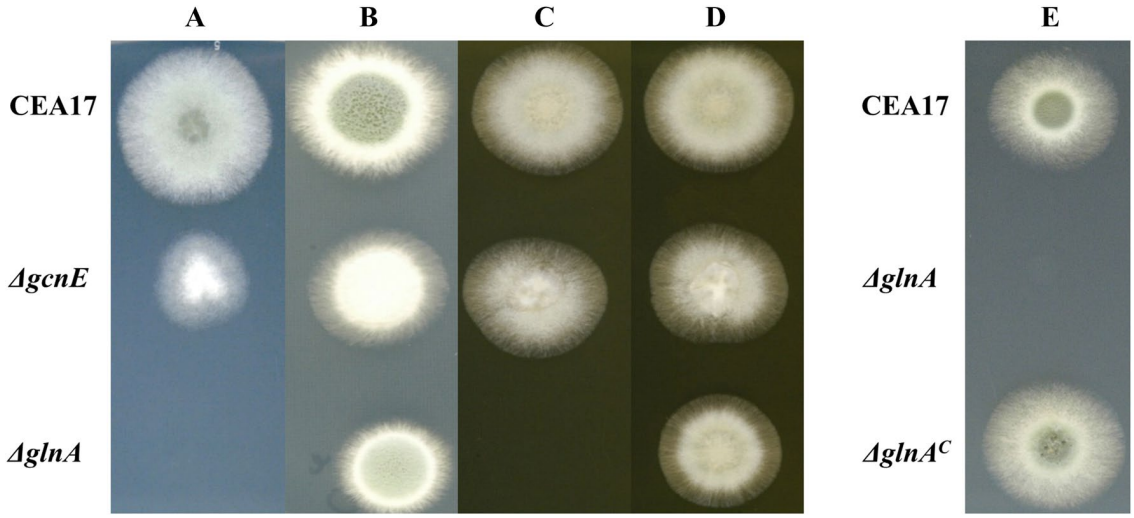

Fig. 5 *A. fumigatus* Δ*glnA* requires glutamine supplementation. Conidia of the wild-type strain CEA17, Δ*gcnE* and Δ*glnA* were grown on AMM-agar (**a, b**) or on malt-peptone agar (**c, d**) at 37 °C for 48 h and 72 h, respectively. Supplementation with 20 mM glutamine complemented the auxotrophy on both media (**b, d**). Complementation with a functional copy of *glnA* in the deletion strain (Δ*glnA*^{C}) restored growth of the strains on AMM-agar in the absence of glutamine (**e**)

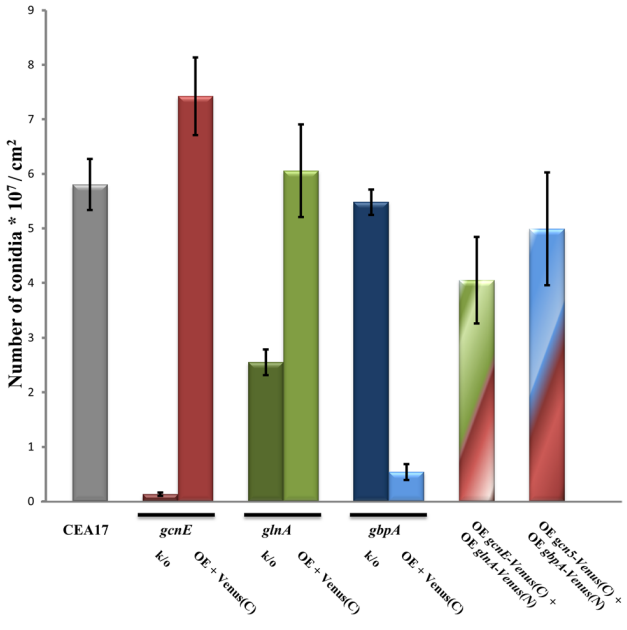

Fig. 6 GlnA and GbpA are required for conidiation in *A. fumigatus*. Equal numbers of conidia for all fungal strains were streaked on AMM-agar plates and incubated for 96 h at 37 °C. Total numbers of conidia were normalized to the surface area. The wild-type strain CEA17 and strains carrying gene deletions or overproduction constructs for GcnE (red), GlnA (green) or GbpA (blue) are represented by different colors. Columns represent the mean of three replicates and errors bars indicate standard deviations. *k/o* knockout, *OE* overexpression

the deletion of the second interaction partner, GbpA, showed no different phenotype (Fig. 5). However, in contrast to GlnA and GcnE whose presence was essential for normal conidiation, overexpression of *gbpA* caused a significant defect in development with a markedly reduced number of generated conidia (Fig. 6). Conidia formation as a result of GbpA overexpression was decreased to approximately 9 and 16% relative to the wild type and hence, comparable to mycelia lacking GcnE (Fig. 1I).

GcnE silences glutamine synthetase activity independent of its acetylation activity

The interaction of GlnA and GcnE found *via* Y2H prompted us to analyze whether the enzymatic activity of GlnA was directly affected by binding of GcnE. Therefore, we measured glutamine synthetase activity using protein extracts of the wild type and Δ*gcnE*. Protein extracts of the wild-type strain showed an activity for glutamine synthetase of approximately 343 U mg^{-1} of protein in the stationary growth phase. In contrast, in the absence of GcnE the enzymatic activity increased to 538 U mg^{-1}, representing a 1.57-fold increase in glutamine synthetase activity (Fig. 7b). To analyze whether the reduction in enzymatic activity resulted from a GcnE-dependent acetylation of GlnA, we analyzed the acetylation patterns of GlnA in mycelia of the wild type *vs.* Δ*gcnE*. Following the Strep-Tag-mediated enrichment of GlnA and digestion with trypsin, LC–MS analysis allowed for the elucidation of post-translational modifications. GlnA from both strains showed no differences in the acetylation pattern at a total coverage of 49–65%. With higher amounts

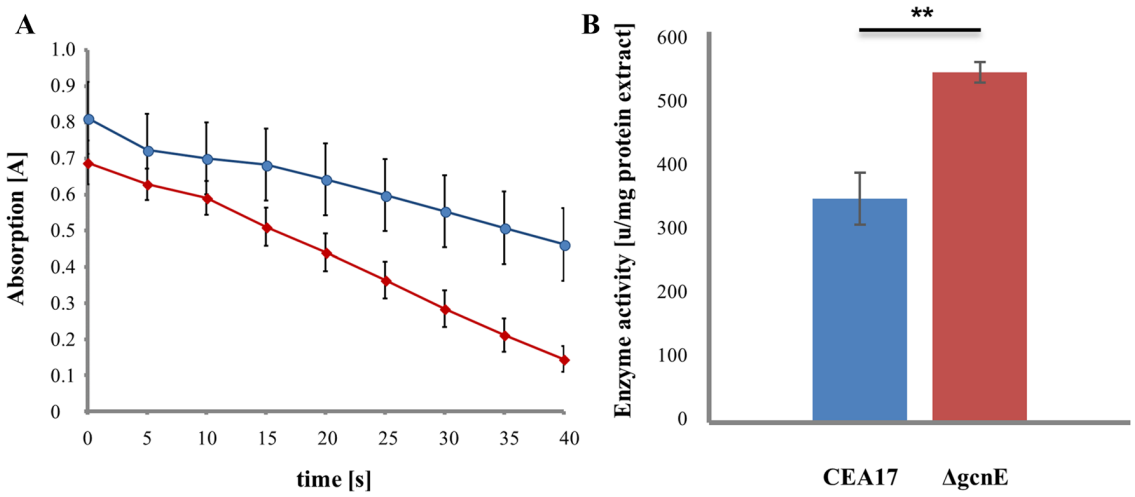

Fig. 7 GcnE-dependent silencing of GlnA. Kinetics of conversion of glutamate to glutamine determined indirectly through NADH oxidation coupled via pyruvate kinase and lactate dehydrogenase. Reactions were started by the addition of 250 µg of protein extracts from *A. fumigatus* as source of GlnA. The linear decrease of NADH (**a**) and total enzymatic activity (**b**) in protein extracts from the wild-type strain CEA17 and *ΔgcnE* are shown in blue and red, respectively. Data represent the mean of three biological replicates and error bars indicate the standard deviation. Two asterisks show significance in a Student's *t* test with $p \leq 0.01$

of Strep-tagged GlnA from the wild type and a coverage of 97%, we detected an acetylation at K15 in the N-terminal region of the glutamine synthetase. However, this acetylation occurred inconsistently in the wild-type strain with an abundance of less than 2% making an active acetylation unlikely. These results indicate that silencing of GlnA is mediated rather by binding of GcnE than by its acetylation activity.

Discussion

The histone acetyltransferase GcnE of *A. fumigatus* is a key factor for the modification of the chromatin architecture and thus plays an important role in transcription regulation (Nützmann et al. 2013). Therefore, the analysis of chromatin remodeling allows for a better understanding of how fungi control their life cycle and also secondary metabolite production in their natural environments as well as during pathogenesis. To further elucidate the cellular function of GcnE, which is known to be a central histone acetyltransferase in other organisms like *S. cerevisiae* or *A. nidulans* (Samara and Wolberger 2011; Nützmann et al. 2011; Canovas et al. 2014), a Y2H screening was performed using a cDNA library of *A. fumigatus*. Modification of the Takara protocol for library construction resulted in an average insert size of 950 bp. A high quality of such libraries is a prerequisite for a successful discovery of prey proteins as longer sequences increase the probability to express functional peptides. The sequence of *gcnE* was codon-optimized for expression in *S. cerevisiae*. The expression of the prey proteins encoded by the cDNA library was ensured by the *S. cerevisiae* strain MNY3 in which the arginine tRNA level was adapted to the codon usage of *A. fumigatus*. The strain displays enhanced transcription of the tRNA molecules $tRNA^{Arg}_{CCG}$, $tRNA^{Arg}_{GCG}$, and $tRNA^{Arg}_{UCG}$ in MNY3 leading to a significant improvement of protein production as demonstrated by Y2H (Nossmann et al. 2017). Heterologous protein production was also previously optimized for bacterial expression systems like *E. coli*, by plasmid-encoded tRNA molecules for rare codons transcribed from plasmids [e.g., Rosetta strains from Novagen (Novy et al. 2001) or BL21-CodonPlus strains from Stratagene].

Here, we have chosen a mating-based system since it enables the analysis of a higher number of cells in each screening (Lopez and Mukhtar 2017). In contrast to the classical Y2H approach (Fields and Song 1989) which only uses the *lacZ* gene as a reporter, four different reporter genes (*HIS3; ADE2; MEL1; AUR1-C*) under the control of three Gal4-dependent promoters were applied. This allows the premature exclusion of false-positive prey sequences, which may bind to one of the promoters (Serebriiskii et al. 2000). Such proteins are usually transcription factors or misfolded peptides encoded by the *A. fumigatus* library. To further enhance the probability of identifying unambiguous interactions, stringent media were used which lack the amino acid histidine and the nucleic acid adenine. A growth-dependent selection enables the most effective identification of interaction partners. Therefore, only bait–prey interactions lead to the expression of the *HIS3* and *ADE2* reporter genes and thus complementation of the respective auxotrophies. To avoid an interference of yeast cells carrying more than one

prey plasmid, a validation of GcnE/GlnA and GcnE/GbpA was achieved by transformation of prey plasmids alone into yeast strain Y187, which was subsequently mated with the bait-containing strain MNY3. For a final validation, a haploid strain carrying the *lacZ* reporter was co-transformed with the respective bait and prey plasmids. This reconfirmation clearly excluded false-positive interactions because of the use of a further promoter/reporter construct in an independent yeast strain. With our optimized screening system we identified two new interaction partners of GcnE, i.e., GbpA (Afu8g00780) and the glutamine synthetase GlnA (Afu4g13120).

For the validation of interactions *in vivo* we applied the BiFC method, which was successfully used in other filamentous fungi like *Acremonium chrysogenum, Neurospora crassa* and *A. nidulans* (Thön et al. 2010; Hoff and Kück 2005; Kollath-Leiss et al. 2014). Also, for *A. fumigatus*, BiFC proved to be a valuable tool (Magnani Dinamarco et al. 2012; Jöhnk et al. 2016). For the BiFC experiments shown here, we used the entire sequences of bait and prey proteins (Fig. 3a, b). As expected, the cytoplasmic protein GlnA containing the entire YFP showed high signal intensity after overexpression using a constitutive *gpdA* promoter but appeared in spotty patches along the hyphae. This could be a hint that the glutamine synthetase is not soluble due to its overproduction since this protein is generally located in the cytoplasm in other eukaryotes (Tate et al. 2018). However, this signal was much stronger than the signal of the bait protein GcnE in the cytoplasm despite using the same promoter. This finding could be due to the fact that GcnE acts as part of the SAGA protein complex and thus, other proteins of the complex might quench the YFP signal.

The function of glutamine synthetase in nitrogen metabolite repression was studied in *N. crassa* by Dunn-Coleman and Garrett (1980). The glutamine synthetase catalyzes the ATP-dependent condensation of glutamate and ammonia to generate glutamine. As also shown here, its loss leads to glutamine auxotrophy (Fig. 5a). The same effect was found for *F. fujikuroi*, where the deletion of *glnA* not only led to auxotrophy but also suggested the involvement of glutamine synthetase in nitrogen metabolite repression (Teichert et al. 2004; Wagner et al. 2013).

The absence of GcnE also led to a drastic decrease in hyphal growth and a nearly complete absence of conidia with a reduction of 97%. Along this line, the absence of the glutamine synthetase GlnA also led to a decrease in the number of conidia by 46% on glutamine-containing agar. Furthermore, the absence of this enzyme could lead to an imbalance of the citric acid cycle, since glutamate is produced by the glutamate dehydrogenase by transfer of an amino group to α-ketoglutarate. This disturbance could constitute an additional challenge for the cell. The loss of the *glnA* (Afu4g13120) gene led to a glutamine auxotrophy for the fungus and demonstrated that the second putative glutamine synthase Afu6g03530 is apparently not responsible for the conversion of glutamate to glutamine. The deletion of the gene *gbpA* displayed no different phenotype compared to the wild-type strain (data not shown). Interestingly, the overexpression of *gbpA* led to reduced conidia formation reaching values comparable to the knockout of *gcnE*. Investigating the acetylation pattern of GbpA revealed no acetylated lysine residues in the wild-type strain (data not shown). Therefore, formally, GbpA acts as repressor by binding to GcnE. Consistently, this effect was overcome by overexpressing both proteins (Fig. 6).

The application of BiFC can not only prove the in vivo interaction of two proteins but might already give a hint on the native compartment in which this interaction takes place. In the case of GcnE and GlnA we assume that their interaction occurs in the cytoplasm where the glutamine synthetase is generally located (Tate et al. 2018). A prerequisite is the accurate translation of the overproduced protein. For other organisms it was shown that orthologous GcnE/Gcn5-like proteins are located in different cellular compartments. While a constitutive nuclear localization was shown for *Cryptococcus neoformans* and *F. fujikuroi*, in *Candida albicans* its localization changed depending on the developmental status of the fungus (Chang et al. 2015; O'Meara et al. 2010; Rösler et al. 2016). In the stationary phase, Gcn5 accumulated in the nucleus but was distributed throughout the cytoplasm during hyphal growth. In *S. cerevisiae* Gcn5 was also shown to translocate back to the cytosol during hypoxia (Dastidar et al. 2012).

In addition to its function as histone acetyltransferase as part of the SAGA/Ada complex, GcnE-contains exhibits a further function as a lysine acetyltransferase (KAT) (Georgakopoulos et al. 2013; Samara and Wolberger 2011) which was also detected in human cell lines where the GcnE homolog targets also other proteins than histones (Lerin et al. 2006; Paolinelli et al. 2009). A reversible lysine acetylation is responsible for the repression of the glutamine synthetase in the actinomycete *Saccharopolyspora erythraea* (You et al. 2016) but such a mode of regulation has not been shown for fungi yet. A comparison of the two proteins revealed a common GNAT domain (IPR000182) using *InterProScan 5* (Jones et al. 2014) but an overall low amino acid-identity (< 1%) and similarity (1.5%). Together with our finding that GcnE did not acetylate GlnA in *A. fumigatus*, these results suggest that these proteins are no functional homologues. Beside the modification of histone proteins, it has become evident that acetylation generally triggers activities of key enzymes in many different pathways (Lundby et al. 2012). As described before, KATs are involved in regulation of many metabolic processes, occurring both in the cytoplasm and mitochondria (reviewed in Soufi et al. 2012; Choudhary

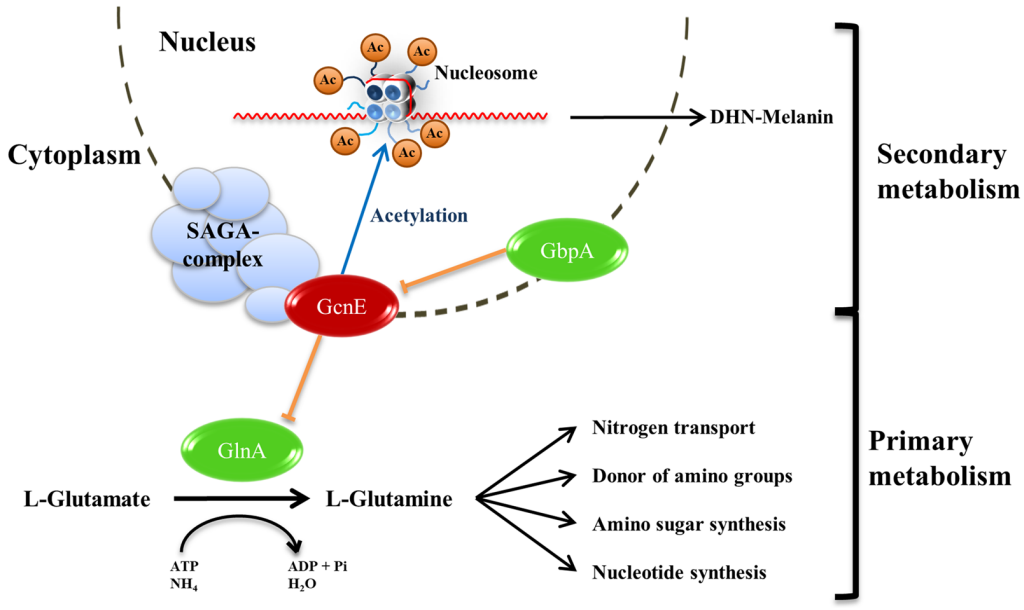

Fig. 8 Model summarizing the activity of GcnE as a mediator between primary and secondary metabolism. The interaction of GcnE with both GlnA and GbpA demonstrates its dual role in histone acetylation and protein regulation in the fungal primary metabolism. Orange arrows mark protein/protein interaction and the resulting inhibition of GlnA activity; the blue arrow indicates acetylation of histones by GcnE. Black arrows mark the physiological processes affected by the identified proteins. *DHN-melanin* 1,8-dihydroxynaphthalene-melanin

et al. 2014). In *Salmonella enterica* lysine acetylation affects the relative activities of key enzymes that control the direction of glycolysis and gluconeogenesis as well as the branching between citrate cycle and glyoxylate bypass (Wang et al. 2010).

Our results showed that in the presence of GcnE, GlnA activity was reduced to 64%. Since it is known that the glutamine synthase activity can be regulated by acetylation of its lysine epsilon amino groups, as shown for an actinomycete (You et al. 2016), it seemed likely that a similar mechanism operates in *A. fumigatus*. However, no differences in the GcnE-dependent acetylation patterns of GlnA were found. By contrast, GcnE binds GlnA at least partially at its C-terminal region where no lysine modification was identified. These data strongly suggest that the mere binding of GcnE is sufficient to inhibit GlnA, indicating a dual role of GcnE beyond to being solely a histone acetyltransferase. Moreover, our findings suggest a role of GcnE as mediator between primary and secondary metabolism (Fig. 8).

Acknowledgements Lisa Reimer is acknowledged for excellent technical assistance. This study was supported by the Ernst-Abbe University of Applied Sciences Jena, by the Leibniz Institute for Natural Product Research and Infection Biology-Hans Knöll Institute Jena and the collaborative research center/transregio 124 FungiNet (Project A1 and Z2) funded by the Deutsche Forschungsgemeinschaft.

References

Altwasser R, Baldin C, Weber J, Guthke R, Kniemeyer O, Brakhage AA, Linde J, Valiante V (2015) Network modeling reveals cross talk of MAP kinases during adaptation to caspofungin stress in *Aspergillus fumigatus*. PLoS One 10(9):e0136932

Ashok Kumar T (2013) CFSSP: Chou and Fasman secondary structure prediction server. Wide Spectr 1(9):15–19

Ballance DJ, Turner G (1985) Development of a high-frequency transforming vector for *Aspergillus nidulans*. Gene 36(3):321–331

Bowyer P, Denning DW (2007) Genomic analysis of allergen genes in *Aspergillus* spp.: the relevance of genomics to everyday research. Med Mycol 45(1):17–26

Bradford MM (1976) A rapid and sensitive method for the quantitation of microgram quantities of protein utilizing the principle of protein-dye binding. Anal Biochem 72:248–254

Brakhage AA, Langfelder K (2002) Menacing mold: the molecular biology of *Aspergillus fumigatus*. Annu Rev Microbiol 56:433–455

Brakhage AA, Van den Brulle J (1995) Use of reporter genes to identify recessive *trans*-acting mutations specifically involved in the regulation of *Aspergillus nidulans* penicillin biosynthesis genes. J Bacteriol 177(10):2781–2788

Breeden L, Nasmyth K (1985) Regulation of the yeast HO gene. Cold Spring Harb Symp Quant Biol 50:643–650

Brown GD, Denning DW, Gow NA, Levitz SM, Netea MG, White TC (2012) Hidden killers: human fungal infections. Sci Transl Med 4(165):165rv113

Canovas D, Marcos AT, Gacek A, Ramos MS, Gutierrez G, Reyes-Dominguez Y, Strauss J (2014) The histone acetyltransferase

GcnE (GCN5) plays a central role in the regulation of *Aspergillus* asexual development. Genetics 197(4):1175–1189
Chang P, Fan X, Chen J (2015) Function and subcellular localization of Gcn5, a histone acetyltransferase in *Candida albicans*. Fungal Genet Biol 81:132–141
Choudhary C, Weinert BT, Nishida Y, Verdin E, Mann M (2014) The growing landscape of lysine acetylation links metabolism and cell signalling. Nat Rev Mol Cell Biol 15(8):536–550
da Silva Ferreira ME, Kress MR, Savoldi M, Goldman MH, Hartl A, Heinekamp T, Brakhage AA, Goldman GH (2006) The akuB(KU80) mutant deficient for nonhomologous end joining is a powerful tool for analyzing pathogenicity in *Aspergillus fumigatus*. Eukaryot Cell 5(1):207–211
Daniel JA, Grant PA (2007) Multi-tasking on chromatin with the SAGA coactivator complexes. Mutat Res 618(1–2):135–148
Dastidar RG, Hooda J, Shah A, Cao TM, Henke RM, Zhang L (2012) The nuclear localization of SWI/SNF proteins is subjected to oxygen regulation. Cell Biosci 2(1):30
Dunn-Coleman NS, Garrett RH (1980) The role fo glutamine synthetase and glutamine metabolism in nitrogen metabolite repression, a regulatory phenomenon in the lower eukaryote *Neurospora crassa*. Mol Gen Genet 179(1):25–32
Dyda F, Klein DC, Hickman AB (2000) GCN5-related *N*-acetyltransferases: a structural overview. Annu Rev Biophys Biomol Struct 29:81–103
Fedorova ND, Khaldi N, Joardar VS, Maiti R, Amedeo P, Anderson MJ, Crabtree J, Silva JC, Badger JH, Albarraq A, Angiuoli S, Bussey H, Bowyer P, Cotty PJ, Dyer PS, Egan A, Galens K, Fraser-Liggett CM, Haas BJ, Inman JM, Kent R, Lemieux S, Malavazi I, Orvis J, Roemer T, Ronning CM, Sundaram JP, Sutton G, Turner G, Venter JC, White OR, Whitty BR, Youngman P, Wolfe KH, Goldman GH, Wortman JR, Jiang B, Denning DW, Nierman WC (2008) Genomic islands in the pathogenic filamentous fungus *Aspergillus fumigatus*. PLoS Genet 4(4):e1000046
Fields S, Song O (1989) A novel genetic system to detect protein–protein interactions. Nature 340(6230):245–246
Georgakopoulos P, Lockington RA, Kelly JM (2013) The Spt-Ada-Gcn5 acetyltransferase (SAGA) complex in *Aspergillus nidulans*. PLoS One 8(6):e65221
Gola S, Munder T, Casonato S, Manganelli R, Vicente M (2015) The essential role of SepF in mycobacterial division. Mol Microbiol 97(3):560–576
Gsaller F, Hortschansky P, Beattie SR, Klammer V, Tuppatsch K, Lechner BE, Rietzschel N, Werner ER, Vogan AA, Chung D, Muhlenhoff U, Kato M, Cramer RA, Brakhage AA, Haas H (2014) The Janus transcription factor HapX controls fungal adaptation to both iron starvation and iron excess. EMBO J 33(19):2261–2276
Hassan AH, Prochasson P, Neely KE, Galasinski SC, Chandy M, Carrozza MJ, Workman JL (2002) Function and selectivity of bromodomains in anchoring chromatin-modifying complexes to promoter nucleosomes. Cell 111(3):369–379
Hillmann F, Bagramyan K, Strassburger M, Heinekamp T, Hong TB, Bzymek KP, Williams JC, Brakhage AA, Kalkum M (2016) The crystal structure of peroxiredoxin Asp f3 provides mechanistic insight into oxidative stress resistance and virulence of *Aspergillus fumigatus*. Sci Rep 6:33396
Hoff B, Kück U (2005) Use of bimolecular fluorescence complementation to demonstrate transcription factor interaction in nuclei of living cells from the filamentous fungus *Acremonium chrysogenum*. Curr Genet 47(2):132–138
Jöhnk B, Bayram O, Abelmann A, Heinekamp T, Mattern DJ, Brakhage AA, Jacobsen ID, Valerius O, Braus GH (2016) SCF ubiquitin ligase F-box protein Fbx15 controls nuclear co-repressor localization, stress response and virulence of the human pathogen *Aspergillus fumigatus*. PLoS Pathog 12(9):e1005899
Jones P, Binns D, Chang HY, Fraser M, Li W, McAnulla C, McWilliam H, Maslen J, Mitchell A, Nuka G, Pesseat S, Quinn AF, Sangrador-Vegas A, Scheremetjew M, Yong SY, Lopez R, Hunter S (2014) *InterProScan 5*: genome-scale protein function classification. Bioinformatics 30(9):1236–1240
Kollath-Leiss K, Bonniger C, Sardar P, Kempken F (2014) BEM46 shows eisosomal localization and association with tryptophan-derived auxin pathway in *Neurospora crassa*. Eukaryot Cell 13(8):1051–1063
Kornberg A, Pricer WE Jr (1951) Enzymatic phosphorylation of adenosine and 2,6-diaminopurine riboside. J Biol Chem 193(2):481–495
Langfelder K, Jahn B, Gehringer H, Schmidt A, Wanner G, Brakhage AA (1998) Identification of a polyketide synthase gene (pksP) of *Aspergillus fumigatus* involved in conidial pigment biosynthesis and virulence. Med Microbiol Immunol 187(2):79–89
Latge JP (1999) *Aspergillus fumigatus* and aspergillosis. Clin Microbiol Rev 12(2):310–350
Lerin C, Rodgers JT, Kalume DE, Kim SH, Pandey A, Puigserver P (2006) GCN5 acetyltransferase complex controls glucose metabolism through transcriptional repression of PGC-1alpha. Cell Metab 3(6):429–438
Linde J, Wilson D, Hube B, Guthke R (2010) Regulatory network modelling of iron acquisition by a fungal pathogen in contact with epithelial cells. BMC Syst Biol 4:148
Lopez J, Mukhtar MS (2017) Mapping protein–protein interaction using high-throughput yeast 2-hybrid. Methods Mol Biol 1610:217–230
Lundby A, Lage K, Weinert BT, Bekker-Jensen DB, Secher A, Skovgaard T, Kelstrup CD, Dmytriyev A, Choudhary C, Lundby C, Olsen JV (2012) Proteomic analysis of lysine acetylation sites in rat tissues reveals organ specificity and subcellular patterns. Cell Rep 2(2):419–431
Magnani Dinamarco T, Brown NA, Couto de Almeida RS, Alves de Castro P, Savoldi M, de Souza Goldman MH, Goldman GH (2012) *Aspergillus fumigatus* calcineurin interacts with a nucleoside diphosphate kinase. Microb Infect 14(11):922–929
Marchler-Bauer A, Bo Y, Han L, He J, Lanczycki CJ, Lu S, Chitsaz F, Derbyshire MK, Geer RC, Gonzales NR, Gwadz M, Hurwitz DI, Lu F, Marchler GH, Song JS, Thanki N, Wang Z, Yamashita RA, Zhang D, Zheng C, Geer LY, Bryant SH (2017) CDD/SPARCLE: functional classification of proteins via subfamily domain architectures. Nucleic Acids Res 45(D1):D200–D203
Munder T, Hinnen A (1999) Yeast cells as tools for target-oriented screening. Appl Microbiol Biotechnol 52(3):311–320
Nossmann M, Pieper J, Hillmann F, Brakhage AA, Munder T (2017) Generation of an arginine-tRNA-adapted *Saccharomyces cerevisiae* strain for effective heterologous protein expression. Curr Genet 64(3):589–598
Novy R, Drott D, Yaeger K, Mierendorf R (2001) Overcoming the codon bias of *E. coli* for enhanced protein expression. Innovations 12:1–3
Nützmann HW, Fischer J, Scherlach K, Hertweck C, Brakhage AA (2013) Distinct amino acids of histone H3 control secondary metabolism in Aspergillus nidulans. Appl Environ Microbiol 79(19):6102–6109. https://doi.org/10.1128/AEM.01578-13
Nützmann HW, Reyes-Dominguez Y, Scherlach K, Schroeckh V, Horn F, Gacek A, Schumann J, Hertweck C, Strauss J, Brakhage AA (2011) Bacteria-induced natural product formation in the fungus *Aspergillus nidulans* requires Saga/Ada-mediated histone acetylation. Proc Natl Acad Sci USA 108(34):14282–14287
O'Meara TR, Hay C, Price MS, Giles S, Alspaugh JA (2010) *Cryptococcus neoformans* histone acetyltransferase Gcn5 regulates fungal adaptation to the host. Eukaryot Cell 9(8):1193–1202
Paolinelli R, Mendoza-Maldonado R, Cereseto A, Giacca M (2009) Acetylation by GCN5 regulates CDC6 phosphorylation in the S phase of the cell cycle. Nat Struct Mol Biol 16(4):412–420

Pray-Grant MG, Schieltz D, McMahon SJ, Wood JM, Kennedy EL, Cook RG, Workman JL, Yates JR III, Grant PA (2002) The novel SLIK histone acetyltransferase complex functions in the yeast retrograde response pathway. Mol Cell Biol 22(24):8774–8786

Quan J, Tian J (2009) Circular polymerase extension cloning of complex gene libraries and pathways. PLoS One 4(7):e6441

Rice P, Longden I, Bleasby A (2000) EMBOSS: the European molecular biology open software suite. Trends Genet TIG 16(6):276–277

Rösler SM, Kramer K, Finkemeier I, Humpf HU, Tudzynski B (2016) The SAGA complex in the rice pathogen *Fusarium fujikuroi*: structure and functional characterization. Mol Microbiol 102(6):951–974

Salah Ud-Din AI, Tikhomirova A, Roujeinikova A (2016) Structure and functional diversity of GCN5-related *N*-acetyltransferases (GNAT). Int J Mol Sci 17(7):1018

Samara NL, Wolberger C (2011) A new chapter in the transcription SAGA. Curr Opin Struct Biol 21(6):767–774

Sarikaya Bayram Ö, Latgé JP, Bayram Ö (2018) MybA, a new player driving survival of the conidium of the human pathogen Aspergillus fumigatus. Curr Genet 64(1):141–146. https://doi.org/10.1007/s00294-017-0740-5

Sellam A, Askew C, Epp E, Lavoie H, Whiteway M, Nantel A (2009) Genome-wide mapping of the coactivator Ada2p yields insight into the functional roles of SAGA/ADA complex in *Candida albicans*. Mol Biol Cell 20(9):2389–2400

Serebriiskii I, Estojak J, Berman M, Golemis EA (2000) Approaches to detecting false positives in yeast two-hybrid systems. Biotechniques 28(2):328–330, 332–326

Soufi B, Soares NC, Ravikumar V, Macek B (2012) Proteomics reveals evidence of cross-talk between protein modifications in bacteria: focus on acetylation and phosphorylation. Curr Opin Microbiol 15(3):357–363

Stajich JE, Harris T, Brunk BP, Brestelli J, Fischer S, Harb OS, Kissinger JC, Li W, Nayak V, Pinney DF, Stoeckert CJ Jr, Roos DS (2012) FungiDB: an integrated functional genomics database for fungi. Nucleic Acids Res 40(Database issue):D675–D681

Tate JJ, Rai R, Cooper TG (2018) More than one way in: three Gln3 sequences required to telieve negative Ure2 regulation and support nuclear Gln3 import in *Saccharomyces cerevisiae*. Genetics 208(1):207–227

Teichert S, Schonig B, Richter S, Tudzynski B (2004) Deletion of the *Gibberella fujikuroi* glutamine synthetase gene has significant impact on transcriptional control of primary and secondary metabolism. Mol Microbiol 53(6):1661–1675

Thon M, Al Abdallah Q, Hortschansky P, Scharf DH, Eisendle M, Haas H, Brakhage AA (2010) The CCAAT-binding complex coordinates the oxidative stress response in eukaryotes. Nucleic Acids Res 38(4):1098–1113

Vo TV, Das J, Meyer MJ, Cordero NA, Akturk N, Wei X, Fair BJ, Degatano AG, Fragoza R, Liu LG, Matsuyama A, Trickey M, Horibata S, Grimson A, Yamano H, Yoshida M, Roth FP, Pleiss JA, Xia Y, Yu H (2016) A proteome-wide fission yeast interactome reveals network evolution principles from yeasts to human. Cell 164(1–2):310–323

Wagner D, Wiemann P, Huss K, Brandt U, Fleissner A, Tudzynski B (2013) A sensing role of the glutamine synthetase in the nitrogen regulation network in *Fusarium fujikuroi*. PLoS One 8(11):e80740

Wang Q, Zhang Y, Yang C, Xiong H, Lin Y, Yao J, Li H, Xie L, Zhao W, Yao Y, Ning ZB, Zeng R, Xiong Y, Guan KL, Zhao S, Zhao GP (2010) Acetylation of metabolic enzymes coordinates carbon source utilization and metabolic flux. Science 327(5968):1004–1007

Wessel D, Flügge UI (1984) A method for the quantitative recovery of protein in dilute solution in the presence of detergents and lipids. Anal Biochem 138(1):141–143

Wiemann P, Guo CJ, Palmer JM, Sekonyela R, Wang CC, Keller NP (2013) Prototype of an intertwined secondary-metabolite supercluster. Proc Natl Acad Sci USA 110(42):17065–17070

You D, Yin BC, Li ZH, Zhou Y, Yu WB, Zuo P, Ye BC (2016) Sirtuin-dependent reversible lysine acetylation of glutamine synthetases reveals an autofeedback loop in nitrogen metabolism. Proc Natl Acad Sci USA 113(24):6653–6658

Yu H, Braun P, Yildirim MA, Lemmens I, Venkatesan K, Sahalie J, Hirozane-Kishikawa T, Gebreab F, Li N, Simonis N, Hao T, Rual JF, Dricot A, Vazquez A, Murray RR, Simon C, Tardivo L, Tam S, Svrzikapa N, Fan C, de Smet AS, Motyl A, Hudson ME, Park J, Xin X, Cusick ME, Moore T, Boone C, Snyder M, Roth FP, Barabasi AL, Tavernier J, Hill DE, Vidal M (2008) High-quality binary protein interaction map of the yeast interactome network. Science 322(5898):104–110

Supplementary material

Table II: Primers used in this study

Primer	Sequence	Application
Gal4AD Fw	TACCACTACAATGGATG	Sequencing of prey sequences in pGADT7
Gal4AD Rv	GCGGGGTTTTTCAGTATCTACG	Sequencing of prey sequences in pGADT7
GbpA 5‘_Fw	CTCCGTACATTCCGAAGGAATCCGTGG	Generation of Afu8g00780 deletion cassette
GbpA 5‘_Rv	TTGGCCTGAGTGGCCATCGAATTCCTGCAGCTTTGGCCAGAGAAGGCTGCGTGCG	Generation of Afu8g00780 deletion cassette
GbpA 3‘_Fw	TTCTAGAATAATTATGTGTAACAAGAAAGAGGATACCTTTGCTTGGTCTCCCGAT	Generation of Afu8g00780 deletion cassette
GbpA 3‘_rv	CGAAAAATGGGGTTGCTTAAGCTCAG	Generation of Afu8g00780 deletion cassette
Gcn5 5'_Fw	GTGGTGTTGTCATGATTGTCTGCG	Generation of Afu4g12650 deletion cassette
Gcn5 5'_Rv	GCCTGAGTGGCCATCGAATTCCTGCAGGGCTTCTTCAACATCCTGCTCC	Generation of Afu4g12650 deletion cassette
Gcn5 3'_Fw	GGGGCATTCTAGAATAATTATGTGTAACAAGAAAGAGCATGGGGGAGCATTCTAGC	Generation of Afu4g12650 deletion cassette
Gcn5 3'_Rv	GGACATAATGGCGACATAGCGAC	Generation of Afu4g12650 deletion cassette
GlnA 5'_Fw	TGCGCAACGGGAGAAAGGGGGA	Generation of Afu4g13120 deletion cassette
GlnA 5'_Rv	TCCTGTGTGAAATTGTTATCCGCTCAGATTGGCAGAATGTGTGATATGA	Generation of Afu4g13120 deletion cassette
GlnA 3'_Fw	GTCGTGACTGGGAAAACCCTGGCGTATGTCTTCGATATCAAAACAAA	Generation of Afu4g13120 deletion cassette
GlnA 3'_Rv	CAGTGCCCGAGTGCCGGAAGTCA	Generation of Afu4g13120 deletion cassette
ptrA_Fw	CTGCAGGAATTCGATGGCCACT	Generation of Afu8g00780 and Afu4g12650 deletion cassette; amplification of pyrithiamine cassette
ptrA_Rv	TCTTTCTTGTTACACATAATTATTCTAGAATGCCCC	Generation of Afu8g00780 and Afu4g12650 deletion cassette; amplification of pyrithiamine cassette
Hph_Fw	ACGCCAGGGTTTTCCCAGTCACGACG	Generation of Afu4g13120 deletion cassette; amplification of hygromycin B cassette
Hph_Rv	TGAGCGGATAACAATTTCACACAGGA	Generation of Afu4g13120 deletion cassette; amplification of hygromycin B cassette

GcnVc_hph Fw	GAGCTCCACCGCGGTGGCGGCCGCTCTAGAAATGCCGGCACTTACATCAGAGAGTG	Generation of plinkerVenusC-hph-GcnE plasmid
GcnVc_hph Rv	CTCCTCCGCCAGATCCGCCGCCTCCACTAGATCCAAGAGAGACACTTACCGACC	Generation of plinkerVenusC-hph-GcnE plasmid
glnAVn_pyr Fw	GAGCTCCACCGCGGTGGCGGCCGCTCTAGAAATGGTGAGTCCTTCAATACATTCGAAT	Generation of plinkerVenusN-ptrA-GlnA plasmid
glnAVn_pyr Rv	CTCCTCCGCCAGATCCGCCGCCTCCACTAGAGTTGCCACCGCAGAGCTATGGAAT	Generation of plinkerVenusN-ptrA-GlnA plasmid
8gVn_pyr Fw	GAGCTCCACCGCGGTGGCGGCCGCTCTAGAAATGGACCTAACCGTCCTTCGCT	Generation of plinkerVenusN-ptrA-GbpA plasmid
8gVn_pyr Rv	CTCCTCCGCCAGATCCGCCGCCTCCACTAGGACGGGAAACCTGACGGCGCTCCGA	Generation of plinkerVenusN-ptrA-GbpA plasmid
GPD in Ven Fw	GAGCTCCACCGCGGTGGCGGCCGCTCTAGAACCCTTGGTTGAATTTAGAACGTGG	Generation of plinkerVenusC-hph and plinkerVenusN-ptrA plasmids containing *gpdA* promoter
GPD in NA Rv	GTATTCGAATGTATTGAAGGACTCACCATTGTGATGTCTGCTCAAGCGGGGTAGC	Generation of plinkerVenusC-hph and plinkerVenusN-ptrA plasmids containing *gpdA* promoter
GPD in GC Rv	CTGTTTCTGGGAATCCGGGCAAGCCGCATTGTGATGTCTGCTCAAGCGGGGTAGC	Generation of plinkerVenusC-hph and plinkerVenusN-ptrA plasmids containing *gpdA* promoter
GPD in N8 Rv	GACATGGAGCGAAGGACGGTTAGGTCCATTGTGATGTCTGCTCAAGCGGGGTAGC	Generation of plinkerVenusC-hph and plinkerVenusN-ptrA plasmids containing *gpdA* promoter
GlnA-Fw	ATGGTGAGTCCTTCAATACATTCGAAT	Linearization plinerVenusN-ptrA-GlnA
GcnE-Fw	ATGCGGCTTGCCCGGATT	Linearization plinerVenusC-hph-GcnE
Fw_8g	ATGGACCTAACCGTCCTTCGCT	Linearization plinerVenusN-ptrA-GbpA
Vn-Tet-Rv	TTCTAGAGCGGCCGCCACCG	Linearization Venus plasmids Rv
Trafo_Fw	GAGCTCCACCGCGGTGGCGGCCGCTCTAGAACCCTTGGTTGAATTTAGAACGTGG	Generation of fragments for transformation
Trafo_Rv	TGAGCGGATAACAATTTCACACAGGA	Generation of fragments for transformation
pGTH Fw	GCGGACATTCGATTTATGCCGTTAT	Linearization of pGTH(P_{GpdA}, T_{tef}, Hyp^{R})

pGTH Rv	GGTGAATTAAACGGTGATGTCTGC	Linearization of pGTH(P_{GpdA}, T_{tef}, Hyp^R)
GlnA_StrepII_Fw	GCTTGAGCAGACATCACCGTTTAATTCACCATGGTGAGTCCTTCAATACATTCGA	Generation of pGTH plasmid
GlnA_StrepII_Rv	TTATTTTTCGAACTGCGGGTGGCTCCACTAGTTGCCACCGCAGAGCTATGGA	Fusion of StrepII (WSHPQFEK) to GlnA
8g_StrepII_Fw	GCTTGAGCAGACATCACCGTTTAATTCACCATGGACCTAACCGTCCTTCGCTCCA	Generation of pGTH plasmid
8g_StrepII_Rv	TTATTTTTCGAACTGCGGGTGGCTCCAAGCGCTGACGGGAAACCTGACGGCGCTCCG	Add StrepII (WSHPQFEK) to GbpA
Strep_pGTH_Rv	AAGTCATAACGGCATAAATCGAATGTCCGCTTATTTTTCGAACTGCGGGTGGCTCCA	Generation of pGTH plasmid

Supplementary figures

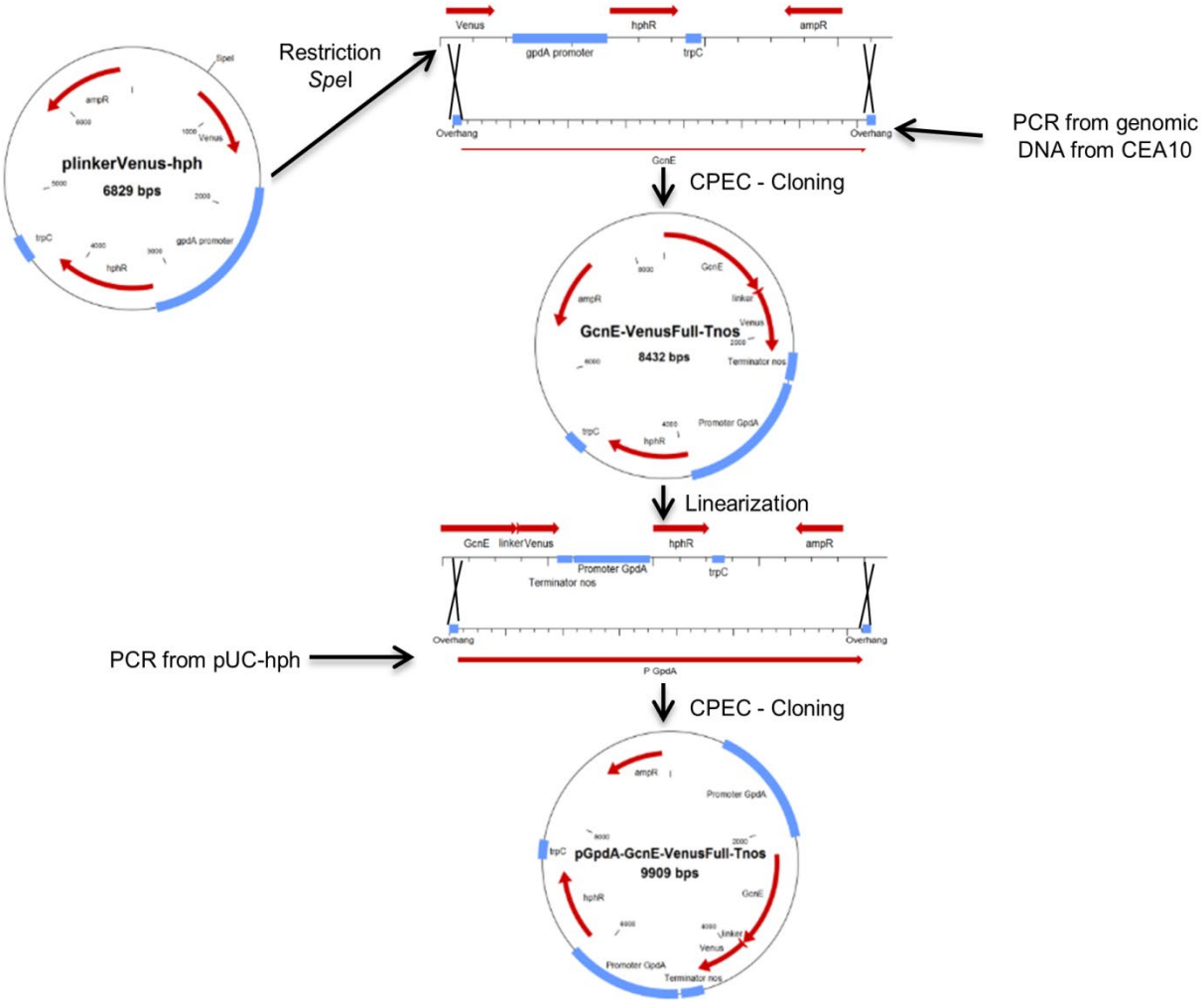

Fig. S1: Example of cloning strategies to generate different expression plasmids for BiFC and pGTH plasmids.

The *gcnE* gene was first cloned into plasmid plinkerVenus-hph to the 5'-end of the entire YFP by applying the CPEC cloning method. Subsequently, the *gpdA* promoter derived from pUC-hph plasmid was inserted by the same method yielding plasmid pGpdA-GcnE-VenusFull-Tnos. The generation of all Venus-constructs followed the same scheme.

A

	Aspergillus fumigatus
Aspergillus oryzae	Identity: **45.1 %** (441/978) Similarity: **64.6 %** (632/978) Gaps: **8.1 %** (79/978)
Aspergillus niger	Identity: **45.0 %** (432/961) Similarity: **63.8 %** (613/961) Gaps: **5.8 %** (56/961)
Aspergillus nidulans	Identity: **12.3 %** (290/2349) Similarity: **20.5 %** (481/2349) Gaps: **62.7 %** (1472/2349)
Saccharomyces cerevisiae	Identity: **10.0 %** (137/1369) Similarity: **18.0 %** (246/1369) Gaps: **62.2 %** (851/1369)

B

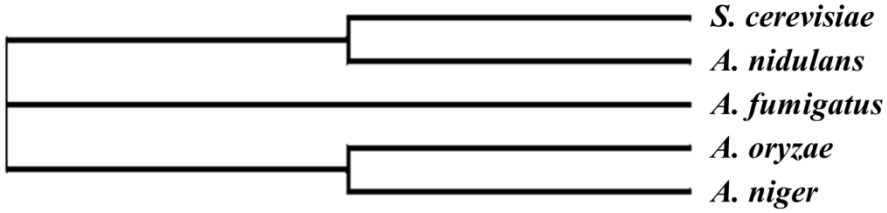

Fig. S2: Sequence comparison of GbpA (Afu8g00780) to orthologues from other *Aspergillus* species and *S. cerevisiae.*

(A) Comparison of the amino acid sequence of GbpA of *A. fumigatus* with that of other *Aspergillus* species [*A. oryzae* (AO090010000059), *A. niger* (An03g01570), *A. nidulans* (AN7246)] and *S. cerevisiae* (NAM7) using Emboss EBI Needle tool; parameters: Matrix: Blosum62; Gap_penalty: 10; Extend_penalty: 0.5 (Rice et al. 2000); **(B)** unrooted tree based on the comparison of amino acid sequences using Clustal Omega multiple sequence alignments (Rice et al. 2000) shows the relationships with following alignment parameters: Dealign input sequences: no, MBED-like clustering: yes, Number of combined: default(0), Max guide tree iterations: default, Max HMM iterations: default

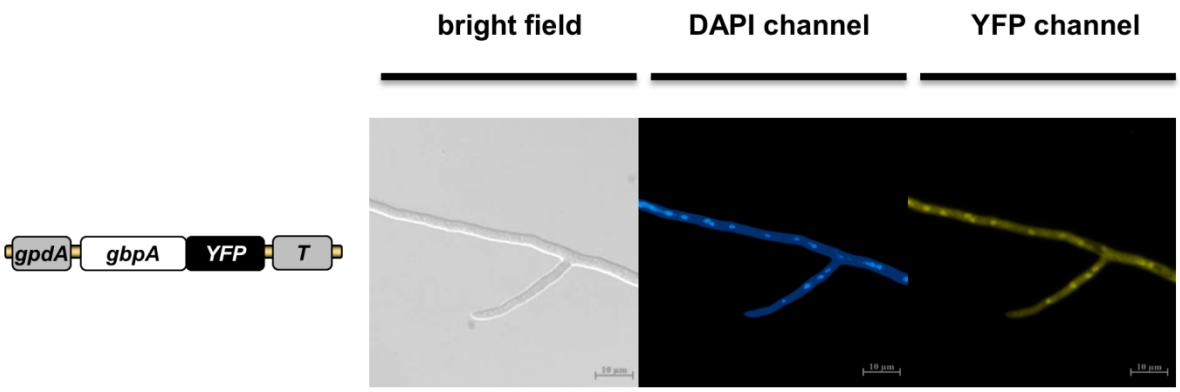

Fig. S3: Fluorescence microscopy to determine GbpA localization *in vivo.*

Microscopic images in bright field mode, and with DAPI and YFP channels. An *A. fumigatus* strain overproducing GbpA with a C-terminal fusion of YFP was analyzed. Co-localization of the DAPI and YFP signal indicates that GbpA partially localizes to the nucleus.

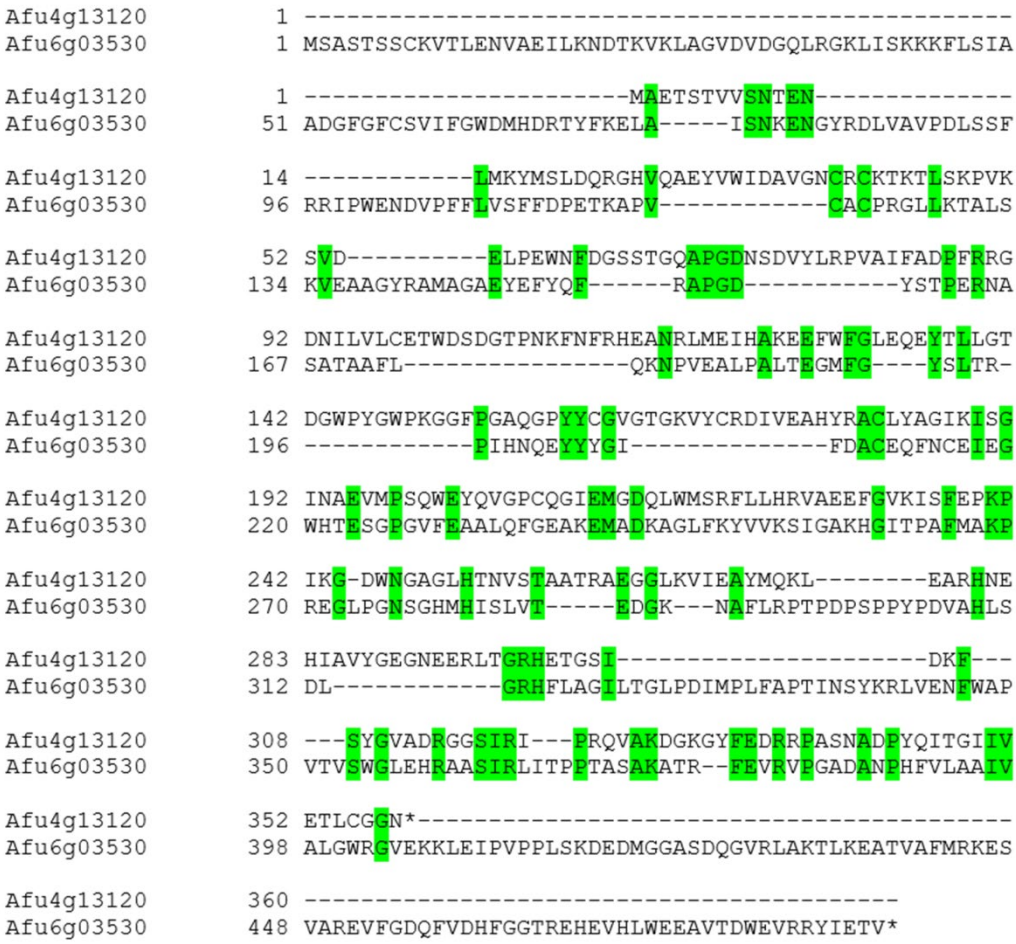

Fig. S4: Pairwise alignment of two putative glutamine synthetases in *A. fumigatus*: Afu4g13120 (GlnA) and Afu6g03530.

Comparison of amino acid sequences using Emboss Needle tool (Rice et al. 2000) with following pairwise alignment parameters: Blosum62; Gap_penalty: 10; Extend_penalty: 0.5

3.2 Manuscript 2 - The Peroxiredoxin Asp f3 Acts as Redox Sensor in *Aspergillus fumigatus*

FORMULAR 1

Manuskript Nr. 2

Titel des Manuskriptes: The Peroxiredoxin Asp f3 Acts as Redox Sensor in *Aspergillus fumigatus*

Autoren: Jana Boysen, Nauman Saeed, Thomas Wolf, Gianni Panagiotou, Falk Hillmann

Bibliographische Informationen: Boysen, J. M., Saeed, N., Wolf, T., Panagiotou, G., & Hillmann, F. (2021a). The Peroxiredoxin Asp f3 Acts as Redox Sensor in *Aspergillus fumigatus*. Genes, 12(5), 668.

https://doi.org/10.3390/genes12050668

Die Kandidatin ist

☒ Erstautor/-in, ☐ Ko-Erstautor/-in, ☐ Korresp. Autor/-in, ☐ Koautor/-in.

Status: publiziert

Anteile (in %) der Autoren / der Autorinnen an der Publikation

Autor/-in	Konzeptionell	Datenanalyse	Experimentell	Verfassen des Manuskriptes	Bereitstellung von Material
Jana M. Boysen	20	70	90	70	0 %
Falk Hillmann	80	20	0	20	80 %

genes

MDPI

Article

The Peroxiredoxin Asp f3 Acts as Redox Sensor in *Aspergillus fumigatus*

Jana Marie Boysen [1,2], Nauman Saeed [1,2], Thomas Wolf [3], Gianni Panagiotou [3] and Falk Hillmann [1,*]

[1] Junior Research Group Evolution of Microbial Interactions, Leibniz-Institute for Natural Product Research and Infection Biology–Hans Knöll Institute (HKI), Beutenbergstr. 11a, 07745 Jena, Germany; Jana.boysen@leibniz-hki.de (J.M.B.); nauman.saeed@leibniz-hki.de (N.S.)
[2] Institute of Microbiology, Friedrich Schiller University Jena, 07743 Jena, Germany
[3] Systemsbiology and Bioinformatics, Leibniz-Institute for Natural Product Research and Infection Biology–Hans Knöll Institute, Beutenbergstr. 11a, 07745 Jena, Germany; thomas.wolf@h-s-o.de (T.W.); gianni.panagiotou@leibniz-hki.de (G.P.)
* Correspondence: Falk.Hillmann@leibniz-hki.de; Tel.: +49-3641-532-1445

Abstract: The human pathogenic fungus *Aspergillus fumigatus* is readily eradicated by the innate immunity of immunocompetent human hosts, but can cause severe infections, such as invasive aspergillosis (IA), in immunocompromised individuals. During infection, the fungal redox homeostasis can be challenged by reactive oxygen species (ROS), either derived from the oxidative burst of innate immune cells or the action of antifungal drugs. The peroxiredoxin Asp f3 was found to be essential to cause IA in mice, but how Asp f3 integrates with fungal redox homeostasis remains unknown. Here, we show that in vivo, Asp f3 acts as a sensor for ROS. While global transcription in fungal hyphae under minimal growth conditions was fully independent of Asp f3, a robust induction of the oxidative stress response required the presence of the peroxiredoxin. Hyphae devoid of Asp f3 failed to activate several redox active genes, like members of the gliotoxin biosynthesis gene cluster and integral members of the Afyap1 regulon, the central activator of the ROS defense machinery in fungi. Upon deletion of the *asp f3* gene Afyap1 displayed significantly reduced nuclear localization during ROS exposure, indicating that Asp f3 can act as an intracellular redox sensor for several target proteins.

Keywords: *Aspergillus fumigatus*; peroxiredoxin Asp f3; AfYap1; transcriptomics; oxidative stress

Citation: Boysen, J.M.; Saeed, N.; Wolf, T.; Panagiotou, G.; Hillmann, F. The Peroxiredoxin Asp f3 Acts as Redox Sensor in *Aspergillus fumigatus*. *Genes* **2021**, *12*, 668. https://doi.org/10.3390/genes12050668

Academic Editor: Ulrike Binder

Received: 16 March 2021
Accepted: 27 April 2021
Published: 29 April 2021

1. Introduction

The ascomycete *Aspergillus fumigatus* is a ubiquitous fungus which is generally involved in the decomposition of (plant based) biomass, thus playing an important role during carbon and nitrogen recycling [1,2]. With its ability to adapt to a wide temperature range, different oxygen and pH levels and nutritional challenges like low iron levels, *A. fumigatus* thrives in many diverse environments and is also known as the most common airborne fungal pathogen. Infection occurs via the widely distributed asexual conidia which after inhalation, germinate and colonize the lung tissue of immuno-compromised patients such as those suffering from HIV, leukemia or active therapeutic immunosuppression following organ and stem cell transplantation [3,4]. Depending on the underlying condition infections range from allergic bronchopulmonary aspergillosis (ABPA) to often fatal invasive aspergillosis (IA), a disease reaching mortality rates in the range of 30–95% [5,6]. Reasons for high mortality are deficiencies in specific and timely diagnostics as well as the limited availability of effective therapeutic treatment [7]. Hence it is imperative to aim for a better understanding of the pathophysiology of *A. fumigatus*, enabling more targeted approaches towards the development of new therapeutic solutions.

The protein Asp f3 was originally found as a prominent allergen on the surface of fungal conidia [8]. Due to its high abundance and affinity to serum immunoglobulin E

(IgE) Asp f3 was also introduced as an auspicious vaccine candidate, protecting Asp f3 immunized mice against invasive pulmonary aspergillosis [9,10]. Recently, we characterized the protein as a dimeric, two-type-cysteine peroxiredoxin Asp f3 which showed peroxidase activity in vitro and protected *A. fumigatus* from external oxidative stress [11]. The protein was furthermore required for virulence in a murine model of pulmonary aspergillosis, and may thus present a promising target for therapeutic applications. Whether its role as a virulence determinant directly relates to its function as a reductive reactive oxygen species (ROS) scavenging enzyme is currently unknown.

Clinical data support an essential role of reactive oxygen species in the defense against fungal infections, as patients suffering from chronic granulomatous disease (CGD) have reduced capability to produce ROS which renders them especially susceptible to *A. fumigatus* infections [7]. The fact that the absence of the major ROS defense activator Yap1 in *A. fumigatus* causes hypersensitivity to ROS, but at the same time does not attenuate its virulence, makes it unlikely that there is a direct correlation between efficient ROS scavenging and virulence. However, ROS may still impact survival of *A. fumigatus* in the host. Only recently host derived ROS were observed to induce the programmed cell death in conidia of the fungus after ingestion by innate immune phagocytes [12]. Here we examine the role of Asp f3 in *A. fumigatus* in the response towards ROS. We show that the absence of Asp f3 does not affect the fungal transcriptome under unstressed conditions but leads to a significant shift in gene expression upon challenge with oxidative stress. Surprisingly, ROS exposure to cells lacking Asp f3 did not activate the AfYap1 regulon, suggesting that Asp f3 acts as an essential redox switch to launch a potent defense against ROS or ROS mediated damages.

2. Materials and Methods

2.1. A. fumigatus Strain and Culture Conditions

All strains and plasmids used in the study are listed in Table 1. The *asp f3* deletion and complemented strains were generated as described by Hillmann et al. [11]. *A. fumigatus* was cultured on/in *Aspergillus* minimal medium (AMM) with 1% Glucose as carbon source and 20 mM $NaNO_3$ as nitrogen source by inoculation with 10^5 conidia if not otherwise noted [13]. Liquid cultures were kept shaking at 180 rpm at 37 °C for 24 h. Conidia were harvested with 0.1% (*v*/*v*) Tween 80 from AMM-agar plates cultivated at 37 °C for 96 h. Mutant-phenotypes were selected by either 250 µg/mL hygromycin B (Invivogen, Toulouse, France) or pyrithiamine (0.1 mg/mL, Sigma-Aldrich, Taufkirchen, Germany), depending on the resistance marker used in transformation [14]. Conidia were counted by a CASY® Modell TT (OLS OMNI Life Science, Bremen, Germany). For long–time storage, conidia were mixed with glycerol at 20% (*v*/*v*) and frozen at −80 °C.

Table 1. Strains of *Aspergillus fumigatus*.

Strain	Genotype	References
A. fumigatus D141	WT	[15]
A. fumigatus Δ*asp f3*	Asp f3::hph; Hyg^R	[11]
A. fumigatus Δ*asp f3*^{C}	Asp f3::hph; Hyg^R Δasp f3::Asp f3; PT^R	[11]
A. fumigatus OE::*Afyap1*^{VENUS}	P_{GpdA}-Afyap1^{Venus}-T_{nos}::ptrA; PT^R	This study
A. fumigatus Δ*asp f3* OE::*Afyap1*^{VENUS}	Asp f3::hph; Hyg^R P_{GpdA}-Afyap1^{Venus}-T_{nos}::ptrA; PT^R	This study

2.2. Construction of Fluorescent Reporter Strains

For the generation of a *VENUS*-Fusion protein expression strain, the gene sequence of *Afyap1* was cloned into plasmid pGpdA-Afyap1-VENUS containing a constitutive *gpdA*-

promoter and *VENUS* gene with a *nos* terminator (Supplementary Figure S1). The target gene (*Afyap1*) was introduced as a N-terminal-fusion to *VENUS* via CPEC and further paired with the *PtrA* resistance cassette which confers resistance to the antimetabolite pyrithiamine [16]. For a list of Primers see Supplementary Table S1. Plasmids were amplified in *E. coli* DH5α, linear fragments for transformation were amplified via PCR (Phusion Flash Polymerase, Thermo Fisher Scientific, Bremen, Germany) and transformed into *A. fumigatus* D141 and Δ*asp f3* via protoplast formation [17,18]. Mutants were confirmed by diagnostic PCR and a detectable *VENUS*-signal during fluorescence microscopy.

2.3. Isolation of Chromosomal DNA

Fungal strains were cultivated for 16 h at 37 °C at 180 rpm in Sabouraud 2% Glucose Bouillon (Carl Roth, Karlsruhe, Germany). The mycelium was harvested through miracloth, washed thoroughly with H_2O, dried and frozen with liquid nitrogen. Frozen mycelium was then ground to a fine powder in a mortar and stored at −20 °C until further use. Isolation of chromosomal DNA was carried out as described previously [19].

2.4. Oxidative Stress Experiments

Reactive oxygen species were produced either by addition of H_2O_2 or directly in vivo we with the xanthine oxidase enzymatic system generating a mixture of H_2O_2 and O_2^- as previously described [11]. Prior to treatment 10^5 conidia were grown in liquid Czapek Dox medium (BD, Franklin Lakes, NJ, USA) in 6-well tissue culture plates (VWR International, Leuven, Belgium) in a final volume of 3 mL and cultured for 48 h until a thin layer of mycelium was formed. A sub-lethal concentration (for Δ*asp f3*) of 150 μM xanthine was supplied. The addition of 100 μg/mL (0.2 units/mL) xanthine oxidase (Sigma-Aldrich, Taufkirchen, Germany) started the reaction. For the transcriptome, analysis reaction was stopped after 15 min and samples were harvested, frozen with liquid nitrogen and stored at −80 °C until further use. All data analyzed originated from three biological replicates.

2.5. RNA Isolation

Total RNA was isolated from ROS treated and untreated mycelia of the wild type and the Δ*asp f3* strain using the RNeasy Plant Mini Kit (Qiagen, Hilden, Germany). Frozen mycelium was transferred to tubes containing glass beads (Sigma-Aldrich, Taufkirchen, Germany), after addition of resuspension buffer cells were disrupted by mechanical force applied via FastPrep (MP Biomedicals, Irvine, CA, USA) for 60 s at high-speed setting (6.0). Further processing was conducted according to the manufacturer's protocol. Extracted RNA was stored at −80 °C. RNA concentration was determined by NanoDrop ND1000 Spectrophotometer (NanoDrop Technologies Inc., Wilmington, DE, USA).

2.6. Analysis of Transcriptome Data

The preparation of cDNA libraries from total RNA and the sequencing was performed by GATC Biotech (GATC Biotech, Konstanz, Germany). According to GATC Protocol samples were enriched for mRNA by isolation of poly(A)+ mRNA, mRNA was fragmented and cDNA synthesis was performed to generate strand specific cDNA libraries. From these libraries 1 × 50 bp single end reads were sequenced with the Genome Sequencer Illumina HiSeq (HiSeq 4000 50bp SR) (Illumina, San Diego, CA, USA). FastQC [20] and Trimmomatic v0.32 [21] were used for quality control and trimming of library adaptors. Mapping of reads was achieved with HiSat2 [22] against the reference genome of *A. fumigatus A293*. The normalized number of reads were analyzed with EdgeR, Limma, DESeq, DESeq2 [23–26] and genes were considered as differentially expressed gene (DEGs) when the differences in the number of reads were statistically significant according to one or more of these tests.

2.7. Gene Expression Analysis by qRT-PCR

A. fumigatus WT and Δ*asp f3* conidia (1×10^9) were grown in 3 mL AMM and CD at 37 °C and 180 rpm for 6 h to induce swelling. After 6 h, swollen conidia were treated with 0.1

M H_2O_2 for 15 min. Swollen conidia were harvested from triplicate samples at 0 and 15 min after the addition of 0.1 M H_2O_2 by centrifugation at 800 *g* and 4 °C for 5 min. Swollen conidia were subsequently lysed with glass beads in the FastPrep (MP Biomedicals, Irvine, CA, USA) for 60 s at 13,000 rpm and processed for total RNA isolation using a Qiagen RNeasy plant mini kit (Qiagen, Hilden, Germany), according to manufacturer's protocol. Extracted RNA was then stored at −20 °C. Concentration of each sample was determined with NanoDrop ND1000 spectrophotometer (NanoDrop Technologies Inc., Wilmington, DE, USA).

RNA was treated with RQ1 RNase-free DNase (Promega, Walldorf, Germany) and transcribed into cDNA (RevertAid First Strand cDNA Synthesis Kit, Thermo Fischer Scientific, Germany), according to the manufacturers protocol. Quantitative real time polymerase chain reaction (qRT-PCR) was performed using the cDNA as a template. The ΔCT method was used to analyze the relative expression of the target genes, normalized to the constitutively expressed *tubA* gene encoding tubulin A. Al primers are listed in Supplementary Table S1. The reactions were carried out in a total volume of 20 µL on Quantstudio3 system (Thermo Fisher Scientific, Bremen, Germany).

2.8. DAPI Staining and Fluorescence Microscopy

A total of 10^5 conidia were incubated at 37 °C for 10 h in 300 µL of CD in ibidi® µ-slide (ibidi, Gräfelfing, Germany) until germination. The nuclei were then stained with NucBlue™ Live ReadyProbes™ Reagent (ThermoFisher, Dreieich, Germany) according to manufacturer's guidelines. Afterwards, 2 mM H_2O_2 was added and after 30 min the samples were subsequently analyzed under the microscope. Fluorescent stain and proteins were excited with 408 nm and 488 nm, respectively, to analyze the localization of AfYap1^{VENUS} in both WT and Δ*asp f3* strains using a Zeiss Axio Observer Spinning Disk Confocal Microscope (ZEISS, Jena, Germany) using ZEN software (Version 2.6). Microscopic images were evenly processed and analyzed with ImageJ software [27].

2.9. Co-Localization Analysis

For the co-localization analysis of AfYap1^{VENUS} and DAPI, the Coloc2 plugin of ImageJ was used to calculate the Pearson's correlation coefficient to identify the intensity correlation of fluorescence signals. GraphPad9 Prism software was used to plot the graph and calculate the *p*-value. Error bars represent ± standard deviation from at least 3 images.

2.10. Preparation of Protein Extracts and Catalase Activity Measurements

Crude protein extracts were prepared from *A. fumigatus* swollen conidia incubated for 6 h in CD medium and treated with 2 mM of H_2O_2 for 45 min. Conidia were harvested by centrifugation and washed thoroughly with PBS. Conidia were re-suspended in assay buffer (Abcam, Cambridge, UK) and disrupted by FastPrep treatment, repeated mixing and sonication for 10 min to enhance the solubilization of proteins. Protein concentration was determined by the Bradford assay [28] and spectrophotometric measurements (UV mini 1240, Shimadzu, Kyoto, Japan). Catalase activity was determined using the catalase activity assay kit (cat. No. ab83464 Catalase Activity Assay Kit, Abcam, Cambridge, UK) according to the manufacturer's instructions and fluorometric measurements in a fluorescence plate reader (Tecan, Männedorf, Switzerland) at excitation and emission wavelengths of 535 and 587 nm, respectively.

2.11. In-Gel Catalase Activity Assay

A. fumigatus conidia of different strains were inoculated in CD medium and grown for 20 h at 37 °C prior to a 5 mM H_2O_2 treatment for 45 min. The mycelium was harvested, frozen in liquid nitrogen and ground to a fine powder. Isolation of native protein occurred according to Lessing et. al. (2007) [29]. Again, protein concentration was measurured via Bradford assay [28] and spectrophotometric measurements (UV mini 1240, Shimadzu, Kyōto, Japan). A total of 30 µg of protein was loaded on an 8–16% polyacrylamide (wt/vo)

Tris-Glycine Gel (Invitrogen™ Novex™ WedgeWell™, Art. Nr.: 15486814). The runtime was for 4 h at 60 V at 4 °C. Catalase activity in the gel was determined with the method described by Goldberg and Hochman [30]. A total of 1 µg catalase from bovine liver (C1345, 2000–5000 units/mg protein, Sigma-Aldrich, Taufkirchen, Germany) was used as a positive control.

2.12. Functional Annotation of Transcriptome Data

Enrichment analyses of genes were carried out with the FungiFun2 package [31]. Default settings were used to enrich genes according to GO and FunCat categories. Hits were deemed significant with a *p*-values < 0.01. Enrichment was carried out for the Go-terms "biological process" and "molecular function". Additional analyses were performed with the AspGD Gene Ontology Term Finder (http://www.aspergillusgenome.org/cgi-bin/GO/goTermFinder, accessed on 28 February 2021) [32].

3. Results

3.1. Global Transcriptome Analysis Reveals a ROS Specific Function of Asp f3

To understand the protective role of Asp f3 during ROS exposure we monitored global transcription in wild type hyphae of *A. fumigatus* (WT) and the ROS sensitive deletion mutant Δ*asp f3*. Both strains were first grown in minimal medium and either left untreated (−ROS) or exposed to H_2O_2 and O_2^- (+ROS), therefore ROS were generated in vivo by the xanthine oxidase enzymatic system for 15 min in biological triplicates. A principal component analysis of the fungal transcriptomes demonstrated a comparatively low cumulative variance in untreated samples, indicating that the lack of Asp f3, despite its abundance as protein, did not significantly impact transcription under ambient growth conditions of fungal hyphae in minimal medium (Figure 1). These results corresponded to a widely indistinguishable phenotype under a wide range of growth conditions with various carbon sources (Supplementary Figure S2).

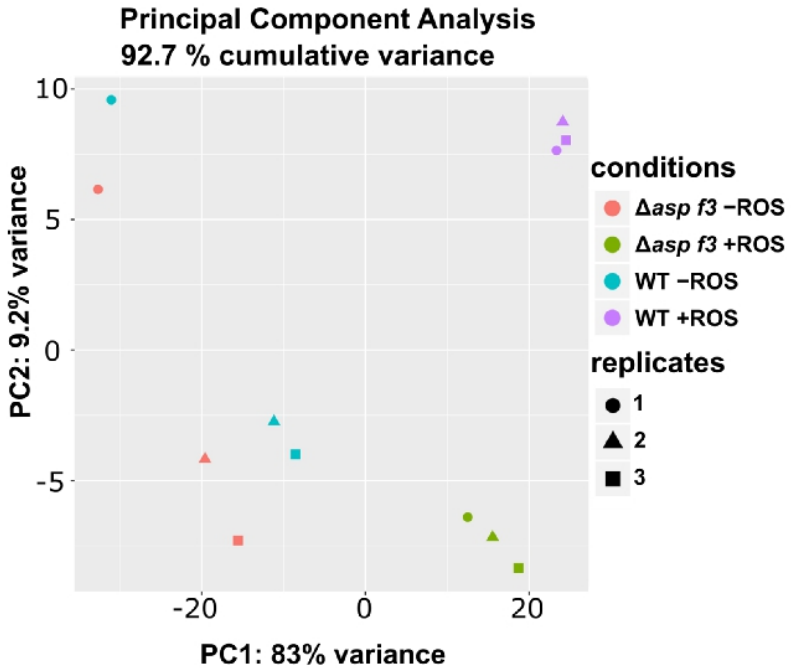

Figure 1. Principal component analysis of transcriptome data from wild type *Aspergillus fumigatus* (WT) and a strain lacking the *asp f3* gene (Δ*asp f3*) grown with (+ROS) or without (−ROS) reactive oxygen species (ROS). The strains, treatments and biological replicates are represented by different colours and symbols, respectively.

In fact, in the absence of ROS, WT and Δ*asp f3* showed an exceptionally high similarity in their genome expression and only seven genes were found to be differentially expressed genes (DEGs). The only DEG commonly identified by all four methods was *asp f3* which remained undetected in the mutant strain, as expected. This indicated that Asp f3 plays a minor role in the absence of ROS and allowed a direct comparison of the ROS-treated samples without a background of genes that directly respond to the absence of Asp f3.

ROS exposure induced a shift in the global transcriptome with nearly identical numbers of DEGs for both strains. For the wild type and Δ*asp f3* mutant we identified 1810 and 1729 ROS dependent DEGs, respectively. The numbers of up- and downregulated genes are likewise similar, identifying 1124 up- and 686 downregulated genes for the WT and 1025 up- and 704 down-regulated genes in Δ*asp f3* (Figure 2A). However, when the DEGs were compared between the two strains, we found only about two thirds of them in congruency. This proportion was comparable for up- as well as for the down-regulated genes (Figure 2B).

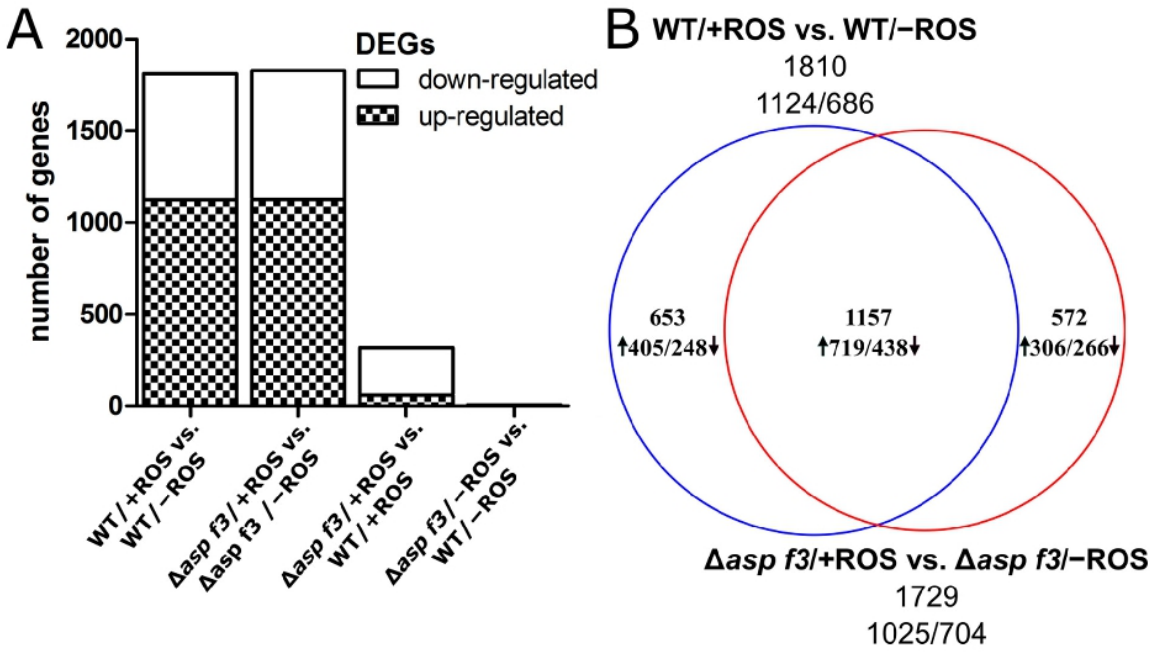

Figure 2. Reactive oxygen species dependent gene expression in *Aspergillus fumigatus* wild type (WT) and hyphae lacking Asp f3 (Δ*asp f3*). (**A**): Comparison of the total number of differentially expressed genes (DEGs) and the direction of their regulation between strains and conditions. (**B**): Venn-diagram of DEGs in the transcriptomes of the WT and Δ*asp f3* during ROS exposure. Given numbers represent the total number of DEGs. Arrows pointing up- or downwards indicate the direction of regulation.

3.2. Transcriptional Induction of the ROS Defense Requires Asp f3

Although the number of ROS induced DEGs was similar in hyphae of the wild type and Δ*asp f3*, 653 genes were differentially expressed only in the wild type, indicating that Asp f3 was required for gene expression under oxidative stress and Δ*asp f3* seems to react differently when challenged with ROS. To get an overview of the effects triggered by loss of the peroxiredoxin we plotted the expression of all genes in WT and Δ*asp f3* under ROS exposure (Figure 3A).

This direct comparison of the treated samples showed 319 DEGs of which 60 were higher expressed in hyphae of the mutant when compared to those of the wild type. The remaining 259 genes showed lower expression in the mutant during ROS exposure. The

lowest was the *asp f3* gene itself with RPKM values of 14 and approximately 5900 in hyphae of the mutant and the wild type, respectively.

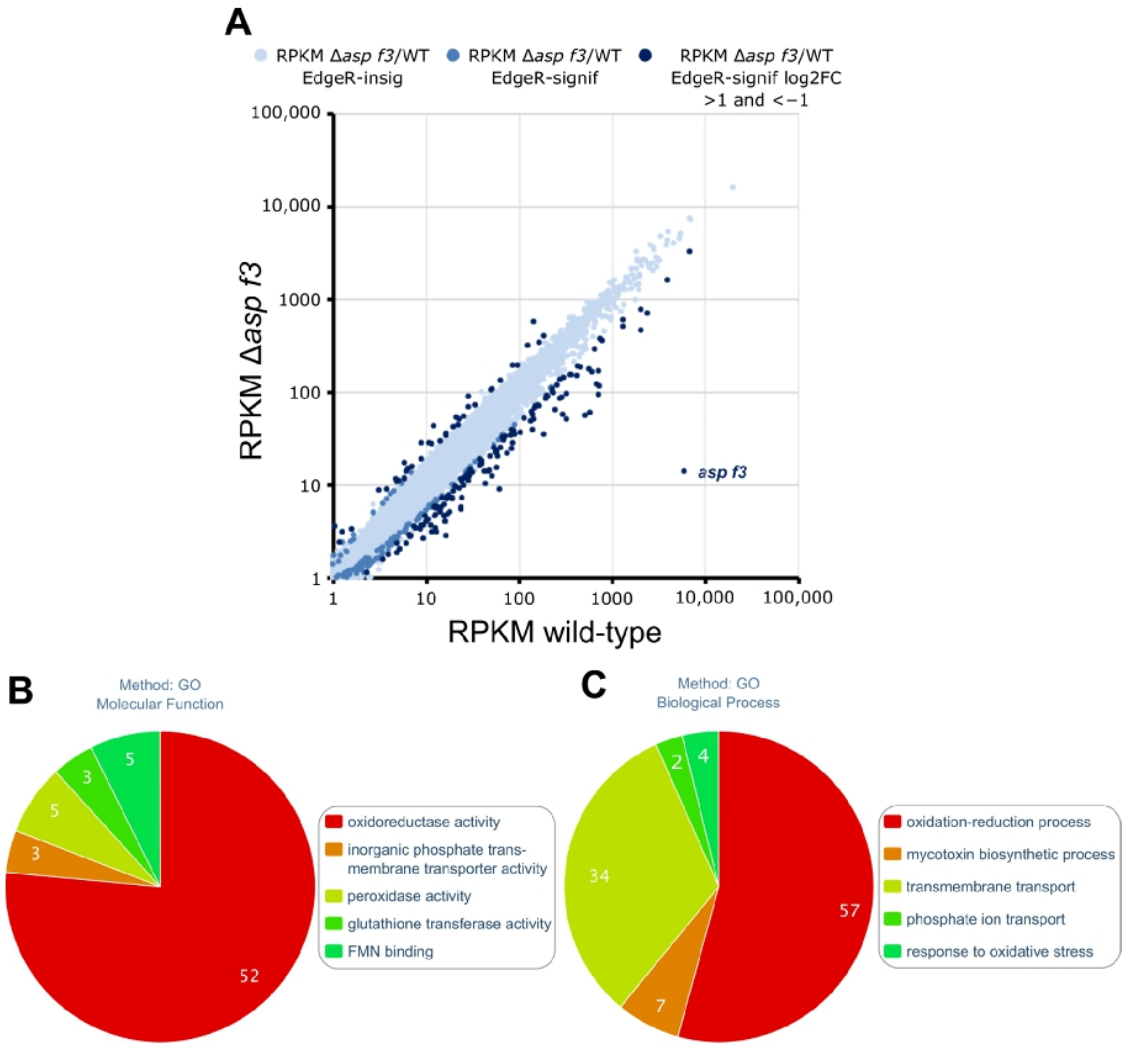

Figure 3. Global transcription in wild type and an *asp f3* deletion mutant of *Aspergillus fumigatus* after treatment with ROS. (**A**): Differential gene expression displayed as RPKM values of single genes in the *asp f3* deletion mutant (Δ*asp f3*) and the wild type (WT) during oxidative stress. Differences in gene expression were defined as either insignificant (bright blue) or significant (blue) according to EdgeR. Genes with log2 fold differences >1 and <−1 are highlighted in dark blue. (**B**,**C**): Gene ontology enrichment according to *Molecular function* (**B**) and *Biological process* (**C**) of genes specifically down-regulated in Δ*asp f3* in response to ROS.

Of the 259 genes that were specifically downregulated in Δ*asp f3* under ROS, 53 genes were not affected by ROS in the wild type. The remaining 205 of these DEGs were up-regulated after ROS exposure of the wild type. A gene ontology analysis for *molecular functions* of the group of genes that lacked ROS dependent expression in the absence of the peroxiredoxin identified primarily oxidoreductase activity, inorganic phosphate transmembrane transporter activity, peroxidase activity and FMN binding as significantly enriched categories (Figure 3B, Supplementary Table S2). *Biological processes* that showed attenuated expression specific to the absence of Asp f3 included categories such as phosphate ion transport, transmembrane transport and mycotoxin biosynthetic processes. The latter was in principle limited to gliotoxin biosynthesis (Figure 3C, Supplementary Table S3). Indeed,

a closer look at the genes of the gliotoxin cluster identified 7 of 12 genes as downregulated, including *gliP*, the gene for the non-ribosomal peptide synthetase. The largest enriched biological processes were oxidation-reduction processes and transmembrane transport. More specifically, the transmembrane transport of phosphate ions and the specific response to oxidative stress was deregulated in the absence of the peroxiredoxin. To analyze whether Asp f3 is required for the activation of ROS defense, catalase activity was determined in total protein extracts from both strains before and after a treatment with H_2O_2 by indirect measurement of catalase activity (Figure 4A). Untreated hyphae ($-H_2O_2$) revealed insignificant differences in catalase activity. Exposure of H_2O_2 to the swollen spores increased catalase activity in both WT and Δ*asp f3*, but ROS dependent upregulation in Δ*asp f3* led to significantly lower activity then in hyphae of the wild type. To determine which catalases were active in the samples both strains were grown for 20 h and challenged with H_2O_2 for 45 min. Proteins were extracted and loaded in equal amounts (30 µg) on a native polyacrylamide gel to perform an in-gel catalase activity assay (Figure 4B,C). Catalase activity was visualized by a negative staining and shows a strong induction of Cat2 in the wild type after challenge with H_2O_2. In contrast to the wild type, Cat2 activity was detectable in the unchallenged sample of Δ*asp f3*. However, exposure to H_2O_2 did not lead to an induction of Cat2 activity. Activity of the spore borne catalase CatA was not observed.

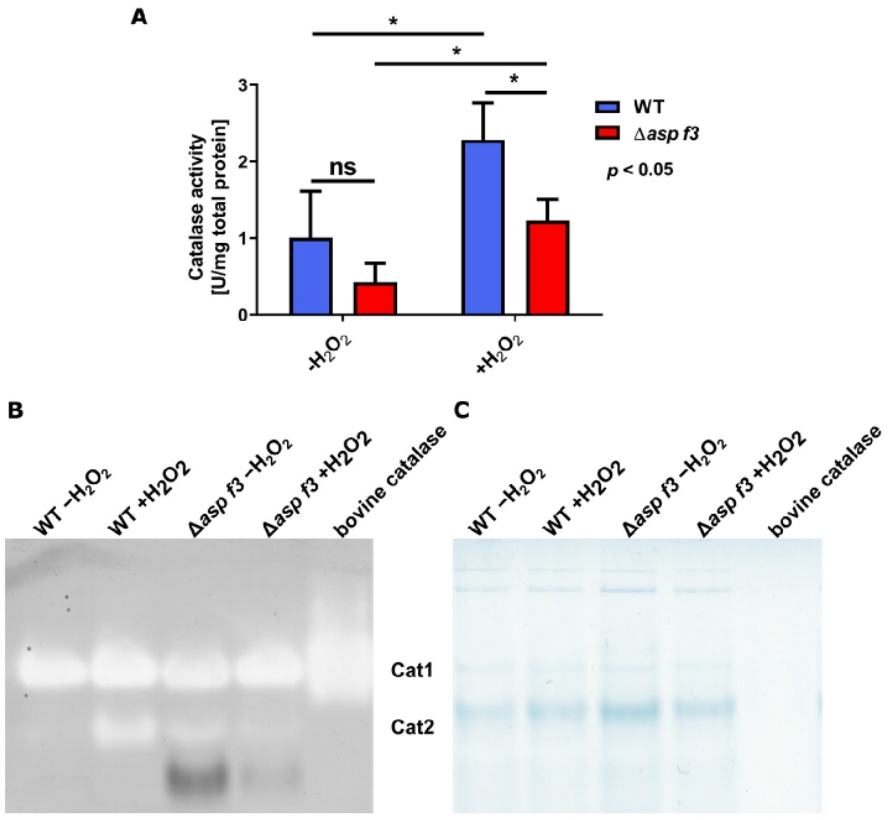

Figure 4. Catalase activity in hyphae of the wild type and the *asp f3* deletion mutant of *Aspergillus fumigatus*. (**A**): Catalase activity was measured in total protein isolated from swollen spores 30 min after stress treatment with either 0 mM ($-H_2O_2$) or 2 mM ($+H_2O_2$) H_2O_2. (**B**): Catalase activity staining was performed according to the method of Goldberg and Hochman [30]. Cultures of wild type and Δ*asp f3* were grown for 20 h and treated with 5 mM H_2O_2. Negative staining shows catalase activity of Cat1 and Cat2 as described previously [29,33] (**C**): Loading control stained with Coomassie. *: $p < 0.05$

3.3. Full ROS Dependent Activation of Several Afyap1 Target Genes Requires Asp f3

Several genes with a major role in the redox-homeostasis and the defense against oxidative stress were upregulated in the wild type (Table 2), among them three confirmed targets of the major activator AfYap1 [29]: the bifunctional catalase-peroxidase (*cat2*, AFUA_8g01670), the Cytochrome c peroxidase (*ccp1*, AFUA_4G09110), and the p-Nitroreductase family protein (*pnr1*, AFUA_5g09910). The latter is not only known to be strongly induced by diverse environmental stresses such as superoxide stress, osmotic stress and heat stress but is also expressed when the fungus is exposed to neutrophils [34,35]. However, other putative AfYap1-targets suggested by Lessing and colleagues [29], such as the mitochondrial peroxiredoxin (Prx1) or methionine synthase, were not significantly affected in the transcriptome data set of the wild type or the mutant. The expression of the putative Afyap1 targets, the *yap1* itself, and several other ROS defense genes was analyzed by qRT-PCR in two different conditions (Figure 5). Expression of ROS defense genes in Czapek-Dox (CD) medium (Figure 5A), which was also used to generate the transcriptome data, was approximately an order of magnitude lower than in *Aspergillus* minimal medium (AMM) which was supplemented with added trace metals as a major difference (Figure 5B). For both wild type and Δ*asp f3* the expression of the *Afyap1* gene was comparably lower in CD than in AMM even without the addition of ROS stress. For both strains the transcript levels were also not significantly affected by the addition of ROS in CD, while a significant induction of the regulator gene *Afyap1* was detected for both strains in AMM. For several other ROS defense genes, including the putative Afyap1 targets *ccp1*, *cat2*, and *pnr1*, ROS dependent activation was lower in hyphae of the *asp f3* deletion mutant. This lack of activation was also more pronounced in the trace metal free CD medium. ROS mediated induction of *catA* and *gpx3* were detected for both strains in both media.

Table 2. Expression of oxidative stress genes in the *Aspergillus fumigatus* wild type and Δ*asp f3* in response to reactive oxygen species (ROS).

	Gene ID	Afyap1 Target *	WT + ROS vs. WT − ROS	Δ*asp f3* + ROS vs. Δ*asp f3* − ROS	Δ*asp f3* + ROS vs. WT + ROS
1	Putative NADH flavin oxidoreductase (AFUA_2g04060)	−	4.16	1.93	−2.65
2	bifunctional catalase-peroxidase (*cat2*, AFUA_8g01670)	+	2.85	0.31	−2.64
3	p-Nitroreductase family protein (*pnr1*, AFUA_5g09910)	+	4.05	2.4	−2.15
4	Oxidoreductase, putative (AFUA_5G01250)	−	2.12	0.39	−1.87
5	Thioredoxin reductase (*trxR*, AFUA_4g12990)	−	2.75	1.79	−1.74
6	Glutathione transferase, putative (AFUA_2g15770)	−	2.53	0.95	−1.66
7	NADH-dependent flavin oxidoreductase, putative (AFUA_7G06420)	−	1.81	0.88	−1.47
8	Glutathione peroxidase (*gpx3*, AFUA_3g12270)	−	1.31	0.35	−1.34
9	Cytochrome c peroxidase (*ccp1*, AFUA_4G09110)	+	1.36	0.21	−1.3
10	Glutathione S-transferase, putative (AFUA_2G00590)	−	0.85	0.22	−1.18

Table 2. *Cont.*

	Gene ID	Afyap1 Target *	WT + ROS vs. WT − ROS	Δ*asp f3* + ROS vs. Δ*asp f3* − ROS	Δ*asp f3* + ROS vs. WT + ROS
11	Ferric-chelate reductase, putative (AFUA_6G13750)	–	0.86	−0.26	−1.14
12	Gliotoxin Cluster e.G. gliM (AFUA_6G09680)	–	−0.3	0.62	−1.12
13	Metalloreductase, putative (AFUA_6g02820)	–	1.21	0.27	−1.1
14	Thioredoxin (Asp29/Trx1) (AFUA_5g11320)	–	1.63	0.7	−1.1
15	Mitochondrial peroxiredoxin Prx1 (AFUA_4G08580)	+	−0.75	−0.66	0.13
16	Methionine synthase MetH/D (AFUA_4G07360)	+	−0.11	−0.02	0.07

* Putative members of the Yap1 regulon according to Lessing et al., 2007 [29].

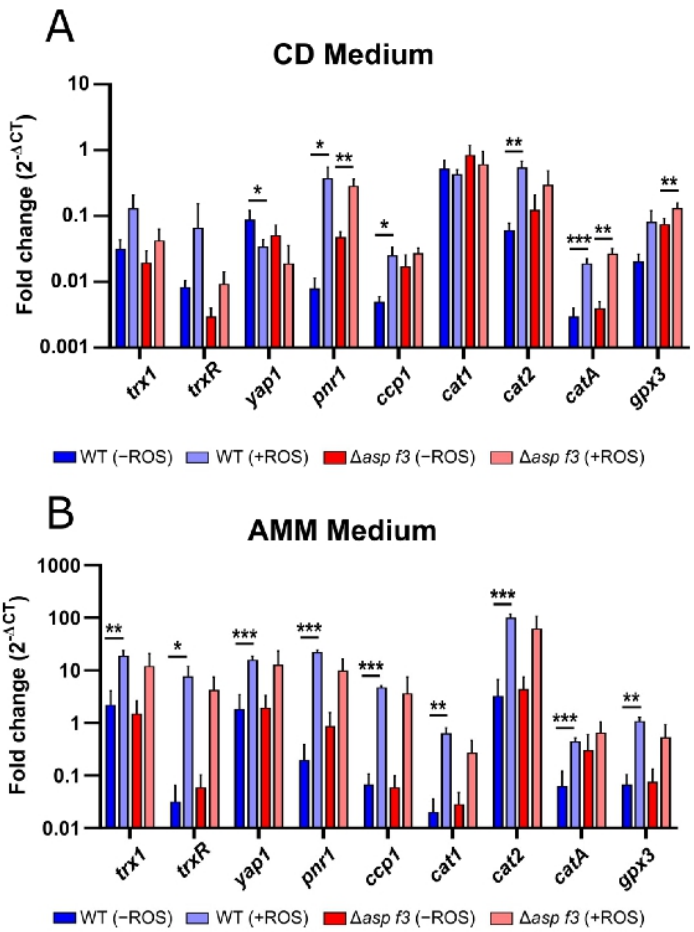

Figure 5. Gene expression of ROS defense genes in wild type (WT) and *aspf3*-deleted (Δ*asp f3*) hyphae of *Aspergillus fumigatus* in Czapek Dox (**A**) and *Aspergillus* minimal medium (**B**) in the absence (−ROS) or presence (+ROS) oxidative stress. Data from qRT-PCR are displayed as logFC normalized to the housekeeping gene *tubA* and represent the mean and SD of three biological replicates. For statistical analysis, Student's t-test with *: $p < 0.1$; **: $p < 0.05$; ***: $p < 0.01$ was used.

3.4. *Asp f3 Is Required for Afyap1 Activation and Nuclear Localization*

The oxidative stress regulator Afyap1 localizes to the nucleus in response to ROS and activates the transcription of target genes, such as *cat2* [29]. The reduced expression levels of *cat2* in Δ*asp f3*, as well as the lower catalase activity in the mutant, prompted us to evaluate whether Afyap1 activation depends on this peroxiredoxin. Thus, we monitored the subcellular localization of the AfYap1-Venus fusion protein in germlings of the wild type and Δ*asp f3* (Figure 6). In the absence of H_2O_2, AfYap1^{VENUS} displayed diffused cytosolic localization in both, wild type and Δ*asp f3* (0 min). An addition of 2 mM H_2O_2, induced nuclear localization of AfYap1^{VENUS} in wild type germlings within 30 min. Conversely, in the Δ*asp f3* background, a larger proportion of the AfYap1^{VENUS} remained diffused in the cytoplasm with only a minor nuclear concentration of the activator. To overcome heterogeneity in the microscopic data, we quantified the fluorescence intensity signals for AfYap1^{VENUS} and DAPI as a nucleus specific signal. Co-localization of the two different fluorescent intensities was determined as Pearson's correlation coefficient (PCC, Figure 7). In the absence of H_2O_2, PCC values were 0.48 and 0.46 for wild type and Δ*asp f3*, respectively. Whereas, after 30 min of H_2O_2 exposure PCC values significantly increased for the wild type (0.80). However, a significantly lower PCC value was observed for Δ*asp f3* (0.61) when compared with the treated wild type indicating that efficient nuclear localization of Afyap1 depends on the peroxiredoxin Asp f3.

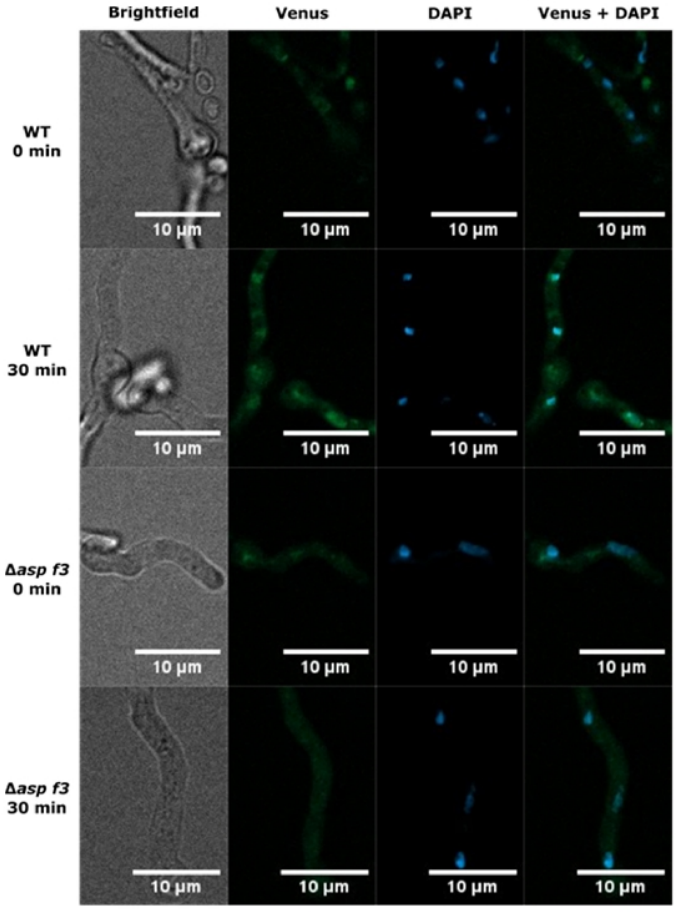

Figure 6. Subcellular localization of AfYap1^{VENUS}. *Aspergillus fumigatus* conidia were incubated in Czapec Dox for 10 h until germination. Both strains were challenged with 2 mM H_2O_2 for 30 min before microscopy. The VENUS-tag shows a green fluorescent signal for the target protein AfYap1, nuclei were stained with NucBlue™ Live ReadyProbes™.

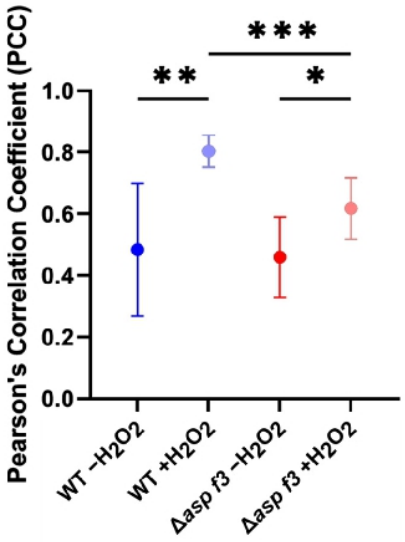

Figure 7. Quantification of co-localization of DAPI and AfYap1^{VENUS} dependent fluorescence signals. Pearson's correlation coefficient (PCC) for DAPI and AfYap1^{VENUS} co-localization calculation in the presence and absence of H_2O_2 in the wild type and Δ*asp f3* background strains. The data represents the mean and standard deviation from at least three independent experiments (n ≥ 3). Significant differences calculated by Student's t-test are shown as *: $p < 0.05$; **: $p < 0.01$; ***: $p < 0.001$.

4. Discussion

The peroxiredoxin Asp f3 is a major allergen and an abundant protein of *A. fumigatus*, as an allergen on the conidial surface, but also within growing hyphae. It was shown to function in the defense against ROS and was essential during invasive aspergillosis in a mouse infection model [11]. However, it remained unclear how this confirmed biochemical function as a peroxiredoxin would serve precisely during infection in the host. In the absence of oxidative stress, the absence of Δ*asp f3* yields an inconspicuous phenotype, nearly indistinguishable from the wild type. Our transcriptome analysis confirmed, under in vitro conditions without ROS exposure, only minor transcriptional changes were detected and the Asp f3 protein appears to be dispensable for growth. This observation is in line with earlier results for *Saccharomyces cerevisiae* which demonstrated that the yeast was still viable despite a deletion of all five peroxiredoxin genes and that single mutants grew like the wild type in aerobic conditions [36]. Interestingly, the authors also showed that the Asp f3 orthologue in yeast, Tsa1p, secured long-term genomic stability by preventing mutations [37,38]. Such a protective function may well be conserved in *A. fumigatus* but would most likely not explain the avirulent phenotype of the Δ*asp f3* strain in the aspergillosis animal model.

While Asp f3 was dispensable in hyphae during the absence of ROS, confrontation with ROS induced major changes in the transcriptome. Resulting from its hypersensitive phenotype, one may have expected a slightly higher expression level of oxidative stress genes to compensate the phenotype, but indeed the opposite was observed. Several ROS defense genes were slightly downregulated under ambient growth conditions, and for others no induction was seen in response to ROS. Amongst the unaffected or even downregulated genes are several which are pivotal to the oxidative stress response or involved in virulence. Several of the genes, including *trxR*, *ccp1* and *gpx3*, also coincide with genes upregulated in *A. fumigatus* conidia when exposed to neutrophils, indicating their relevance during virulence [35]. Although not all of these gene products may be crucial to defend against innate immune cells, it confirms the presence of a perceptible exposure to ROS. Furthermore, TrxR was recently described as an essential gene which not only affects oxidative stress resistance but is needed for full virulence in animal models

of both *Galleria melonella* and immunosuppressed mice [39]. Seven genes of the gliotoxin gene cluster are downregulated in Δ*asp f3*, including *gliP*, which encodes the nonribosomal peptide synthase catalysing the first step in the biosynthesis of gliotoxin. This mycotoxin is produced in vivo during infections and is known to mediate immunosuppressive effects on human cells [40–43]. When interacting with human neutrophils, gliotoxin was shown to re-organize the actin-skeleton, thus inhibiting phagocytosis and further inhibiting the respiratory burst and other neutrophil functions such as superoxide production [44,45]. Additionally, deletion of *gliP* was shown to attenuate virulence in mice immunosuppressed with hydrocortisone [42,46]. With regard to its reversible dithiol linkage, a regulatory link between gliotoxin biosynthesis and the fungal redox state seems likely and has previously been observed [47]. We saw a mild H_2O_2 dependent upregulation in the wild type and the opposite tendency in the absence of Asp f3. Such downregulation of the gliotoxin gene cluster in the Δ*asp f3* strain may lead to lower levels of the mycotoxin during infection which might thus attenuate its virulence potential in the lung environment in the host.

Some of the downregulated genes in Δ*asp f3* were confirmed regulatory targets of Afyap1. Furthermore, *Afyap1*^{VENUS} overexpression in a Δ*asp f3* background could not compensate for the absence of Asp f3. These results suggested that Afyap1 and Asp f3 could be functionally interconnected, especially as a reversible disulphide bond formation is known to regulate Yap1 localization and activity. In baker's yeast, activation of Yap1 was first reported to occur by the glutathione peroxidase (Gpx3), acting as the hydroperoxide receptor and redox transducer [48]. In our transcriptome the Gpx3 orthologue of *A. fumigatus* was clearly upregulated in the wild type in response to ROS but transcription remained unchanged in Δ*asp f3* after ROS treatment. It should not be excluded that lower levels of Gpx3 in the mutant may attenuate Afyap1 activation, either via direct interaction or as a member in a redox relay system.

Peroxiredoxin dependent activation of the Yap1 regulator has also been proposed for filamentous fungi previously [49]. In *Aspergillus nidulans*, the Yap1 orthologue is coined NapA and regulates a wide set of genes far beyond ROS defense. Neither GpxA (Gpx3 in *A. fumigatus*) or two other peroxiredoxins, TpxA (AFUA_4g08580, Prx1 in *A. fumigatus*) and TpxB (AFUA_8G07130 in *A. fumigatus*), were found to be involved in NapA activation [50], making it seem unlikely that their orthologous proteins would fulfil this role in *A. fumigatus*. Both peroxiredoxins were slightly downregulated under oxidative stress, independent of Asp f3. Another peroxiredoxin, Tsa1p was shown to activate Yap1 in specific yeast strains [51]. Asp f3 is most likely not a true homologue of Tsa1p, as the amino acid identity between the two proteins is lower when comparing Asp f3 to Ahp1 (18% and 37%, respectively). In contrast to Tsa1p, Ahp1p is specific for alkylhydroperoxides [52].

We found Asp f3 to be the peroxiredoxin that mediates nuclear retention of Afyap1 under ROS exposure in *A. fumigatus*, indicating that this function may well be conserved for its homologue in *A. nidulans*-PrxA, which was found to be involved in oxidative stress defense and suspected to be the regulatory peroxiredoxin for NapA [49,53]. We speculate that this occurs via direct interaction of the two proteins and that rather its cellular abundance rather than specific biochemical properties of Asp f3 determine this interaction. As Afyap1 was previously found to be dispensable for virulence in a mouse model of aspergillosis our results also suggest that another, Afyap1 independent function of Asp f3 must be essential during infection conditions. A previous study has identified that iron availability may be compromised in response to oxidative stress [54] and Asp f3 may represent a regulatory hub between these interconnected stress responses.

5. Conclusions

Aspergillus fumigatus puts immunocompromised patients at a high risk of severe and often fatal infections. It is thus imperative to find not only more reliable diagnostic tools but also research a more targeted approach for antimycotic treatment. In this study we investigated the in vivo function of Asp f3, a protein that plays an essential in virulence. A transcriptomic approach showed clear differences between the wild type and the highly

ROS-sensitive Δ*asp* f3 mutants. Further investigations led to the conclusion that Asp f3 deficient mutants suffer from a deregulation of the oxidative stress response due to lacking nuclear retention of the regulator Afyap1. However, loss of Afyap1 does not lead to avirulence of *A. fumigatus*, strongly suggesting additional cellular effects upon challenge with ROS.

Supplementary Materials: The following are available online at https://www.mdpi.com/article/10.3390/genes12050668/s1, Figure S1: Overexpression construct for Afyap1^{VENUS}. A Vector Map of gpdA-*Afyap1-VENUS* including the pyrithiamine resistance gene *thiA (ptrA)* gene of *Aspergillus oryzae* as a selectable marker for successful transformation in *A. fumigatus*. Figure S2: Growth of *Aspergillus fumigatus* on minimal media (AMM) with various carbon sources. 2×10^4 conidia of the wild type (D141) and the *asp f3* deletion mutant (Δ*asp f3*) were point-inoculated on AMM with indicated supplements (% *w*/*v*) as carbon/nutrient sources and incubated at 37 °C for 48 h. The *Afyap1* deletion strain (Δ*Afyap1*) and its wild type like parent CEA17Δ*aku*^{BKU80} (CEA17) are shown for comparison. Table S1: Primer list for the generation of *Afyap1*^{VENUS}. Table S2: Results of the gene enrichment analysis (GO-term search, molecular function). Table S3: Results of the gene enrichment analysis (GO-term search, biological process).

Author Contributions: Conceptualization, F.H.; methodology, J.M.B., N.S., T.W., software, T.W., G.P.; formal analysis, J.M.B., N.S., T.W., F.H.; resources, G.P., F.H.; data curation, J.M.B., T.W., G.P.; writing—original draft preparation, J.M.B., N.S., T.W.; writing—review and editing J.M.B., N.S., T.W., G.P., F.H.; visualization, J.M.B., N.S.; supervision, G.P., F.H.; funding acquisition, G.P., F.H.; All authors have read and agreed to the published version of the manuscript.

Funding: This study was supported by the Leibniz Institute for Natural Product Research and Infection Biology–Hans Knöll Institute, Jena and funded by a grant of the Deutsche Forschungsgemeinschaft (DFG, German Research Foundation DFG, HI 1574-2/1).

Institutional Review Board Statement: Not applicable.

Informed Consent Statement: Not applicable.

Data Availability Statement: The sequencing data have been deposited in NCBI's Gene Expression Omnibus database and are accessible through GEO Series accession number GSE173349 (https://www.ncbi.nlm.nih.gov/geo/query/acc.cgi?acc=GSE173349, accessed on 28 February 2021).

Conflicts of Interest: The authors declare no competing interests.

References

1. Brakhage, A.A.; Langfelder, K. Menacing mold: The molecular biology of *Aspergillus fumigatus*. *Annu. Rev. Microbiol.* **2002**, *56*, 433–455. [CrossRef]
2. Latgé, J.-P. Aspergillus fumigatus and aspergillosis. *Clin. Microbiol. Rev.* **1999**, *12*, 310–350. [CrossRef]
3. Tekaia, F.; Latgé, J.-P. *Aspergillus fumigatus*: Saprophyte or pathogen? *Curr. Opin. Microbiol.* **2005**, *8*, 385–392. [CrossRef]
4. Rhodes, J.C. *Aspergillus fumigatus*: Growth and virulence. *Med. Mycol.* **2006**, *44*, S77–S81. [CrossRef] [PubMed]
5. Schrettl, M.; Bignell, E.; Kragl, C.; Joechl, C.; Rogers, T.; Arst, H.N., Jr.; Haynes, K.; Haas, H. Siderophore biosynthesis but not reductive iron assimilation is essential for *Aspergillus fumigatus* virulence. *J. Exp. Med.* **2004**, *200*, 1213–1219. [CrossRef]
6. Willger, S.D.; Grahl, N.; Willger, S.D.; Grahl, N.; Cramer, R.A., Jr. *Aspergillus fumigatus* metabolism: Clues to mechanisms of in vivo fungal growth and virulence. *Med. Mycol.* **2009**, *47*, S72–S79. [CrossRef]
7. Brown, G.D.; Denning, D.W.; Gow, N.A.; Levitz, S.M.; Netea, M.G.; White, T.C. Hidden killers: Human fungal infections. *Sci. Transl. Med.* **2012**, *4*, rv113–rv165. [CrossRef]
8. Asif, A.R.; Oellerich, M.; Amstrong, V.W.; Riemenschneider, B.; Monod, M.; Reichard, U. Proteome of Conidial Surface Associated Proteins of *Aspergillus fumigatus* Reflecting Potential Vaccine Candidates and Allergens. *J. Proteome Res.* **2006**, *5*, 954–962. [CrossRef] [PubMed]
9. Ito, J.I.; Lyons, J.M.; Hong, T.B.; Tamae, D.; Liu, Y.-K.; Wilczynski, S.P.; Kalkum, M. Vaccinations with recombinant variants of *Aspergillus fumigatus* allergen Asp f 3 protect mice against invasive aspergillosis. *Infect. Immun.* **2006**, *74*, 5075–5084. [CrossRef] [PubMed]
10. Diaz-Arevalo, D.; Bagramyan, K.; Hong, T.B.; Ito, J.I.; Kalkum, M. CD4+ T cells mediate the protective effect of the recombinant Asp f3-based anti-aspergillosis vaccine. *Infect. Immun.* **2011**, *79*, 2257–2266. [CrossRef] [PubMed]
11. Hillmann, F.; Bagramyan, K.; Straßburger, M.; Heinekamp, T.; Hong, T.B.; Bzymek, K.P.; Williams, J.C.; Brakhage, A.A.; Kalkum, M. The crystal structure of peroxiredoxin Asp f3 provides mechanistic insight into oxidative stress resistance and virulence of *Aspergillus fumigatus*. *Sci. Rep.* **2016**, *6*, 33396. [CrossRef]

12. Shlezinger, N.; Irmer, H.; Dhingra, S.; Beattie, S.R.; Cramer, R.A.; Braus, G.H.; Sharon, A.; Hohl, T.M. Sterilizing immunity in the lung relies on targeting fungal apoptosis-like programmed cell death. *Science* **2017**, *357*, 1037. [CrossRef]
13. Brakhage, A.A.; Van den Brulle, J. Use of reporter genes to identify recessive trans-acting mutations specifically involved in the regulation of *Aspergillus nidulans* penicillin biosynthesis genes. *J. Bacteriol.* **1995**, *177*, 2781–2788. [CrossRef] [PubMed]
14. Weidner, G.; d'Enfert, C.; Koch, A.; Mol, P.C.; Brakhage, A.A. Development of a homologous transformation system for the human pathogenic fungus *Aspergillus fumigatus* based on the pyrG gene encoding orotidine 5"-monophosphate decarboxylase. *Curr. Genet.* **1998**, *33*, 378–385. [CrossRef]
15. Reichard, U.; Büttner, S.; Eiffert, H.; Staib, F.; Rüchel, R. Purification and characterisation of an extracellular serine proteinase from *Aspergillus fumigatus* and its detection in tissue. *J. Med. Microbiol.* **1990**, *33*, 243–251. [CrossRef]
16. Quan, J.; Tian, J. Circular polymerase extension cloning of complex gene libraries and pathways. *PLoS ONE* **2009**, *4*, e6441. [CrossRef]
17. Ballance, D.; Turner, G. Development of a high-frequency transforming vector for *Aspergillus nidulans*. *Gene* **1985**, *36*, 321–331. [CrossRef]
18. Tilburn, J.; Sarkar, S.; Widdick, D.; Espeso, E.; Orejas, M.; Mungroo, J.; Penalva, M.; Arst, H., Jr. The *Aspergillus* PacC zinc finger transcription factor mediates regulation of both acid-and alkaline-expressed genes by ambient pH. *Embo J.* **1995**, *14*, 779–790. [CrossRef] [PubMed]
19. Cenis, J. Rapid extraction of fungal DNA for PCR amplification. *Nucleic Acids Res.* **1992**, *20*, 2380. [CrossRef] [PubMed]
20. Andrews, S. FastQC: A Quality Control Tool for High Throughput Sequence Data. 2010. Available online: http://www.bioinformatics.babraham.ac.uk/projects/fastqc (accessed on 29 April 2021).
21. Bolger, A.M.; Lohse, M.; Usadel, B. Trimmomatic: A flexible trimmer for Illumina sequence data. *Bioinformatics* **2014**, *30*, 2114–2120. [CrossRef] [PubMed]
22. Kim, D.; Paggi, J.M.; Park, C.; Bennett, C.; Salzberg, S.L. Graph-based genome alignment and genotyping with HISAT2 and HISAT-genotype. *Nat. Biotechnol.* **2019**, *37*, 907–915. [CrossRef] [PubMed]
23. Ritchie, M.E.; Phipson, B.; Wu, D.; Hu, Y.; Law, C.W.; Shi, W.; Smyth, G.K. limma powers differential expression analyzes for RNA-sequencing and microarray studies. *Nucleic Acids Res.* **2015**, *43*, e47. [CrossRef] [PubMed]
24. Robinson, M.D.; McCarthy, D.J.; Smyth, G.K. edgeR: A Bioconductor package for differential expression analysis of digital gene expression data. *Bioinformatics* **2010**, *26*, 139–140. [CrossRef] [PubMed]
25. Anders, S.; Huber, W. Differential expression analysis for sequence count data. *Nat. Preced.* **2010**. [CrossRef]
26. Love, M.I.; Huber, W.; Anders, S. Moderated estimation of fold change and dispersion for RNA-seq data with DESeq2. *Genome Biol.* **2014**, *15*, 1–21. [CrossRef]
27. Abràmoff, M.D.; Magalhães, P.J.; Ram, S.J. Image processing with ImageJ. *Biophotonics Int.* **2004**, *11*, 36–42.
28. Bradford, M.M. A rapid and sensitive method for the quantitation of microgram quantities of protein utilizing the principle of protein-dye binding. *Anal. Biochem.* **1976**, *72*, 248–254. [CrossRef]
29. Lessing, F.; Kniemeyer, O.; Wozniok, I.; Loeffler, J.; Kurzai, O.; Haertl, A.; Brakhage, A.A. The *Aspergillus fumigatus* transcriptional regulator AfYap1 represents the major regulator for defense against reactive oxygen intermediates but is dispensable for pathogenicity in an intranasal mouse infection model. *Eukaryot. Cell* **2007**, *6*, 2290–2302. [CrossRef]
30. Goldberg, I.; Hochman, A. Purification and characterization of a novel type of catalase from the bacterium *Klebsiella pneumoniae*. *Biochim. Biophys. Acta (BBA) Gen. Subj.* **1989**, *991*, 330–336. [CrossRef]
31. Priebe, S.; Kreisel, C.; Horn, F.; Guthke, R.; Linde, J. FungiFun2: A comprehensive online resource for systematic analysis of gene lists from fungal species. *Bioinformatics* **2015**, *31*, 445–446. [CrossRef] [PubMed]
32. Cerqueira, G.C.; Arnaud, M.B.; Inglis, D.O.; Skrzypek, M.S.; Binkley, G.; Simison, M.; Miyasato, S.R.; Binkley, J.; Orvis, J.; Shah, P. The *Aspergillus* Genome Database: Multispecies curation and incorporation of RNA-Seq data to improve structural gene annotations. *Nucleic Acids Res.* **2014**, *42*, D705–D710. [CrossRef] [PubMed]
33. Paris, S.; Wysong, D.; Debeaupuis, J.-P.; Shibuya, K.; Philippe, B.; Diamond, R.D.; Latgé, J.-P. Catalases of *Aspergillus fumigatus*. *Infect. Immun.* **2003**, *71*, 3551–3562. [CrossRef] [PubMed]
34. Takahashi, H.; Kusuya, Y.; Hagiwara, D.; Takahashi-Nakaguchi, A.; Sakai, K.; Gonoi, T. Global gene expression reveals stress-responsive genes in *Aspergillus fumigatus* mycelia. *BMC Genom.* **2017**, *18*, 1–15. [CrossRef] [PubMed]
35. Sugui, J.A.; Kim, H.S.; Zarember, K.A.; Chang, Y.C.; Gallin, J.I.; Nierman, W.C.; Kwon-Chung, K.J. Genes differentially expressed in conidia and hyphae of *Aspergillus fumigatus* upon exposure to human neutrophils. *PLoS ONE* **2008**, *3*, e2655. [CrossRef] [PubMed]
36. Wong, C.M.; Siu, K.L.; Jin, D.Y. Peroxiredoxin-null yeast cells are hypersensitive to oxidative stress and are genomically unstable. *J. Biol. Chem.* **2004**, *279*, 23207–23213. [CrossRef]
37. Tang, H.-M.V.; Siu, K.-L.; Wong, C.-M.; Jin, D.-Y. Loss of yeast peroxiredoxin Tsa1p induces genome instability through activation of the DNA damage checkpoint and elevation of dNTP levels. *PLoS Genet.* **2009**, *5*, e1000697. [CrossRef]
38. West, J.D.; Roston, T.J.; David, J.B.; Allan, K.M.; Loberg, M.A. Piecing together how peroxiredoxins maintain genomic stability. *Antioxidants* **2018**, *7*, 177. [CrossRef]
39. Binder, J.; Shadkchan, Y.; Osherov, N.; Krappmann, S. The essential thioredoxin reductase of the human pathogenic mold *Aspergillus fumigatus* is a promising antifungal target. *Front. Microbiol.* **2020**, *11*, 1383. [CrossRef] [PubMed]

40. Kupfahl, C.; Heinekamp, T.; Geginat, G.; Ruppert, T.; Hartl, A.; Hof, H.; Brakhage, A.A. Deletion of the gliP gene of *Aspergillus fumigatus* results in loss of gliotoxin production but has no effect on virulence of the fungus in a low-dose mouse infection model. *Mol. Microbiol.* **2006**, *62*, 292–302. [CrossRef]
41. Sugui, J.A.; Rose, S.R.; Nardone, G.; Swamydas, M.; Lee, C.-C.R.; Kwon-Chung, K.J.; Lionakis, M.S. Host immune status-specific production of gliotoxin and bis-methyl-gliotoxin during invasive aspergillosis in mice. *Sci. Rep.* **2017**, *7*, 10977. [CrossRef]
42. Sugui, J.A.; Pardo, J.; Chang, Y.C.; Zarember, K.A.; Nardone, G.; Galvez, E.M.; Müllbacher, A.; Gallin, J.I.; Simon, M.M.; Kwon-Chung, K.J. Gliotoxin is a virulence factor of *Aspergillus fumigatus*: gliP deletion attenuates virulence in mice immunosuppressed with hydrocortisone. *Eukaryot. Cell* **2007**, *6*, 1562–1569. [CrossRef]
43. Lewis, R.E.; Wiederhold, N.P.; Chi, J.; Han, X.Y.; Komanduri, K.V.; Kontoyiannis, D.P.; Prince, R.A. Detection of gliotoxin in experimental and human aspergillosis. *Infect. Immun.* **2005**, *73*, 635–637. [CrossRef] [PubMed]
44. Coméra, C.; André, K.; Laffitte, J.; Collet, X.; Galtier, P.; Maridonneau-Parini, I. Gliotoxin from *Aspergillus fumigatus* affects phagocytosis and the organization of the actin cytoskeleton by distinct signalling pathways in human neutrophils. *Microbes Infect.* **2007**, *9*, 47–54. [CrossRef] [PubMed]
45. Cramer, R.A.; Gamcsik, M.P.; Brooking, R.M.; Najvar, L.K.; Kirkpatrick, W.R.; Patterson, T.F.; Balibar, C.J.; Graybill, J.R.; Perfect, J.R.; Abraham, S.N. Disruption of a nonribosomal peptide synthetase in *Aspergillus fumigatus* eliminates gliotoxin production. *Eukaryot. Cell* **2006**, *5*, 972–980. [CrossRef]
46. Hof, H.; Kupfahl, C. Gliotoxin in *Aspergillus fumigatus*: An example that mycotoxins are potential virulence factors. *Mycotoxin Res.* **2009**, *25*, 123. [CrossRef] [PubMed]
47. Gallagher, L.; Owens, R.A.; Dolan, S.K.; O'Keeffe, G.; Schrettl, M.; Kavanagh, K.; Jones, G.W.; Doyle, S. The *Aspergillus fumigatus* protein GliK protects against oxidative stress and is essential for gliotoxin biosynthesis. *Eukaryot. Cell* **2012**, *11*, 1226–1238. [CrossRef]
48. Delaunay, A.; Pflieger, D.; Barrault, M.-B.; Vinh, J.; Toledano, M.B. A thiol peroxidase is an H2O2 receptor and redox-transducer in gene activation. *Cell* **2002**, *111*, 471–481. [CrossRef]
49. Mendoza-Martínez, A.E.; Cano-Domínguez, N.; Aguirre, J. Yap1 homologs mediate more than the redox regulation of the antioxidant response in filamentous fungi. *Fungal Biol.* **2020**, *124*, 253–262. [CrossRef]
50. Mendoza-Martínez, A.E.; Lara-Rojas, F.; Sánchez, O.; Aguirre, J. NapA Mediates a Redox Regulation of the Antioxidant Response, Carbon Utilization and Development in *Aspergillus nidulans*. *Front. Microbiol.* **2017**, *8*, 516. [CrossRef]
51. Okazaki, S.; Naganuma, A.; Kuge, S. Peroxiredoxin-mediated redox regulation of the nuclear localization of Yap1, a transcription factor in budding yeast. *Antioxid Redox Signal.* **2005**, *7*, 327–334. [CrossRef]
52. Park, S.G.; Cha, M.K.; Jeong, W.; Kim, I.H. Distinct physiological functions of thiol peroxidase isoenzymes in *Saccharomyces cerevisiae*. *J. Biol. Chem.* **2000**, *275*, 5723–5732. [CrossRef] [PubMed]
53. Xia, Y.; Yu, H.; Zhou, Z.; Takaya, N.; Zhou, S.; Wang, P. Peroxiredoxin System of *Aspergillus nidulans* Resists Inactivation by High Concentration of Hydrogen Peroxide-Mediated Oxidative Stress. *J. Microbiol. Biotechnol.* **2018**, *28*, 145–156. [CrossRef] [PubMed]
54. Kurucz, V.; Krüger, T.; Antal, K.; Dietl, A.-M.; Haas, H.; Pócsi, I.; Kniemeyer, O.; Emri, T. Additional oxidative stress reroutes the global response of *Aspergillus fumigatus* to iron depletion. *BMC Genom.* **2018**, *19*, 357. [CrossRef] [PubMed]

Supplementary Information - Boysen et al.,

Supplementary Figures

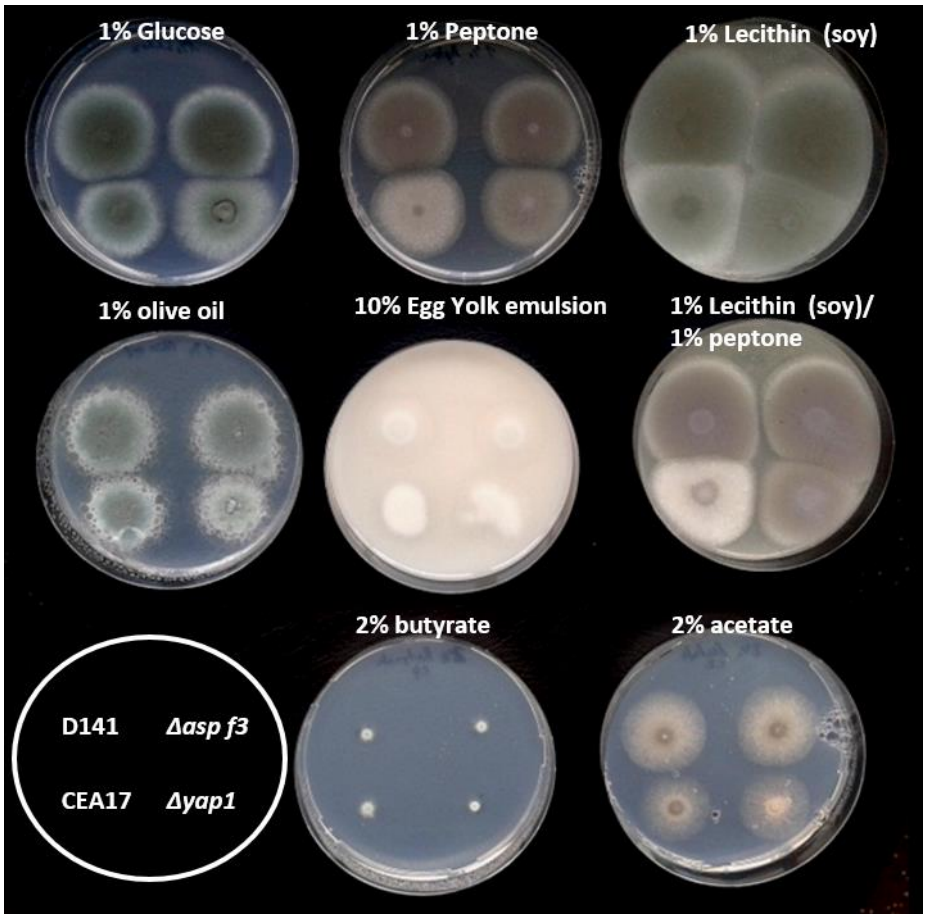

Supplementary Fig. 1: Growth of *Aspergillus fumigatus* on minimal media (AMM) with various carbon sources. 2×10^4 conidia of the wild type (D141) and the *asp f3* deletion mutant (*ΔaspF3*) were point-inoculated on AMM with indicated supplements (% w/v) as carbon/nutrient sources and incubated at 37°C for 48 h. The *Afyap1* deletion strain (*Δyap1)* and its wild type like parent CEA17ΔakuB^{KU80} (CEA17) are shown for comparison.

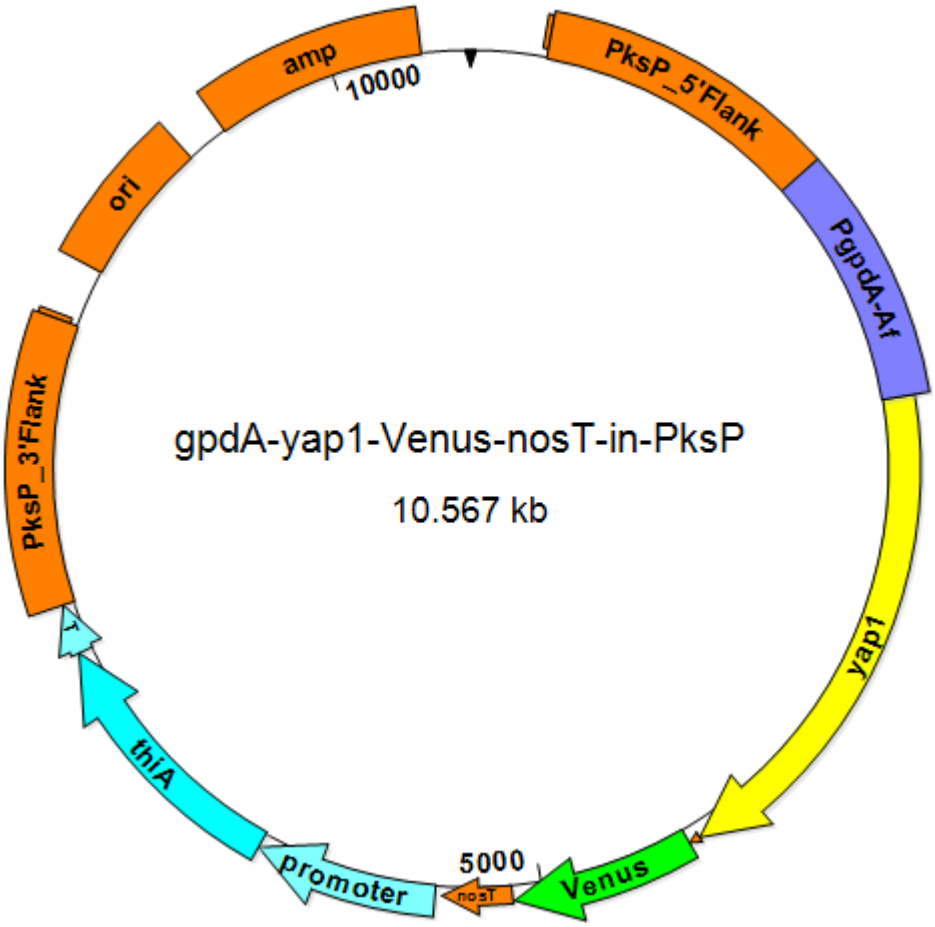

Supplementary Fig. 2: Overexpression construct for *Afyap1*^{VENUS}. **A** Vector Map of gpdA-*Afyap1-VENUS* including the pyrithiamine resistance gene *thiA* (*ptrA*) gene of *Aspergillus oryzae* as a selectable marker for successful transformation in *A. fumigatus*.

Supplementary Table 1: Results of the gene enrichment analysis (GO-term search, molecular function)

GO name	GO ID	Gene ID
oxidoreductase activity	GO:0016491	AFUA_1G02820; AFUA_1G03250; AFUA_1G12460; AFUA_1G14520; AFUA_1G14540; AFUA_1G15610; AFUA_2G00170; AFUA_2G00460; AFUA_2G04060; AFUA_2G04330; AFUA_2G06000; AFUA_2G09580; AFUA_2G16570; AFUA_2G17850; AFUA_3G00180; AFUA_3G00865; AFUA_3G01290; AFUA_3G01780; AFUA_3G03030; AFUA_3G09540; AFUA_3G12270; AFUA_3G15350; AFUA_4G09920; AFUA_4G12990; AFUA_4G14490; AFUA_5G01030; AFUA_5G01250; AFUA_5G01290; AFUA_5G01450; AFUA_5G02020; AFUA_5G07000; AFUA_5G08900; AFUA_5G09910; AFUA_5G10060; AFUA_5G10070; AFUA_5G14000; AFUA_5G14800; AFUA_6G00280; AFUA_6G02820; AFUA_6G09670; AFUA_6G10120; AFUA_6G10720; AFUA_6G13750; AFUA_7G06260; AFUA_7G06420; AFUA_7G06600; AFUA_8G01550; AFUA_8G01630; AFUA_4G09110; AFUA_8G01670; AFUA_6G02280; AFUA_4G10770;
inorganic phosphate transmembrane transporter activity	GO:0005315	AFUA_3G03010; AFUA_7G06350; AFUA_8G01850;
peroxidase activity	GO:0004601	AFUA_3G12270; AFUA_4G09110; AFUA_8G01670; AFUA_6G02280; AFUA_4G10770;
glutathione transferase activity	GO:0004364	AFUA_2G00590; AFUA_3G10830 (GstA); AFUA_6G09690;
FMN binding	GO:0010181	AFUA_1G02820; AFUA_2G04060; AFUA_3G00865; AFUA_5G01450 AFUA_7G06420;

Supplementary Table 2: Results of the gene enrichment analysis (GO-term search, biological process)

GO name	GO ID	Gene ID
Oxidation-reduction process	GO:0055114	AFUA_1G02820 (*Pst2*); AFUA_1G03250; AFUA_1G12460; AFUA_1G14520; AFUA_1G14540; AFUA_1G15610; AFUA_2G00170; AFUA_2G00460; AFUA_2G04060; AFUA_2G04330; AFUA_2G06000; AFUA_2G09580; AFUA_2G16570; AFUA_2G17850; AFUA_3G00180; AFUA_3G00865; AFUA_3G01290; AFUA_3G01780; AFUA_3G02300; AFUA_3G03030; AFUA_3G09540; AFUA_3G10830 (*GstA*); AFUA_3G12270; AFUA_3G15050; AFUA_3G15350; AFUA_4G09920; AFUA_4G12990 (trr1); AFUA_4G14490; AFUA_5G01030; AFUA_5G01250; AFUA_5G01290; AFUA_5G01450; AFUA_5G02020; AFUA_5G07000; AFUA_5G08900; AFUA_5G09910; AFUA_5G10060; AFUA_5G10070; AFUA_5G11320; AFUA_5G14000; AFUA_5G14800; AFUA_6G00280; AFUA_6G02820; AFUA_6G09670 (*GliC*); AFUA_6G09730 (*GliF*); AFUA_6G10120 (*ToxD*); AFUA_6G10720; AFUA_6G13750; AFUA_7G06260; AFUA_7G06420; AFUA_7G06600; AFUA_8G01550; AFUA_8G01630; AFUA_4G09110 (*ccp1*); AFUA_8G01670 (*Cat2*); AFUA_6G02280 (*asp f3*);
mycotoxin biosynthetic process	GO:0043386	AFUA_6G09660 (*GliP*); AFUA_6G09670 (*GliC*), AFUA_6G09680 (*GliM*), AFUA_6G09690 (*GliG*), AFUA_6G09710 (*GliA*), AFUA_6G09720 (*GliN*), AFUA_6G09730 (*GliF*),
transmembrane transport	GO:0055085	AFUA_1G10390; AFUA_1G12620; AFUA_1G13350; AFUA_1G13360; AFUA_1G17160; AFUA_2G02040; AFUA_2G05840; AFUA_2G16860; AFUA_3G03010; AFUA_3G11490; AFUA_3G12010; AFUA_3G14560; AFUA_3G15250; AFUA_4G00120; AFUA_4G01050; AFUA_4G12260; AFUA_4G13820; AFUA_4G13830; AFUA_5G00790; AFUA_5G07970; AFUA_5G11980; AFUA_6G03860; AFUA_6G04360; AFUA_6G09710 (GliA); AFUA_6G12550; AFUA_7G00390; AFUA_7G05100; AFUA_7G06350; AFUA_7G06390; AFUA_8G00770; AFUA_8G01850; AFUA_8G04470; AFUA_8G06610
phosphate ion transport	GO:0006817	AFUA_3G03010, AFUA_7G06350, AFUA_8G01850,
response to oxidative stress	GO:0006979	AFUA_3G12270, AFUA_4G09110 (ccp1), AFUA_8G01670 (Cat2), AFUA_4G10770,

Supplementary Table 3: Primer list for the generation of *Afyap1*^{VENUS}

Primer	Sequence	Application
PksP_5'F_OH_BB_F	GCCTCTTCGCTATTACGCCAGCAATTCGAGGATGTCTTCCG	Amplification of PksP 5'Flank
PksP_5'F_OH_gpdA_R	CGGAACAATGTTAATCCACAAACTACGGAGTAGTGATTATCCTGGACC	Amplification of PksP 5'Flank
PksP_3'F_OH_Pth_F_neu	GGGGCATTCTAGAATAATTATGTGTAACAAGAAAGAGGGGTGGAGTTGTGCATACC	Amplification of PksP 3'Flank
PksP_3'F_OH_BB_R_neu	GTTGGCCGATTCATTAATGCAGTTCATTGGGGGCGGTTACTCG	Amplification of PksP 3'Flank
PksP_5'F_F	CAATTCGAGGATGTCTTCCG	Generation of Afyap1-VENUS overexpression fragment
PksP_3'F_R	GGCTTTGTCCAATCACATCCAGC	Generation of Afyap1-VENUS overexpression fragment
PgpdA_F_1	GTAGTTTGTGGATTAACATTGTTCCG	Amplification of *gpdA*-promoter sequence
P_gpdA_rev	TGTGTAGATTCGTCTGGTACTGAGC	Amplification of *gpdA*-promoter sequence
Yap1_F	ATGGCGGACTACAATACTC	Amplification of Afyap1-Gene
Yap1_OH_Link_V_R	CCTCCGCCAGATCCGCCGCCTCCTTTGACGCGACCCATGATGTCC	Amplification of Afyap1-Gene
pUC_BB_fw	CTGCATTAATGAATCGGCCAACGC	Generation of pUC-vector backbone
pUC_BB_rev	CTGGCGTAATAGCGAAGAGGC	Generation of pUC-vector backbone
VENUS_Link_Fwd	GGAGGCGGCGGATCTGGCGGAGG	Generation of combined Linker-VENUS and pyrithiamine resistance cassette
Pth fwd	TCTTTCTTGTTACACATAATTATTCTAGAATGCCCC	Generation of combined Linker-VENUS and pyrithiamine resistance cassette

3.3 Manuscript 3 - Natural products in the predatory defence of the filamentous fungal pathogen *Aspergillus fumigatus*

FORMULAR 1

Manuskript Nr. 3

Titel des Manuskriptes: Natural products in the predatory defence of the filamentous fungal pathogen *Aspergillus fumigatus*

Autoren: Jana Boysen, Nauman Saeed, Falk Hillmann

Bibliographische Informationen: Boysen, J. M., Saeed, N., & Hillmann, F. (2021b). Natural products in the predatory defence of the filamentous fungal pathogen *Aspergillus fumigatus*. Beilstein journal of organic chemistry, 17(1), 1814-1827.
https://doi.org/10.3762/bjoc.17.124

Die Kandidatin ist

☐ Erstautor/-in, ☒ Ko-Erstautor/-in, ☐ Korresp. Autor/-in, ☐ Koautor/-in.

Status: publiziert

Anteile (in %) der Autoren / der Autorinnen an der Publikation

Autor/-in	Konzeptionell	Datenanalyse	Experimentell	Verfassen des Manuskriptes	Bereitstellung von Material
Jana M. Boysen	40 %	50%	-	45 %	-
Nauman Saeed	30%	50%	-	30 %	-
Falk Hillmann	30%	0%	-	25%	-

BEILSTEIN JOURNAL OF ORGANIC CHEMISTRY

Natural products in the predatory defence of the filamentous fungal pathogen *Aspergillus fumigatus*

Jana M. Boysen[‡1,2], Nauman Saeed[‡1,2] and Falk Hillmann[*1]

Review

Open Access

Address:
[1]Junior Research Group Evolution of Microbial Interactions, Leibniz-Institute for Natural Product Research and Infection Biology – Hans Knöll Institute (HKI), Beutenbergstr. 11a, 07745 Jena, Germany and [2]Institute of Microbiology, Friedrich Schiller University Jena, Jena, Germany

Email:
Falk Hillmann[*] - falk.hillmann@leibniz-hki.de

* Corresponding author ‡ Equal contributors

Keywords:
amoeba predation; *Aspergillus fumigatus*; fungal ecology; non-ribosomal peptides; polyketides; secondary metabolism; virulence

Beilstein J. Org. Chem. **2021,** *17,* 1814–1827.
https://doi.org/10.3762/bjoc.17.124

Received: 15 January 2021
Accepted: 14 July 2021
Published: 28 July 2021

This article is part of the thematic issue "Chemical ecology".

Guest Editor: C. Beemelmanns

Abstract

The kingdom of fungi comprises a large and highly diverse group of organisms that thrive in diverse natural environments. One factor to successfully confront challenges in their natural habitats is the capability to synthesize defensive secondary metabolites. The genetic potential for the production of secondary metabolites in fungi is high and numerous potential secondary metabolite gene clusters have been identified in sequenced fungal genomes. Their production may well be regulated by specific ecological conditions, such as the presence of microbial competitors, symbionts or predators. Here we exemplarily summarize our current knowledge on identified secondary metabolites of the pathogenic fungus *Aspergillus fumigatus* and their defensive function against (microbial) predators.

Introduction

To thrive in their natural habitats all organisms from bacteria and fungi to plants and animals need access to sufficient nutritional sources and have to defend themselves against both, competitors and predators (Figure 1). Fungi are ubiquitous, living a mostly saprophytic, parasitic or symbiotic lifestyle in various habitats including soil, water, other organisms and even salt-flats and arctic glaciers [1,2]. As fungi are not able to physically leave their habitats they must rely on mechanical barriers, physiological adaptations and chemical defence mechanisms to optimize their living conditions and resist competitors, parasites and predators [3-5]. These bioactive compounds are often considered as secondary metabolites (SM) which are involved in communication, symbiotic interactions, pathogenicity or chemical defence, e.g., by toxin production [6]. With penicillin

Beilstein J. Org. Chem. **2021,** *17,* 1814–1827.

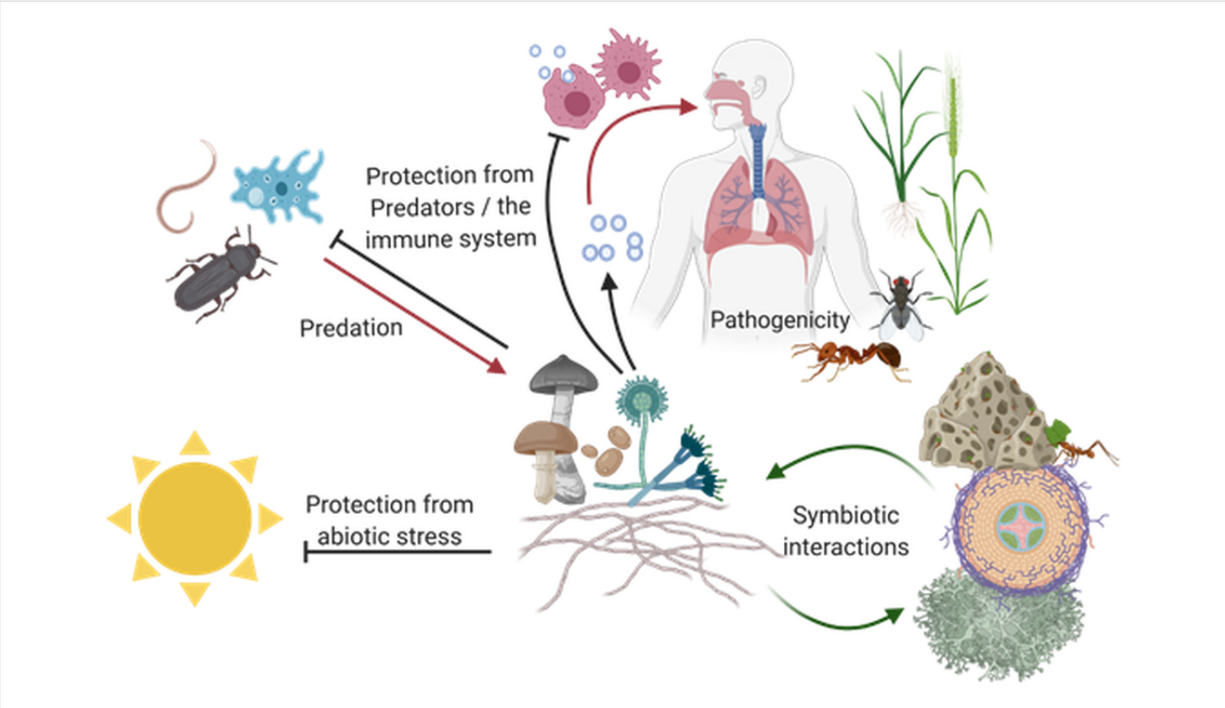

Figure 1: Schematic overview of fungal interactions in the environment. Fungi can be found in essentially all terrestrial habitats comprising saprophytic, parasitic, symbiotic or predatory lifestyles [6]. Independent of their ecological niche, they have to protect themselves against abiotic stresses, competitors and predators while also communicating with their host or partners during parasitic/pathogenic or symbiotic interactions. This figure was created with biorender.com.

as the prime example fungal secondary metabolites have raised scientific and pharmaceutical interests for nearly one century. Today's sequencing and bioinformatic analyses of fungal genomes revealed that the genetic potential far exceeds the number of known metabolites and the interest of scientists to gain access to them remains high [7-9].

Genes associated with these bioactive compounds are often organized in biosynthetic gene clusters (BGCs) which are physically linked, commonly regulated and often belong to a few distinct classes of molecules like non-ribosomal peptides (NRP), polyketides (PK), terpenes or indole alkaloids [10,11]. The vast majority of fungal BGCs is found in the genomes of members of the Basidiomycota and Ascomycota including the genus *Penicillium* in which the first BGC was identified in 1990 [12-14]. *Penicillium* species belong to the Pezizomycotina, a subdivision within the Ascomycotina including several species that are closely associated with humans at many different levels. Aside from being a source of many medically relevant compounds including antibiotics like penicillin they offer food sources in the form of naturally grown truffles (e.g., *Tuber melanosporum*) or recently cultivated meat alternatives like Quorn® (*Fusarium venenatum*) [15-17]. Species of *Aspergillus*, such as *Aspergillus fumigatus, Aspergillus flavus* and *Aspergillus niger* can affect the health of humans, plants and lifestock by acting as pathogens. It is firmly established that the ability to produce mycotoxins contributes to the virulence potential of these fungi, but as they all thrive in environmental reservoirs they must also provide an ecological advantage to their producer [18].

Indeed, many of these pathogenic fungi also produce compounds with antibacterial, antifungal and insecticidal properties to ward of both competitors and predators. The mycotoxins aflatoxin B1 (**1**) from *Aspergillus flavus* and patulin (**2**), produced by *Aspergillus* and *Penicillium* species, exhibit insecticidal activity against *Drosophila melanogaster* and might thus prevent feeding competition [19-21] (Figure 2). But not only mycotoxins protect from predation: *A. flavus* sclerotia are protected from sap beetles by asparasone and *Neurospora crassa's* neurosporin A prevents springtail grazing [22,23]. Grazing by *Folsomia candida* springtails on *Fusarium graminearum* induces several metabolites, of which especially the bisnaphthopyrone pigment aurofusarin (**3**) was shown to have antifeedant effects not only on springtails but also on mealworm *Tenebrio molitor* and woodlouse *Trichorhina tomentosa*. Not only *Fusarium* species produce bisnaphthopyrones like aurofusarin but also *Aspergillus* and *Penicilllium* species produce these metabolites which show antifeedant effects on a wide variety of arthropods [24].

Beilstein J. Org. Chem. 2021, 17, 1814–1827.

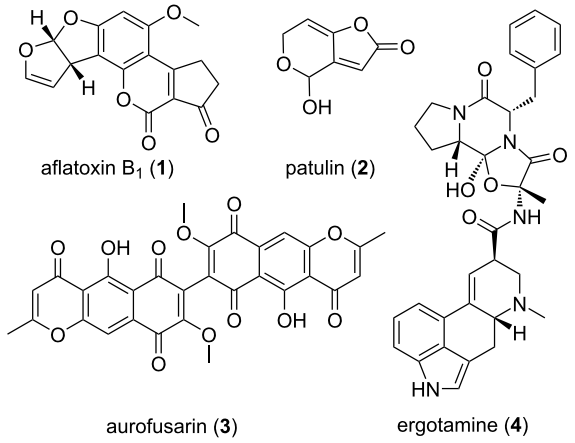

Figure 2: Fungal derived bioactive natural compounds with ecological and/or economic relevance.

Some fungal compounds can have deleterious effects on humans, livestock or crops, like the ergot alkaloids, e.g., ergotamine (**4**) present in the sclerotia of the ergot fungus *Claviceps purpurea*, which can contaminate grain products like flour. In the middle ages these contaminations caused vast epidemics of "St. Anthony's fire", a severe poisoning which could lead to death and mutilation in humans. However, midwives already knew the therapeutic potential of ergot alkaloids as early as 1582 and used it for abortion or to aid childbirth. The ecological significance of ergot alkaloids remains unclear, but they are assumed to be a feeding deterrent due to their toxicity and bad taste [25-28].

To trigger the synthesis of new SMs a number of approaches have been exploited so far, including co-cultivation with other species [9]. Amoebae offer promising possibilities to not only discover new SM but also to discover their ecological role as amoeba often cohabitate with fungi in their natural environments, especially the soil. Some, like *Protostelium aurantium*, were recently found to be exclusively fungivorous, feeding on both yeasts and filamentous fungi alike [29]. Additionally, amoeba closely resemble human phagocytic cells and the interactions of fungi and amoeba often parallels interactions of fungi and macrophages as was shown for *Aspergillus fumigatus* and its interactions with *Acanthamoeba castellanii* [30]. Thus, the adaptations that protect fungi against amoeba that were gained in the 'environmental school of virulence' might also protect fungi from the immune system [31]. Therefore, to study their interactions with human pathogenic fungi like *A. fumigatus*, one of the most common airborne fungal pathogens, might lead to new insight in virulence mechanisms and the role of SMs therein [32]. The aim of this review is to depict the fungal secondary metabolite potential and its role in an ecological context using *A. fumigatus* as an example because of its high medical importance and its diverse profile of secondary metabolites which seems to fulfil dual roles: targeting innate immune cells during virulence and protect from environmental predators in natural habitats.

Review

Natural products of Aspergillus fumigatus

The genus *Aspergillus* comprises a large number of species that are not only of scientific but also of pharmaceutical and commercial interest. While the non-pathogenic *A. niger* is used as industrial workhorse, for example in the production of citric acid, other representatives contaminate food stocks with mycotoxins (*A. flavus*) or can cause severe infections (*A. fumigatus*, *A. terreus*). Despite their different role for humans, they commonly share a high potential for the production of secondary metabolites, measured by the predicted number of secondary metabolite gene clusters identified by numerous genome sequencing projects. Due to its clinical importance as an opportunistic pathogen *A. fumigatus* is of great interest among them [33,34].

As a saprophytic decomposer of organic material in the soil, *A. fumigatus* encounters not only numerous competitors but also fungivorous predators like amoebae (e.g., *P. aurantium*), nematodes (e.g., *Aphelenchus avenae*) or arthropods like insects, mites and springtails (e.g., *F. candida*) [35-39]. However, the fungus may also act as a pathogen causing often lethal infections in immune-compromised patients, and thus its secondary metabolism was extensively studied in recent years [38,40,41]. Analysis of the *A. fumigatus* genome sequence and metabolomics revealed its potential to synthesize more than 200 compounds and the presence of over 30 secondary metabolite associated gene clusters [7,42-44]. The products of many of those gene clusters are already known and span the whole range of secondary metabolite classes. Table 1 provides an overview of the major secondary metabolites from *A. fumigatus* and lists their ecological roles as well as their impact on virulence.

Gliotoxin

Gliotoxin (GT, **5**) is the non-ribosomal peptide (NRP) derived epipolythiodioxopiperazine (ETP's) class toxin of several fungal genera including *Aspergillus*, *Penicillium*, *Trichoderma*, and *Leptosphaera* (Figure 3) [112]. Among the ascomycetes, *A. fumigatus* may well be the major GT producer and the identification of its heterocyclic structure by Bell and colleagues in 1958 builds the foundation to understand its role in invasive aspergillosis [113]. In *A. fumigatus* 13 genes form a 28 kb biosynthetic cluster of gliotoxin, of which *gliZ* (a zinc-finger transcription factor) and *gliP* (an NRPS) together with global regulator LaeA regulate its expression at the genomic level

Beilstein J. Org. Chem. **2021,** *17,* 1814–1827.

Table 1: Overview of *Aspergillus fumigatus* secondary metabolites and their roles during virulence and in their ecological context.

Metabolite	Class	Virulence factor	Role in virulence	Ecological role/ toxicity	Reference
DHN-melanin	polyketide, phenolic polymer, pigment	yes	- prevents recognition by the immune system - prevents phagosomal acidification	- protection against UV-stress - prevents recognition by predators (e.g., amoeba) - prevents phagolysosome maturation	[45-50]
endocrocin	polyketide, pigment	–	- inhibits chemotaxis of neutrophils	- protection against UV-stress	[47,51-53]
ferricrocin	siderophore	yes	- iron homeostasis	- iron homeostasis	[54,55]
fumagillin	mero-terpenoid	–	- inhibitor of phagocyte activity - damages epithelial cells - inhibitor of methionine aminopeptidase	- cilioinhibitory - antimicrobial - antiprotozoal	[56-62]
fumigaclavine	ergot alkaloid	–	- reduces production of TNF-α – toxic to mammalian cells	- antibacterial - insecticidal - antifeedant	[63-67]
fumipyrrole	non-ribosomal peptide	–	–	- enhances growth and sporulation	[68]
fumiquinozalines	tryptophan derived peptidyl alkaloid	–	not determined	- antibacterial - antifungal	[69-72]
fumisoquin	isoquinolone alkaloid	–	not determined	- inhibits bacterial replication	[73,74]
fumitremorgin	indole diketo-piperazine alkaloid	–	- inhibitor of breast cancer resistance protein	- antifungal - antifeedant - insecticidal	[72,75]
fusarinine C/ triacetylfusarinine C	siderophore	yes	- iron acquisition	- iron acquisition	[54,55,76]
fungisporin	non-ribosomal peptide	–	not determined	- antibacterial	[41,77]
gliotoxin	epipolythiopiperazine	yes	- inhibition of immune response	- cilioinhibitory - antimicrobial - protects against amoeba predation	[78-82]
helvolic acid/ protostadienol	fusidane-type steroid	–	- cilioinhibitory	- antibacterial - antiprotozoal - antifungal	[72,83-88]
hexadehydro-astechrome	non-ribosomal peptide, tryptophan-derived iron(III) complex	yes	- iron homeostasis	- iron homeostasis	[89,90]
neosartoricin/ fumicycline	prenylated polyketide, meroterpenoid	–	- inhibition of immune response	not determined	[41,91,92]
nidulanin A	tetracyclo-peptide/ isoprene	–	not determined	not determined	[93]
pseurotin	heterocyclic γ-lactam	–	- inhibition of IgE production	- antibacterial	[94-97]
pyripyropene A	sesqui-terpenoid	–	- acetyltransferase inhibitor	- nematicide - insecticidal	[98-100]
sphingofungin A–D	sphingosine-like compound	not determined	- inhibition of serine palmitoyl transferase	- antifungal	[101-104]
trypacidin	polyketide, anthraquinone, pigment	–	- toxic to lung cells	- antiprotozoal - antiphagocytic	[53,105-107]
verruculogen	indole diketo-piperazine alkaloid	not determined	- alters electrophysical properties of human nasal epithelial cells	- antifungal	[72,108-110]

Beilstein J. Org. Chem. **2021,** *17,* 1814–1827.

Table 1: Overview of *Aspergillus fumigatus* secondary metabolites and their roles during virulence and in their ecological context. (continued)

xanthocillin	tyrosine-derived isocyanide	–	- copper homeostasis	- copper homeostasis	[111]

[112,114-116] (Figure 3). Whereas GliT (a gliotoxin oxidoreductase) catalyses the oxidation of reactive dithiol gliotoxin (**6**) to gliotoxin and a distantly localized *S*-adenosylmethionine-dependent gliotoxin bisthiomethyltransferase (*GtmA*) is responsible for the formation of bis(methyl)gliotoxin (**7**) to maintain the GT concentration at sub-lethal levels via redox cycling and S-methylation of active disulfides in GT, respectively [117,118]. Furthermore, in terms of exogenous factors, not only GT itself but several other biotic and abiotic factors, including neutrophilic granulocytes, media composition, pH, temperature and aeration, are known to regulate gliotoxin biosynthesis [115,119,120].

The biological activity of ETP's like gliotoxin is mediated by the active disulfide bridge that targets vulnerable thiols or catalyses oxidative burst formation via redox cycling [78]. In previous studies, these cytotoxic activities of gliotoxin were shown to be immunosuppressive in humans [79-81]. Sugui and colleagues (2007) also demonstrated that a gliotoxin lacking strain of *A. fumigatus* is avirulent in mice treated with cortisone acetate [121]. Nevertheless, the fact that gliotoxin is not only produced by pathogenic *A. fumigatus* suggests a role of gliotoxin in natural microenvironments. In vitro studies have also revealed the amoebicidal activities of gliotoxin on its natural co-inhabitant *Dictyostelium discoideum* [82]. However, these pathogenic activities sometimes prove to be beneficial for other co-habitants, comparable to how *Trichoderma virens* protects cotton seedlings from its pathogen *Pythium ultimum* [122].

Trypacidin

The spore-born toxin trypacidin (**8**) is a polyketide that belongs to an anthraquinone-derived class of secondary metabolites (Figure 4) [107]. In *A. fumigatus*, the trypacidin biosynthetic cluster (*tpc*) is comprised of 13 genes that spans over a 25 kb sub-telomeric region on chromosome 4 [53,105]. It is one of the conidial secondary metabolites that are regulated by global transcriptional regulators LaeA and BrlA in *A. fumigatus* [51,123-126]. Nevertheless, trypacidin production is also regulated by cluster specific transcriptional regulators TpcD/E [53]. Though the precise mechanism of action of trypacidin remains to be elucidated, it was shown to exhibit antiprotozoal, antiphagocytic and cytotoxic activities in vitro. Gauthier and colleagues (2012) have shown that in lung cells trypacidin mediates in necrosis-mediated death [107]. In another study, absence of trypacidin was shown to be linked with increased phagocytic rates in murine alveolar macrophages and phagocytic amoeba *D. discoideum*. The authors further showed that trypacidin reduced the viability of amoebae which signifies its role in conidial protection in the environment [105].

Fumagillin

Fumagillin (**9**) belongs to the meroterpenoid class of secondary metabolites. It was discovered in 1949 from *A. fumigatus* [127].

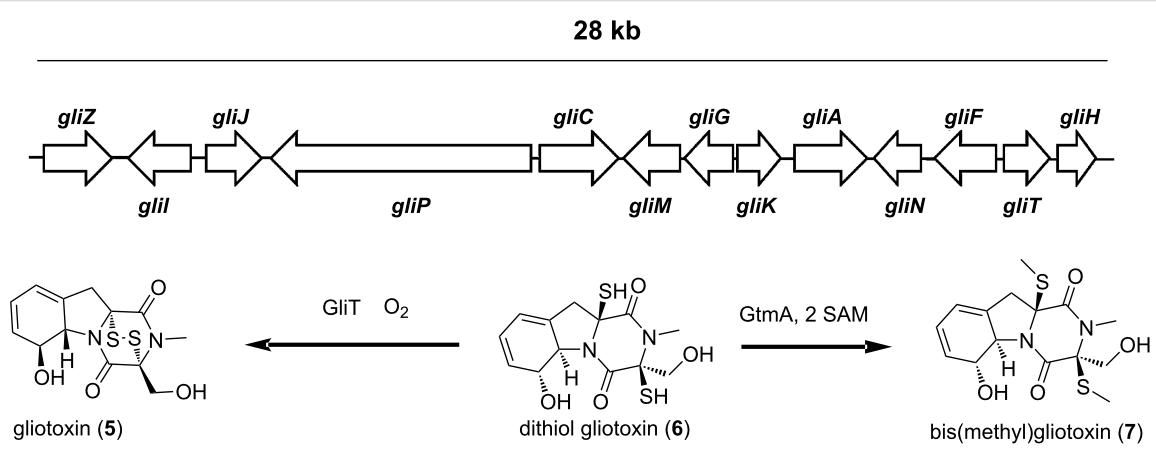

Figure 3: Gliotoxin biosynthetic gene cluster and it major biosynthetic transformations: Gliotoxin (**5**) is the oxidized form of dithiol-gliotoxin (**6**) catalysed by the gliotoxin oxidoreductase GliT. Dithiol-gliotoxin can be methylated to bis(methyl)gliotoxin (**7**) via the S-adenosyl-methionine (SAM) dependent bisthiomethyltransferase GtmA which is not part of the *gli*-cluster.

Beilstein J. Org. Chem. **2021,** *17,* 1814–1827.

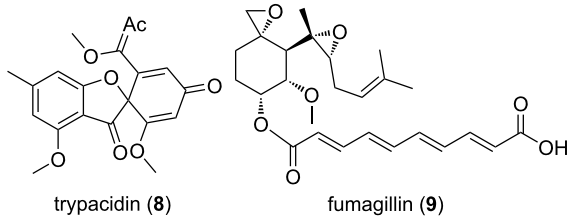

Figure 4: Amoebicidal secondary metabolites trypacidin and fumagillin of *Aspergillus fumigatus*.

Strikingly, unlike other secondary metabolite synthesizing clusters, the fumagillin biosynthetic cluster is intertwined with the pseurotin gene cluster and designated as the *fma* cluster [95,128]. Wiemann and colleagues (2013) have shown the existence of a similarly intertwined pattern in both close and distant relatives of *A. fumigatus*, and therefore suggested a role of these metabolites in survival. In *A. fumigatus*, the *fma* cluster is located on the sub-telomeric region on chromosome 8 and is comprised of 15 genes. At the cellular level fumagillin is regulated by both cluster specific regulator FumR (FapR) and global regulator LaeA [95].

Fumagillin consists of a cyclohexane ring and decatetraenedioic acid connected via an ester bond. There is also a methoxy group, an epoxide and a terpene derived aliphatic chain that contains another epoxide, linked to cyclohexane. These unstable di-epoxides are responsible for the biological activity of fumagillin, which targets the active site of the methionine aminopeptidase type-2 (MetAP-2) enzyme [129]. MetAP-2 is involved in cell proliferation, translation and post-translational modifications of nascent polypeptides and is therefore essential for cell viability [130,131]. Additionally, fumagillin is also known to be overproduced upon caspofungin treatment and damage to the cell walls while fumagillin aids in immune evasion by reducing ROS levels, degranulation and actin filamentation in neutrophils [60,132]. In nature, several fungal species are known to produce caspofungin which could trigger fumagillin production in natural environments [132,133]. *A. fumigatus* possesses an additional MetAP-2 gene in the *fma* cluster that protects itself against its own toxin [134]. Fumagillin has therapeutic potential for the treatment of intestinal microsporidiosis and nosemiasis in honey bees [58,135]. Overall, antibiotic, immunosuppressive, antitumor and antiangiogenic properties have been attributed to fumagillin [129,136-140]. Specific antibiotic activities were demonstrated against the pathogen *Entamoeba histolytica* and later against eukaryotic parasites such as *Trypanosoma* and *Plasmodium* the causative agent of malaria [141,142]. In comparison to gliotoxin, we found only minor cytotoxic activities of fumagillin against the model amoebae *D. discoideum* [82]. It could still be conceivable that other amoeba could reveal higher sensitivity, but tests against the fungivorous amoeba *P. aurantium* were not yet conducted.

DHN-melanin

Melanins are a heterogenous group of hydrophobic phenolic polymers that are found in a range of organisms including bacteria, plants, fungi and even animals. The melanin pigments are of mostly dark colours like black or brown and are associated with virulence in plant- and animal-pathogenic fungi [143-145]. Three types of melanins are known to be produced by fungi of which *A. fumigatus* is able to produce two – pyomelanin and dihydroxynaphthalene melanin (DHN-melanin). While the water-soluble pyomelanin is synthesized via the tyrosine degradation pathway, the DHN-melanin synthesis relies on its own SM-gene-cluster [146-148]. The DHN-melanin of *A. fumigatus* is a heteropolymer formed through the polymerization of 1,8-dihydroxynaphtalene (1,8-DHN) monomers (**10**) and is responsible for the unique greyish-green colour of *A. fumigatus* conidia (Figure 5).

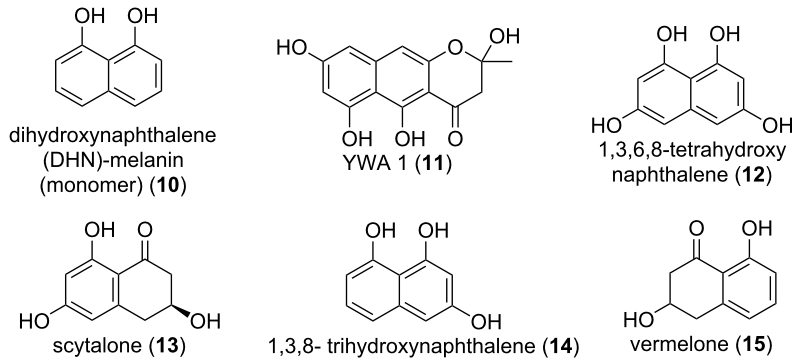

Figure 5: Intermediates of the DHN-melanin biosynthesis in *Aspergillus fumigatus*.

Beilstein J. Org. Chem. **2021,** *17,* 1814–1827.

The genetics and biochemistry of its biosynthesis are well established: the 19 kb gene cluster contains 6 genes and lies downstream of the conidiation pathway. The polyketide synthase PksP combines the starter units acetyl-CoA and malonyl-CoA into the heptaketide naphthopyrone YWA1 (**11**). The hydrolytic activity of Ayg1 shortens the heptaketide to the pentaketide 1,3,6,8-tetrahydroxynaphthalene (1,3,6,8-THN) (**12**) and is further reduced by reductase Arp2 to scytalone (**13**), which in turn is dehydrated by Arp1 to 1,3,8-trihydroxynaphthalene (1,3,8-THN) (**14**). Again, Arp2 reduces 1,3,8-THN to vermelone (**15**) before it is dehydrated to 1,8-dihydroxynaphthalene (1,8-DHN) (**10**) by Abr1, a multi-copper reductase. In a last step polymerization of 1,8-DHN monomers is facilitated by the laccase Abr2 [45,149-152]. Knock out mutants of either *ayg1*, *arp2*, or *abr2* lead to different coloured conidia while loss of *pksP* aborts DHN-melanin synthesis completely which leads to white spores [45]. DHN-melanin is a heterogeneous polymer, as such it does not have a unique structure. Its insolubility aggravates any structural analyses of the deciphering of repetitive motives. However, there were studies doing either computational predictions or artificial oxidative polymerization studies of 1,8-DHN monomers [144,153].

Next to offering the conidia protection from UV radiation, DHN-melanin was shown to be a key factor to survival during both predation and virulence. When preyed upon by fungivorous amoeba like *P. aurantium* melanised conidia where not only internalized less than Δ*pksP* conidia but were also able to prevent maturation of phagolysosomes [50,147]. During infection DHN-melanin masks the pathogen-associated molecular patterns on the spore-surface and is thus less likely to be recognized by the immune system. The Δ*pksP* strain lacks this protection and is more easily recognized by the immune system, thus triggering a stronger immune response, including a higher pro-inflammatory response and increased recognition and ingestion by phagocytes rendering the Δ*pksP* strain less virulent. Additionally, melanised conidia are more likely to survive internalization by lung epithelial cells [147,154,155]. Although DHN-melanin is generally associated with immune evasion it was recently found to be recognized in higher animals via the C-type lectin receptor (MelLec) which interacts with the naphthalenediol domain of DHN-melanin. Additionally, the surfactant protein D (SP-D), a soluble C-type lectin receptor (CLR), is also able to recognise DHN-melanin and opsonize it to increase the immune response. However, MelLec receptors are only present on some endothelial and myeloid cells [156,157].

Fumigaclavines

Fumigaclavine C (**19**) is a tryptophan-derived indole alkaloid which was so far only shown to be produced by *A. fumigatus* while other fumigaclavines can for example also be found in *Penicillium* ssp. (fumigaclavine A (**18**) and B (**17**)) [66,158]. In all fungi, alkaloid biosynthetic pathways share a common basis, starting with the prenylation of L-tryptophan to dimethylallyltryptophan (DMAT). During several steps DMAT is converted to chanoclavine-I aldehyde, the last mutual intermediate. Branching into different pathways after this intermediate is mainly due to differences in the function of EasA, the enzyme catalysing the next biosynthetic step. In *A. fumigatus* EasA acts as a reductase and after additional steps chanoclavine-I aldehyde is converted into festuclavine (**16**) (Figure 6). Festuclavine is then oxidized to fumigaclavine B (**17**) which in turn is acetylated to fumigaclavine A (**18**). Finally a reverse prenylation of fumigaclavine A leads to fumigaclavine C (**19**), the final product of fumigaclavine biosynthesis [159]. Biosynthesis of the intermediate festuclavine as well as fumigaclavines A–C is dependent on LaeA regulation [124].

Its numerous bioactive effects hold the potential for a pharmaceutical use since it was shown to be an effective inhibitor of tumor necrosis factor-alpha (TNF-α) production by preventing the activation of TLR4 by lipopolysaccharide (LPS) and was thus proposed for potential use against atherosclerosis [67]. Furthermore fumigaclavine C has also proven effective against MCF-7 breast cancer cells by arresting the cell cycle and promoting apoptosis while showing no cytotoxicity against RAW 264.7 cells, thus demonstrating their selectivity [65,67]. Further, fumigaclavine was shown to exhibit antibacterial properties and to contribute to virulence in the model insect *Galleria mellonella* [66].

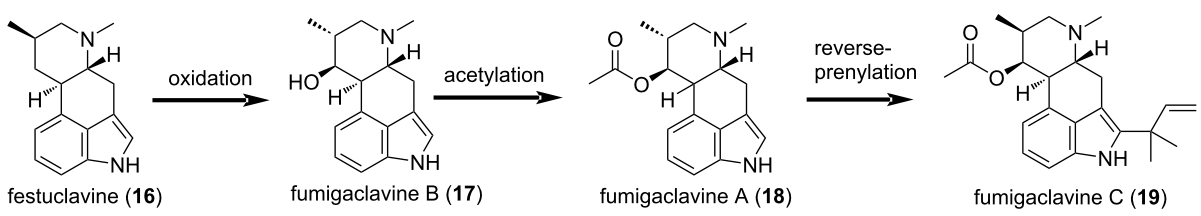

Figure 6: Intermediates and products of the fumigaclavine C biosynthesis.

Beilstein J. Org. Chem. **2021,** *17,* 1814–1827.

Fumitremorgins

The class of fumitremorgins comprises several diketopiperazine alkaloids which are tremorgenic mycotoxins. However, there are several fumitremorgin-like indole alkaloids including tryprostatins, spiro- and cyclotryprostatins and verruculogen besides fumitremorgins themselves. They occur most often in *Aspergillus* and *Penicillium* species [160]. Fumitremorgin A (**20**), B (**21**) and C (**22**) can all be found in *A. fumigatus* (Figure 7). They are based on the precursers L-tryptophan and L-proline and are further derived from breviamide F, proposedly via tryprostatin B which is hydroxylated and methylated to tryprostatin A. Oxidative closure of the ringstructure then results in fumitremorgin C. Further modification of the structure leads to fumitremorgin B and verruculogen, which shares the same pathway [97,160-162]. Which enzyme is responsible for the conversion of verruculogen to fumitremorgin A remains to be elucidated. Like several other clusters, the biosynthesis of fumitremorgins is dependent on LaeA [124].

Fumitremorgin B was shown to have antifungal properties against phytopathogenic fungi, antifeedant properties against army-worm larvae and toxic on brine shrimp [72]. It was further shown to be cytotoxic and inhibiting cell cycle progression at G2/M phase [163]. Fumitremorgin C was shown to effect mammalian cells and inhibit the breast cancer resistance protein which imparts multidrug resistance and thus resistance to chemotherapeutics in breast cancer treatment [75,164].

Helvolic acid

Helvolic acid (HA) (**23**) is a fusidane-type antibiotic that belongs to the triterpenoid class of secondary metabolites. Originally, it was discovered from *A. fumigatus* but later several other members of the sub phylum Pezizomycotina were also found to be HA producers [165-168]. In *A. fumigatus*, the biosynthetic cluster of HA is comprised of 9 genes that spans over a 16.3 kb region on chromosome 4 (Figure 8). The cluster contains an oxidosqualine cyclase (*helA*), three Cytochrome P450 (*helB1*, *helB2*, *helB3*), a short-chain dehydrogenase/reductase (*helC*) and two acetyltransferases (*helD1*, *helD2*) and a 3-ketosteroid-Δ^1-dehydrogenase [83,169]. Helvolic acid is a tetracyclic compound containing two keto groups, two acetates and one carboxyl group which do not equally contribute to function [169]. Lv and colleagues have shown that the presence of both the C-20 carboxyl group and the 3-keto group are crucial for its antibacterial activity whereas, acetylation of the C-6 hydroxy group reduces the activity of HA [169]. Previous studies have also shown the antitrypanosomal, antifungal and cilioinhibitory properties of HA [72,83,86-88]. For these properties and little cross-resistance helvolic acid is of great pharmaceutical importance. On the other hand, these antibiotic activi-

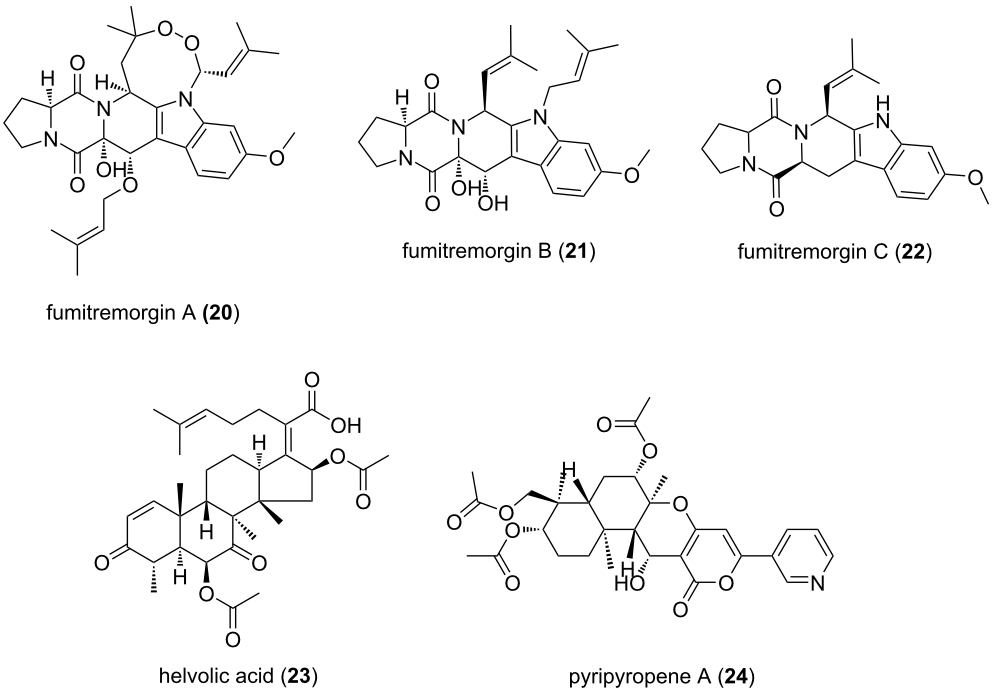

Figure 7: Bioactive secondary metabolites of *Aspergillus fumigatus*.

Beilstein J. Org. Chem. **2021,** *17,* 1814–1827.

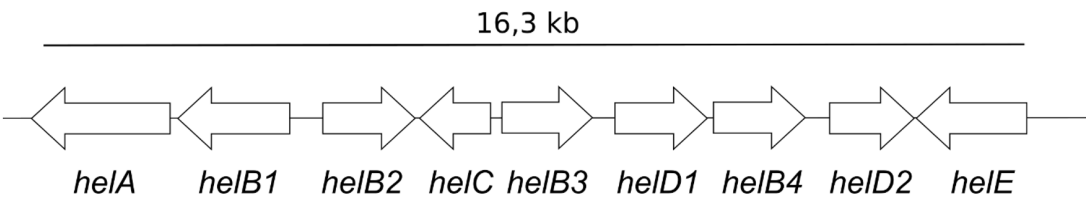

Figure 8: Helvolic acid gene cluster of *A. fumigatus*.

ties of HA could alter the soil microflora in natural habitats, an ecological role of HA that requires further investigation.

Pyripyropene A

Pyripyropene A (PPPA) (**24**) belongs to the meroterpenoid class of secondary metabolites. It was originally isolated from *A. fumigatus*, but later several other pyripyropene A producing members of *Aspergillus* and *Penicillium* ssp. were identified [98,99,170,171]. In A. fumigatus 9 genes form a pyripyropene A (pyr) biosynthetic cluster that spans a 23 kb region on chromosome 6 [172]. Chemically, pyripyropene (PP) analogs are meroterpenoids containing a fused pyridyl α-pyrone moiety and eight contiguous stereocenters [170]. Metabolically, PPPA noncovalently binds within the fifth transmembrane domain of acyl-coenzyme A (CoA):cholesterol acyltransferase ACAT2 and renders it inactive [173]. In vivo, PPPA-mediated ACAT2 inhibition was shown to protect the mice from atherosclerosis, ACAT2 enzyme mediates in lipid metabolism and is localized in the liver and intestines [174]. Furthermore, PPPA was also shown to exhibit insecticidal properties against aphids [100].

Conclusion

Increasing access to sequenced microbial genomes offers a glimpse at the untapped potential we have yet to gain access to. Fungi in particular harbor great potential to produce novel secondary metabolites with ecological and pathogenic importance. As a medically relevant fungal pathogen *A. fumigatus* is the subject of much research and since sequencing of its genome in 2005 its potential for the production of secondary metabolites was scrutinized frequently [7,43,175]. In recent years many of its BGCs could be matched with either long known or newly discovered bioactive compounds and while the bioactive potential and the ecological role of many well studied metabolites like DHN-melanin or gliotoxin is well known, newer metabolites often cannot be associated with a biological function. Due to its clinical significance, the highest interest in secondary metabolites of *A. fumigatus* was driven by its pathobiology, e.g., a role in cytotoxicity, immunosuppression or antifungal drug resistance. In natural habitats these molecules may fulfill analogous functions, such as the defense against phagocytic predators by gliotoxin [78-82]. Indeed, the need for survival is the driving force of evolution and fungi like *A. fumigatus* were able to cultivate an impressive arsenal of protective mechanism from DHN-melanin which offers mostly passive protection to more active compounds like fumigaclavines or helvolic acid with their antibacterial and antifungal activities, respectively [50,63,72,147]. Since SM activities are most often closely related to ecological conditions mimicking of more natural cultivation conditions might lead to the discovery of new compounds and their ecological role.

In the past few years, protists like *D. discoideum* and *Acanthamoeba castellani* have been widely used for the identification of virulence attributes of pathogenic fungi, including *Aspergillus* spp., for their similarity with human phagocytic cells [32]. Nevertheless, the precise identity of amoeboid, nematode and arthropod predators that target filamentous fungi in their environmental niches remained elusive and has been limited by their biological complexity. It was thus surprising to find that the environmentally abundant, fungivorous amoeba *P. aurantium* does not only graze on yeast but can specifically target filamentous fungi such as *A. fumigatus*. The mechanism of action was coined ruphocytosis and involved a locally distinct disruption of the cell wall of the fungal hyphae to feed on the fungal cytoplasm [29]. It is well conceivable that this amoeba will target a range of different filamentous fungi, and that this biotic cell wall stress can be exploited as an ecological trigger for the production and identification of new bioactive compounds in the future.

Funding

Work in the authors' lab was supported by the Deutsche Forschungsgemeinschaft (DFG, German Research Foundation) under Germany's Excellence Startegy - EXC 2051 - Project-ID 390713860 and the research grants DFG HI1574/2-1 und HI1574/4-1. The graphical abstract and Figure 1 were created with BioRender.com.

ORCID® iDs

Jana M. Boysen - https://orcid.org/0000-0001-5877-0006
Nauman Saeed - https://orcid.org/0000-0003-3627-7725
Falk Hillmann - https://orcid.org/0000-0002-5493-930X

References

1. Blackwell, M. *Am. J. Bot.* **2011,** *98,* 426–438. doi:10.3732/ajb.1000298
2. Cantrell, S. A.; Dianese, J. C.; Fell, J.; Gunde-Cimerman, N.; Zalar, P. *Mycologia* **2011,** *103,* 1161–1174. doi:10.3852/11-108
3. Sutherland, I. W. *Trends Microbiol.* **2001,** *9,* 222–227. doi:10.1016/s0966-842x(01)02012-1
4. Costa-Orlandi, C. B.; Sardi, J. C. O.; Pitangui, N. S.; de Oliveira, H. C.; Scorzoni, L.; Galeane, M. C.; Medina-Alarcón, K. P.; Melo, W.; Marcelino, M. Y.; Braz, J. D.; Fusco-Almeida, A. M.; Mendes-Giannini, M. J. S. *J. Fungi* **2017,** 3. doi:10.3390/jof3020022
5. Kowalski, C. H.; Morelli, K. A.; Schultz, D.; Nadell, C. D.; Cramer, R. A. *Proc. Natl. Acad. Sci. U. S. A.* **2020,** *117,* 22473–22483. doi:10.1073/pnas.2003700117
6. Spiteller, P. *Nat. Prod. Rep.* **2015,** *32,* 971–993. doi:10.1039/c4np00166d
7. Nierman, W. C.; Pain, A.; Anderson, M. J.; Wortman, J. R.; Kim, H. S.; Arroyo, J.; Berriman, M.; Abe, K.; Archer, D. B.; Bermejo, C.; Bennett, J.; Bowyer, P.; Chen, D.; Collins, M.; Coulsen, R.; Davies, R.; Dyer, P. S.; Farman, M.; Fedorova, N.; Fedorova, N.; Feldblyum, T. V.; Fischer, R.; Fosker, N.; Fraser, A.; García, J. L.; García, M. J.; Goble, A.; Goldman, G. H.; Gomi, K.; Griffith-Jones, S.; Gwilliam, R.; Haas, B.; Haas, H.; Harris, D.; Horiuchi, H.; Huang, J.; Humphray, S.; Jiménez, J.; Keller, N.; Khouri, H.; Kitamoto, K.; Kobayashi, T.; Konzack, S.; Kulkarni, R.; Kumagai, T.; Lafton, A.; Latgé, J.-P.; Li, W.; Lord, A.; Lu, C.; Majoros, W. H.; May, G. S.; Miller, B. L.; Mohamoud, Y.; Molina, M.; Monod, M.; Mouyna, I.; Mulligan, S.; Murphy, L.; O'Neil, S.; Paulsen, I.; Peñalva, M. A.; Pertea, M.; Price, C.; Pritchard, B. L.; Quail, M. A.; Rabbinowitsch, E.; Rawlins, N.; Rajandream, M.-A.; Reichard, U.; Renauld, H.; Robson, G. D.; de Córdoba, S. R.; Rodríguez-Peña, J. M.; Ronning, C. M.; Rutter, S.; Salzberg, S. L.; Sanchez, M.; Sánchez-Ferrero, J. C.; Saunders, D.; Seeger, K.; Squares, R.; Squares, S.; Takeuchi, M.; Tekaia, F.; Turner, G.; de Aldana, C. R. V.; Weidman, J.; White, O.; Woodward, J.; Yu, J.-H.; Fraser, C.; Galagan, J. E.; Asai, K.; Machida, M.; Hall, N.; Barrell, B.; Denning, D. W. *Nature* **2005,** *438,* 1151–1156. doi:10.1038/nature04332
8. Khaldi, N.; Seifuddin, F. T.; Turner, G.; Haft, D.; Nierman, W. C.; Wolfe, K. H.; Fedorova, N. D. *Fungal Genet. Biol.* **2010,** *47,* 736–741. doi:10.1016/j.fgb.2010.06.003
9. Brakhage, A. A.; Schroeckh, V. *Fungal Genet. Biol.* **2011,** *48,* 15–22. doi:10.1016/j.fgb.2010.04.004
10. Keller, N. P.; Turner, G.; Bennett, J. W. *Nat. Rev. Microbiol.* **2005,** *3,* 937–947. doi:10.1038/nrmicro1286
11. Gacek, A.; Strauss, J. *Appl. Microbiol. Biotechnol.* **2012,** *95,* 1389–1404. doi:10.1007/s00253-012-4208-8
12. Krause, D. J.; Kominek, J.; Opulente, D. A.; Shen, X.-X.; Zhou, X.; Langdon, Q. K.; DeVirgilio, J.; Hulfachor, A. B.; Kurtzman, C. P.; Rokas, A.; Hittinger, C. T. *Proc. Natl. Acad. Sci. U. S. A.* **2018,** *115,* 11030–11035. doi:10.1073/pnas.1806268115
13. Smith, D. J.; Burnham, M. K. R.; Edwards, J.; Earl, A. J.; Turner, G. *Bio/Technology* **1990,** *8,* 39–41. doi:10.1038/nbt0190-39
14. Keller, N. P. *Nat. Rev. Microbiol.* **2019,** *17,* 167–180. doi:10.1038/s41579-018-0121-1
15. O'Donnell, K.; Cigelnik, E.; Casper, H. H. *Fungal Genet. Biol.* **1998,** *23,* 57–67. doi:10.1006/fgbi.1997.1018
16. Martin, F.; Kohler, A.; Murat, C.; Balestrini, R.; Coutinho, P. M.; Jaillon, O.; Montanini, B.; Morin, E.; Noel, B.; Percudani, R.; Porcel, B.; Rubini, A.; Amicucci, A.; Amselem, J.; Anthouard, V.; Arcioni, S.; Artiguenave, F.; Aury, J.-M.; Ballario, P.; Bolchi, A.; Brenna, A.; Brun, A.; Buée, M.; Cantarel, B.; Chevalier, G.; Couloux, A.; Da Silva, C.; Denoeud, F.; Duplessis, S.; Ghignone, S.; Hilselberger, B.; Iotti, M.; Marçais, B.; Mello, A.; Miranda, M.; Pacioni, G.; Quesneville, H.; Riccioni, C.; Ruotolo, R.; Splivallo, R.; Stocchi, V.; Tisserant, E.; Viscomi, A. R.; Zambonelli, A.; Zampieri, E.; Henrissat, B.; Lebrun, M.-H.; Paolocci, F.; Bonfante, P.; Ottonello, S.; Wincker, P. *Nature* **2010,** *464,* 1033–1038. doi:10.1038/nature08867
17. Karwehl, S.; Stadler, M. Exploitation of Fungal Biodiversity for Discovery of Novel Antibiotics. In *How to Overcome the Antibiotic Crisis : Facts, Challenges, Technologies and Future Perspectives;* Stadler, M.; Dersch, P., Eds.; Springer International Publishing: Cham, Switzerland, 2016; pp 303–338. doi:10.1007/82_2016_496
18. Spiteller, P. *Chem. – Eur. J.* **2008,** *14,* 9100–9110. doi:10.1002/chem.200800292
19. Zeng, R. S. L.; Niu, G.; Wen, Z.; Schuler, M. A.; Berenbaum, M. R. *J. Chem. Ecol.* **2006,** *32,* 1459–1471. doi:10.1007/s10886-006-9062-7
20. González-Osnaya, L.; Soriano, J. M.; Moltó, J. C.; Mañes, J. *Food Addit. Contam.* **2007,** *24,* 1268–1274. doi:10.1080/02652030701361556
21. Reiss, J. *Chem.-Biol. Interact.* **1975,** *10,* 339–342. doi:10.1016/0009-2797(75)90055-1
22. Cary, J. W.; Harris-Coward, P. Y.; Ehrlich, K. C.; Di Mavungu, J. D.; Malysheva, S. V.; De Saeger, S.; Dowd, P. F.; Shantappa, S.; Martens, S. L.; Calvo, A. M. *Fungal Genet. Biol.* **2014,** *64,* 25–35. doi:10.1016/j.fgb.2014.01.001
23. Zhao, Y.; Ding, J.; Yuan, W.; Huang, J.; Huang, W.; Wang, Y.; Zheng, W. *Environ. Microbiol.* **2017,** *19,* 3920–3929. doi:10.1111/1462-2920.13791
24. Xu, Y.; Vinas, M.; Alsarrag, A.; Su, L.; Pfohl, K.; Rohlfs, M.; Schäfer, W.; Chen, W.; Karlovsky, P. *Nat. Commun.* **2019,** *10,* 3579. doi:10.1038/s41467-019-11377-5
25. Eadie, M. J. *Lancet Neurol.* **2003,** *2,* 429–434. doi:10.1016/s1474-4422(03)00439-3
26. Tudzynski, P.; Correia, T.; Keller, U. *Appl. Microbiol. Biotechnol.* **2001,** *57,* 593–605. doi:10.1007/s002530100801
27. Tudzynski, P.; Scheffer, J. *Mol. Plant Pathol.* **2004,** *5,* 377–388. doi:10.1111/j.1364-3703.2004.00237.x
28. Schardl, C. L.; Panaccione, D. G.; Tudzynski, P. Ergot Alkaloids – Biology and Molecular Biology. *The Alkaloids: Chemistry and Biology;* Academic Press, 2006; Vol. 63, pp 45–86. doi:10.1016/s1099-4831(06)63002-2
29. Radosa, S.; Ferling, I.; Sprague, J. L.; Westermann, M.; Hillmann, F. *Environ. Microbiol.* **2019,** *21,* 1809–1820. doi:10.1111/1462-2920.14588
30. Van Waeyenberghe, L.; Baré, J.; Pasmans, F.; Claeys, M.; Bert, W.; Haesebrouck, F.; Houf, K.; Martel, A. *Environ. Microbiol. Rep.* **2013,** *5,* 819–824. doi:10.1111/1758-2229.12082
31. Brunke, S.; Mogavero, S.; Kasper, L.; Hube, B. *Curr. Opin. Microbiol.* **2016,** *32,* 89–95. doi:10.1016/j.mib.2016.05.010
32. Tosetti, N.; Croxatto, A.; Greub, G. *Microb. Pathog.* **2014,** *77,* 125–130. doi:10.1016/j.micpath.2014.07.009
33. Sanchez, J. F.; Somoza, A. D.; Keller, N. P.; Wang, C. C. C. *Nat. Prod. Rep.* **2012,** *29,* 351–371. doi:10.1039/c2np00084a
34. Show, P. L.; Oladele, K. O.; Siew, Q. Y.; Aziz Zakry, F. A.; Lan, J. C.-W.; Ling, T. C. *Front. Life Sci.* **2015,** *8,* 271–283. doi:10.1080/21553769.2015.1033653

35. Stötefeld, L.; Scheu, S.; Rohlfs, M. *Ecol. Entomol.* **2012,** *37,* 323–329. doi:10.1111/j.1365-2311.2012.01373.x
36. Rohlfs, M. Fungal secondary metabolism in the light of animal–fungus interactions: from mechanism to ecological function. In *Biosynthesis and Molecular Genetics of Fungal Secondary Metabolites;* Zeilinger, S.; Martín, J. F.; García-Estrada, C., Eds.; Springer: New York, NY, USA, 2015; Vol. 3, pp 177–198. doi:10.1007/978-1-4939-2531-5_9
37. Künzler, M. *PLoS Pathog.* **2018,** *14,* e1007184. doi:10.1371/journal.ppat.1007184
38. Brakhage, A. A.; Langfelder, K. *Annu. Rev. Microbiol.* **2002,** *56,* 433–455. doi:10.1146/annurev.micro.56.012302.160625
39. Novohradská, S.; Ferling, I.; Hillmann, F. *Front. Cell. Infect. Microbiol.* **2017,** *7,* 497. doi:10.3389/fcimb.2017.00497
40. Latge, J.-P. *Clin. Microbiol. Rev.* **1999,** *12,* 310–350. doi:10.1128/cmr.12.2.310
41. Bignell, E.; Cairns, T. C.; Throckmorton, K.; Nierman, W. C.; Keller, N. P. *Philos. Trans. R. Soc., B* **2016,** *371,* 20160023. doi:10.1098/rstb.2016.0023
42. Frisvad, J. C.; Rank, C.; Nielsen, K. F.; Larsen, T. O. *Med. Mycol.* **2009,** *47* (Suppl. 1), S53–S71. doi:10.1080/13693780802307720
43. Inglis, D. O.; Binkley, J.; Skrzypek, M. S.; Arnaud, M. B.; Cerqueira, G. C.; Shah, P.; Wymore, F.; Wortman, J. R.; Sherlock, G. *BMC Microbiol.* **2013,** *13,* 91. doi:10.1186/1471-2180-13-91
44. Lind, A. L.; Wisecaver, J. H.; Lameiras, C.; Wiemann, P.; Palmer, J. M.; Keller, N. P.; Rodrigues, F.; Goldman, G. H.; Rokas, A. *PLoS Biol.* **2017,** *15,* e2003583. doi:10.1371/journal.pbio.2003583
45. Heinekamp, T.; Thywißen, A.; Macheleidt, J.; Keller, S.; Valiante, V.; Brakhage, A. A. *Front. Microbiol.* **2013,** *3,* 440. doi:10.3389/fmicb.2012.00440
46. Gómez, B. L.; Nosanchuk, J. D. *Curr. Opin. Infect. Dis.* **2003,** *16,* 91–96. doi:10.1097/00001432-200304000-00005
47. Nguyen, K.-H.; Chollet-Krugler, M.; Gouault, N.; Tomasi, S. *Nat. Prod. Rep.* **2013,** *30,* 1490–1508. doi:10.1039/c3np70064j
48. Brakhage, A. A.; Liebmann, B. *Med. Mycol.* **2005,** *43* (Suppl. 1), S75–S82. doi:10.1080/13693780400028967
49. Jahn, B.; Langfelder, K.; Schneider, U.; Schindel, C.; Brakhage, A. A. *Cell. Microbiol.* **2002,** *4,* 793–803. doi:10.1046/j.1462-5822.2002.00228.x
50. Ferling, I.; Dunn, J. D.; Ferling, A.; Soldati, T.; Hillmann, F. *mBio* **2020,** *11*. doi:10.1128/mbio.00862-20
51. Lim, F. Y.; Hou, Y.; Chen, Y.; Oh, J.-H.; Lee, I.; Bugni, T. S.; Keller, N. P. *Appl. Environ. Microbiol.* **2012,** *78,* 4117–4125. doi:10.1128/aem.07710-11
52. Berthier, E.; Lim, F. Y.; Deng, Q.; Guo, C.-J.; Kontoyiannis, D. P.; Wang, C. C. C.; Rindy, J.; Beebe, D. J.; Huttenlocher, A.; Keller, N. P. *PLoS Pathog.* **2013,** *9,* e1003289. doi:10.1371/journal.ppat.1003289
53. Throckmorton, K.; Lim, F. Y.; Kontoyiannis, D. P.; Zheng, W.; Keller, N. P. *Environ. Microbiol.* **2016,** *18,* 246–259. doi:10.1111/1462-2920.13007
54. Hissen, A. H. T.; Wan, A. N. C.; Warwas, M. L.; Pinto, L. J.; Moore, M. M. *Infect. Immun.* **2005,** *73,* 5493–5503. doi:10.1128/iai.73.9.5493-5503.2005
55. Schrettl, M.; Bignell, E.; Kragl, C.; Joechl, C.; Rogers, T.; Arst, H. N., Jr.; Haynes, K.; Haas, H. *J. Exp. Med.* **2004,** *200,* 1213–1219. doi:10.1084/jem.20041242
56. Kato, N.; Suzuki, H.; Okumura, H.; Takahashi, S.; Osada, H. *Biosci., Biotechnol., Biochem.* **2013,** *77,* 1061–1067. doi:10.1271/bbb.130026
57. Ehlers, T.; Furness, S.; Robinson, T. P.; Zhong, H. A.; Goldsmith, D.; Aribser, J.; Bowen, J. P. *Curr. Top. Med. Chem.* **2016,** *16,* 1478–1488. doi:10.2174/1568026615666150915121204
58. van den Heever, J. P.; Thompson, T. S.; Curtis, J. M.; Ibrahim, A.; Pernal, S. F. *J. Agric. Food Chem.* **2014,** *62,* 2728–2737. doi:10.1021/jf4055374
59. Mendoza, Y.; Diaz-Cetti, S.; Ramallo, G.; Santos, E.; Porrini, M.; Invernizzi, C. *J. Econ. Entomol.* **2017,** *110,* 1–5. doi:10.1093/jee/tow228
60. Fallon, J. P.; Reeves, E. P.; Kavanagh, K. *J. Med. Microbiol.* **2010,** *59,* 625–633. doi:10.1099/jmm.0.018192-0
61. Fallon, J. P.; Reeves, E. P.; Kavanagh, K. *Microbiology (Reading, U. K.)* **2011,** *157,* 1481–1488. doi:10.1099/mic.0.043786-0
62. Guruceaga, X.; Ezpeleta, G.; Mayayo, E.; Sueiro-Olivares, M.; Abad-Diaz-De-Cerio, A.; Aguirre Urízar, J. M.; Liu, H. G.; Wiemann, P.; Bok, J. W.; Filler, S. G.; Keller, N. P.; Hernando, F. L.; Ramirez-Garcia, A.; Rementeria, A. *Virulence* **2018,** *9,* 1548–1561. doi:10.1080/21505594.2018.1526528
63. Pinheiro, E. A. A.; Carvalho, J. M.; dos Santos, D. C. P.; Feitosa, A. d. O.; Marinho, P. S. B.; Guilhon, G. M. S. P.; de Souza, A. D. L.; da Silva, F. M. A.; Marinho, A. M. d. R. *Nat. Prod. Res.* **2013,** *27,* 1633–1638. doi:10.1080/14786419.2012.750316
64. Ma, H.-Y.; Song, Y.-C.; Mao, Y.-Y.; Jiang, J.-H.; Tan, R.-X.; Luo, L. *Planta Med.* **2006,** *72,* 387–392. doi:10.1055/s-2005-916235
65. Li, Y.-X.; Himaya, S. W. A.; Dewapriya, P.; Zhang, C.; Kim, S.-K. *Mar. Drugs* **2013,** *11,* 5063–5086. doi:10.3390/md11125063
66. Panaccione, D. G.; Arnold, S. L. *Sci. Rep.* **2017,** *7,* 8930. doi:10.1038/s41598-017-09107-2
67. Du, R. H.; Li, E. G.; Cao, Y.; Song, Y. C.; Tan, R. X. *Life Sci.* **2011,** *89,* 235–240. doi:10.1016/j.lfs.2011.06.015
68. Macheleidt, J.; Scherlach, K.; Neuwirth, T.; Schmidt-Heck, W.; Straßburger, M.; Spraker, J.; Baccile, J. A.; Schroeder, F. C.; Keller, N. P.; Hertweck, C.; Heinekamp, T.; Brakhage, A. A. *Mol. Microbiol.* **2015,** *96,* 148–162. doi:10.1111/mmi.12926
69. Lim, F. Y.; Ames, B.; Walsh, C. T.; Keller, N. P. *Cell. Microbiol.* **2014,** *16,* 1267–1283. doi:10.1111/cmi.12284
70. Garcia Silva, M.; Araçari Jacometti Cardoso Furtado, N.; Tallarico Pupo, M.; José Vieira Fonseca, M.; Said, S.; Alves da Silva Filho, A.; Kenupp Bastos, J. *Microbiol. Res.* **2004,** *159,* 317–322. doi:10.1016/j.micres.2004.06.003
71. Belofsky, G. N.; Anguera, M.; Jensen, P. R.; Fenical, W.; Köck, M. *Chem. – Eur. J.* **2000,** *6,* 1355–1360. doi:10.1002/(sici)1521-3765(20000417)6:8<1355::aid-chem1355>3.0.co;2-s
72. Li, X.-J.; Zhang, Q.; Zhang, A.-L.; Gao, J.-M. *J. Agric. Food Chem.* **2012,** *60,* 3424–3431. doi:10.1021/jf300146n
73. Baccile, J. A.; Spraker, J. E.; Le, H. H.; Brandenburger, E.; Gomez, C.; Bok, J. W.; Macheleidt, J.; Brakhage, A. A.; Hoffmeister, D.; Keller, N. P.; Schroeder, F. C. *Nat. Chem. Biol.* **2016,** *12,* 419–424. doi:10.1038/nchembio.2061
74. Khalid, S.; Baccile, J. A.; Spraker, J. E.; Tannous, J.; Imran, M.; Schroeder, F. C.; Keller, N. P. *ACS Chem. Biol.* **2018,** *13,* 171–179. doi:10.1021/acschembio.7b00731
75. González-Lobato, L.; Real, R.; Prieto, J. G.; Álvarez, A. I.; Merino, G. *Eur. J. Pharmacol.* **2010,** *644,* 41–48. doi:10.1016/j.ejphar.2010.07.016

76. Lehner, S. M.; Atanasova, L.; Neumann, N. K. N.; Krska, R.; Lemmens, M.; Druzhinina, I. S.; Schuhmacher, R. *Appl. Environ. Microbiol.* **2013,** *79,* 18–31. doi:10.1128/aem.02339-12
77. Ali, H.; Ries, M. I.; Lankhorst, P. P.; van der Hoeven, R. A. M.; Schouten, O. L.; Noga, M.; Hankemeier, T.; van Peij, N. N. M. E.; Bovenberg, R. A. L.; Vreeken, R. J.; Driessen, A. J. M. *PLoS One* **2014,** *9,* e98212. doi:10.1371/journal.pone.0098212
78. Scharf, D. H.; Brakhage, A. A.; Mukherjee, P. K. *Environ. Microbiol.* **2016,** *18,* 1096–1109. doi:10.1111/1462-2920.13080
79. Yamada, A.; Kataoka, T.; Nagai, K. *Immunol. Lett.* **2000,** *71,* 27–32. doi:10.1016/s0165-2478(99)00155-8
80. Schlam, D.; Canton, J.; Carreño, M.; Kopinski, H.; Freeman, S. A.; Grinstein, S.; Fairn, G. D. *mBio* **2016,** *7*. doi:10.1128/mbio.02242-15
81. Gardiner, D. M.; Waring, P.; Howlett, B. J. *Microbiology (Reading, U. K.)* **2005,** *151,* 1021–1032. doi:10.1099/mic.0.27847-0
82. Hillmann, F.; Novohradská, S.; Mattern, D. J.; Forberger, T.; Heinekamp, T.; Westermann, M.; Winckler, T.; Brakhage, A. A. *Environ. Microbiol.* **2015,** *17,* 2858–2869. doi:10.1111/1462-2920.12808
83. Mitsuguchi, H.; Seshime, Y.; Fujii, I.; Shibuya, M.; Ebizuka, Y.; Kushiro, T. *J. Am. Chem. Soc.* **2009,** *131,* 6402–6411. doi:10.1021/ja8095976
84. Lodeiro, S.; Xiong, Q.; Wilson, W. K.; Ivanova, Y.; Smith, M. L.; May, G. S.; Matsuda, S. P. T. *Org. Lett.* **2009,** *11,* 1241–1244. doi:10.1021/ol802696a
85. Kimura, M.; Kushiro, T.; Shibuya, M.; Ebizuka, Y.; Abe, I. *Biochem. Biophys. Res. Commun.* **2010,** *391,* 899–902. doi:10.1016/j.bbrc.2009.11.160
86. Ganaha, M.; Yoshii, K.; Ōtsuki, Y.; Iguchi, M.; Okamoto, Y.; Iseki, K.; Ban, S.; Ishiyama, A.; Hokari, R.; Iwatsuki, M.; Otoguro, K.; Ōmura, S.; Hashimoto, T.; Noji, M.; Umeyama, A. *Chem. Pharm. Bull.* **2016,** *64,* 988–990. doi:10.1248/cpb.c16-00220
87. Amitani, R.; Taylor, G.; Elezis, E.-N.; Llewellyn-Jones, C.; Mitchell, J.; Kuze, F.; Cole, P. J.; Wilson, R. *Infect. Immun.* **1995,** *63,* 3266–3271. doi:10.1128/iai.63.9.3266-3271.1995
88. Kong, F.-D.; Huang, X.-L.; Ma, Q.-Y.; Xie, Q.-Y.; Wang, P.; Chen, P.-W.; Zhou, L.-M.; Yuan, J.-Z.; Dai, H.-F.; Luo, D.-Q.; Zhao, Y.-X. *J. Nat. Prod.* **2018,** *81,* 1869–1876. doi:10.1021/acs.jnatprod.8b00382
89. Yin, W.-B.; Baccile, J. A.; Bok, J. W.; Chen, Y.; Keller, N. P.; Schroeder, F. C. *J. Am. Chem. Soc.* **2013,** *135,* 2064–2067. doi:10.1021/ja311145n
90. Wiemann, P.; Lechner, B. E.; Baccile, J. A.; Velk, T. A.; Yin, W.-B.; Bok, J. W.; Pakala, S.; Losada, L.; Nierman, W. C.; Schroeder, F. C. *Front. Microbiol.* **2014,** *5,* 530. doi:10.3389/fmicb.2014.00530
91. König, C. C.; Scherlach, K.; Schroeckh, V.; Horn, F.; Nietzsche, S.; Brakhage, A. A.; Hertweck, C. *ChemBioChem* **2013,** *14,* 938–942. doi:10.1002/cbic.201300070
92. Chooi, Y.-H.; Fang, J.; Liu, H.; Filler, S. G.; Wang, P.; Tang, Y. *Org. Lett.* **2013,** *15,* 780–783. doi:10.1021/ol303435y
93. Andersen, M. R.; Nielsen, J. B.; Klitgaard, A.; Petersen, L. M.; Zachariasen, M.; Hansen, T. J.; Blicher, L. H.; Gotfredsen, C. H.; Larsen, T. O.; Nielsen, K. F.; Mortensen, U. H. *Proc. Natl. Acad. Sci. U. S. A.* **2013,** *110,* E99–E107. doi:10.1073/pnas.1205532110
94. Mehedi, M. A. U.; Molla, A. H.; Khondkar, P.; Sultana, S.; Islam, M. A.; Rashid, M. A.; Chowdhury, R. *Asian J. Chem.* **2010,** *22,* 2611–2614.
95. Wiemann, P.; Guo, C.-J.; Palmer, J. M.; Sekonyela, R.; Wang, C. C. C.; Keller, N. P. *Proc. Natl. Acad. Sci. U. S. A.* **2013,** *110,* 17065–17070. doi:10.1073/pnas.1313258110
96. Ishikawa, M.; Ninomiya, T.; Akabane, H.; Kushida, N.; Tsujiuchi, G.; Ohyama, M.; Gomi, S.; Shito, K.; Murata, T. *Bioorg. Med. Chem. Lett.* **2009,** *19,* 1457–1460. doi:10.1016/j.bmcl.2009.01.029
97. Maiya, S.; Grundmann, A.; Li, X.; Li, S.-M.; Turner, G. *ChemBioChem* **2007,** *8,* 1736–1743. doi:10.1002/cbic.200700202
98. Omura, S.; Tomoda, H.; Kim, Y. K.; Nishida, H. *J. Antibiot.* **1993,** *46,* 1168–1169. doi:10.7164/antibiotics.46.1168
99. Hu, J.; Furutani, A.; Yamamoto, K.; Oyama, K.; Mitomi, M.; Anzai, H. *Biotechnol. Biotechnol. Equip.* **2014,** *28,* 818–826. doi:10.1080/13102818.2014.960140
100. Goto, K.; Horikoshi, R.; Mitomi, M.; Oyama, K.; Hirose, T.; Sunazuka, T.; Ōmura, S. *J. Antibiot.* **2018,** *71,* 785–797. doi:10.1038/s41429-018-0064-9
101. VanMiddlesworth, F.; Dufresne, C.; Wincott, F. E.; Mosley, R. T.; Wilson, K. E. *Tetrahedron Lett.* **1992,** *33,* 297–300. doi:10.1016/s0040-4039(00)74115-3
102. VanMiddlesworth, F.; Giacobbe, R. A.; Lopez, M.; Garrity, G.; Bland, J. A.; Bartizal, K.; Fromtling, R. A.; Polishook, J.; Zweerink, M.; Edison, A. M. *J. Antibiot.* **1992,** *45,* 861–867. doi:10.7164/antibiotics.45.861
103. Rank, C. Mapping of secondary metabolism in biotechnologically important Aspergillus species. Ph.D. Thesis, Technical University of Denmark, Lyngby, Denmark, 2010.
104. Kobayashi, S.; Furuta, T.; Hayashi, T.; Nishijima, M.; Hanada, K. *J. Am. Chem. Soc.* **1998,** *120,* 908–919. doi:10.1021/ja9730829
105. Mattern, D. J.; Schoeler, H.; Weber, J.; Novohradská, S.; Kraibooj, K.; Dahse, H.-M.; Hillmann, F.; Valiante, V.; Figge, M. T.; Brakhage, A. A. *Appl. Microbiol. Biotechnol.* **2015,** *99,* 10151–10161. doi:10.1007/s00253-015-6898-1
106. Balan, J.; Ebringer, L.; Nemec, P.; Kováč, Š.; Dobias, J. *J. Antibiot., Ser. A* **1963,** *16,* 157–160.
107. Gauthier, T.; Wang, X.; Sifuentes Dos Santos, J.; Fysikopoulos, A.; Tadrist, S.; Canlet, C.; Artigot, M. P.; Loiseau, N.; Oswald, I. P.; Puel, O. *PLoS One* **2012,** *7,* e29906. doi:10.1371/journal.pone.0029906
108. Khoufache, K.; Puel, O.; Loiseau, N.; Delaforge, M.; Rivollet, D.; Coste, A.; Cordonnier, C.; Escudier, E.; Botterel, F.; Bretagne, S. *BMC Microbiol.* **2007,** *7,* No. 1. doi:10.1186/1471-2180-7-1
109. Gallagher, R. T.; Latch, G. C. M. *Appl. Environ. Microbiol.* **1977,** *33,* 730–731. doi:10.1128/aem.33.3.730-731.1977
110. Wang, F.; Fang, Y.; Zhu, T.; Zhang, M.; Lin, A.; Gu, Q.; Zhu, W. *Tetrahedron* **2008,** *64,* 7986–7991. doi:10.1016/j.tet.2008.06.013
111. Lim, F. Y.; Won, T. H.; Raffa, N.; Baccile, J. A.; Wisecaver, J.; Rokas, A.; Schroeder, F. C.; Keller, N. P. *mBio* **2018,** *9*. doi:10.1128/mbio.00785-18
112. Bok, J. W.; Chung, D.; Balajee, S. A.; Marr, K. A.; Andes, D.; Nielsen, K. F.; Frisvad, J. C.; Kirby, K. A.; Keller, N. P. *Infect. Immun.* **2006,** *74,* 6761–6768. doi:10.1128/iai.00780-06
113. Bell, M. R.; Johnson, J. R.; Wildi, B. S.; Woodward, R. B. *J. Am. Chem. Soc.* **1958,** *80,* 1001. doi:10.1021/ja01537a065
114. Bok, J. W.; Balajee, S. A.; Marr, K. A.; Andes, D.; Nielsen, K. F.; Frisvad, J. C.; Keller, N. P. *Eukaryotic Cell* **2005,** *4,* 1574–1582. doi:10.1128/ec.4.9.1574-1582.2005
115. Cramer, R. A., Jr.; Gamcsik, M. P.; Brooking, R. M.; Najvar, L. K.; Kirkpatrick, W. R.; Patterson, T. F.; Balibar, C. J.; Graybill, J. R.; Perfect, J. R.; Abraham, S. N.; Steinbach, W. J. *Eukaryotic Cell* **2006,** *5,* 972–980. doi:10.1128/ec.00049-06

116. Kupfahl, C.; Heinekamp, T.; Geginat, G.; Ruppert, T.; Härtl, A.; Hof, H.; Brakhage, A. A. *Mol. Microbiol.* **2006,** *62,* 292–302. doi:10.1111/j.1365-2958.2006.05373.x
117. Scharf, D. H.; Remme, N.; Heinekamp, T.; Hortschansky, P.; Brakhage, A. A.; Hertweck, C. *J. Am. Chem. Soc.* **2010,** *132,* 10136–10141. doi:10.1021/ja103262m
118. Schrettl, M.; Carberry, S.; Kavanagh, K.; Haas, H.; Jones, G. W.; O'Brien, J.; Nolan, A.; Stephens, J.; Fenelon, O.; Doyle, S. *PLoS Pathog.* **2010,** *6,* e1000952. doi:10.1371/journal.ppat.1000952
119. McDonagh, A.; Fedorova, N. D.; Crabtree, J.; Yu, Y.; Kim, S.; Chen, D.; Loss, O.; Cairns, T.; Goldman, G.; Armstrong-James, D.; Haynes, K.; Haas, H.; Schrettl, M.; May, G.; Nierman, W. C.; Bignell, E. *PLoS Pathog.* **2008,** *4,* e1000154. doi:10.1371/journal.ppat.1000154
120. Sugui, J. A.; Kim, H. S.; Zarember, K. A.; Chang, Y. C.; Gallin, J. I.; Nierman, W. C.; Kwon-Chung, K. J. *PLoS One* **2008,** *3,* e2655. doi:10.1371/journal.pone.0002655
121. Sugui, J. A.; Pardo, J.; Chang, Y. C.; Zarember, K. A.; Nardone, G.; Galvez, E. M.; Müllbacher, A.; Gallin, J. I.; Simon, M. M.; Kwon-Chung, K. J. *Eukaryotic Cell* **2007,** *6,* 1562–1569. doi:10.1128/ec.00141-07
122. Vargas, W. A.; Mukherjee, P. K.; Laughlin, D.; Wiest, A.; Moran-Diez, M. E.; Kenerley, C. M. *Microbiology (Reading, U. K.)* **2014,** *160,* 2319–2330. doi:10.1099/mic.0.079210-0
123. Coyle, C. M.; Kenaley, S. C.; Rittenour, W. R.; Panaccione, D. G. *Mycologia* **2007,** *99,* 804–811. doi:10.1080/15572536.2007.11832512
124. Perrin, R. M.; Fedorova, N. D.; Bok, J. W.; Cramer, R. A.; Wortman, J. R.; Kim, H. S.; Nierman, W. C.; Keller, N. P. *PLoS Pathog.* **2007,** *3,* e50. doi:10.1371/journal.ppat.0030050
125. Twumasi-Boateng, K.; Yu, Y.; Chen, D.; Gravelat, F. N.; Nierman, W. C.; Sheppard, D. C. *Eukaryotic Cell* **2009,** *8,* 104–115. doi:10.1128/ec.00265-08
126. Upadhyay, S.; Torres, G.; Lin, X. *Eukaryotic Cell* **2013,** *12,* 1641–1652. doi:10.1128/ec.00217-13
127. Hanson, F. R.; Eble, T. E. *J. Bacteriol.* **1949,** *58,* 527–529. doi:10.1128/jb.58.4.527-529.1949
128. Lin, H.-C.; Chooi, Y.-H.; Dhingra, S.; Xu, W.; Calvo, A. M.; Tang, Y. *J. Am. Chem. Soc.* **2013,** *135,* 4616–4619. doi:10.1021/ja312503y
129. Sin, N.; Meng, L.; Wang, M. Q. W.; Wen, J. J.; Bornmann, W. G.; Crews, C. M. *Proc. Natl. Acad. Sci. U. S. A.* **1997,** *94,* 6099–6103. doi:10.1073/pnas.94.12.6099
130. Mauriz, J. L.; Martín-Renedo, J.; García-Palomo, A.; Tuñón, M. J.; González-Gallego, J. *Curr. Drug Targets* **2010,** *11,* 1439–1457. doi:10.2174/1389450111009011439
131. Vetro, J. A.; Dummitt, B.; Chang, Y.-H. Methionine Aminopeptidase. In *Aminopeptidases in Biology and Disease;* Hooper, N. M.; Lendeckel, U., Eds.; Proteases in Biology and Disease, Vol. 2; Springer: Boston, MA, USA, 2004; pp 17–44. doi:10.1007/978-1-4419-8869-0_2
132. Conrad, T.; Kniemeyer, O.; Henkel, S. G.; Krüger, T.; Mattern, D. J.; Valiante, V.; Guthke, R.; Jacobsen, I. D.; Brakhage, A. A.; Vlaic, S.; Linde, J. *BMC Syst. Biol.* **2018,** *12,* 88. doi:10.1186/s12918-018-0620-8
133. Netzker, T.; Fischer, J.; Weber, J.; Mattern, D. J.; König, C. C.; Valiante, V.; Schroeckh, V.; Brakhage, A. A. *Front. Microbiol.* **2015,** *6,* 299. doi:10.3389/fmicb.2015.00299
134. Guruceaga, X.; Perez-Cuesta, U.; Abad-Diaz de Cerio, A.; Gonzalez, O.; Alonso, R. M.; Hernando, F. L.; Ramirez-Garcia, A.; Rementeria, A. *Toxins* **2019,** *12,* 7. doi:10.3390/toxins12010007
135. Molina, J.-M.; Tourneur, M.; Sarfati, C.; Chevret, S.; de Gouvello, A.; Gobert, J.-G.; Balkan, S.; Derouin, F. *N. Engl. J. Med.* **2002,** *346,* 1963–1969. doi:10.1056/nejmoa012924
136. Keller, N.; Bok, J.; Chung, D.; Perrin, R. M.; Keats Shwab, E. *Med. Mycol.* **2006,** *44* (Suppl. 1), S83–S85. doi:10.1080/13693780600835773
137. Romsdahl, J.; Wang, C. C. C. *Med. Chem. Commun.* **2019,** *10,* 840–866. doi:10.1039/c9md00054b
138. Wang, J.; Sheppard, G. S.; Lou, P.; Kawai, M.; BaMaung, N.; Erickson, S. A.; Tucker-Garcia, L.; Park, C.; Bouska, J.; Wang, Y.-C. *Cancer Res.* **2003,** *63,* 7861–7869.
139. Yamaoka, M.; Yamamoto, T.; Ikeyama, S.; Sudo, K.; Fujita, T. *Cancer Res.* **1993,** *53,* 5233–5236.
140. Tucker, L. A.; Zhang, Q.; Sheppard, G. S.; Lou, P.; Jiang, F.; McKeegan, E.; Lesniewski, R.; Davidsen, S. K.; Bell, R. L.; Wang, J. *Oncogene* **2008,** *27,* 3967–3976. doi:10.1038/onc.2008.14
141. McCowen, M. C.; Callender, M. E.; Lawlis, J. F., Jr. *Science* **1951,** *113,* 202–203. doi:10.1126/science.113.2930.202
142. Arico-Muendel, C.; Centrella, P. A.; Contonio, B. D.; Morgan, B. A.; O'Donovan, G.; Paradise, C. L.; Skinner, S. R.; Sluboski, B.; Svendsen, J. L.; White, K. F.; Debnath, A.; Gut, J.; Wilson, N.; McKerrow, J. H.; DeRisi, J. L.; Rosenthal, P. J.; Chiang, P. K. *Bioorg. Med. Chem. Lett.* **2009,** *19,* 5128–5131. doi:10.1016/j.bmcl.2009.07.029
143. Eisenman, H. C.; Casadevall, A. *Appl. Microbiol. Biotechnol.* **2012,** *93,* 931–940. doi:10.1007/s00253-011-3777-2
144. Cecchini, M. M.; Reale, S.; Manini, P.; d'Ischia, M.; De Angelis, F. *Chem. – Eur. J.* **2017,** *23,* 8092–8098. doi:10.1002/chem.201701951
145. Tsai, H.-F.; Washburn, R. G.; Chang, Y. C.; Kwon-Chung, K. J. *Mol. Microbiol.* **1997,** *26,* 175–183. doi:10.1046/j.1365-2958.1997.5681921.x
146. Schmaler-Ripcke, J.; Sugareva, V.; Gebhardt, P.; Winkler, R.; Kniemeyer, O.; Heinekamp, T.; Brakhage, A. A. *Appl. Environ. Microbiol.* **2009,** *75,* 493–503. doi:10.1128/aem.02077-08
147. Perez-Cuesta, U.; Aparicio-Fernandez, L.; Guruceaga, X.; Martin-Souto, L.; Abad-Diaz-de-Cerio, A.; Antoran, A.; Buldain, I.; Hernando, F. L.; Ramirez-Garcia, A.; Rementeria, A. *Int. Microbiol.* **2020,** *23,* 55–63. doi:10.1007/s10123-019-00078-0
148. Tsai, H.-F.; Wheeler, M. H.; Chang, Y. C.; Kwon-Chung, K. J. *J. Bacteriol.* **1999,** *181,* 6469–6477. doi:10.1128/jb.181.20.6469-6477.1999
149. Fujii, I.; Yasuoka, Y.; Tsai, H.-F.; Chang, Y. C.; Kwon-Chung, K. J.; Ebizuka, Y. *J. Biol. Chem.* **2004,** *279,* 44613–44620. doi:10.1074/jbc.m406758200
150. Langfelder, K.; Jahn, B.; Gehringer, H.; Schmidt, A.; Wanner, G.; Brakhage, A. A. *Med. Microbiol. Immunol.* **1998,** *187,* 79–89. doi:10.1007/s004300050077
151. Tsai, H.-F.; Fujii, I.; Watanabe, A.; Wheeler, M. H.; Chang, Y. C.; Yasuoka, Y.; Ebizuka, Y.; Kwon-Chung, K. J. *J. Biol. Chem.* **2001,** *276,* 29292–29298. doi:10.1074/jbc.m101998200
152. Sugareva, V.; Härtl, A.; Brock, M.; Hübner, K.; Rohde, M.; Heinekamp, T.; Brakhage, A. A. *Arch. Microbiol.* **2006,** *186,* 345–355. doi:10.1007/s00203-006-0144-2
153. Manini, P.; Bietti, M.; Galeotti, M.; Salamone, M.; Lanzalunga, O.; Cecchini, M. M.; Reale, S.; Crescenzi, O.; Napolitano, A.; De Angelis, F.; Barone, V.; d'Ischia, M. *ACS Omega* **2018,** *3,* 3918–3927. doi:10.1021/acsomega.8b00155

154. Chai, L. Y. A.; Netea, M. G.; Sugui, J.; Vonk, A. G.; van de Sande, W. W. J.; Warris, A.; Kwon-Chung, K. J.; Kullberg, B. J. *Immunobiology* **2010,** *215,* 915–920. doi:10.1016/j.imbio.2009.10.002
155. Thywißen, A.; Heinekamp, T.; Dahse, H.-M.; Schmaler-Ripcke, J.; Nietsche, S.; Zipfel, P. F.; Brakhage, A. A. *Front. Microbiol.* **2011,** *2,* 96. doi:10.3389/fmicb.2011.00096
156. Stappers, M. H. T.; Clark, A. E.; Aimanianda, V.; Bidula, S.; Reid, D. M.; Asamaphan, P.; Hardison, S. E.; Dambuza, I. M.; Valsecchi, I.; Kerscher, B.; Plato, A.; Wallace, C. A.; Yuecel, R.; Hebecker, B.; da Glória Teixeira Sousa, M.; Cunha, C.; Liu, Y.; Feizi, T.; Brakhage, A. A.; Kwon-Chung, K. J.; Gow, N. A. R.; Zanda, M.; Piras, M.; Zanato, C.; Jaeger, M.; Netea, M. G.; van de Veerdonk, F. L.; Lacerda, J. F.; Campos, A.; Carvalho, A.; Willment, J. A.; Latgé, J.-P.; Brown, G. D. *Nature* **2018,** *555,* 382–386. doi:10.1038/nature25974
157. Wong, S. S. W.; Rani, M.; Dodagatta-Marri, E.; Ibrahim-Granet, O.; Kishore, U.; Bayry, J.; Latgé, J.-P.; Sahu, A.; Madan, T.; Aimanianda, V. *J. Biol. Chem.* **2018,** *293,* 4901–4912. doi:10.1074/jbc.m117.815852
158. Kozlovskii, A. G.; Zhelifonova, V. P.; Antipova, T. V. *Appl. Biochem. Microbiol.* **2013,** *49,* 1–10. doi:10.1134/s0003683813010092
159. Robinson, S. L.; Panaccione, D. G. *Toxins* **2015,** *7,* 201–218. doi:10.3390/toxins7010201
160. Li, S.-M. *J. Antibiot.* **2011,** *64,* 45–49. doi:10.1038/ja.2010.128
161. Grundmann, A.; Li, S.-M. *Microbiology (Reading, U. K.)* **2005,** *151,* 2199–2207. doi:10.1099/mic.0.27962-0
162. Yamazaki, M.; Fujimoto, H.; Kawasaki, T. *Chem. Pharm. Bull.* **1980,** *28,* 245–254. doi:10.1248/cpb.28.245
163. Cui, C.-B.; Kakeya, H.; Osada, H. *Tetrahedron* **1997,** *53,* 59–72. doi:10.1016/s0040-4020(96)00978-7
164. Rabindran, S. K.; Ross, D. D.; Doyle, L. A.; Yang, W.; Greenberger, L. M. *Cancer Res.* **2000,** *60,* 47–50.
165. Chain, E.; Florey, H.; Jennings, M.; Williams, T. *Br. J. Exp. Pathol.* **1943,** *24,* 108.
166. Rank, C.; Larsen, T. O.; Frisvad, J. C. Functional systems biology of Aspergillus. In *Aspergillus: molecular biology and genomics;* Machida, M.; Gomi, K., Eds.; Caister Academic Press: Norfolk, UK, 2010; pp 173–198.
167. Tamiya, H.; Ochiai, E.; Kikuchi, K.; Yahiro, M.; Toyotome, T.; Watanabe, A.; Yaguchi, T.; Kamei, K. *J. Infect. Chemother.* **2015,** *21,* 385–391. doi:10.1016/j.jiac.2015.01.005
168. Cole, R. J.; Jarvis, B. B.; Schweikert, M. A. *Handbook of secondary fungal metabolites;* Elsevier, 2003.
169. Lv, J.-M.; Hu, D.; Gao, H.; Kushiro, T.; Awakawa, T.; Chen, G.-D.; Wang, C.-X.; Abe, I.; Yao, X.-S. *Nat. Commun.* **2017,** *8,* 1644. doi:10.1038/s41467-017-01813-9
170. Tomoda, H.; Nishida, H.; Kim, Y. K.; Obata, R.; Sunazuka, T.; Omura, S.; Bordner, J.; Guadliana, M.; Dormer, P. G.; Smith, A. B., III. *J. Am. Chem. Soc.* **1994,** *116,* 12097–12098. doi:10.1021/ja00105a078
171. Kim, Y. K.; Tomoda, H.; Nishida, H.; Sunazuka, T.; Obata, R.; Omura, S. *J. Antibiot.* **1994,** *47,* 154–162. doi:10.7164/antibiotics.47.154
172. Itoh, T.; Tokunaga, K.; Matsuda, Y.; Fujii, I.; Abe, I.; Ebizuka, Y.; Kushiro, T. *Nat. Chem.* **2010,** *2,* 858–864. doi:10.1038/nchem.764
173. Das, A.; Davis, M. A.; Tomoda, H.; Ômura, S.; Rudel, L. L. *J. Biol. Chem.* **2008,** *283,* 10453–10460. doi:10.1074/jbc.m709460200
174. Ohshiro, T.; Matsuda, D.; Sakai, K.; Degirolamo, C.; Yagyu, H.; Rudel, L. L.; Ōmura, S.; Ishibashi, S.; Tomoda, H. *Arterioscler., Thromb., Vasc. Biol.* **2011,** *31,* 1108–1115. doi:10.1161/atvbaha.111.223552
175. Raffa, N.; Keller, N. P. *PLoS Pathog.* **2019,** *15,* e1007606. doi:10.1371/journal.ppat.1007606

License and Terms

3.4 Manuscript 4 - Peroxiredoxin Asp f3 Is Essential for *Aspergillus fumigatus* To Overcome Iron Limitation during Infection

FORMULAR 1

Manuskript Nr. 4

Titel des Manuskriptes: Peroxiredoxin Asp f3 Is Essential for *Aspergillus fumigatus* To Overcome Iron Limitation during Infection

Autoren: Victor Brantl, Jana M. Boysen, Annie Yap, Evgeny Golubtsov, Dominik Ruf, Thorsten Heinekamp, Maria Straßburger, Karl Dichtl, Hubertus Haas, Falk Hillmann, Johannes Wagener

Bibliographische Informationen: Brantl, V., Boysen, J. M., Yap, A., Golubtsov, E., Ruf, D., Heinekamp, T., Straßburger, M., Dichtl, K., Haas, H., Hillmann, F., Wagener, J. (2021). Peroxiredoxin Asp f3 Is Essential for *Aspergillus fumigatus* To Overcome Iron Limitation during Infection. *Mbio*, *12*(4), e00976-21. https://doi.org/10.1128/mBio.00976-21

Der Kandidat / Die Kandidatin ist (bitte ankreuzen)

☐ Erstautor/-in, ☐ Ko-Erstautor/-in, ☐ Korresp. Autor/-in, ☒ Koautor/-in.

Status : publiziert

Anteile (in %) der Autoren / der Autorinnen an der Publikation

Autor/-in	Konzeptionell	Datenanalyse	Experimentell	Verfassen des Manuskriptes	Bereitstellung von Material
Jana M. Boysen	10 %	10 %	10 %	5 %	-
Victor Brant	20%	50 %	50 %	20 %	-
Johannes Wagener	60 %	30 %	-	50 %	60 %

AMERICAN SOCIETY FOR MICROBIOLOGY | mBio®

RESEARCH ARTICLE

Peroxiredoxin Asp f3 Is Essential for *Aspergillus fumigatus* To Overcome Iron Limitation during Infection

Victor Brantl,[a] Jana M. Boysen,[b,c] Annie Yap,[d] Evgeny Golubtsov,[e] Dominik Ruf,[a] Thorsten Heinekamp,[f] Maria Straßburger,[g] Karl Dichtl,[a] Hubertus Haas,[d] Falk Hillmann,[b] Johannes Wagener[a,e,h]

[a]Max von Pettenkofer-Institut für Hygiene und Medizinische Mikrobiologie, Medizinische Fakultät, LMU München, Munich, Germany
[b]Evolution of Microbial Interactions, Leibniz Institute for Natural Product Research and Infection Biology—Hans Knöll Institute, Jena, Germany
[c]Institute of Microbiology, Friedrich Schiller University Jena, Jena, Germany
[d]Institute of Molecular Biology, Medical University of Innsbruck, Innsbruck, Austria
[e]Institut für Hygiene und Mikrobiologie, Julius-Maximilians-Universität Würzburg, Würzburg, Germany
[f]Department of Molecular and Applied Microbiology, Leibniz Institute for Natural Product Research and Infection Biology—Hans Knöll Institute, Jena, Germany
[g]Transfer Group Anti-infectives, Leibniz Institute for Natural Product Research and Infection Biology—Hans Knöll Institute, Jena, Germany
[h]Department of Clinical Microbiology, School of Medicine, Trinity College Dublin, The University of Dublin, St James's Hospital Campus, Dublin, Ireland

ABSTRACT *Aspergillus fumigatus* is an important fungal pathogen that causes allergic reactions but also life-threatening infections. One of the most abundant *A. fumigatus* proteins is Asp f3. This peroxiredoxin is a major fungal allergen and known for its role as a virulence factor, vaccine candidate, and scavenger of reactive oxygen species. Based on the hypothesis that Asp f3 protects *A. fumigatus* against killing by immune cells, we investigated the susceptibility of a conditional *aspf3* mutant by employing a novel assay. Surprisingly, Asp f3-depleted hyphae were killed as efficiently as the wild type by human granulocytes. However, we identified an unexpected growth defect of mutants that lack Asp f3 under low-iron conditions, which explains the avirulence of the Δ*aspf3* deletion mutant in a murine infection model. *A. fumigatus* encodes two Asp f3 homologues which we named Af3l (Asp f3-like) 1 and Af3l2. Inactivation of Af3l1, but not of Af3l2, exacerbated the growth defect of the conditional *aspf3* mutant under iron limitation, which ultimately led to death of the double mutant. Inactivation of the iron acquisition repressor SreA partially compensated for loss of Asp f3 and Af3l1. However, Asp f3 was not required for maintaining iron homeostasis or siderophore biosynthesis. Instead, we show that it compensates for a loss of iron-dependent antioxidant enzymes. Iron supplementation restored the virulence of the Δ*aspf3* deletion mutant in a murine infection model. Our results unveil the crucial importance of Asp f3 to overcome nutritional immunity and reveal a new biological role of peroxiredoxins in adaptation to iron limitation.

IMPORTANCE Asp f3 is one of the most abundant proteins in the pathogenic mold *Aspergillus fumigatus*. It has an enigmatic multifaceted role as a fungal allergen, virulence factor, reactive oxygen species (ROS) scavenger, and vaccine candidate. Our study provides new insights into the cellular role of this conserved peroxiredoxin. We show that the avirulence of a Δ*aspf3* mutant in a murine infection model is linked to a low-iron growth defect of this mutant, which we describe for the first time. Our analyses indicated that Asp f3 is not required for maintaining iron homeostasis. Instead, we found that Asp f3 compensates for a loss of iron-dependent antioxidant enzymes. Furthermore, we identified an Asp f3-like protein which is partially functionally redundant with Asp f3. We highlight an unexpected key role of Asp f3 and its partially redundant homologue Af3l1 in overcoming the host's nutritional immunity. In addition, we uncovered a new biological role of peroxiredoxins.

KEYWORDS Asp f3, *Aspergillus fumigatus*, peroxiredoxin, iron regulation, virulence

Citation Brantl V, Boysen JM, Yap A, Golubtsov E, Ruf D, Heinekamp T, Straßburger M, Dichtl K, Haas H, Hillmann F, Wagener J. 2021. Peroxiredoxin Asp f3 is essential for *Aspergillus fumigatus* to overcome iron limitation during infection. mBio 12:e00976-21. https://doi.org/10.1128/mBio.00976-21.

Editor Jean-Paul Latge, IMBB-FORTH

Address correspondence to Johannes Wagener, wagenerj@tcd.ie.

Received 31 March 2021
Accepted 9 July 2021
Published 17 August 2021

Several molds in the genus *Aspergillus* are important opportunistic fungal pathogens that cause a broad range of human diseases (1). These include severe invasive infections in immunocompromised patients, so-called invasive aspergillosis (IA; mortality, approximately 30 to 95%), chronic noninvasive (aspergilloma) or semi-invasive colonization of body cavities in healthy or generally immunocompetent individuals, and allergic diseases such as allergic bronchopulmonary aspergillosis (ABPA) and asthma (2–4). In most cases, *Aspergillus fumigatus* is the causative agent (1, 4).

Neutrophils play a major role in the defense against IA (1, 4, 5). Because of this, IA occurs almost exclusively in patients with primary or secondary immunodeficiencies that correlate with neutrophil dysfunction (2, 3). In contrast, allergic diseases result from the exuberant response of the immune system to allergens. Continuing inhalation of *Aspergillus* conidia and hyphal fragments or transient or chronic colonization of the respiratory tract by aspergilli may cause a hypersensitive immune reaction in atopic individuals. This hypersensitivity is typically characterized by IgE and IgG antibodies directed against *Aspergillus* antigens (6, 7). Asp f3 is a highly abundant protein in *A. fumigatus* and was identified, among others, as a major fungal allergen (8, 9). Cutaneous hypersensitivity or positive antibodies in serum against *Aspergillus* antigens, including Asp f3, indicate sensitization, which was proposed as obligatory criterion for diagnosing ABPA (10).

The cellular role of Asp f3 in *A. fumigatus* remained unknown for a long time. In a proteomic approach, Lessing and colleagues showed that Asp f3 is the most upregulated protein in *A. fumigatus* after exposure to hydrogen peroxide (11). Deletion of the encoding gene, *aspf3*, results in complete loss of virulence in a murine infection model (12). Based on its amino acid sequence, Asp f3 is a peroxiredoxin. This biochemical function was later demonstrated with crude extracts of *Aspergillus* in an enzymatic assay (12). The Δ*aspf3* deletion mutant is highly susceptible to hydrogen peroxide and the organic hydroperoxide *tert*-butyl hydroperoxide (*t*-bOOH) (12). It was therefore suggested that Asp f3 has an important function in peroxide detoxification and thereby contributes to virulence, making the pathogen more resistant to reactive oxygen species (ROS) which are released by innate immune cells (e.g., granulocytes) to counter the infection (11, 12). Interestingly, Asp f3 was additionally proposed as a vaccine candidate against IA, since Asp f3-primed $CD4^+$ T cells can protect immunosuppressed mice from experimentally induced pulmonary aspergillosis (13, 14).

We recently established a novel killing assay to quantify the antifungal activity of granulocytes (15). In the present study, we used this assay to study the role of Asp f3 for *Aspergillus* to withstand killing by human granulocytes. Unexpectedly, we found that an Asp f3-depleted mutant is not more susceptible to killing than the wild type. In contrast, we detected a severe growth phenotype of Asp f3-lacking mutants under low-iron conditions. Furthermore, we identified an additional peroxiredoxin with partial functional redundancy, which we named Af3l1 (Asp f3-like 1). Importantly, supplementation with iron restored virulence of the Δ*aspf3* deletion mutant in a murine infection model. Based on our results, we highlight an unexpected key role of Asp f3 and its partially redundant homologue Af3l1 to overcome nutritional immunity during infection. In addition, we uncover a new biological role of peroxiredoxins.

RESULTS

Asp f3-depleted hyphae are H_2O_2 sensitive but not more efficiently killed by human granulocytes. ROS are of central importance for the host defense against invasive *Aspergillus* infections. This is evidenced by that fact that patients with chronic granulomatous disease (CGD), a hereditary inability of immune cells to produce various ROS, are at high risk for invasive aspergillosis (16). However, it remains controversial whether ROS directly kill the pathogens or indirectly mediate the immune defense, e.g., by promoting neutrophil degranulation and extracellular trap formation (5). The Δ*aspf3* deletion mutant is one of very few *A. fumigatus* mutants described that showed both increased susceptibility to ROS and avirulence in a murine infection model (12). To study the role of human granulocytes in inactivating *A. fumigatus* that lacks the

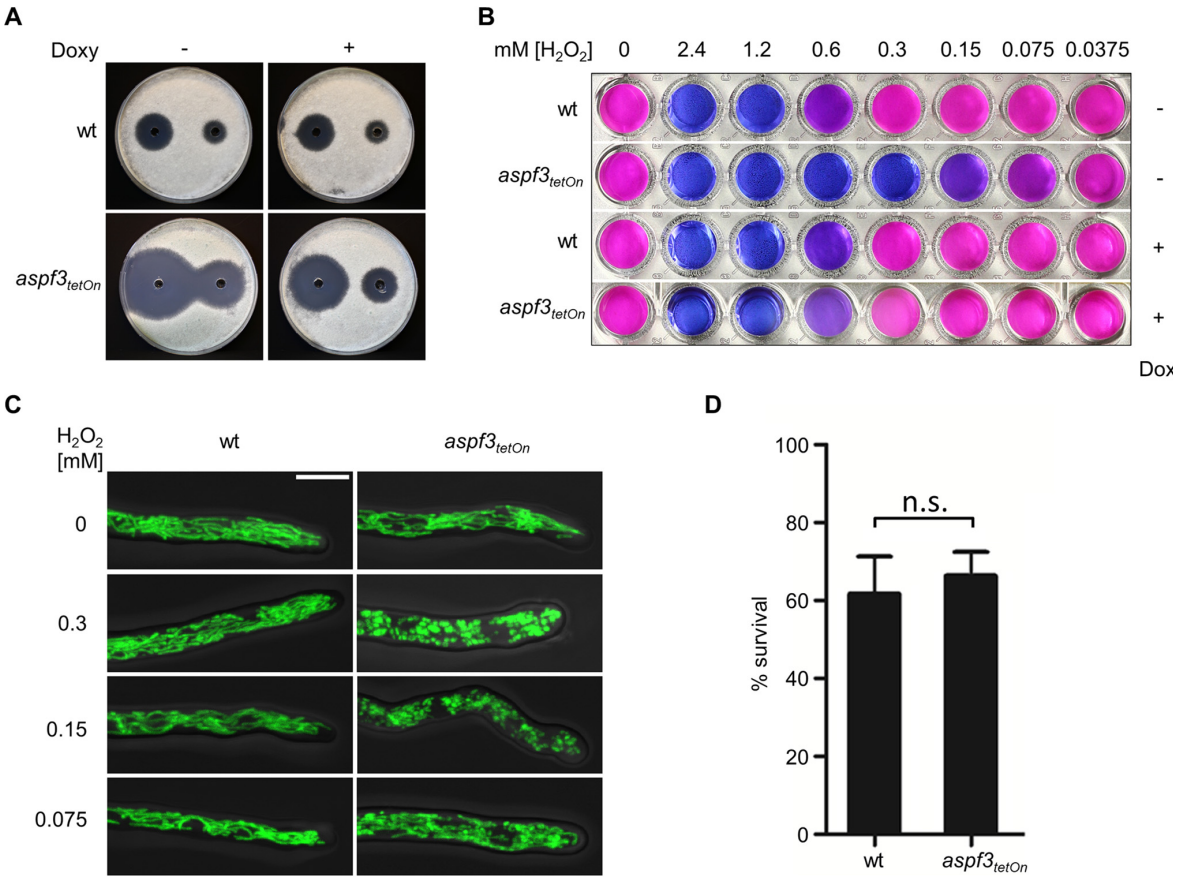

FIG 1 An Asp f3-depleted mutant is hypersensitive to hydrogen peroxide but is not more effectively killed by human granulocytes. (A) Conidia (4×10^5) of the indicated strains were spread on AMM agar plates. When indicated, medium was supplemented with doxycycline (7.5 μg ml^{-1}; Doxy). Fifty microliters of 300 mM (left) or 100 mM (right) H_2O_2 was applied in the punch holes of each agar plate. Images were taken after 30 h of incubation at 37°C. (B) Conidia (1.5×10^4) of the indicated strains were inoculated in 100 μl RPMI 1640 per well in a 96-well plate and incubated at 37°C with 5% CO_2. After 10 h, 100 μl medium supplemented with resazurin and, when indicated, H_2O_2 was added to a final concentration of 0.002% (wt/vol) resazurin and the indicated final concentration of H_2O_2. The plate was then incubated for another 24 h at 37°C with 5% CO_2. (C) Conidia of the indicated strains expressing mitochondrion-targeted GFP (mtGFP) were inoculated in RPMI 1640 and incubated at 37°C with 5% CO_2. After 10 h, medium was supplemented with the indicated H_2O_2 concentrations. After 2 h of incubation, samples were fixed and analyzed with a confocal laser scanning microscope. The depicted representative images are overlays of bright-field and GFP fluorescence images of optical stacks covering the entire hypha in focus. Bar, 5 μm (applicable to all images). (D) Conidia of the indicated strains expressing mtGFP were inoculated in RPMI 1640. Human granulocytes (PMNs) were added after 10 h of incubation at 37°C with 5% CO_2. After 2 h coincubation (37°C, 5% CO_2), samples were fixed and stained with calcofluor white. The ratio of vital hyphae (defined as hyphae with tubular or partially tubular mitochondrial morphology in more than 40% of a hyphal volume) was determined as described in Materials and Methods. The data in the graph are based on the results of three independent experiments. Statistical significance (n.s., not significant [$P > 0.05$]) was calculated with a two-tailed unpaired (assuming unequal variances) Student's *t* test. The error bars indicate standard deviations.

peroxide detoxification enzyme Asp f3, we constructed a conditional *aspf3* mutant by replacing the endogenous promoter with a doxycycline-inducible Tet-On promoter system (*aspf3*$_{tetOn}$). Growth of the wild type and of the induced or repressed *aspf3*$_{tetOn}$ mutant was indistinguishable with respect to germination, growth rate, and formation of conidia (asexual spores) under normal growth conditions (data not shown). However, under repressed conditions, the conditional *aspf3*$_{tetOn}$ mutant exhibited a severe susceptibility to hydrogen peroxide on solid agar and in liquid medium (Fig. 1A and B), very similar to a Δ*aspf3* deletion mutant characterized in previous studies. Induction of the conditional promoter partially rescued the increased hydrogen peroxide susceptibility of the mutant (Fig. 1A and B).

To assess the susceptibility of the *aspf3*$_{tetOn}$ mutant to killing by human granulocytes, we constructed a derivative that constitutively expresses mitochondrion-

targeted green fluorescent protein (mtGFP). This reporter, which we called MitoFLARE, allows visualizing and quantifying of hydrogen peroxide- as well as granulocyte-induced cell death of *Aspergillus* hyphae (15). Hydrogen peroxide readily induced fragmentation of the tubular mitochondrial network, thereby clearly indicating the increased ROS susceptibility of the conditional *aspf3*$_{tetOn}$ mutant under repressed conditions compared to the induced strain or to the mtGFP-expressing wild type (Fig. 1C). Next, we analyzed the susceptibility of the *aspf3*$_{tetOn}$ mutant to killing induced by granulocytes isolated from human blood (15). Surprisingly, the *aspf3*$_{tetOn}$ mutant under repressed conditions was not more prone to granulocyte-induced killing than the wild type (Fig. 1D).

Unexpected growth phenotype under low-iron conditions. Due to its drastically increased susceptibility to peroxides, we expected the conditional *aspf3*$_{tetOn}$ mutant under repressed conditions to be significantly more sensitive to killing by human granulocytes. We therefore attempted to confirm our result in an independent assay that relies on measuring the metabolic activity of the surviving fungi after killing by granulocytes with a colorimetric assay (e.g., see references 17–20). To this end, we inoculated conidia of the wild type and the *aspf3*$_{tetOn}$ strain under inducing and noninducing conditions in RPMI 1640 medium and incubated the respective well plates at 37°C overnight to obtain *Aspergillus* hyphae for exposing to granulocytes. Even though carbonate-buffered RPMI 1640 medium was used, the well plate was incubated at an atmospheric carbon dioxide concentration. This condition unveiled a growth defect (granulocyte independent) of the *aspf3*$_{tetOn}$ mutant under repressed conditions (Fig. 2A).

Apparently, the alkalization of the medium due to atmospheric carbon dioxide concentration and successive loss of the bicarbonate buffer caused precipitation of media components (Fig. 2A; also, see Fig. S1A in the supplemental material). We therefore tested which essential medium supplement can reconstitute growth of the Asp f3-depleted *Aspergillus* mutant. Of the three tested essential metals, i.e., iron, zinc, and copper, iron (Fe^{2+}) showed a striking effect (Fig. S1B). Supplementation of the precipitated RPMI 1640 medium with iron sulfate chelated with EDTA ($FeSO_4$-EDTA), which keeps iron soluble and bioavailable, apparently fully restored growth (Fig. 2B). To confirm these results, we artificially depleted media from free iron by adding bathophenanthrolinedisulfonic acid (BPS) or lactoferrin, a multifunctional protein with antibacterial and antifungal properties that binds iron. As shown in Fig. S1C and Fig. 2D and E, BPS and 2.5 mg ml^{-1} lactoferrin from bovine milk significantly inhibited growth of the *aspf3*$_{tetOn}$ mutant under repressed conditions. Very similar results were obtained for a Δ*aspf3* deletion mutant compared to its wild type (Fig. 2D and F). Doxycycline induced the conditional promoter of the *aspf3*$_{tetOn}$ mutant and fully rescued growth but did not affect the susceptibility of the Δ*aspf3* deletion mutant (Fig. 2D and E). Supplementation of the medium with iron, however, fully restored growth of both mutants, the repressed *aspf3*$_{tetOn}$ strain and the Δ*aspf3* strain (Fig. 2G and Fig. S1). This demonstrates that Asp f3 plays an important role in growth of *A. fumigatus* under low-iron conditions.

Identification of an Asp f3 homologue with functional overlap under low-iron but not under oxidative-stress conditions. Asp f3 belongs to the atypical 2-Cys group of peroxiredoxins (12, 21, 22). BLAST searches revealed that *A. fumigatus* encodes two other Asp f3-like (Af3l) proteins, Afu5g01440 (Af3l1) and Afu6g12500 (Af3l2), both of which remained uncharacterized. All three proteins harbor a conserved redoxin (PF08534) protein family (Pfam) (23) pattern that is not found in any other *A. fumigatus* proteins. The opportunistic pathogenic yeast *Candida albicans* encodes three Asp f3/Af3l1/Af3l2 homologues (CaAhp1, CaAhp2, and CaTrp99) and baker's yeast (*Saccharomyces cerevisiae*) only one (ScAhp1). Similar to *A. fumigatus*, other *Aspergillus* species, such as *Aspergillus niger*, *Aspergillus flavus* and *Aspergillus nidulans*, each encode three Asp f3/Af3l1/Af3l2 homologues. In all these species, the identified proteins are consistent with the proteins that harbor the conserved redoxin (PF08534) protein family pattern.

Alignments of the identified predicted proteins and analysis of transcription start based on RNA sequencing data (24) revealed that the start sites of translation of Af3l1,

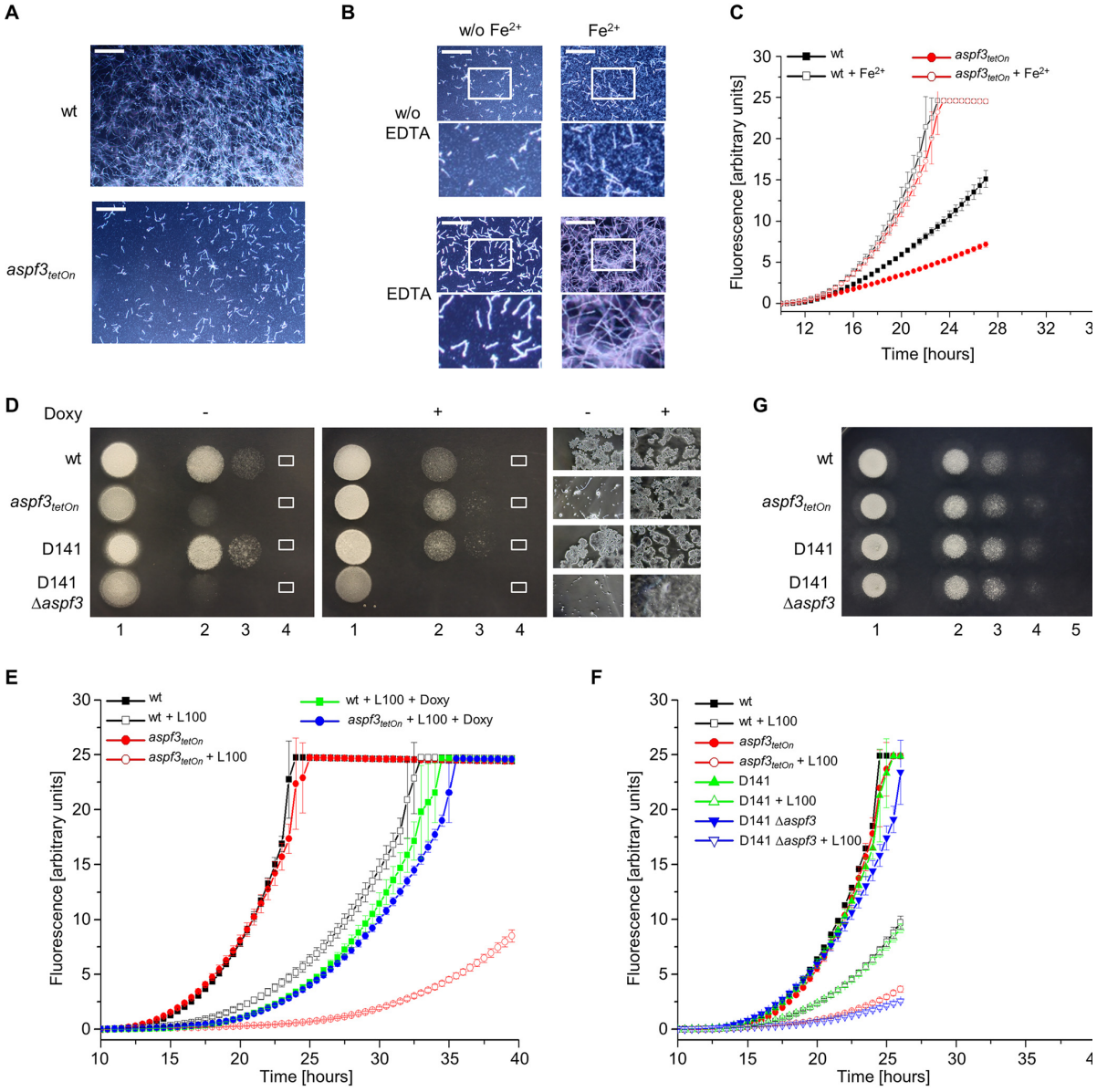

FIG 2 Asp f3 is important for growth under low-iron conditions. (A and B) Conidia (1.5×10^4) of the indicated strains (A) or of the *aspf3*$_{tetOn}$ strain (B) were inoculated in RPMI 1640 medium supplemented with 0.002% (wt/vol) resazurin per well in a 96-well plate. When indicated, medium was additionally supplemented with or without (w/o) 5 μg ml^{-1} $FeSO_4$ (Fe^{2+}) or 50 μg ml^{-1} EDTA. Plates were incubated at 37°C at atmospheric CO_2 concentration, causing partial precipitation of the medium. Representative dark-field images were taken after 10 h. Magnifications of the framed sections of the images are shown in the lower rows. Bars, 250 μm. (C, E, and F) Conidia (1.5×10^4) of the indicated strains were inoculated in RPMI 1640 medium supplemented with 0.002% (wt/vol) resazurin per well in a 96-well plate. When indicated, medium was additionally supplemented with 100 ng ml^{-1} $FeSO_4$ (Fe^{2+}), 7.5 μg ml^{-1} doxycycline (Doxy), or 100 μg ml^{-1} lactoferrin (L100). The plate was then incubated at 37°C with 5% CO_2. Resorufin fluorescence was documented over time with a microplate reader and plotted in the graphs. The error bars indicate standard deviations for three technical replicates. (D and G) In a series of 10-fold dilutions derived from a starting suspension of 5×10^7 conidia ml^{-1} of the indicated strains, aliquots of 3 μl were spotted on peptone agarose plates (1% [wt/vol] agarose, 1% [wt/vol] peptone; pH 7.0) supplemented with 2.5 mg ml^{-1} lactoferrin. When indicated, medium was additionally supplemented with 7.5 μg ml^{-1} doxycycline (Doxy). The plate depicted in panel G was additionally supplemented with 5 μg ml^{-1} $FeSO_4$. Representative images were taken after 30 h (D) or 24 h (G) incubation at 37°C. (D) Magnifications of the framed sections of the images are shown on the right.

Af3l2, and the *A. flavus* proteins encoded by AFLA_053060 and AFLA_019280 were most likely incorrectly annotated in the genome database (wrong start codon or splice sites). The corrected protein sequences, including full alignments thereof, are shown in Fig. S2. The tree depicted in Fig. 3A and Fig. S2 shows agglomerative clustering of the

full alignments of Asp f3-like proteins based on average distance and indicates that Af3l1 and Asp f3 are more similar than Af3l2 and Asp f3. The *A. nidulans* Asp f3 homologue PrxA (AN8692) was recently characterized and is reported to have a function similar to that previously described for Asp f3 in *A. fumigatus* (25).

In contrast to Asp f3, Af3l1 and related proteins, Af3l2 and its homologues (CaTrp99, An3687, and Afl053060) have an N-terminal extension of approximately 25 amino acids preceding the conserved redoxin domain (Fig. 3A). Analysis of the respective sequences with MitoFates (26) indicates that these are mitochondrial targeting signals. Af3l2 and its homologues are therefore most likely mitochondrial proteins. Interestingly, the Af3l2-like proteins lack the so-called "resolving" cysteine (C_R) in the N-terminal part of the protein which is highly conserved in the Asp f3- and Af3l1-like proteins and in ScAhp1 as well as in CaAhp1 (Fig. S2). This cysteine is essential for forming homodimers and for the peroxidase activities of Asp f3 and AnPrxA (12, 25).

We asked whether Af3l1 and Af3l2 have functions similar to those of the peroxiredoxins Asp f3 or AnPrxA. We therefore constructed mutants that lack *af3l1* or *af3l2*. No growth phenotypes were found under standard growth conditions for both gene deletion mutants (Fig. 3B). Besides this, hydrogen peroxide susceptibility and growth rates under low-iron conditions of the Δ*af3l1* and Δ*af3l2* deletion mutants were similar to those of the wild type (Fig. S3A and B). To check for potential functional redundancy of the enzyme, we constructed double and triple mutants. As shown in Fig. 3C and D, deletion of *af3l1*, *af3l2*, or both did not significantly alter growth or the hydrogen peroxide susceptibility of the $aspf3_{tetOn}$ mutant under repressed conditions. Significant differences were observed under low-iron conditions. Growth of the $aspf3_{tetOn}$ Δ*af3l1* double mutant and of the Δ*af3l1* Δ*af3l2* $aspf3_{tetOn}$ triple mutant under repressed conditions was drastically reduced compared to that of the $aspf3_{tetOn}$ single mutant in the presence of lactoferrin (Fig. 3E and F). Growth reduction under low-iron conditions of the $aspf3_{tetOn}$ Δ*af3l1* mutant and that of the Δ*af3l1* Δ*af3l2* $aspf3_{tetOn}$ mutant were comparable. Deletion of *af3l2* did not change the low-iron susceptibility of the $aspf3_{tetOn}$ mutant under repressed conditions (Fig. 3E and F). Notably, the $aspf3_{tetOn}$ Δ*af3l1* and the Δ*af3l1* Δ*af3l2* $aspf3_{tetOn}$ mutants were constructed independently but showed very similar increase of low-iron susceptibility under repressed conditions compared to the $aspf3_{tetOn}$ mutant (Fig. 3E and F). Induction of the Tet-On promoter restored growth of the conditional $aspf3_{tetOn}$ Δ*af3l1* mutant and the Δ*af3l1* Δ*af3l2* $aspf3_{tetOn}$ mutant under low-iron conditions compared to the wild type (Fig. 3E and Fig. S4). This clearly demonstrates that Af3l1 is partially functionally redundant with Asp f3 under low-iron conditions.

Asp f3 and Af3l1 are essential for survival under low-iron conditions. Growth of the $aspf3_{tetOn}$ Δ*af3l1* double mutant under repressed and low-iron conditions was almost abolished. Nevertheless, the $aspf3_{tetOn}$ Δ*af3l1* conidia were overall able to germinate and form short hyphae, but hyphae then stopped growing (Fig. 3E and 4A). We asked whether these fungi die during germination. The $aspf3_{tetOn}$ Δ*af3l1* mutant was transformed with a construct expressing mtGFP to visualize mitochondria, in order to quantify viability of individual hyphae (27). Mitochondrial morphology and dynamics of the resulting strain were analyzed over time under repressed conditions (Fig. 4; Videos S1 to S3). As shown in Fig. 4, the germlings still showed dynamic mitochondrial morphology after 12, 24, and 48 h. After 72 h, approximately 70% of the hyphae showed clear evidence of cell death (lysis of mitochondria and release of mtGFP to the cytoplasm, arrest of mitochondrial dynamics, and fading of GFP fluorescence). This indicates that the $aspf3_{tetOn}$ Δ*af3l1* hyphae are unable to grow but remain alive for an extended period.

Inactivation of the iron acquisition repressor SreA partially compensates for loss of Asp f3 and Af3l1. Iron uptake of *A. fumigatus* is under the control of a complex regulatory network. The two major regulators of iron homeostasis are SreA and HapX (28, 29). Under iron sufficiency or iron excess conditions, SreA suppresses high-affinity iron uptake and HapX triggers iron detoxification pathways. In contrast, under iron starvation, HapX activates a transcriptional response that results in repression of iron-

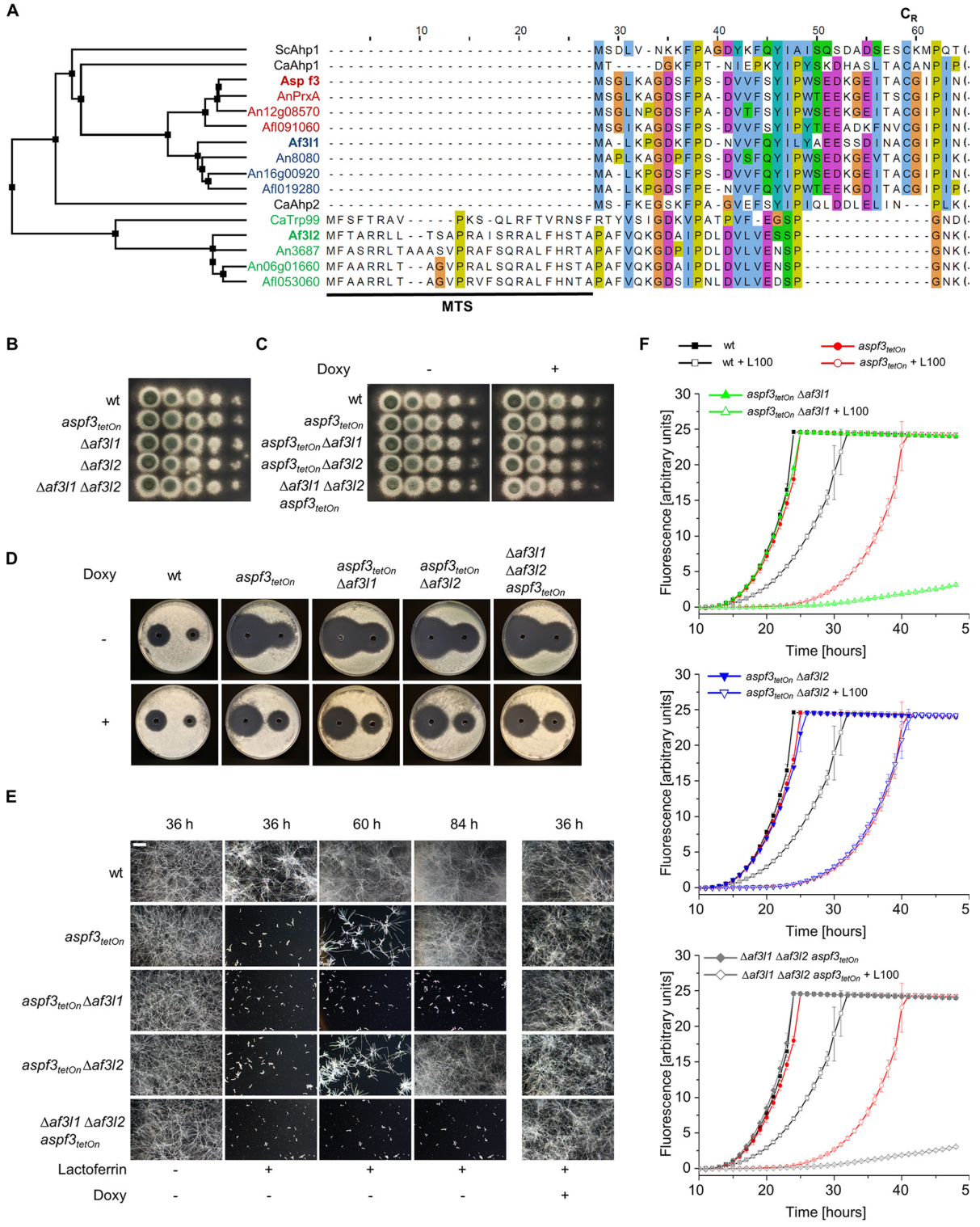

FIG 3 Identification and functional characterization of the Asp f3 homologues Af3l1 and Af3l2. (A) Average distance tree and alignment of the N-terminal sequences of Asp f3 and its homologues and putative paralogues in *A. fumigatus* (Af3l1 and Af3l2), *A. nidulans* (AnPrxA, An8080, and An3687), *A. flavus*

(Continued on next page)

consuming pathways and induction of iron uptake. We speculated that the low-iron growth deficiency of *Aspergillus* mutants lacking Asp f3 is related to incomplete derepression of iron acquisition enzymes. Deletion of *sreA* slightly improved the hydrogen peroxide tolerance of wild-type *A. fumigatus* and of the $aspf3_{tetOn}$ mutant and the $aspf3_{tetOn}$ Δ*af3l1* mutant under repressed conditions (Fig. 5A). The growth delay of the wild type observed under low-iron conditions was not improved upon deletion of *sreA* (Fig. 5C). In contrast, deletion of *sreA* significantly improved growth under low-iron conditions of the repressed $aspf3_{tetOn}$ and $aspf3_{tetOn}$ Δ*af3l1* mutants (Fig. 5B and C). However, it did not reach wild-type levels. This suggests either that the low-iron growth deficiency upon depletion of Asp f3 and Af3l1 is partially related to derepression of iron acquisition or that inactivation of SreA partially compensates for the defect caused by loss of peroxiredoxins indirectly by derepression of iron acquisition or by increasing the conidial iron content. In any case, these data underline a link between peroxiredoxin function and iron homeostasis.

Asp f3 has no major impact on iron homeostasis. Siderophore biosynthesis is vital for growth of *A. fumigatus* under low-iron conditions (28, 29). We speculated that impaired growth of the $aspf3_{tetOn}$ Δ*af3l1* mutant under low-iron conditions could be linked to a role of the peroxiredoxins in siderophore biosynthesis regulation. We therefore analyzed production of the extracellular siderophores triacetylfusarinine C and fusarinine C and of the intracellular siderophore ferricrocin of the $aspf3_{tetOn}$ mutant, the $aspf3_{tetOn}$ Δ*af3l1* mutant, and the wild type under noninduced and induced conditions. As shown in Fig. 6A, B, and C, we found no significant differences with respect to siderophore biosynthesis in the different strains under repressed conditions. Interestingly, induction of *aspf3* expression with doxycycline seemed to result in a minor increase of fusarinine C synthesis. Nevertheless, this suggests that the growth deficiency of $aspf3_{tetOn}$ and $aspf3_{tetOn}$ Δ*af3l1* mutants under repressed conditions is not related to siderophore biosynthesis. As siderophore biosynthesis is regulated by SreA, these data also indicate that peroxiredoxins do not directly affect SreA activity (see above).

To analyze a potential direct impact of Asp f3 on iron homeostasis during germination, we analyzed transcript levels of iron-regulated genes in conidia and germinating hyphae under low-iron conditions with Northern blot analysis. Altered iron homeostasis, as seen for example in mutants that lack intracellular siderophores (e.g., a Δ*sidA* mutant), was previously shown to cause a characteristic "iron starvation signature" in the conidial transcriptome (30). As shown in Fig. S5A, *hapX* (encoding an iron-regulatory transcription factor, already mentioned above) and *ftrA* (encoding an iron permease involved in reductive iron assimilation) were not upregulated in conidia of the $aspf3_{tetOn}$ mutant which were obtained from mycelium on solid agar under repressed conditions. Furthermore, transcript levels of *mirB* (encoding a siderophore transporter) and *ftrA* of the $aspf3_{tetOn}$ mutant under repressed conditions were not significantly changed during germination under low-iron conditions (Fig. S5B). Taken together, these data indicate that Asp f3 is not a central regulator of fungal iron homeostasis.

FIG 3 Legend (Continued)

(Afl091060, Afl019280, and Afl053060), *A. niger* (An12g08570, An16g00920, and An06g01660), *S. cerevisiae* (ScAhp1), and *C. albicans* (CaAhp1, CaAhp2, and CaTrp99). The black bar indicates a putative mitochondrial targeting signal (MTS). A conserved resolving cysteine (C_R) is indicated. Sequences of Af3l1, Af3l2, Afl019280, and Afl053060 have been corrected taking into account most likely incorrectly annotated start codons or splice sites for the respective sequences in genome databases. Alignment (MAFFT, Clustal color scheme) is based on total protein sequences; the average distance tree was generated with BLOSUM62. The full alignment is available in Fig. S2. (B and C) In a series of 10-fold dilutions derived from a starting suspension of 5×10^7 conidia ml^{-1} of the indicated strains, aliquots of 3 μl were spotted on AMM agar plates. When indicated, medium was supplemented with 7.5 μg ml^{-1} doxycycline (Doxy). Representative images were taken after 30 h of incubation at 37°C. (D) Conidia (4×10^5) of the indicated strains were spread on AMM agar plates. When indicated, medium was supplemented with doxycycline (7.5 μg ml^{-1}; Doxy). Fifty microliters of 300 mM (left) or 100 mM (right) H_2O_2 was applied in the punch holes of each agar plate. Images were taken after 30 h of incubation at 37°C. (E and F) Conidia (1.5×10^3 [E] or 1.5×10^4 [F]) of the indicated strains were inoculated in RPMI 1640 medium supplemented with 100 ng ml^{-1} $FeSO_4$ per well in 96-well plates. For panel F, medium was additionally supplemented with 0.002% (wt/vol) resazurin. When indicated, medium was additionally supplemented with 100 μg ml^{-1} lactoferrin (L100) or 7.5 μg ml^{-1} doxycycline (Doxy). Plates were then incubated at 37°C with 5% CO_2. (E) After the indicated incubation time, representative dark-field images were taken. Bar, 250 μm (applicable to all images). (F) Resorufin fluorescence was documented over time with a microplate reader and plotted in the graph. The error bars indicate standard deviations for three technical replicates.

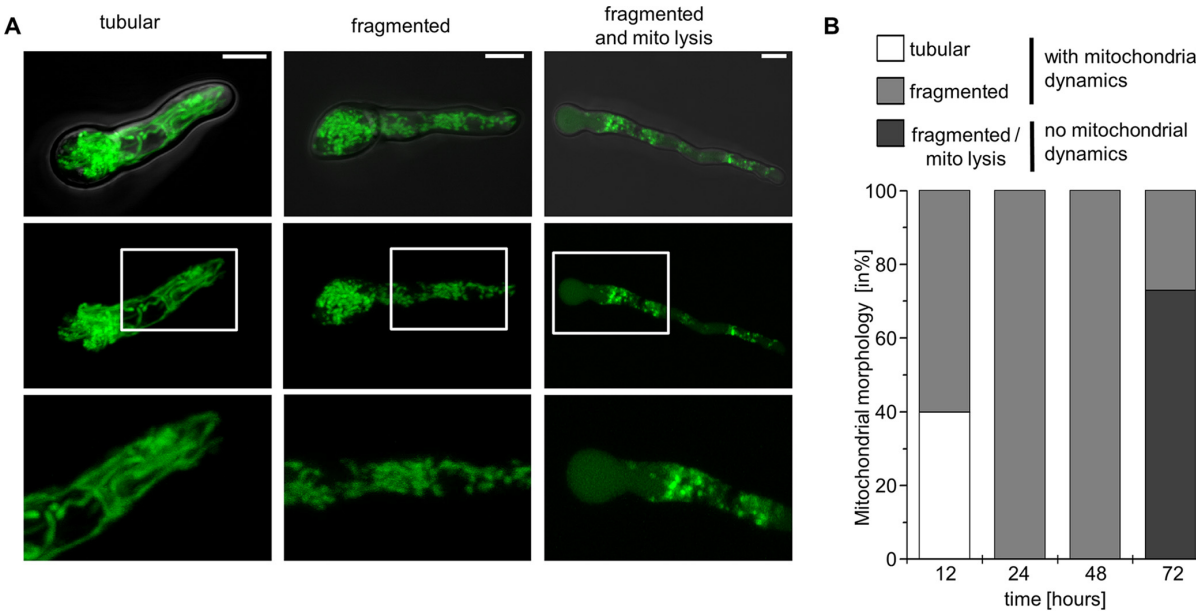

FIG 4 Asp f3 and Af3l1 are essential for survival under iron-limited conditions. (A and B) Conidia of the *aspf3*$_{tetOn}$ Δ*af3l1* mutant expressing mitochondrion-targeted GFP (mtGFP) were inoculated in RPMI 1640 supplemented with 100 ng ml^{-1} $FeSO_4$ and 200 μg ml^{-1} lactoferrin under repressed conditions (no doxycycline). Samples were incubated at 37°C with 5% CO_2 and then analyzed with a laser scanning microscope. (A) Representative GFP fluorescence images of hyphae with tubular (left) and fragmented (middle and right) mitochondrial morphology after 12 h, 24 h, and 72 h of incubation, respectively. The hypha on the right shows cytosolic fluorescence, which indicates disruption of mitochondrial integrity (mito lysis) and release of mtGFP to the cytosol. Depicted are images of optical stacks covering the entire hyphae in focus (middle row), magnifications of the framed sections therein (bottom row), and overlays of bright-field and GFP fluorescence images (top row). Bars, 5 μm. (B) The viability of 100 individual hyphae per time point was analyzed in independent samples after 12, 24, 48, and 72 h of incubation based on the mitochondrial morphology and dynamics. Hyphae which exhibited a tubular or fragmented mitochondrial morphology with mitochondrial dynamics were considered alive. Hyphae which exhibited a fragmented mitochondrial morphology without mitochondrial dynamics with or without cytosolic fluorescence or no fluorescence were considered dead.

Expression of *aspf3* is responsive to iron availability. Because of the unexpected low-iron growth phenotype of the *aspf3* mutant, we investigated whether *aspf3* expression is subject to iron regulation at the transcriptional level (Fig. 6B). The analysis of the short-term adaptation from iron starvation to iron sufficiency has previously proven to be a highly sensitive tool for identifying iron-dependent regulation (31, 32). The *A. fumigatus* wild type and mutants lacking either SreA or HapX, which both encode key iron regulators, were cultured under iron starvation for 18 h (−Fe). Subsequently, iron was added, and cultivation was continued for another hour (sFe). While SreA transcriptionally represses iron acquisition during iron sufficiency, HapX transcriptionally activates iron acquisition and represses iron consumption during iron starvation. Furthermore, HapX activates iron-consuming pathways and iron detoxification during short-term adaptation from iron starvation to iron sufficiency (28, 29). As strain and growth condition controls, we analyzed the transcript levels of the genes that encode the siderophore transporter MirB (*mirB*, mentioned above) and the heme iron-dependent mycelial catalase Cat1 (*cat1*). In agreement with previous reports (31, 32), *mirB* showed a decreased transcript level in the Δ*hapX* mutant during iron starvation and was significantly downregulated during short-term adaptation to iron sufficiency, with a slightly increased transcript level in the Δ*sreA* mutant. In contrast, *cat1* expression was downregulated in a HapX-dependent manner during iron starvation and induced during short-term adaptation from iron starvation to iron sufficiency. Lack of SreA caused an increased *cat1* transcript level during the short-term adaptation, which is most likely a result of increased iron acquisition and, consequently, increased activation of HapX in this strain.

During iron starvation, the wild type and the mutant strains displayed similar *aspf3* transcript levels. Upon short-term adaptation to iron sufficiency, the *aspf3* transcript

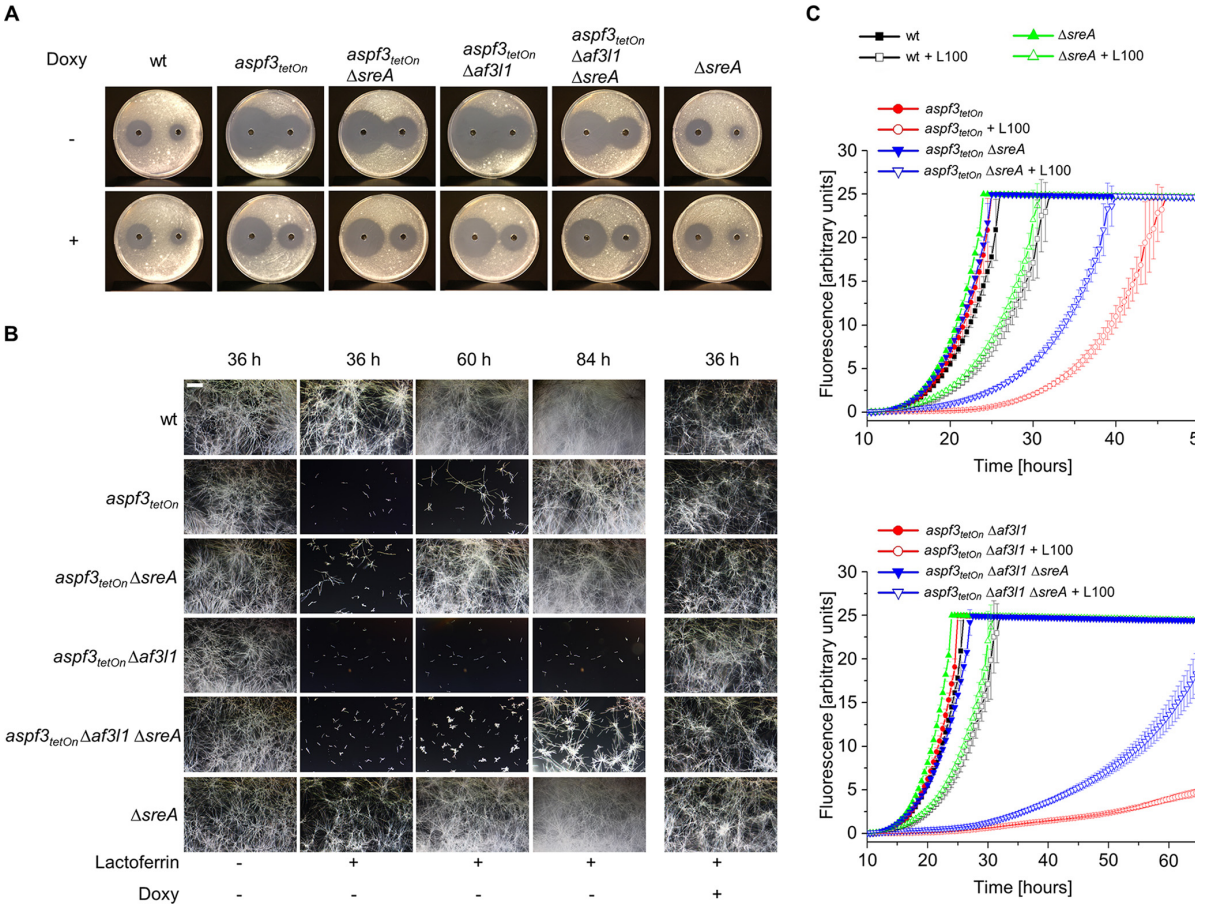

FIG 5 Deletion of the iron acquisition repressor *sreA* partially compensates for loss of Asp f3 and Af3l1. (A) Conidia (4×10^5) of the indicated strains were spread on AMM agar plates. When indicated, medium was supplemented with doxycycline (7.5 μg ml^{-1}; Doxy). Fifty microliters of 300 mM (left) or 100 mM (right) H_2O_2 was applied in the punch holes of each agar plate. Images were taken after 30 h of incubation at 37°C. (B and C) Conidia (1.5×10^3 [B] or 1.5×10^4 [C]) of the indicated strains were inoculated in RPMI 1640 medium supplemented with 100 ng ml^{-1} $FeSO_4$ per well in 96-well plates. For panel C, medium was additionally supplemented with 0.002% (wt/vol) resazurin. When indicated, medium was additionally supplemented with 100 μg ml^{-1} lactoferrin (L100) or 7.5 μg ml^{-1} doxycycline (Doxy). Plates were then incubated at 37°C with 5% CO_2. (B) After the indicated incubation time, representative dark-field images were taken. Bar, 250 μm (applicable to all images). (C) Resorufin fluorescence was documented over time with a microplate reader and plotted in the graph. The error bars indicate standard deviations for three technical replicates.

level decreased slightly in the wild type and was more pronounced in the Δ*sreA* mutant, while it was largely unaffected in the Δ*hapX* mutant. The enhanced downregulation of *aspf3* during short-term adaptation to iron sufficiency in the Δ*sreA* mutant compared to the wild type could be explained by the fact that lack of SreA leads to elevated iron uptake, which would then increase the slight iron repression observed in the wild type. The lacking downregulation of *aspf3* in the Δ*hapX* mutant indicates that HapX is required for repression of *aspf3* during short-term adaptation to iron sufficiency. These data demonstrate that *aspf3* expression is modulated by iron availability at the transcript level and responds to iron availability largely inversely compared to *cat1*.

ROS susceptibility of the repressed *aspf3*$_{tetOn}$ and *aspf3*$_{tetOn}$ Δ*af3l1* mutants is further increased under low-iron conditions. Our data indicated that compared to the wild type, *cat1* and *aspf3* are inversely regulated in an iron- and HapX-dependent manner. The shift from iron starvation to iron sufficiency caused an increase of *cat1* expression and a decrease of *aspf3* expression. Notably, many antioxidant enzymes, such as the major catalases in *A. fumigatus* (Cat1 and Cat2) and the cytochrome *c*

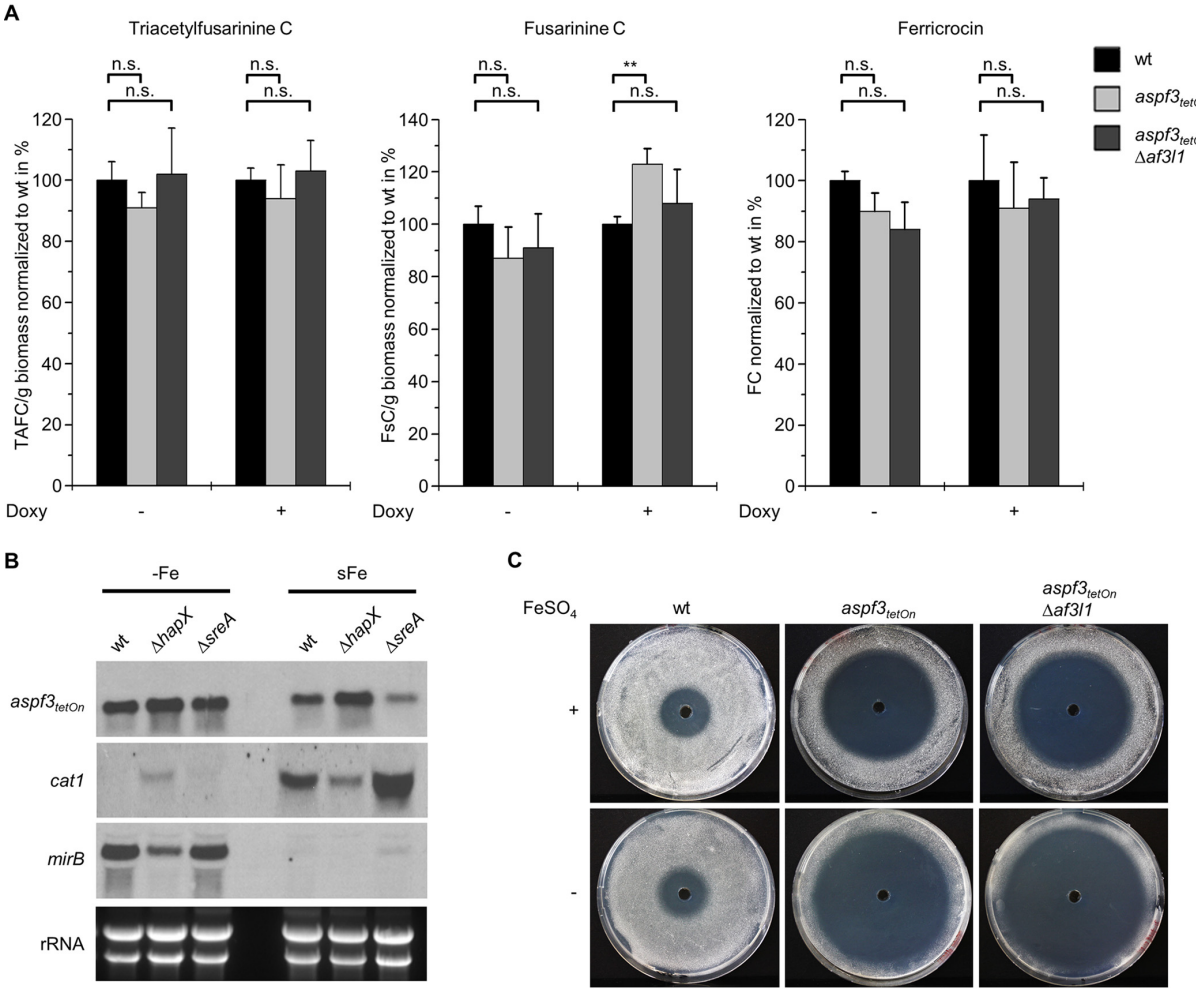

FIG 6 Siderophore biosynthesis is not changed in the *aspf3 af3l1* mutant, but *aspf3* expression is iron responsive. (A) Production of the extracellular (triacetylfusarinine C and fusarinine C) and intracellular (ferricrocin) siderophores in submersed growth for 18 h at 37°C in a liquid AMM variant as described in Materials and Methods was normalized to biomass and wild type (wt). When indicated, medium was supplemented with doxycycline (10 μg ml^{-1}; Doxy). Statistical significance (n.s., not significant [$P > 0.05$]; **, $P < 0.01$) was calculated with one-way ANOVA with *post hoc* Tukey's HSD test. The error bars indicate standard deviations for three technical replicates. (B) Conidia (1×10^6) of *A. fumigatus* ATCC 46645 (wt) and of the Δ*hapX* and Δ*sreA* mutants were inoculated in 100 ml of the liquid AMM variant in shake flasks and incubated for 18 h under iron-depleted conditions at 37°C (−Fe). Subsequently, $FeSO_4$ was added to a final concentration of 0.03 mM, and the cultures were incubated for one more hour at 37°C to monitor short-term adaptation from iron starvation to iron sufficiency (sFe). Total RNA was isolated before (−Fe) and after (sFe) iron addition and subjected to Northern blot analysis with *aspf3*, *cat1*, and *mirB* hybridization probes. Ethidium bromide-stained rRNA is shown as a control for RNA loading and quality. (C) Conidia (1×10^6) of the indicated strains were spread on peptone agarose plates (1% [wt/vol] agarose, 1% [wt/vol] peptone; pH 7.0). When indicated, medium was supplemented with 5 μg ml^{-1} $FeSO_4$ (Fe^{2+}). Fifty microliters of 100 mM H_2O_2 was applied in the punch holes of each agar plate. Images were taken after 48 h of incubation at 37°C.

peroxidase (Ccp1), functionally depend on iron. We asked whether Asp f3 and Af3l1 are especially required under low-iron conditions to counter oxidative stress. As shown in Fig. 6C, the hydrogen peroxide inhibition zones of the wild type were indistinguishable on peptone agarose, which is low in iron, and on peptone agarose supplemented with iron sulfate. In marked contrast, the reduced availability iron on the peptone agarose medium drastically increased the hydrogen peroxide susceptibility of the *aspf3*$_{tetOn}$ and *aspf3*$_{tetOn}$ Δ*af3l1* mutants under repressed conditions.

Iron restores virulence of the Δ*aspf3* mutant in a mammalian infection model. Our results demonstrated that lactoferrin specifically inhibits growth of the *aspf3*$_{tetOn}$ mutant and the *aspf3*$_{tetOn}$ Δ*af3l1* mutant under repressed conditions by sequestering

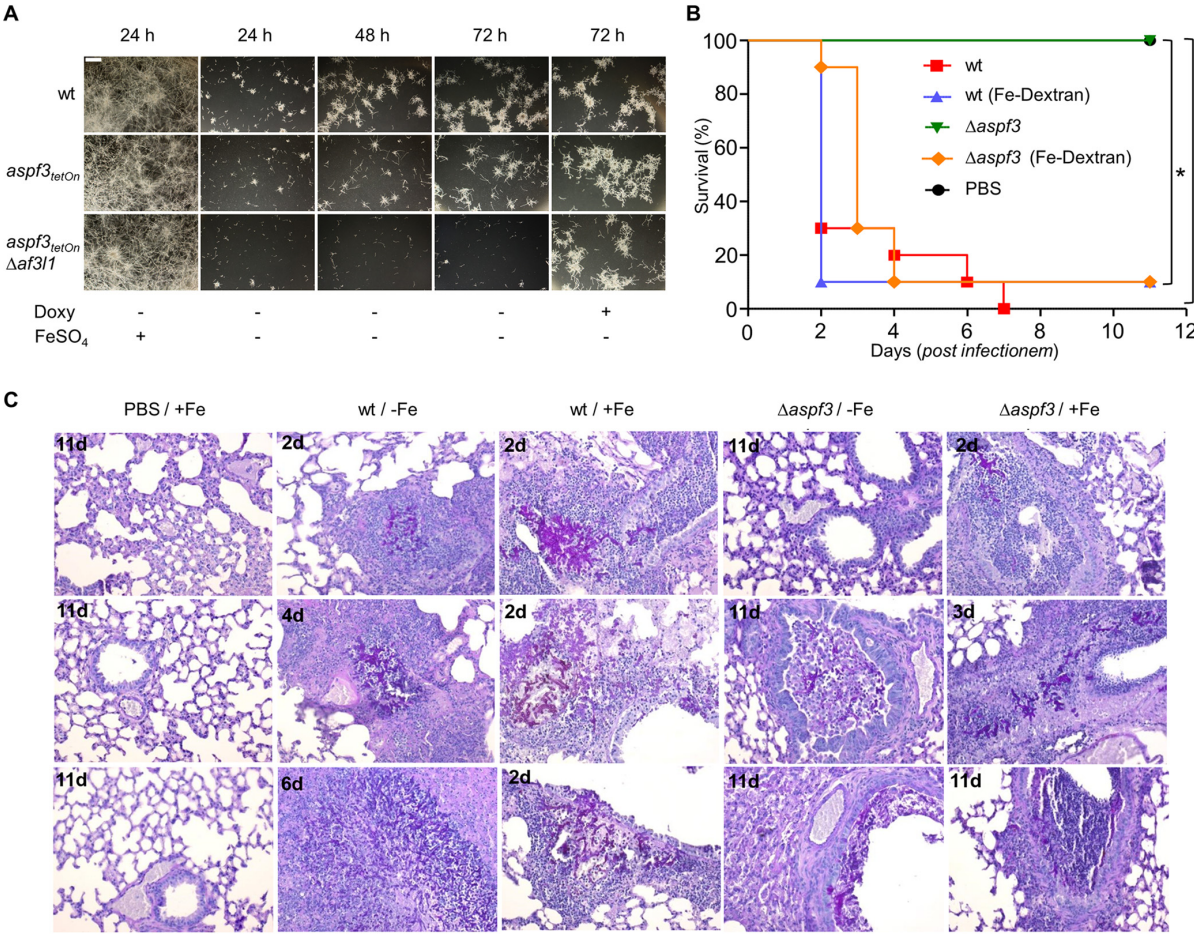

FIG 7 The avirulence of the Δ*aspf3* mutant is linked to the iron deprivation in the host. (A) Conidia (1.5×10^3 per well) of the indicated strains were inoculated in 60% (vol/vol) serum in ddH_2O in a 96-well plate. When indicated, medium was supplemented with 50 μg ml^{-1} $FeSO_4$ or 7.5 μg ml^{-1} doxycycline (Doxy). Plates were then incubated at 37°C for the indicated times. After the indicated incubation times, representative dark-field images were taken. Bar, 250 μm (applicable to all images). (B) Survival of mice after intranasal infection with conidia of *A. fumigatus* D141 (wt) and the Δ*aspf3* mutant. Immunosuppressed mice were left untreated or loaded with iron (iron dextran) prior to intranasal infection with conidia ($n = 10$ per strain/treatment group). A control group ($n = 4$) was infected with PBS as a mock control. The percentage of survivors after each day of infection is shown in the graph. *, $P < 0.001$ (log-rank test and the Gehan-Wilcoxon test). (C) Histology of lungs from mice infected with *A. fumigatus*. Lung sections were stained with periodic acid-Schiff (PAS). The presence of tissue invasive fungal hyphae (magenta) and infiltration of immune cells (purple nuclei) was confirmed in lungs of mice infected with wild-type conidia in the presence (+Fe) or absence (−Fe) of iron and in lung sections infected with the Δ*aspf3* strain with Fe. Fungal hyphae and immune cells were rarely found in Δ*aspf3*-strain-infected lungs without Fe. Numbers in the upper left corners indicate days postinfection.

available iron. This supports a model where nutritional immunity could be responsible for the previously reported avirulence of the Δ*aspf3* deletion mutant in a murine infection model (12). To further substantiate this model, we tested whether the *aspf3*$_{tetOn}$ and the *aspf3*$_{tetOn}$ Δ*af3l1* mutants have specific difficulties growing in serum. Serum is known to be a harsh environment for *Aspergillus* because iron is bound to transferrin and difficult to access (33, 34). As shown in Fig. 7A, growth of the *aspf3*$_{tetOn}$ mutant and, even more so, that of the *aspf3*$_{tetOn}$ Δ*af3l1* mutant in 60% (vol/vol) serum under repressed conditions was significantly reduced compared to that of the wild type. The induction of the conditional promoter with doxycycline restored growth of the two peroxiredoxin mutants to wild-type levels. In agreement with the sequestration of iron being the cause of the reduced growth of the mutants in serum, iron supplementation drastically improved growth of these strains.

This suggests that the avirulence of an Δ*aspf3* deletion mutant is primarily linked to the low-iron environment under host infection conditions. To confirm this hypothesis,

we performed a murine infection experiment under conditions that overturn the low-iron conditions in the lungs of a nonneutropenic host. For this, mice were immunosuppressed with cortisone acetate, exposed to high iron levels by intraperitoneal injection of iron dextran, and infected intranasally with conidia of wild-type *A. fumigatus* D141 or of the corresponding Δ*aspf3* deletion mutant. For wild-type conidia, such a dose caused a lethal outcome of the infection within 2 to 7 days, independent of iron supplementation. As expected from the previous study, conidia of the Δ*aspf3* deletion mutant were avirulent. However, iron supplementation reconstituted their virulence up to wild-type levels (Fig. 7B). Iron-dependent virulence of the Δ*aspf3* strain was reflected by histopathological analysis of the lungs of infected mice (Fig. 7C). While tissue invasive hyphae and infiltration of immune cells were frequently found in the wild-type within 2 to 6 days postinfection, tissue invasion was not observed in lungs infected with the Δ*aspf3* mutant. Extensive hyphal growth of the mutant was in turn detected after iron supplementation. This shows that the avirulence of the Δ*aspf3* mutant is tightly linked to its inability to cope with low-iron conditions and demonstrates that Asp f3 is an essential key player for *A. fumigatus* to overcome iron limitation during infection of a host.

DISCUSSION

Asp f3 is one of the most abundant proteins in *A. fumigatus* and is known for its multifaceted role as an allergen, ROS scavenger, virulence factor, and vaccine candidate (8, 10, 12–14). However, despite being studied for more than 2 decades, the cellular function of Asp f3 remains unknown. A Δ*aspf3* deletion mutant is highly susceptible to ROS. It was therefore proposed that the avirulence of the Δ*aspf3* deletion mutant in a murine infection model is attributed to more ROS-mediated damage caused by innate immune cells (12, 35, 36). However, we could not observe more efficient killing of the *aspf3*$_{tetOn}$ hyphae by human granulocytes under repressed conditions compared to wild-type hyphae. This indicates that it is not in the first instance the increased susceptibility to killing by immune cells which is the cause of the avirulence of the Δ*aspf3* deletion mutant.

In our study we discovered a new role of the peroxiredoxin Asp f3 and its homologue Af3l1, which they redundantly exert. The Δ*aspf3* deletion mutant and the conditional *aspf3*$_{tetOn}$ mutant under repressed conditions have severe problems growing under iron-limited conditions. Additional deletion of *af3l1* significantly reinforces this growth defect. A second Asp f3 homologue, Af3l2, appears not to be involved in iron homeostasis, as the deletion of the encoding gene did not reinforce the investigated phenotype. This is in agreement with the finding that Af3l2, in contrast to Asp f3 and Af3l1, harbors a putative N-terminal mitochondrial targeting signal which presumably guides this protein to a subcellular compartment distinct from that of Asp f3 and Af3l1.

Homologues of Asp f3 and Af3l1 are found in other fungal pathogens. Close homologues in *A. nidulans* (AnPrxA), *C. albicans* (CaAhp1), and *S. cerevisiae* (ScAhp1) were shown to have a role in detoxification of ROS, similar to what was previously described for *A. fumigatus* Asp f3 (12, 25, 37, 38). To our knowledge, neither Asp f3 nor any of its homologues in other species has been linked to iron homeostasis or growth under iron-limited conditions. We speculated that Asp f3 and Af3l1 could be involved in iron homeostasis or siderophore biosynthesis. However, the expression of genes which are typically regulated dependent on the intracellular iron availability, such as those encoding the iron-regulatory transcription factor HapX, the iron permease FtrA, and the siderophore transporter MirB, were not significantly altered in the *aspf3*$_{tetOn}$ mutant under repressed and low-iron conditions compared to the wild type. Moreover, biosynthesis of the extracellular siderophores triacetylfusarinine C and fusarinine C and of the intracellular siderophore ferricrocin was not significantly changed in mutants lacking Asp f3 and Af3l1. These results strongly argue against a key regulatory role of Asp f3 and Af3l1 in maintaining iron homeostasis of *A. fumigatus* under low-iron conditions.

Interestingly, deletion of *sreA*, a gene which encodes the important iron acquisition repressor SreA, partially compensates for the growth defect of the repressed *aspf3*$_{tetOn}$

and *aspf3*$_{tetOn}$ Δ*af3l1* mutants under iron-limited conditions. Surprisingly, ROS tolerance of the *aspf3*$_{tetOn}$ and *aspf3*$_{tetOn}$ Δ*af3l1* mutants under repressed conditions was also slightly improved upon deletion of *sreA*. The only partial compensations indicate that the low-iron growth deficiency and the ROS susceptibility are not mediated via SreA hyperactivity in the repressed *aspf3*$_{tetOn}$ and *aspf3*$_{tetOn}$ Δ*af3l1* mutants. This is underlined by the fact that siderophore production, which is regulated by SreA (31), was wild type-like in *aspf3*$_{tetOn}$ and *aspf3*$_{tetOn}$ Δ*af3l1* mutants. Congruently, it suggests that the ROS susceptibility and the low-iron growth deficiency are linked, as SreA seemingly affects both.

Our data demonstrate that iron depletion with lactoferrin remarkably inhibits germination of *A. fumigatus* conidia which lack Asp f3. Even though lactoferrin was reported to have multiple antimicrobial activities (39), the specific susceptibility of the *aspf3* mutant found in this study is unambiguously linked to the iron sequestration. First, other iron-depleting conditions, e.g., adding the iron chelator BPS, caused a very similar growth defect. Second, supplementation of the lactoferrin-containing medium with iron fully suppressed the growth defect. Lactoferrin is found in excessive amounts in many body fluids, including lung secretions, where it serves as an antimicrobial peptide and sequesters iron (40, 41).

An adequate supply of essential trace elements is crucial for fungal and bacterial pathogens to establish an infection (28, 42). Because of this, metazoa evolved multiple mechanisms to deprive possibly invading microbes from essential trace elements such as iron, a concept which is called nutritional immunity (43). Our results demonstrate that Asp f3 and its homologue Af3l1 are essentially required to grow and to survive under iron-limited conditions. Importantly, we could show that Asp f3 and Af3l1 are required to overcome the iron limitation in human serum. Furthermore, we could show that supplementation with iron restores the tissue invasive growth and the virulence of the Δ*aspf3* deletion mutant even in the nonneutropenic murine infection model used here. Together, this indicates that the avirulence of the Δ*aspf3* deletion is primarily caused by the inability of the mutant to grow under iron-limited conditions, rather than resulting from an increased susceptibility to innate immune cells. It should not be ruled out at this point that *in vivo* innate immune cells, such as neutrophilic granulocytes, may additionally limit the access to iron, e.g., via the well-documented release of lactoferrin (44), or in addition may more efficiently inactivate the mutant because of the increased ROS susceptibility under iron-deprived conditions. In agreement with this model, *aspf3* expression is regulated in a HapX- and iron availability-dependent manner. This makes Asp f3 an important virulence factor which is specifically required to overcome iron-depriving nutritional immunity during infection of the host. In summary, this study highlights for the first time the crucial role of a peroxiredoxin as a virulence factor which is specifically required to overcome iron-depriving nutritional immunity during infection of the host.

What is the mechanism by which Asp f3 and Af3l1 enable the mold to grow and survive under iron-limited conditions? A recent study performed with baker's yeast revealed that yeast cells that starve produce nontoxic levels of ROS, which results in the unconventional secretion of normally intracellular antioxidant enzymes, including the Asp f3/Af3l1 homologue ScAhp1 (45). The authors concluded that there is a mechanism whereby antioxidants maintain the cells in a form necessary for growth in case they later return to normal conditions. Interestingly, Asp f3 was also found to be secreted despite lacking a conventional secretion signal in several independent studies (14, 46–48). It is conceivable that *A. fumigatus* and other fungi also rely on antioxidant enzymes to constrain their ROS formation under stressful conditions, such as iron deprivation or germination (49–51). We propose that Asp f3 and Af3l1 play a major role here. The main antioxidant enzymes, e.g., Cat1 (mycelial catalase), Cat2 (catalase-peroxidase), and Ccp1 (cytochrome *c* peroxidase), all functionally depend on iron, an essential constituent of their heme groups, and are consequently transcriptionally downregulated during iron starvation to spare iron and to prevent futile protein synthesis (31,

TABLE 1 *A. fumigatus* strains used in this work

Strain or genotype	Relevant genetic modification	Parental strain	Reference
D141			66
Δ*aspf3*	*aspf3*::*hygro*^{r}	D141	12
AfS35 (wt, if not stated differently)	*akuA*::*loxP*	D141	52
aspf3$_{tetOn}$	*aspf3(p)*::*ptrA-tetOn*	AfS35	This work
Δ*af3l1*	*af3l1*::*six-xylP-β-rec-trpCt-ptrA-six*	AfS35	This work
Δ*af3l2*	*af3l2*::*six-xylP-β-rec-trpCt-ptrA-six*	AfS35	This work
Δ*af3l1* Δ*afl2*	*af3l1*::*six af3l2*::*six-xylP-β-rec-trpCt-ptrA-six*	Δ*af3l1*	This work
aspf3$_{tetOn}$ Δ*af3l1*	*af3l1*::*six-xylP-β-rec-trpCt-ptrA-six*	*aspf3*$_{tetOn}$	This work
aspf3$_{tetOn}$ Δ*af3l2*	*af3l2*::*six-xylP-β-rec-trpCt-ptrA-six*	*aspf3*$_{tetOn}$	This work
Δ*af3l1* Δ*af3l2 aspf3*$_{tetOn}$	*aspf3(p)*::*ptrA-tetOn*	Δ*af3l1* Δ*afl2*	This work
Δ*sreA*	*sreA*::*six-xylP-β-rec-trpCt-ptrA-six*	AfS35	This work
aspf3$_{tetOn}$ Δ*sreA*	*sreA*::*six-xylP-β-rec-trpCt-ptrA-six*	*aspf3*$_{tetOn}$	This work
aspf3$_{tetOn}$ Δ*af3l1* Δ*sreA*	*af3l1*::*six sreA*::*six-xylP-β-rec-trpCt-ptrA-six*	*aspf3*$_{tetOn}$ Δ*af3l1*	This work
wt + mtGFP	pCH005	AfS35	15
aspf3$_{tetOn}$ + mtGFP	pCH005	*aspf3*$_{tetOn}$	This work
aspf3$_{tetOn}$ Δ*af3l1* + mtGFP	pCH005	*aspf3*$_{tetOn}$ Δ*af3l1*	This work
ATCC 46645			31
Δ*sreA*	*sreA*::*hygro*^{r}	ATCC 46645	31
Δ*hapX*	*hapX*::*hygro*^{r}	ATCC 46645	32
Δ*sidA*	*sidA*::*hygro*^{r}	ATCC 46645	67

32, 49). Since peroxiredoxins do not depend on heme, Asp f3 and Af3l1 can step in and could allow the mold to overcome the stress conditions during iron deprivation. In line with this model, we found that (i) even the hyphae of the iron-deprived *aspf3*$_{tetOn}$ Δ*af3l1* mutant under repressed conditions stay alive for several days, reminiscent of the starving yeast cells which depend on antioxidant enzymes to continue to grow (45); (ii) the transcription of *cat1* and that of *aspf3* are inversely regulated depending on iron availability; and (iii) the susceptibility of the repressed *aspf3*$_{tetOn}$ and *aspf3*$_{tetOn}$ Δ*af3l1* mutants to hydrogen peroxide increases even further under low-iron conditions. Future studies will have to explore the cellular function of these peroxiredoxins during iron deprivation in further detail.

MATERIALS AND METHODS

Strains, culture conditions, and chemicals. The strains used and constructed in this study are listed in Table 1. The strains used in this study are derivatives of the *A. fumigatus* strain D141. The Δ*aspf3* deletion mutant is a direct derivative of D141 and was described previously (12). The D141 derivative AfS35 is a nonhomologous end joining-deficient strain (52, 53) and was used as progenitor (wild type [wt]) for all mutants constructed in this study. The conditional *aspf3*$_{tetOn}$ mutant was constructed as described before (54). Briefly, the doxycycline-inducible *oliC-tetOn* promoter cassette derived from pJW128 was inserted before the coding sequence of *aspf3* by double-crossover homologous recombination. Deletion mutants were constructed by replacing the coding region of the respective genes with a self-excising hygromycin B resistance cassette that was obtained from pSK528, essentially as described before (53, 55). Mitochondria were visualized with mitochondrion-targeted green fluorescent protein (mtGFP). To this end, strains were transformed with pCH005, which expresses an N-terminal mitochondrial targeting signal fused to a GFP derivative (sGFP), essentially as described before (56).

Strains were cultured on *Aspergillus* minimal medium (AMM) (57) to harvest conidia if not stated differently. Experiments were performed on or in AMM, RPMI 1640 medium (11835-063; Gibco, Thermo Fisher, Waltham, MA), or peptone medium (pH 7.0) (LP0034B; Oxoid, Thermo Fisher Scientific, Rockford, IL, USA). If not stated differently, experiments performed in RPMI 1640 included incubation with 5% CO_2 and solid media were supplemented with 2% (wt/vol) agar (214030; BD Bioscience, Heidelberg, Germany) or agarose (141098; Serva, Heidelberg, Germany). Resazurin (R7017), paraformaldehyde (158127), bathophenanthrolinedisulfonic acid (BPS; 146617) and calcofluor white (F3543) were obtained from Sigma-Aldrich (St. Louis, MO, USA), hydrogen peroxide (H_2O_2; 8070.2), EDTA (8040.1) and $FeSO_4$ (P015.1) were obtained from Carl Roth (Karlsruhe, Germany), doxycycline was obtained from Clontech (631311; Mountain View, CA, USA), and Percoll was obtained from GE Healthcare (10253000; Uppsala, Sweden). Lactoferrin from bovine milk was purchased from Ingredia (PEP10LAC02; Ingredia SA, Arras Cedex, France).

MitoFLARE assay with human granulocytes and growth experiment in serum. Viability of *Aspergillus* hyphae after exposure to human granulocytes was analyzed as previously described (15). Briefly, 3×10^3 conidia of the indicated strains that express mtGFP were inoculated in 300 μl RPMI 1640 per well in μ-Slide 8-well slides (number 80826; Ibidi, Martinsried, Germany). Slides were incubated at

37°C with 5% CO_2. After 10 h of incubation, 1.5×10^6 granulocytes resuspended in 100 μl RPMI 1640 were added per well. After the indicated incubation time, samples were fixed with 4% (wt/vol) paraformaldehyde for 10 min followed by staining with calcofluor white (1 mg ml^{-1} in double-distilled water [ddH_2O]) for 10 min. Samples were subsequently washed with phosphate-buffered saline (PBS). In each experiment, 60 hyphae per sample and three samples per condition were analyzed using a fluorescence microscope and a 63× objective with oil immersion by an assessor who was blind to sample identity. Samples with different strains were randomly located in each μ-Slide 8-well slide. The calcofluor white and GFP fluorescence and the mitochondrial morphology were analyzed as described before (15). Prior to the blind analysis of an experiment, the killing efficacy of each batch of isolated granulocytes was evaluated with a nonblind wild-type control sample. Experiments where excessive or no significant killing was observed were excluded and not considered in the subsequent statistical analysis (hyphal vitality of wild type after killing for 2 h of $<$30% or $>$90%). On that score, of four experiments, one (25%) was excluded because of too-high killing activity and no experiment (0%) because of too-low killing activity. Statistical significance was calculated with a two-tailed unpaired (assuming unequal variances) Student's *t* test posttest. Statistical analysis was done with GraphPad Prism 5 (GraphPad Software, La Jolla, CA, USA).

Granulocytes and serum for the growth inhibition experiment were isolated from the blood of healthy adult volunteers. For serum outgrowth experiments, 1.5×10^3 conidia of the indicated strains were inoculated in 60% (vol/vol) serum in ddH_2O per well in a 96-well plate. The plates were incubated at 37°C for the indicated time. The method for isolating the granulocytes was described before (15). Volunteers gave informed written consent; collection was conducted according to the Declaration of Helsinki and was approved by the Ethics Committee of the LMU München.

Analysis of metabolic activity. The metabolic activity of *Aspergillus* hyphae was analyzed over time with a resazurin reduction assay (58). Conidia (1.5×10^4) were inoculated in 200 μl RPMI 1640 supplemented with 0.002% (wt/vol) resazurin per well in a 96-well plate (Z707902; TPP, Sigma-Aldrich). Strains were inoculated in triplicate for each experiment. When indicated, medium was additionally supplemented with lactoferrin or $FeSO_4$. Well plates were sealed with a Breathe-Easy sealing membrane (Z380059; Sigma-Aldrich) and incubated. Plates were subsequently incubated at 37°C with 5% CO_2 and analyzed over time in a BMG Labtech CLARIOstar microplate reader (excitation, 550-15 nm; dichroic mirror, 568.8 nm; emission, 590-20 nm; excitation and detection from the top; BMG Labtech, Ortenberg, Germany).

Microscopy. Fluorescence microscopy to obtain images or to analyze mitochondrial dynamics was performed with a Leica SP5 inverted confocal laser scanning microscope (Leica Microsystems, Mannheim, Germany) equipped with a climate chamber (The Cube & The Box, Life Imaging Services, Switzerland). Quantitative analysis of the killing activity of human granulocytes against *Aspergillus* hyphae was performed with a Leica DM IRB inverted microscope (Leica Microsystems). If not stated differently, 3×10^3 conidia were inoculated in 300 μl medium per well in a μ-Slide 8-well slide for fluorescence microscopy. Conventional bright- and dark-field images were taken with an EOS 550D digital camera (Canon, Tokyo, Japan) fitted to an Axiovert 25 inverted microscope (Carl Zeiss MicroImaging, Göttingen, Germany).

Bioinformatics. Sequences were obtained from FungiDB (59), the *Saccharomyces* Genome Database (60), and the *Candida* Genome Database (61). Alignments were performed with Jalview (62) and MAFFT (multiple alignment using fast Fourier transform); the average distance tree was generated with BLOSUM62.

Murine infection experiment. Prior to infection, *A. fumigatus* D141 and the Δ*aspf3* mutant were grown on malt peptone (MP) agar with 19 g $liter^{-1}$ malt extract broth (CP75.1; Carl Roth) and 15 g $liter^{-1}$ agar (5210.2; Carl Roth) with or without 1% (wt/vol) iron dextran (Mediferran; Medistar; 200 mg/ml iron [II] ion) at 37°C for 5 days. Conidia were harvested with sterile PBS with 0.01% (vol/vol) Tween 20 with or without 2% (wt/vol) iron dextran. Conidia were quantified using an automatic cell counter (CASY, model TT; OLS OMNI Life Science, Bremen, Germany). Specific-pathogen-free female outbred CD-1 mice (18 to 20 g; 6 to 8 weeks old) were obtained from Charles River, Germany. Animals were housed under standard conditions in individually ventilated cages and fed normal mouse chow and water *ad libitum*. All animals were cared for in accordance with the European animal welfare regulation, and animal experiments were approved by the responsible federal/state authority and ethics committee in accordance with the German animal welfare act (permit no. 03-009/15). Mice were immunosuppressed with two single doses of 1 g cortisone acetate (C3130-25G, Sigma-Aldrich) per kg of body weight, which were injected intraperitoneally 3 days before and immediately prior to infection with conidia (day 0). Iron loading of mice was achieved by intraperitoneal (i.p.) injection of 20 mg of iron dextran. Subsequently, mice were anesthetized by an intraperitoneal anesthetic combination of midazolam, fentanyl, and medetomidine. Conidia (1×10^6) in 20 μl PBS were applied to the nares of the mice. Deep anesthesia ensured inhalation of the conidial inocula. Anesthesia was terminated by subcutaneous injection of flumazenil, naloxone, and atipamezole. Infected animals were monitored twice daily to check weight loss and dyspnea. Analysis of the survival data for the murine infection model was assessed with the log-rank test and the Gehan-Wilcoxon test, and *P* values of $<$0.05 were considered significant.

Histopathological analysis. Lungs of sacrificed mice were fixed in buffered formalin and embedded in paraffin. Sections of 4 μm were deparaffinized, hydrated in water, and stained with periodic acid-Schiff stain (PAS) using standard protocols. Briefly, sections were oxidized by staining with 1% PA solution for 5 min, incubated with Schiff's reagent for 15 min, and rinsed with tap water between treatments. Counterstaining was carried out with hematoxylin for 30 s, followed by thorough washes with tap water. Stained sections were visualized by light microscopy.

Quantitative analysis of siderophore biosynthesis. For analysis of siderophore production, *A. fumigatus* wild-type and mutant strains were grown for 18 h at 37°C in a liquid *Aspergillus* minimal

medium variant (63) with 20 mM glutamine as the nitrogen source and 1% glucose as the carbon source, omitting addition of iron to generate iron starvation conditions using 10^6 conidia ml^{-1} for inoculation. Production of secreted triacetylfusarinine C and fusarinine C as well of intracellular ferricrocin was quantified from culture supernatants and cell extracts as described previously (64). Produced fungal biomass was harvested by filtration and weighted after freeze-drying for normalization of siderophore production to biomass. Experiments were carried out in triplicate. Statistical significance was calculated with one-way analysis of variance (ANOVA) with a *post hoc* Tukey's honestly significant difference (HSD) test calculator (https://astatsa.com/).

Northern blot analysis. To analyze hyphae, conidia of the respective strains were cultured in a liquid *Aspergillus* minimal medium variant (63) with 20 mM glutamine as the nitrogen source and 1% glucose as the carbon source, omitting addition of iron to generate iron starvation conditions. Complete medium (2% [wt/vol] glucose, 0.2% [wt/vol] peptone, 0.1% [wt/vol] yeast extract, 0.1% [wt/vol] Casamino Acids, 7 mM KCl, 2 mM $MgSO_4$, 11 mM KH_2PO_4, and trace elements as described in the recipe for AMM but without iron, with pH adjusted with HCl to 6.5) was used to obtain conidia for RNA isolation and Northern blot analysis. RNA isolation and Northern blot analysis, using 10 μg of extracted RNA, were performed essentially as described previously (65). The digoxigenin-labeled hybridization probes used in this study were generated by PCR. Primers used were 5′-ATGTCTGGACTCAAGGCCG and 5′-TTACAGGTGCTTGAGGACGG for *aspf3*, 5′-CCAATGCGGTATGTCCCT and 5′-GAGTCATGAGCAGTGGCA for *cat1*, 5′-AAGCCGAGAAAAAGGGGG and 5′-AACCCAGATGAAGCCCAG for *mirB*, 5′-ATGGCAAAAGACGTATTTGC and 5′-TCAGACAAGGGATGCTC for *ftrA*, and 5′-TCGGTGGAAAGAAGTGCC and 5′-CGAGTCCGTTTGGGTATC for *hapX*.

SUPPLEMENTAL MATERIAL

Supplemental material is available online only.

VIDEO S1, AVI file, 4.4 MB.

VIDEO S2, AVI file, 17.6 MB.

VIDEO S3, AVI file, 17.6 MB.

FIG S1, PDF file, 0.3 MB.

FIG S2, PDF file, 0.6 MB.

FIG S3, PDF file, 0.2 MB.

FIG S4, PDF file, 0.2 MB.

FIG S5, PDF file, 0.1 MB.

ACKNOWLEDGMENTS

J.W. conceived the study. J.W. and V.B. wrote the manuscript. H.H. and F.H. reviewed and edited the manuscript. A.Y. and H.H. planned and performed the quantitative analysis of siderophore biosynthesis and Northern blot analyses (Fig. 6A and B and Fig. S5); J.M.B., T.H., M.S., and F.H. planned and performed the murine infection experiment and the histopathological analysis (Fig. 7B and C); all other experiments and analyses were planned and performed by V.B., E.G., D.R., K.D., and J.W. All authors read and authorized the manuscript.

This work was in part supported by the German Research Foundation (J.W., DFG–WA 3016/4-1; J.W. and F.H., DFG–HI 1574/2-1), the Austrian Science Fund (FWF) doctoral program Host Response in Opportunistic Infections (HOROS; W1253 to H.H.), the Verein zur Förderung von Wissenschaft und Forschung an der Medizinischen Fakultät der Ludwig-Maximilians-Universität München e.V., the Förderprogramm für Forschung und Lehre (FöFoLe) of the Medical Faculty of the LMU München, and the Graduate School of Life Sciences (GSLS) at the University of Würzburg.

REFERENCES

1. Sugui JA, Kwon-Chung KJ, Juvvadi PR, Latgé J-P, Steinbach WJ. 2014. Aspergillus fumigatus and related species. Cold Spring Harb Perspect Med 5:a019786. https://doi.org/10.1101/cshperspect.a019786.
2. Kosmidis C, Denning DW. 2015. The clinical spectrum of pulmonary aspergillosis. Thorax 70:270–277. https://doi.org/10.1136/thoraxjnl-2014-206291.
3. Kousha M, Tadi R, Soubani AO. 2011. Pulmonary aspergillosis: a clinical review. Eur Respir Rev 20:156–174. https://doi.org/10.1183/09059180.00001011.
4. Brown GD, Denning DW, Gow NAR, Levitz SM, Netea MG, White TC. 2012. Hidden killers: human fungal infections. Sci Transl Med 4:165rv13. https://doi.org/10.1126/scitranslmed.3004404.
5. Espinosa V, Rivera A. 2016. First line of defense: innate cell-mediated control of pulmonary aspergillosis. Front Microbiol 7:272. https://doi.org/10.3389/fmicb.2016.00272.
6. Tracy MC, Okorie CUA, Foley EA, Moss RB. 2016. Allergic bronchopulmonary aspergillosis. J Fungi (Basel) 2:17. https://doi.org/10.3390/jof2020017.
7. Page ID, Richardson M, Denning DW. 2015. Antibody testing in aspergillosis–quo vadis? Med Mycol 53:417–439. https://doi.org/10.1093/mmy/myv020.
8. Hemmann S, Ismail C, Blaser K, Menz G, Crameri R. 1998. Skin-test reactivity and isotype-specific immune responses to recombinant Asp f 3, a major allergen of Aspergillus fumigatus. Clin Exp Allergy 28:860–867. https://doi.org/10.1046/j.1365-2222.1998.00329.x.
9. Hemmann S, Blaser K, Crameri R. 1997. Allergens of Aspergillus fumigatus and Candida boidinii share IgE-binding epitopes. Am J Respir Crit Care Med 156:1956–1962. https://doi.org/10.1164/ajrccm.156.6.9702087.
10. Agarwal R, Chakrabarti A, Shah A, Gupta D, Meis JF, Guleria R, Moss R, Denning DW, ABPA complicating asthma ISHAM working group. 2013.

Allergic bronchopulmonary aspergillosis: review of literature and proposal of new diagnostic and classification criteria. Clin Exp Allergy 43:850–873. https://doi.org/10.1111/cea.12141.
11. Lessing F, Kniemeyer O, Wozniok I, Loeffler J, Kurzai O, Haertl A, Brakhage AA. 2007. The Aspergillus fumigatus transcriptional regulator AfYap1 represents the major regulator for defense against reactive oxygen intermediates but is dispensable for pathogenicity in an intranasal mouse infection model. Eukaryot Cell 6:2290–2302. https://doi.org/10.1128/EC.00267-07.
12. Hillmann F, Bagramyan K, Straßburger M, Heinekamp T, Hong TB, Bzymek KP, Williams JC, Brakhage AA, Kalkum M. 2016. The crystal structure of peroxiredoxin Asp f3 provides mechanistic insight into oxidative stress resistance and virulence of Aspergillus fumigatus. Sci Rep 6:33396. https://doi.org/10.1038/srep33396.
13. Ito JI, Lyons JM, Hong TB, Tamae D, Liu Y-K, Wilczynski SP, Kalkum M. 2006. Vaccinations with recombinant variants of Aspergillus fumigatus allergen Asp f 3 protect mice against invasive aspergillosis. Infect Immun 74:5075–5084. https://doi.org/10.1128/IAI.00815-06.
14. Diaz-Arevalo D, Bagramyan K, Hong TB, Ito JI, Kalkum M. 2011. CD4+ T cells mediate the protective effect of the recombinant Asp f3-based antiaspergillosis vaccine. Infect Immun 79:2257–2266. https://doi.org/10.1128/IAI.01311-10.
15. Ruf D, Brantl V, Wagener J. 2018. Mitochondrial fragmentation in Aspergillus fumigatus as early marker of granulocyte killing activity. Front Cell Infect Microbiol 8:128. https://doi.org/10.3389/fcimb.2018.00128.
16. Boyle KB, Stephens LR, Hawkins PT. 2012. Activation of the neutrophil NADPH oxidase by Aspergillus fumigatus. Ann N Y Acad Sci 1273:68–73. https://doi.org/10.1111/j.1749-6632.2012.06821.x.
17. Bianchi M, Hakkim A, Brinkmann V, Siler U, Seger RA, Zychlinsky A, Reichenbach J. 2009. Restoration of NET formation by gene therapy in CGD controls aspergillosis. Blood 114:2619–2622. https://doi.org/10.1182/blood-2009-05-221606.
18. Lee MJ, Liu H, Barker BM, Snarr BD, Gravelat FN, Al Abdallah Q, Gavino C, Baistrocchi SR, Ostapska H, Xiao T, Ralph B, Solis NV, Lehoux M, Baptista SD, Thammahong A, Cerone RP, Kaminskyj SGW, Guiot M-C, Latgé J-P, Fontaine T, Vinh DC, Filler SG, Sheppard DC. 2015. The fungal exopolysaccharide galactosaminogalactan mediates virulence by enhancing resistance to neutrophil extracellular traps. PLoS Pathog 11:e1005187. https://doi.org/10.1371/journal.ppat.1005187.
19. Loures FV, Röhm M, Lee CK, Santos E, Wang JP, Specht CA, Calich VLG, Urban CF, Levitz SM. 2015. Recognition of Aspergillus fumigatus hyphae by human plasmacytoid dendritic cells is mediated by dectin-2 and results in formation of extracellular traps. PLoS Pathog 11:e1004643. https://doi.org/10.1371/journal.ppat.1004643.
20. Gazendam RP, van de Geer A, van Hamme JL, Tool ATJ, van Rees DJ, Aarts CEM, van den Biggelaar M, van Alphen F, Verkuijlen P, Meijer AB, Janssen H, Roos D, van den Berg TK, Kuijpers TW. 2016. Impaired killing of Candida albicans by granulocytes mobilized for transfusion purposes: a role for granule components. Haematologica 101:587–596. https://doi.org/10.3324/haematol.2015.136630.
21. Harper AF, Leuthaeuser JB, Babbitt PC, Morris JH, Ferrin TE, Poole LB, Fetrow JS. 2017. An atlas of peroxiredoxins created using an active site profile-based approach to functionally relevant clustering of proteins. PLoS Comput Biol 13:e1005284. https://doi.org/10.1371/journal.pcbi.1005284.
22. Rocha MC, de Godoy KF, Bannitz-Fernandes R, Fabri JHTM, Barbosa MMF, de Castro PA, Almeida F, Goldman GH, da Cunha AF, Netto LES, de Oliveira MA, Malavazi I. 2018. Analyses of the three 1-Cys peroxiredoxins from Aspergillus fumigatus reveal that cytosolic Prx1 is central to H2O2 metabolism and virulence. Sci Rep 8:12314. https://doi.org/10.1038/s41598-018-30108-2.
23. Mistry J, Chuguransky S, Williams L, Qureshi M, Salazar GA, Sonnhammer ELL, Tosatto SCE, Paladin L, Raj S, Richardson LJ, Finn RD, Bateman A. 2021. Pfam: the protein families database in 2021. Nucleic Acids Res 49:D412–D419. https://doi.org/10.1093/nar/gkaa913.
24. Sturm L, Geißel B, Martin R, Wagener J. 2020. Differentially regulated transcription factors and ABC transporters in a mitochondrial dynamics mutant can alter azole susceptibility of Aspergillus fumigatus. Front Microbiol 11:1017. https://doi.org/10.3389/fmicb.2020.01017.
25. Xia Y, Yu H, Zhou Z, Takaya N, Zhou S, Wang P. 2018. Peroxiredoxin system of Aspergillus nidulans resists inactivation by high concentration of hydrogen peroxide-mediated oxidative stress. J Microbiol Biotechnol 28:145–156. https://doi.org/10.4014/jmb.1707.07024.
26. Fukasawa Y, Tsuji J, Fu S-C, Tomii K, Horton P, Imai K. 2015. MitoFates: improved prediction of mitochondrial targeting sequences and their cleavage sites. Mol Cell Proteomics 14:1113–1126. https://doi.org/10.1074/mcp.M114.043083.
27. Geißel B, Loiko V, Klugherz I, Zhu Z, Wagener N, Kurzai O, van den Hondel C, Wagener J. 2018. Azole-induced cell wall carbohydrate patches kill Aspergillus fumigatus. Nat Commun 9:3098. https://doi.org/10.1038/s41467-018-05497-7.
28. Misslinger M, Hortschansky P, Brakhage AA, Haas H. 2021. Fungal iron homeostasis with a focus on Aspergillus fumigatus. Biochim Biophys Acta Mol Cell Res 1868:118885. https://doi.org/10.1016/j.bbamcr.2020.118885.
29. Haas H. 2014. Fungal siderophore metabolism with a focus on Aspergillus fumigatus. Nat Prod Rep 31:1266–1276. https://doi.org/10.1039/c4np00071d.
30. Wallner A, Blatzer M, Schrettl M, Sarg B, Lindner H, Haas H. 2009. Ferricrocin, a siderophore involved in intra- and transcellular iron distribution in Aspergillus fumigatus. Appl Environ Microbiol 75:4194–4196. https://doi.org/10.1128/AEM.00479-09.
31. Schrettl M, Kim HS, Eisendle M, Kragl C, Nierman WC, Heinekamp T, Werner ER, Jacobsen I, Illmer P, Yi H, Brakhage AA, Haas H. 2008. SreA-mediated iron regulation in Aspergillus fumigatus. Mol Microbiol 70:27–43. https://doi.org/10.1111/j.1365-2958.2008.06376.x.
32. Schrettl M, Beckmann N, Varga J, Heinekamp T, Jacobsen ID, Jöchl C, Moussa TA, Wang S, Gsaller F, Blatzer M, Werner ER, Niermann WC, Brakhage AA, Haas H. 2010. HapX-mediated adaption to iron starvation is crucial for virulence of Aspergillus fumigatus. PLoS Pathog 6:e1001124. https://doi.org/10.1371/journal.ppat.1001124.
33. Hissen AHT, Chow JMT, Pinto LJ, Moore MM. 2004. Survival of Aspergillus fumigatus in serum involves removal of iron from transferrin: the role of siderophores. Infect Immun 72:1402–1408. https://doi.org/10.1128/IAI.72.3.1402-1408.2004.
34. Petzer V, Wermke M, Tymoszuk P, Wolf D, Seifert M, Ovaçin R, Berger S, Orth-Höller D, Loacker L, Weiss G, Haas H, Platzbecker U, Theurl I. 2019. Enhanced labile plasma iron in hematopoietic stem cell transplanted patients promotes Aspergillus outgrowth. Blood Adv 3:1695–1700. https://doi.org/10.1182/bloodadvances.2019000043.
35. Philippe B, Ibrahim-Granet O, Prévost MC, Gougerot-Pocidalo MA, Sanchez Perez M, Van der Meeren A, Latgé JP. 2003. Killing of Aspergillus fumigatus by alveolar macrophages is mediated by reactive oxidant intermediates. Infect Immun 71:3034–3042. https://doi.org/10.1128/IAI.71.6.3034-3042.2003.
36. Washburn RG, Gallin JI, Bennett JE. 1987. Oxidative killing of Aspergillus fumigatus proceeds by parallel myeloperoxidase-dependent and -independent pathways. Infect Immun 55:2088–2092. https://doi.org/10.1128/iai.55.9.2088-2092.1987.
37. Lee J, Spector D, Godon C, Labarre J, Toledano MB. 1999. A new antioxidant with alkyl hydroperoxide defense properties in yeast. J Biol Chem 274:4537–4544. https://doi.org/10.1074/jbc.274.8.4537.
38. Truong T, Zeng G, Qingsong L, Kwang LT, Tong C, Chan FY, Wang Y, Seneviratne CJ. 2016. Comparative ploidy proteomics of Candida albicans biofilms unraveled the role of the AHP1 gene in the biofilm persistence against amphotericin B. Mol Cell Proteomics 15:3488–3500. https://doi.org/10.1074/mcp.M116.061523.
39. Kell DB, Heyden EL, Pretorius E. 2020. The biology of lactoferrin, an iron-binding protein that can help defend against viruses and bacteria. Front Immunol 11:1221. https://doi.org/10.3389/fimmu.2020.01221.
40. Singh PK, Parsek MR, Greenberg EP, Welsh MJ. 2002. A component of innate immunity prevents bacterial biofilm development. Nature 417:552–555. https://doi.org/10.1038/417552a.
41. Travis SM, Conway BA, Zabner J, Smith JJ, Anderson NN, Singh PK, Greenberg EP, Welsh MJ. 1999. Activity of abundant antimicrobials of the human airway. Am J Respir Cell Mol Biol 20:872–879. https://doi.org/10.1165/ajrcmb.20.5.3572.
42. Gerwien F, Skrahina V, Kasper L, Hube B, Brunke S. 2018. Metals in fungal virulence. FEMS Microbiol Rev 42:fux050. https://doi.org/10.1093/femsre/fux050.
43. Nairz M, Weiss G. 2020. Iron in infection and immunity. Mol Aspects Med 75:100864. https://doi.org/10.1016/j.mam.2020.100864.
44. Lepanto MS, Rosa L, Paesano R, Valenti P, Cutone A. 2019. Lactoferrin in aseptic and septic inflammation. Molecules 24:1323. https://doi.org/10.3390/molecules24071323.
45. Cruz-Garcia D, Brouwers N, Malhotra V, Curwin AJ. 2020. Reactive oxygen species triggers unconventional secretion of antioxidants and Acb1. J Cell Biol 219:e201905028. https://doi.org/10.1083/jcb.201905028.
46. Singh B, Oellerich M, Kumar R, Kumar M, Bhadoria DP, Reichard U, Gupta VK, Sharma GL, Asif AR. 2010. Immuno-reactive molecules identified from

the secreted proteome of Aspergillus fumigatus. J Proteome Res 9:5517–5529. https://doi.org/10.1021/pr100604x.
47. Ramirez-Garcia A, Pellon A, Buldain I, Antoran A, Arbizu-Delgado A, Guruceaga X, Rementeria A, Hernando FL. 2018. Proteomics as a tool to identify new targets against Aspergillus and Scedosporium in the context of cystic fibrosis. Mycopathologia 183:273–289. https://doi.org/10.1007/s11046-017-0139-3.
48. Souza JAM, de Matos Baltazar L, Carregal VM, Gouveia-Eufrasio L, de Oliveira AG, Dias WG, Campos Rocha M, Rocha de Miranda K, Malavazi I, de Assis Santos D, Frézard FJG, da Gloria de Souza D, Teixeira MM, Soriani FM. 2019. Characterization of Aspergillus fumigatus extracellular vesicles and their effects on macrophages and neutrophils functions. Front Microbiol 10:2008. https://doi.org/10.3389/fmicb.2019.02008.
49. Kurucz V, Krüger T, Antal K, Dietl A-M, Haas H, Pócsi I, Kniemeyer O, Emri T. 2018. Additional oxidative stress reroutes the global response of Aspergillus fumigatus to iron depletion. BMC Genomics 19:357. https://doi.org/10.1186/s12864-018-4730-x.
50. Semighini CP, Harris SD. 2008. Regulation of apical dominance in Aspergillus nidulans hyphae by reactive oxygen species. Genetics 179:1919–1932. https://doi.org/10.1534/genetics.108.089318.
51. Malagnac F, Lalucque H, Lepère G, Silar P. 2004. Two NADPH oxidase isoforms are required for sexual reproduction and ascospore germination in the filamentous fungus Podospora anserina. Fungal Genet Biol 41:982–997. https://doi.org/10.1016/j.fgb.2004.07.008.
52. Krappmann S, Sasse C, Braus GH. 2006. Gene targeting in Aspergillus fumigatus by homologous recombination is facilitated in a nonhomologous end- joining-deficient genetic background. Eukaryot Cell 5:212–215. https://doi.org/10.1128/EC.5.1.212-215.2006.
53. Wagener J, Echtenacher B, Rohde M, Kotz A, Krappmann S, Heesemann J, Ebel F. 2008. The putative alpha-1,2-mannosyltransferase AfMnt1 of the opportunistic fungal pathogen Aspergillus fumigatus is required for cell wall stability and full virulence. Eukaryot Cell 7:1661–1673. https://doi.org/10.1128/EC.00221-08.
54. Helmschrott C, Sasse A, Samantaray S, Krappmann S, Wagener J. 2013. Upgrading fungal gene expression on demand: improved systems for doxycycline-dependent silencing in Aspergillus fumigatus. Appl Environ Microbiol 79:1751–1754. https://doi.org/10.1128/AEM.03626-12.
55. Hartmann T, Dümig M, Jaber BM, Szewczyk E, Olbermann P, Morschhäuser J, Krappmann S. 2010. Validation of a self-excising marker in the human pathogen Aspergillus fumigatus by employing the beta-rec/six site-specific recombination system. Appl Environ Microbiol 76:6313–6317. https://doi.org/10.1128/AEM.00882-10.
56. Neubauer M, Zhu Z, Penka M, Helmschrott C, Wagener N, Wagener J. 2015. Mitochondrial dynamics in the pathogenic mold Aspergillus fumigatus: therapeutic and evolutionary implications. Mol Microbiol 98:930–945. https://doi.org/10.1111/mmi.13167.
57. Hill TW, Kafer E. 2001. Improved protocols for Aspergillus salt stock solutions. Fungal Genet Newsl 48:20–21. https://doi.org/10.4148/1941-4765.1173.
58. Monteiro MC, de la Cruz M, Cantizani J, Moreno C, Tormo JR, Mellado E, De Lucas JR, Asensio F, Valiante V, Brakhage AA, Latgé J-P, Genilloud O, Vicente F. 2012. A new approach to drug discovery: high-throughput screening of microbial natural extracts against Aspergillus fumigatus using resazurin. J Biomol Screen 17:542–549. https://doi.org/10.1177/1087057111433459.
59. Basenko EY, Pulman JA, Shanmugasundram A, Harb OS, Crouch K, Starns D, Warrenfeltz S, Aurrecoechea C, Stoeckert CJ, Kissinger JC, Roos DS, Hertz-Fowler C. 2018. FungiDB: an integrated bioinformatic resource for fungi and oomycetes. J Fungi (Basel) 4:39. https://doi.org/10.3390/jof4010039.
60. Engel SR, Dietrich FS, Fisk DG, Binkley G, Balakrishnan R, Costanzo MC, Dwight SS, Hitz BC, Karra K, Nash RS, Weng S, Wong ED, Lloyd P, Skrzypek MS, Miyasato SR, Simison M, Cherry JM. 2014. The reference genome sequence of Saccharomyces cerevisiae: then and now. G3 (Bethesda) 4:389–398. https://doi.org/10.1534/g3.113.008995.
61. Skrzypek MS, Binkley J, Binkley G, Miyasato SR, Simison M, Sherlock G. 2017. The Candida Genome Database (CGD): incorporation of Assembly 22, systematic identifiers and visualization of high throughput sequencing data. Nucleic Acids Res 45:D592–D596. https://doi.org/10.1093/nar/gkw924.
62. Waterhouse AM, Procter JB, Martin DMA, Clamp M, Barton GJ. 2009. Jalview version 2—a multiple sequence alignment editor and analysis workbench. Bioinformatics 25:1189–1191. https://doi.org/10.1093/bioinformatics/btp033.
63. Pontecorvo G, Roper JA, Hemmons LM, Macdonald KD, Bufton AWJ. 1953. The genetics of Aspergillus nidulans. Adv Genet 5:141–238. https://doi.org/10.1016/s0065-2660(08)60408-3.
64. Misslinger M, Lechner BE, Bacher K, Haas H. 2018. Iron-sensing is governed by mitochondrial, not by cytosolic iron-sulfur cluster biogenesis in Aspergillus fumigatus. Metallomics 10:1687–1700. https://doi.org/10.1039/c8mt00263k.
65. Oberegger H, Schoeser M, Zadra I, Abt B, Haas H. 2001. SREA is involved in regulation of siderophore biosynthesis, utilization and uptake in Aspergillus nidulans. Mol Microbiol 41:1077–1089. https://doi.org/10.1046/j.1365-2958.2001.02586.x.
66. Staib F, Mishra SK, Rajendran C, Voigt R, Steffen J, Neumann KH, Hartmann CA, Heins G. 1980. A notable Aspergillus from a mortal aspergilloma of the lung. New aspects of the epidemiology, serodiagnosis and taxonomy of Aspergillus fumigatus. Zentralbl Bakteriol A 247:530–536.
67. Schrettl M, Bignell E, Kragl C, Joechl C, Rogers T, Arst HN, Haynes K, Haas H. 2004. Siderophore biosynthesis but not reductive iron assimilation is essential for Aspergillus fumigatus virulence. J Exp Med 200:1213–1219. https://doi.org/10.1084/jem.20041242.

Supplementary fig. 1

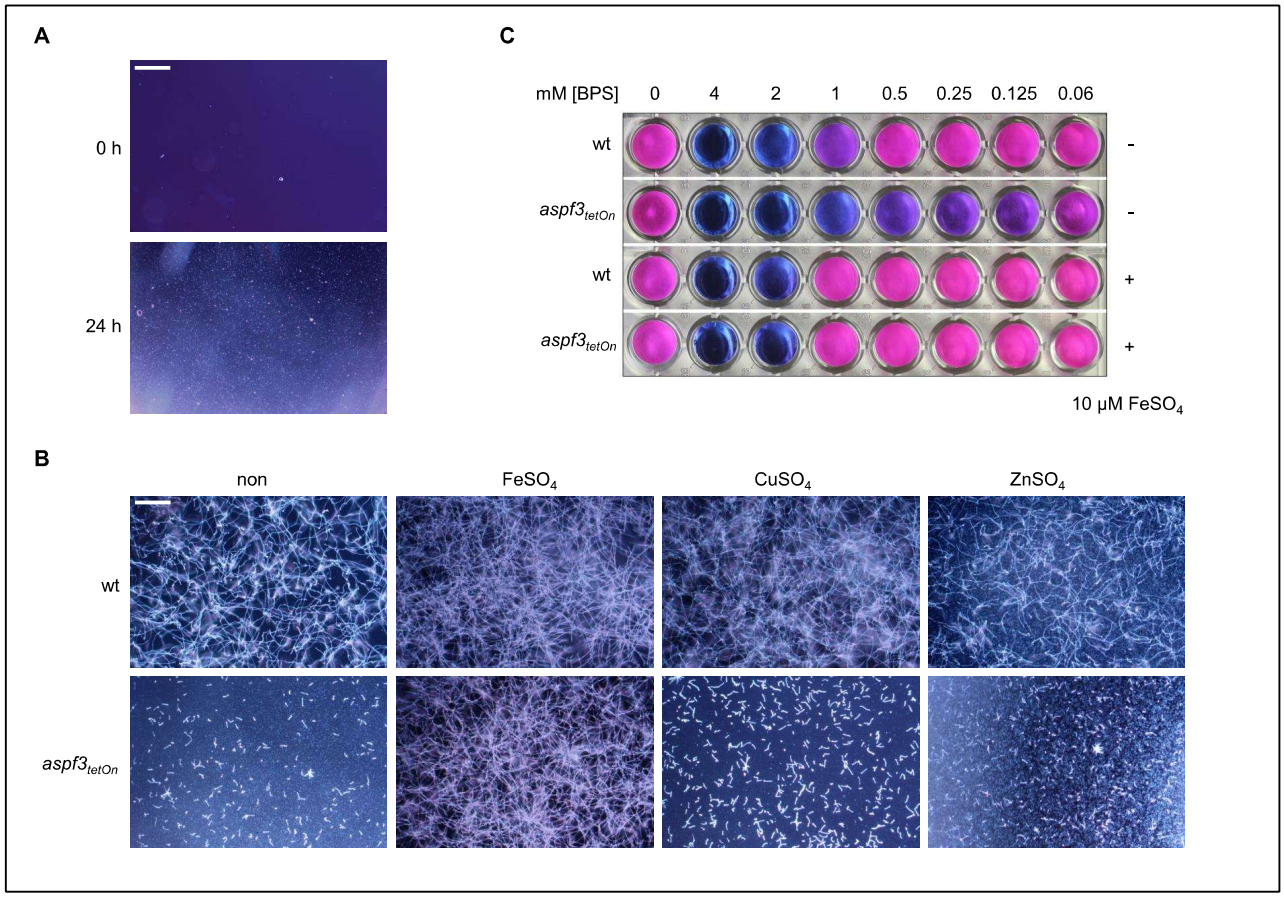

Supplementary fig. 2

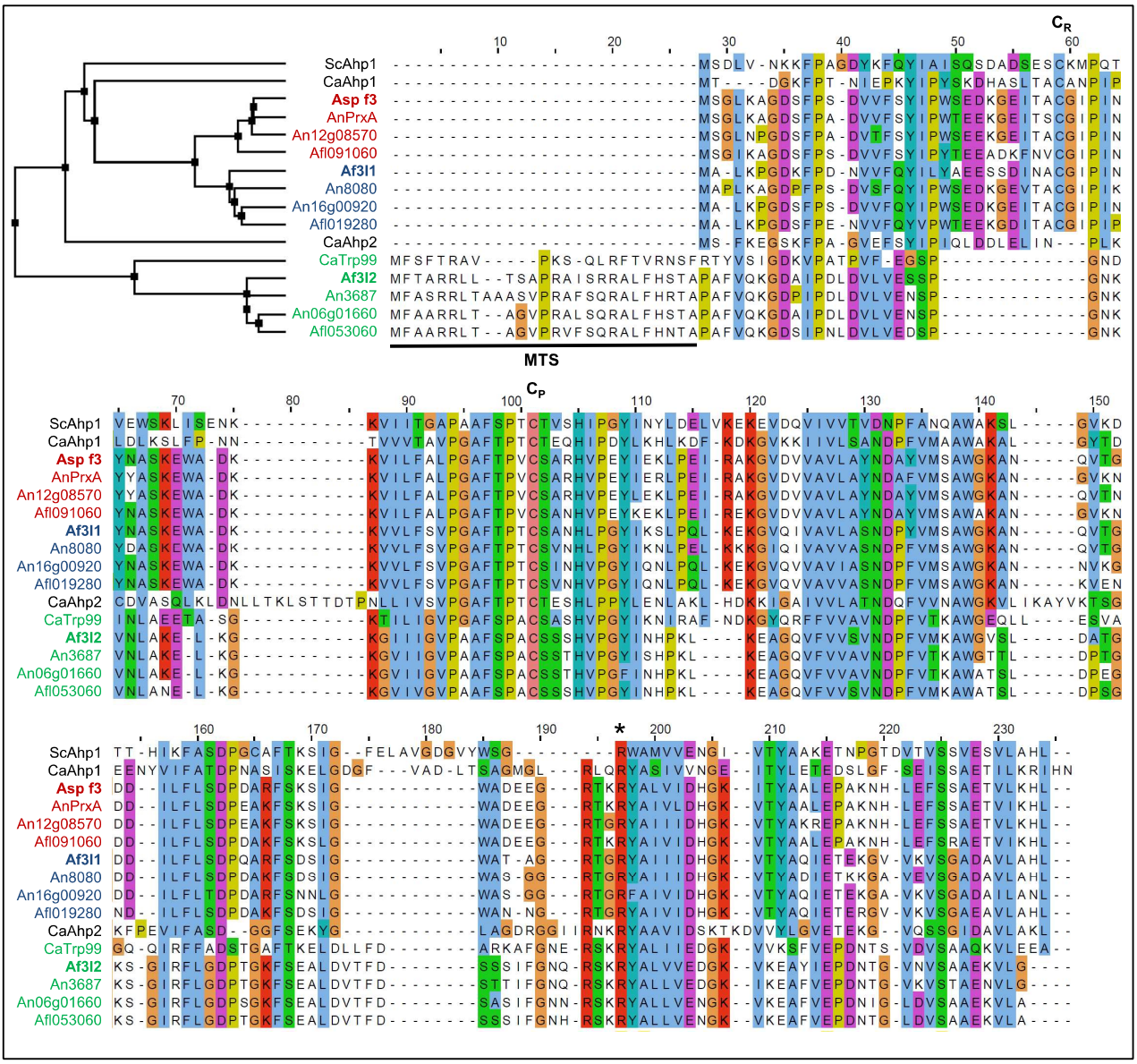

Supplementary fig. 3

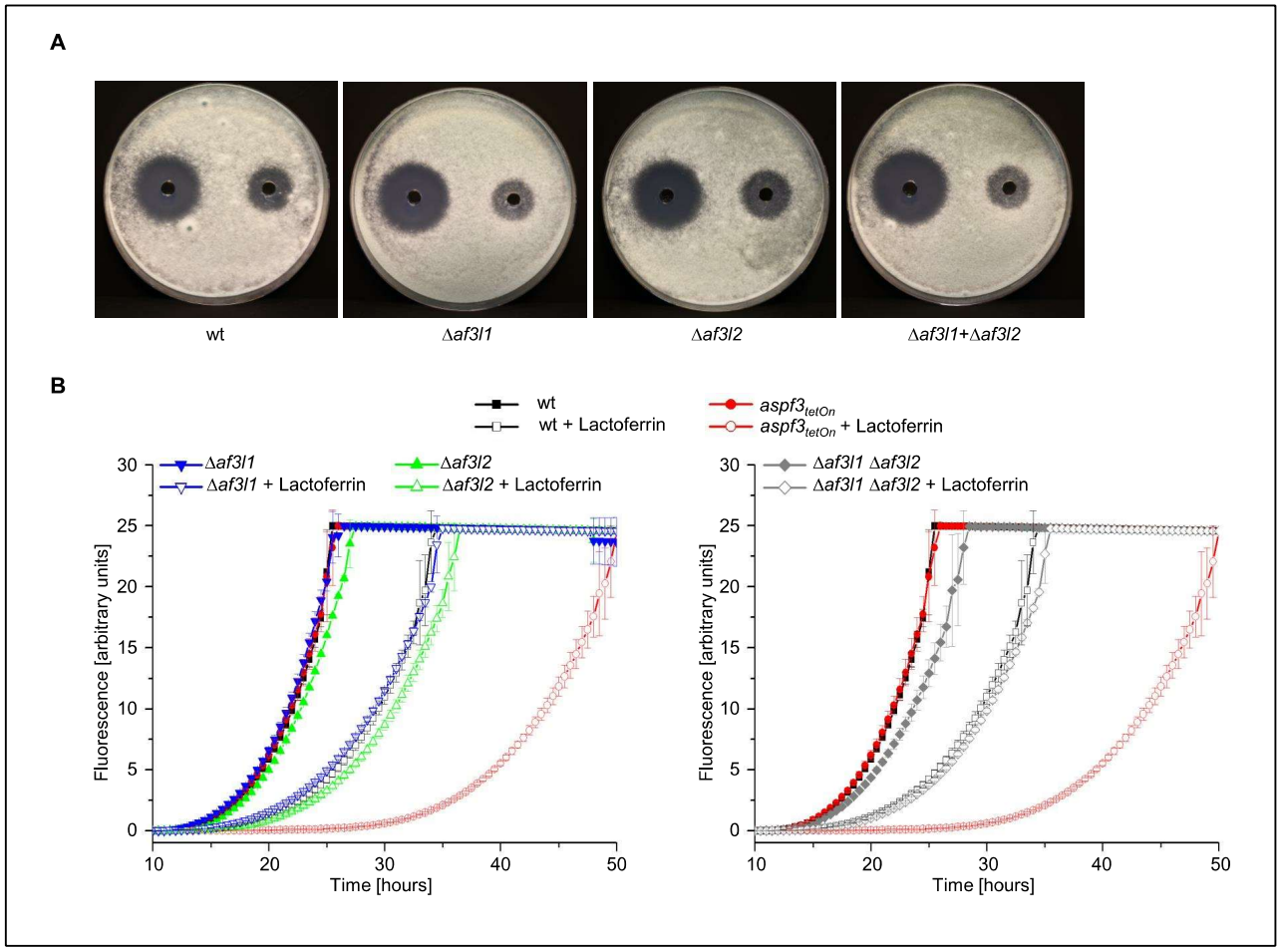

Supplementary fig. 4

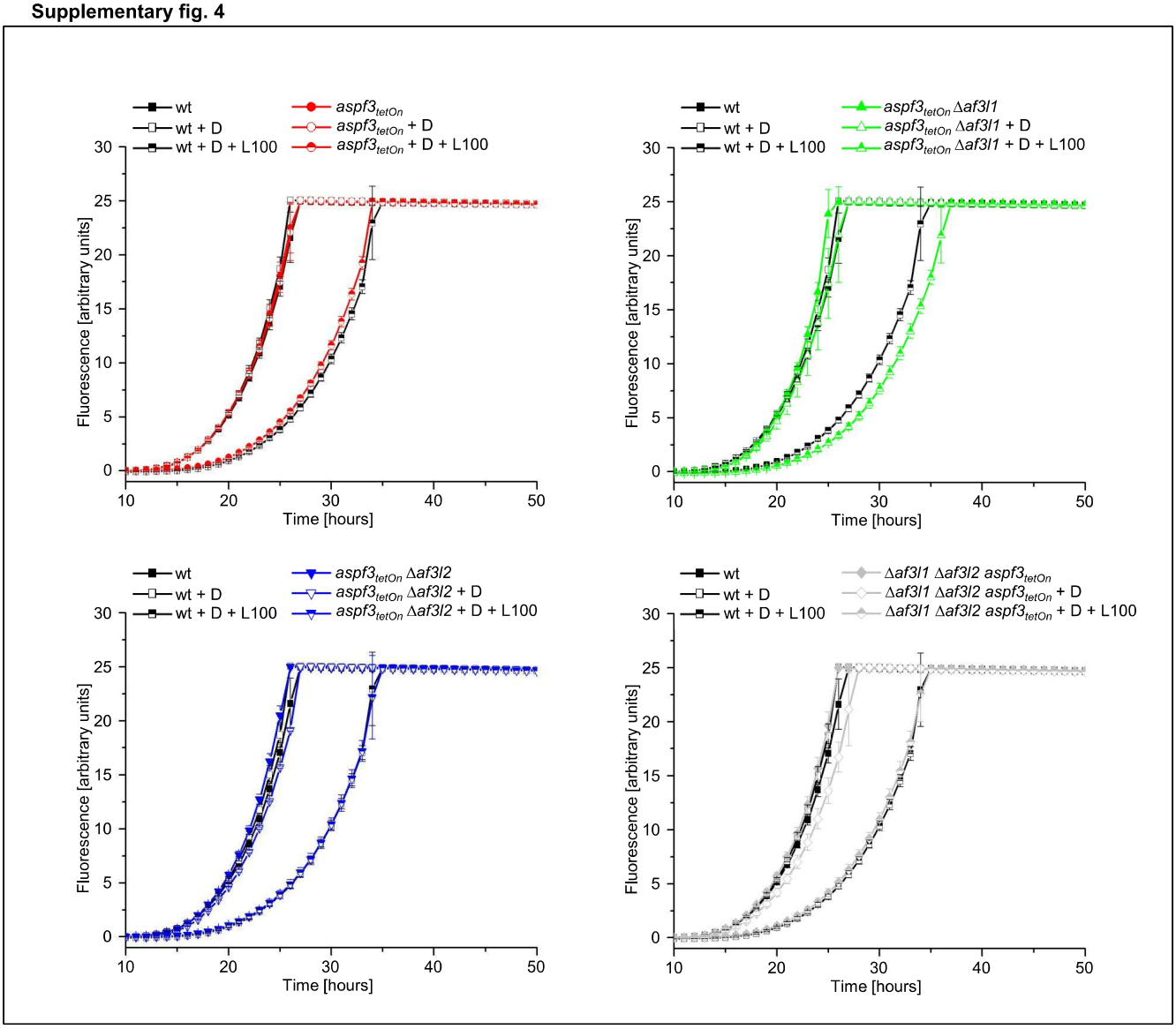

Supplementary figure 5

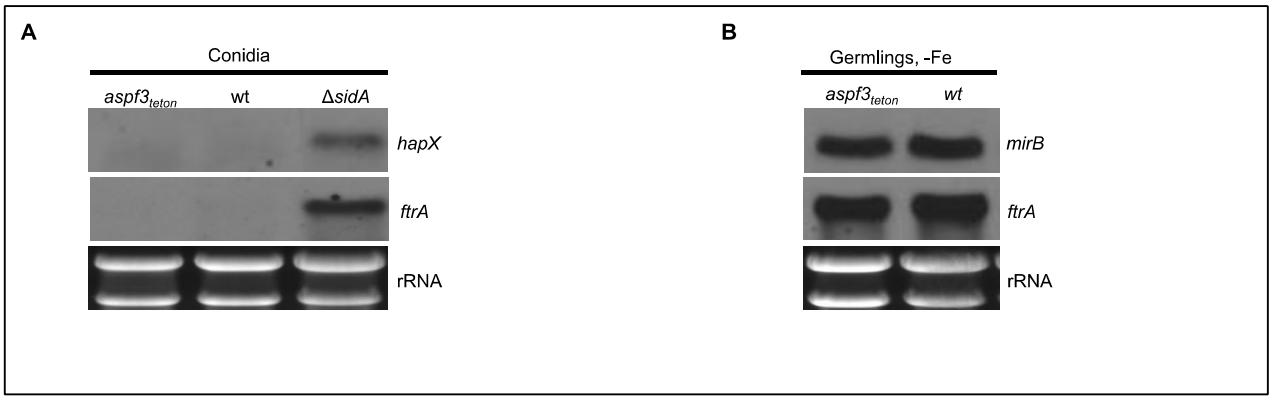

3.5 Manuscript 5 - The protein disulphide isomerase PdiA is involved in low temperature adaptation of *Aspergillus fumigatus*

FORMULAR 1

Manuskript Nr. 5

Titel des Manuskriptes: The protein disulphide isomerase PdiA is involved in low temperature adaptation of *Aspergillus fumigatus*

Autoren: Jana M. Boysen, Elena Shekhova, Olaf Kniemeyer, Axel A. Brakhage, Falk Hillmann

Bibliographische Informationen: -

Die Kandidatin ist

☒ Erstautor/-in, ☐ Ko-Erstautor/-in, ☐ Korresp. Autor/-in, ☐ Koautor/-in.

Status: in Vorbereitung

Anteile (in %) der Autoren / der Autorinnen an der Publikation

Autor/-in	Konzeptionell	Datenanalyse	Experimentell	Verfassen des Manuskriptes	Bereitstellung von Material
Jana M. Boysen	20%	90 %	90 %	90 %	-
Falk Hillmann	40%	-	-	-	80 %

The protein disulphide isomerase PdiA is involved in low temperature adaptation of *Aspergillus fumigatus*

Jana Boysen[1,2], Elena Shekova[3], Olaf Kniemeyer[3], Axel A. Brakhage[2,3], Falk Hillmann[1,*]

[1]Junior Research Group Evolution of Microbial Interactions Leibniz-Institute for Natural Product Research and Infection Biology – Hans Knöll Institute (HKI), Beutenbergstr. 11a, 07745 Jena, Germany

[2]Institute of Microbiology, Friedrich Schiller University Jena, Jena, Germany

[3]Department of Molecular and Applied Microbiology, Leibniz-Institute for Natural Product Research and Infection Biology – Hans Knöll Institute, Beutenbergstr. 11a, 07745 Jena, Germany

*Corresponding author:

Falk Hillmann (Falk.Hillmann@leibniz-hki.de)

Abstract

The opportunistic fungal pathogen *Aspergillus fumigatus* is the causative agent of life threatening infections in immunocompromised patients when inhaled conidia germinate in the lung alveoli and invade the lung tissue. *In vivo* germination of *A. fumigatus* conidia in the lung depends on Asp f3, a two-cysteine-type peroxiredoxin that is crucial for redox and iron homeostasis during the onset of germination. To identify the role of Asp f3 in the redox homeostasis of the fungus, we took a proteomics approach and compared the global protein oxidation state in the wild type and a strain lacking the *asp f3* gene. Although major enzymes of primary metabolic pathways were highly prone to Cystein oxidation, this did not lead to a detectable loss of function. The major target of protein oxidation was the protein disulphide isomerase PdiA, which was highly induced and oxidized in a Δ*asp f3* background. Fungal cells devoid of PdiA were viable but revealed temperature dependent growth deficiency indicating that protein maturation via PdiA is dependent on Asp f3.

Key Words: *Aspergillus fumigatus*, Allergen Asp F3, Redox-proteom, reactive oxygen species, protein folding, protein oxidation

Introduction

Aspergillus fumigatus is an ascomycete with a generally saprophytic lifestyle and ubiquitous distribution. It thrives in soil and compost heaps and contributes to the decomposition and recycling of biomass (Latgé, 1999). Its wide distribution is attributed to its high adaptability, enabling *A. fumigatus* to adjust competently to changes in pH, oxygen levels and temperature as well as changes in nutrition (Tekaia and Latgé, 2005). In addition, its versatility enables *A. fumigatus* to be an opportunistic pathogen, able to cause a range of diseases from fungal asthma and chronic pulmonary aspergillosis to invasive aspergillosis (IA), depending on the underlying condition. During IA, conidia are able to germinate inside the lung and penetrate epithelial as well as endothelial barriers, subsequently followed by the destruction of tissue and angio-invasion. Mortality rates can be up to 95 % in an overall rising number of cases estimated to be >300,000 for IA alone (Bongomin et al., 2017; McCarthy and Walsh, 2017). High-risk groups include chronic granulomatous disease (CGD) and immunosuppression following organ or hematopoietic stem cell transplantation (Segal, 2009; Gavaldà et al., 2014; Warris, 2014). Phagocytes of CGD-patients lack a functional NADPH-oxidase rendering them defective in the production of superoxide anion ($\cdot O_2^-$) and its metabolites (Yu et al., 2021). The resulting immune deficiency and the high risk for fungal infections, especially IA, highlight the importance of reactive oxygen species (ROS) during the hosts defence against the fungus.

Recently we described the peroxiredoxin Asp f3 of *A. fumigatus* and its significance for protection against ROS as well as virulence (Hillmann et al., 2016). Asp f3 is known as one of *A. fumigatus* major allergens and is thus highly abundant. Its additional affinity to serum immunoglobulin (Ig)E makes it an auspicious vaccine candidate and was shown to protect against IPA in Asp f3 immunized mice (Ito et al., 2006; Diaz-Arevalo et al., 2011). Loss of Asp f3 leads to hypersensitivity against ROS, low concentrations leading to a halt in germination and hyphal formation. Furthermore, the Asp f3 deletion strain was avirulent in a murine model of pulmonary aspergillosis (Hillmann et al., 2016). Interestingly, deletion of Afyap1, the major activator of ROS defence, was found to be a major regulatory target of Aspf3 (Boysen et al., 2021). However, this is unlikely to cause the avirulent phenotype, as Afyap1 itself is not essential to cause virulence in immunosuppressed mice (Lessing et al., 2007). Rather, the role of Asp f3 in virulence may be related to iron homeostasis during conidial germination, as conidia lacking the *asp f3* gene were unable to germinate in the iron-limiting environment of

the murine lung (Brantl et al., 2021). Although, these findings indicate a role for Asp f3 in cellular redox sensing, its molecular targets have not yet been elucidated. Therefore, we aimed to identify crucial protein targets of ROS using a Δ*asp f3* strain in a redox proteomics approach. Our results illustrate an impact of ROS on the global protein oxidation state of *A. fumigatus* in the presence and absence of Asp f3. We show that ROS exposure in an Asp f3 deficient background affects the protein oxidation pattern of a variety of metabolic enzymes. While oxidation of several distinct targets of oxidative damage did not necessarily lead to a reduction in enzymatic activity of those proteins, it might affect their cellular redox balance or stability. Especially high oxidation levels were detected for the protein disulphide isomerase PdiA, which may influence the protein folding machinery. A *pdiA* deletion mutant was viable but revealed a growth deficiency and sensitivity to different stress factors.

Material and Methods

A. fumigatus strain and culture conditions

All fungal strains included in this study are listed in Table 1. Unless otherwise specified fungal strains of *A. fumigatus* were cultured on/in *Aspergillus* minimal medium (AMM) with 1% [w/v] glucose as carbon source and 20 mM $NaNO_3$ as nitrogen source. 10^5 conidia were used for inoculation (Brakhage and Van den Brulle, 1995). Liquid cultures were shake at 180 rpm at 37°C for 24 hours. Conidia were harvested with 0.1 %(v/v) Tween 80 from mycelium cultivated on AMM-agar plates at 37°C for 72-96 h. Mutant-phenotypes were selected by addition of different selection markers, hygromycin B (250 µg/mL, Invivogen, Toulouse, France) or pyrithiamine (0.1 mg/mL, Sigma-Aldrich, Taufkirchen, Germany), as specified for the specific strain. Conidia numbers were measured in a CASY® Modell TT (OLS OMNI Life Science, Bremen, Germany). A 20 % (v/v) glycerol stock was used for long time storage of conidia at -80°C.

A. fumigatus gene deletion, complementation and recombination

For the generation of *pdiA* deletion mutants, *pdiA* was exchanged against a hygromycin resistance cassette through homologous recombination. For complementation *pdiA* and the pyrithiamine resistance cassette integrated to the *pksP* gene locus and allowed a straight forward identification of complemented strains by the white conidia resulting from a disrupted DHN-melanin biosynthesis. Plasmids (pUC_dpdiA_hph, pUC_dpksP_pdiAC_pth) were amplified in *Escherichia coli* DH5α, digested with restriction enzymes and transformed

as linear fragments into *A. fumigatus* D141 and Δasp f3 *via* protoplast formation (Ballance and Turner, 1985; Tilburn et al., 1995). Confirmation of mutants occurred by Southern blot and diagnostic PCR for KO and complementation mutants, respectively.

Isolation of chromosomal DNA

For DNA isolation fungal strains were cultivated for 16-18 h at 37°C at 180 rpm in Sabouraud Bouillon (2% [w/v] glucose, Carl Roth, Karlsruhe, Germany). Mycelium was harvested through miracloth, washed thoroughly with water, dried and frozen with liquid nitrogen. With mortar and pestle, frozen mycelium was ground to fine powder and stored at -20°C until further use. Isolation of chromosomal DNA was done following protocol described previously (Cenis, 1992).

Oxidative stress treatments

For the oxidative stress treatment 10^5 spores of *A. fumigatus* were inoculated in 6-well plates with 3 ml Czapek Dox (CD) medium (BD Biosciences) per well. Mycelium of one plate was isolated as a single sample (one replicate). Samples were incubated for 24 h at 37° prior to treatment with concentrations of 150 µM hypoxanthine and 0.2 u/mL xanthine oxidase for the *in vivo* generation of reactive oxygen species. After 15 minutes, samples were harvested quickly and frozen with liquid nitrogen.

Preparation of native protein extracts

For the enzyme assays, crude protein extracts were prepared from *A. fumigatus* mycelium grown for 16 h in AMM. The mycelium was harvested through miracloth, washed thoroughly with water, dried and frozen with liquid nitrogen. Frozen mycelium was then ground to fine powder and 100 mg were resuspended in 500 µl phosphate buffered saline (PBS) at pH 7.4. Samples were then mixed vigorously, sonicated for 10 minutes and mixed again for better solubilisation of proteins. After centrifugation, the supernatant containing the proteins were transferred to new tubes. Protein concentration was determined by the Bradford assay (Bradford, 1976) or in a Spectrophotometer (UV mini1240, Shimadzu, Kyoto, Japan).

Enzymatic assays

Enzymatic activity of MDH and KARI was measured with enzymatic activity assays.

Activity of malate dehydrogenase was measured through the NADH oxidation rate, which can be measured at 340 nm in an oxaloacetate dependent reaction. The method was performed according to Steffan and McAlister-Henn (1992).

KARI activity was measured at 340 nm through the oxidation rate of NADPH. Here, KARI catalyses the reaction of 2-acetolactate and NADPH to 2,3-dihydroxy-3-methylbutyrate and $NADP^+$. The assay was performed according to Tyagi *et al*. (2005), however, measurements were performed at room temperature.

Indirect labelling of Oxidized Cysteines for Redox Proteomics

The wild type (WT) strain D141 and Δ*asp f3* were grown in three biological replicates. CD medium with additional Hutner's Trace elements (1mL/L) ,to guarantee sufficient supply of micronutrients like iron, were inoculated with 10^5 spores and grown in liquid culture for 20 h at 37°C (Hutner et al., 1950). Cultures were then shifted for 30 min at 37°C with 150 µM H_2O_2 before harvesting at 4°C. Mycelia were stored at -80°C until further use.

Proteins were, with slight modifications, isolated and purified as described previously using a method based on trichloroacetic acid (TCA) and acetone precipitation (Kniemeyer et al., 2006; Baldin et al., 2015). In brief: 100 µg of ground mycelium were incubated over night at -20°C in TCA/Acetone. After centrifugation the supernatant was removed and the pellet washed repeatedly with 90% chilled Acetone. The pellet was allowed to dry at room temperature (RT) and was resuspended in lysis buffer (8 M Urea, 2 % [w/v] Chaps, 20 mM Tris-HCl, 1 mM EDTA, at pH 8) with 50 mM Iodoacetamide (IAM) to block reduced cysteines. For better lysis, samples were sonicated for 10 minutes. Subsequently the reaction was stopped by the addition of 4 parts chilled 1 % TCA/Acetone and stored for 1 h at -20°C for protein precipitation. The pellet was again washed repeatedly with 90% [v/v] acetone and dried at RT. Pellets were again resuspended in lysis buffer. Prior to labelling, protein concentration was adjusted to 25 µg in a defined volume for all samples. TCEP (tris(2-carboxyethyl)phosphine, Calbiochem) was added to obtain a final concentration of 800 µM and samples were incubated for 30 min in the dark. Labelling solution (BODIPY FL IAM (Bodipy® FL C1-1A)) was added to a final concentration of 300 µM and incubated for 20 min in darkness. Samples were cleared from excess labelling substrate by the use of BioRad Micro Spin Colums (BioRad, Feldkirchen, Germany).

2-D polyacrylamide gel electrophoresis (2-D PAGE)

For 2D-gelelectrophoresis, proteins are separated according to their isoelectric point (first dimension) on a pH gradient and according to their size (second dimension) in an SDS polyacrylamide gel. For isoelectric focusing IPG gel strips with a non-linear pH gradient from 3-11(GE Healthcare Life Sciences, Germany) were used. For the second dimension vertical SDS-PAGE gels (12.5 % Criterion Tris-HCl, BioRad, Feldkirchen, Germany) were used. Preparation and execution of isoelectric focusing and the SDS-PAGE were performed as described preciously (Barker et al., 2012; Kroll et al., 2016).

Proteins on the gel were visualized by scanning with a Typhoon 9410 scanner (GE Healthcare Life Sciences, Germany) with a resolution of 100 µM. Delta2D software Version 4.8 (DECODON, Greifswald, Germany) was used for analysing and merging of images as well as spot detection. Significantly, different spots were defined by a ratio greater than two and a *p*-value below 0.5 in student's *t*-test.

For identification of differentially oxidized proteins, protein spots were excised from the gels and treated with an in-gel trypsin digestion according to the protocol by Shevchenko et al. (1996). Matrix-assisted laser desorption ionization-tandem time-of-flight (MALDI-TOF/TOF) mass spectrometry was used to analyse extracted peptides on a Bruker ultrafleXtreme MALDI-TOF/TOF device (Bruker Daltonics, Germany) and were analysed and identified as described previously (Vödisch et al., 2009; Kroll et al., 2016).

Results

Loss of Asp f3 changes the protein oxidation pattern after treatment with reactive oxygen species

To analyse the protein oxidation pattern, mycelia of the wild type and Δ*asp f3* strain were treated with oxidative stress in biological triplicates and evaluated for changes in the protein oxidation pattern. The results showed an overall elevated rate of protein oxidation, but only about 25 proteins showed significant changes in oxidation as identified with the Delta2D software. Several protein targets showed differences in oxidation as indicated in a merged image of the 2D-gel electrophoresis (Figure 1), even though abundance was low. Overall, 16 proteins were picked of which seven different proteins were successfully identified by MALDI-TOF/TOF (Table 2). These oxidation targets belong to a number of different protein families. When analysed with the FunCat classification algorithm, target genes show significant (p>0.05) enrichment in the categories “tricarboxylic-acid pathway” (AFUA_3G04170, AFUA_6G05210), “lysosomal protein degradation” (AFUA_3G11400) and “electron transport” (AFUA_2G06150, AFUA_6G05210, AFUA_7G05470) belonging to the FunCat main categories “energy”, “protein fate (folding, modification, destination)” and “electron transport”, respectively. A GO-term analysis assigned the protein targets to seven categories listed in Table 2. Although four of the selected proteins cluster together in the GO-term “oxidation-reduction-process”, they are not part of the same cellular processes. The protein identified from spot seven is Asp f3 itself, which is prominently visible and strongly oxidized in the wild type but absent in Δ*asp f3*, as expected. Of the six identified target proteins, AFUA_7g05470 and AFUA_3g04170, although assigned a putative function, were not further characterized. The other four target genes were identified as protein disulphide isomerase (PdiA, AFUA_2g06150), aspartic endopeptidase Pep2 (AFUA_3g11400), ketol-acid reductoisomerase (KARI, AFUA_3g14490) and malate dehydrogenase (MDH, AFUA_6g05210).

Protein oxidation reduces ketol-acid reductoisomerase activity

Two of the proteins strongly oxidized in Δ*asp f3* are the NAD-dependent malate dehydrogenase (MDH) and the ketol-acid reductoisomerase (KARI). To determine if oxidative damage can affect the enzymatic activity we performed assays using total protein (Table 3). Enzyme activity was measured from three biological replicates. For the MDH, the enzymatic

activity revealed an NAD^+ dependent malate oxidation to oxaloacetate at 54 µM/min and 57µM/min per mg of protein for the wild type and Δ*asp f3*, respectively. Thus, the activity of the enzyme was not significantly affected in the absence of Asp f3. KARI activity was determined to be 11.6 µM/min and 17.7 µM/min per mg of protein for the wild type and Δ*asp f3*, respectively. In contrast to the MDH, KARI activity was generally much lower, but likewise enzymatic activity was not reduced. Instead, measured values were higher in a Δ*asp f3* background, indicating that oxidation of KARI might alter its enzymatic activity and thus Asp f3 signalling may affect central metabolic pathways in the fungus.

Deletion of PdiA is not lethal for *A. fumigatus* but affects growth and sporulation

One of the proteins most affected by ROS-induced oxidation was the protein disulphide isomerase PdiA. As a member of the PDI family PdiA contains a thioredoxin-like domain and is functionally associated with three catalytic activities, namely disulphide exchange, thiol redox activity and a chaperone (Nigam et al., 2001; Wilkinson and Gilbert, 2004; Laurindo et al., 2012; Ali Khan and Mutus, 2014).

PDIs are important in protein folding and the unfolded protein response (UPR) and its induction and altered oxidation state indicated that these pathways are highly affected by elevated ROS levels. We thus constructed *pdiA* deletion and complementation strains (Figure 2). A plate assay showed that Δ*pdiA* is severely impaired in radial growth on different media (Figure 3 A-B). On AMM and Malt Peptone (MP) medium Δ*pdiA* showed a significant deficit in radial growth compared to both the wild type and the complemented strain. These growth defects were less pronounced on Czapek-Dox medium. Reconstitution of *pdiA* under the control of the constitutive *gpdA*-promoter in the genetic locus of *pksP* reverted stress sensitivity to wild type levels. In addition to the growth deficit, sporulation was also significantly impaired with Δ*pdiA* producing approximately one third of the conidia of the wild type (Figure 3 C).

PdiA is not essential in defence against ROS

As PdiA was highly expressed in Δ*asp f3*, we anticipated that deletion of the *pdiA* gene could also yield a ROS sensitive phenotype. Strains were treated with different sources of oxidative stress in an agar diffusion assay, including menadione, hydrogen peroxide and tert-butylhydroperoxid (t-BOOH) (Figure 3 D-E). However, when challenged with different

concentrations of hydrogen peroxide and t-BOOH inhibition zones of Δ*pdiA* equal the wild type. Indeed, plates treated with menadione even show a significantly smaller inhibition zone than the wild type, indicating that PdiA itself could be a target of ROS. Overall, PdiA activity may require functional Asp f3 but is not directly involved in redox homeostasis.

***PdiA* affects stress tolerance and growth at ambient temperature**

Although addition of oxidative stress revealed that Δ*pdiA* is not redox sensitive, we decided to test further stress conditions as a deletion of *pdiA* was not previously characterized for *A. fumigatus*. Included in the range of stress factors were salt (NaCl) and osmotic stress (sorbitol), cell wall stress (CongoRed, Calcofluor White), ER stress (DTT) and antibiotic treatment with Azoles (Itraconazole, Voriconazole) and different temperatures.

Cell wall stress applied as CongoRed and Calcofluor White had a slightly enhancing effects on the growth of Δ*pdiA*. While on normal AMM Δ*pdiA* shows a clear growth deficit, addition of CongoRed and Calcofluor White are more effective on wild type hyphae (Figure 4). However, a broad white ring around the colony indicated impaired conidiation in Δ*pdiA*, which onset was delayed when compared to the wild type. Osmotic stress in form of high Sorbitol concentrations had the same effect and enhance growth of Δ*pdiA* above WT-levels, though sporulation areas were less defined than with CongoRed and Calcofluor White. Surprisingly, ER-stress imposed by DTT, an inhibitor of disulphide bond formation, does not lead to a strong inhibition of growth in Δ*pdiA*, though different results were expected due to previous studies in *S. cerevisae* (Holst et al., 1997). Instead there is no difference in growth between the WT and Δ*pdiA*. Complementation of Δ*pdiA* showed even stronger growth, which may result from the constitutive expression of *pdiA.* In contrast, salt stress showed a weaker growth of Δ*pdiA* than the WT but indeed, all strains tested showed significant salt sensitivity with Δ*pdiA* exhibiting the weakest phenotype. Resistance to azoles depended strongly on the azole used. Voriconazole on one hand affected the fungus already at 0.25 µg/mL and higher concentrations up to 1 µg/mL led to a very effective inhibition of *A. fumigatus* growth (Figure 5 A-C). For Δ*pdiA* growth differences compared to the WT were more pronounced at higher concentrations (0.5-0.75 µg/mL), and less at 0.25 µg/mL. Itraconazole on the other hand had hardly any effect at the tested concentrations and the difference between WT and Δ*pdiA*, although significant, did not compare to the differences found on AMM medium without addition of itraconazole (Figure 5 A,D,E). Yet the Δ*pdiA* complementation strain grew

faster than the wild type, even when challenged with itraconazole. The same effect could be seen with lower concentrations (0.25 µg/mL) of voriconazole, but was lost at higher exposures. Last, we tested the impact of PdiA at different temperatures (Figure 5 A,F,G). *A. fumigatus* is usually considered a thermophile, which thrives at higher temperatures in active compost heaps, or tissues of warm blooded hosts. At 37°C and 45°C PdiA had only little, but significant effect on the radial growth of the fungus. However, a growth defect was detected for the Δ*pdiA* strain at 30°C, which was even more pronounced at 20°C, indicating that PdiA target proteins are primarily required at lower temperatures.

Discussion

The peroxiredoxin Asp f3 is a key player in *A. fumigatus* defence against the constant threat of external reactive oxygen species and in addition plays an important role during virulence. So far, we know that the absence of Asp f3 results in a redox sensitive phenotype and avirulence in a murine model of pulmonary aspergillosis. *A. fumigatus* virulence has long been associated with oxidative stress as the lack thereof in CGD patients renders them more susceptible to fungal infections, especially those caused by *A. fumigatus* (Yu et al., 2021). Thus, we tried to identify potential protein targets suffering strong oxidative damage in the absence of Asp f3, damage that might be strong enough to explain the strong sensitivity to oxidative stress as well as virulence. However, we could show very recently that the avirulence of Δ*asp f3* is caused by a sensitivity to iron limitation rather than the direct impact of ROS (Brantl et al., 2021). Furthermore, we could show that the absence of Asp f3 affects the oxidative stress answer regulated by Afyap1 by preventing Afyap1 accumulation in the nucleus upon exposure to oxidative stress. Nevertheless, we selected several protein target genes exhibiting stronger oxidation in the Δ*asp f3* background than the WT after xanthine oxidase treatment. One of the target proteins is the aspartic endopeptidase Pep2, a homologue of vacuolar proteinase A of *Saccharomyces cerevisiae* (Reichard et al., 1990). It is associated with the conidial surface and as thus more strongly expressed in dormant conidia than the mycelium (Asif et al., 2006). It is immunoreactive and exposition to neutrophils causes elevated expression of Pep2 in conidia (Singh et al., 2010; Suh et al., 2012). Since deletion of Pep2 does not affect the *A. fumigatus* phenotype, oxidative inactivation we considered it irrelevant for the redox sensitive phenotype (Reichard et al., 1990).

As a component of the citric acid cycle the malate dehydrogenase catalyses the oxidation of L-malate to oxaloacetate and is well-studied (Goward and Nicholls, 1994; Takahashi-Íñiguez et al., 2016). As part of this major cellular machinery, its function is important for the whole organism and makes the MDH a potentially interesting primary target of oxidative damage. Although it was not characterized specifically in *A. fumigatus,* MDH is mentioned throughout different research topics. It is expressed during early development, has a higher protein abundance in spores than in mycelium, protein expression is downregulated by induction of protein kinase A subunit *pkaC1* and underlies regulation by *phoB*^{PHO80} (de Gouvêa et al., 2008; Grosse et al., 2008; Teutschbein et al., 2010; Suh et al., 2012). Albeit a potentially interesting

target we could show that higher oxidation does not correlate with its primary enzymatic activity indicating that this part of the citric acid cycle is not a primary target of ROS.

KARI is part of the branched-chain amino acid biosynthesis and catalyses the chemical reaction of (R)-2,3-dihydroxy-3-methylbutanoate and NADP+ to (S)-2-hydroxy-methyl-3-oxobutanoate and NADPH and H^+ (Chunduru et al., 1989). It is involved in several metabolic pathways and a key enzyme in the biosynthesis of branched chain amino acids (BCAA) valine, leucine and isoleucine. Since BCAAs are produced in bacteria, fungi and higher plants but not mammals, it was proposed as a potential target for antifungals, including treatment of Aspergillosis (Durner et al., 1993; Morya et al., 2011; Morya et al., 2012). With examples of its major importance for conidiation, growth and virulence of the insect- and plant pathogenic fungi *Metarhizium robertsii* and *Fusarium graminearum*, respectively, it seems possible that a loss of KARI-function might have a strong impact on the *A. fumigatus* phenotype (Liu et al., 2014; Luo et al., 2020). Granting our results revealed a reduced KARI activity following protein oxidation, but overall the enzyme was still functional. Nonetheless, KARI remains an interesting target for potential antifungals.

The protein disulphide isomerase A PdiA was found to be highly expressed and oxidized in the absence of Asp f3. PdiA is a homologue of *S. cerevisiae* Pdi1, a key player of the protein folding machinery and the unfolded protein response (UPR). Although most organisms, including yeast, contain several PDI-like proteins, deletion of Pdi1 in yeast is lethal but can be complemented by overexpressing its homologues (Farquhar et al., 1991; Nørgaard et al., 2001). In addition to their functions in the ER, PDIs are also described as cell surface located, where they are suggested to act mainly as reductases but are also able to perform isomerase activities (Jiang et al., 1999; Laurindo et al., 2012). PdiA of *A. fumigatus* was also isolated from the conidial surface, described as immunoreactive and even proposed as a possible vaccine candidate (Asif et al., 2006; Singh et al., 2010). Due to its importance in other organisms and its role for protein folding and especially in the unfolded protein response, we expected loss of PdiA to have severe consequences. However, different from *S. cervisiae*, *pdiA* was not an essential gene in *A. fumigatus*, though we observed impaired growth and sporulation in Δ*pdiA* compared to the WT. The deletion strain coped generally well with the addition of different stress factors. Although it stays significantly smaller than the wild type under most conditions, it has to be taken into account that even on a non-stress standard medium (e.g. AMM) growth

is already impaired. In relation, the impact of the applied stresses, with a few exceptions including low temperatures and voriconazol treatment, seems much less severe. The reason might be a functional redundancy of different PDIs. Like yeast *A.fumigatus* contains at least one more PDI (tigA, AFUA_5g12260) (Richie et al., 2009). Also, deletion of yeast *pdi1* was lethal, but overexpressions of the normally lowly expressed homologues were able to save the phenotype (Nørgaard et al., 2001). Additionally, since repeated oxidation and reduction cycles are part of PDI function, higher oxidation levels would hardly indicate loss of function. Enhanced presence of oxidized PdiA might rather indicate an increased requirement for folding assistance or a backlog of oxidized PdiA due to a lack of sufficient redox equivalents to revert PdiA back to its reduced state.

Our results show that the ROS sensitivity and avirulence of Δ*asp f3* are most likely not related to oxidative inactivation of important protein targets upon challenge with oxidative stress. Instead, Brantl and colleagues (2021) could identify a sensitivity to iron limitation as a key factor. However, we provide a deletion mutant of the protein disulphide isomerase A of *A. fumigatus*. Loss of PdiA, though not lethal, leads to a deficiency in growth and conidiation and renders the fungus especially sensitive to low temperatures. This indicates that another PDI, possibly tigA, is able to compensate at least partly for its loss. Since protein folding and the unfolded protein response are important cellular processes, valuable information might be gained by rasearching and understanding their interplay in the future.

Acknowledgement

We thank technical assistant Till Kindl for his support.

Funding

This study was supported by the Leibniz Institute for Natural Product Research and Infection Biology – Hans Knöll Institute Jena and by a grant of the Deutsche Forschungsgemeinschaft (DFG, German Research Foundation DFG, HI 1574-2/1).

List of Figures and Tables

Table 1. Strains of A. *fumigatus*.

Strain	Genotype	References
***A. fumigatus* D141**	WT	(Reichard et al., 1990)
A.°fumigatus* Δ*asp f3	*asp f3*::*hph*; Hyg^R	(Hillmann et al., 2016)
***A.°fumigatus* Δ*asp f3*^{C}**	*asp f3*::*hph*; Hyg^R Δ*asp f3*::*asp f3*; PT^R	(Hillmann et al., 2016)
A.°fumigatus* Δ*pdiA	*pdiA*::*hph*; Hyg^R	This study
***A.°fumigatus* Δ*pdiA*^{C}**	*pdiA*::*hph*; Hyg^R *pdiA*::pksP; PT^R	This study

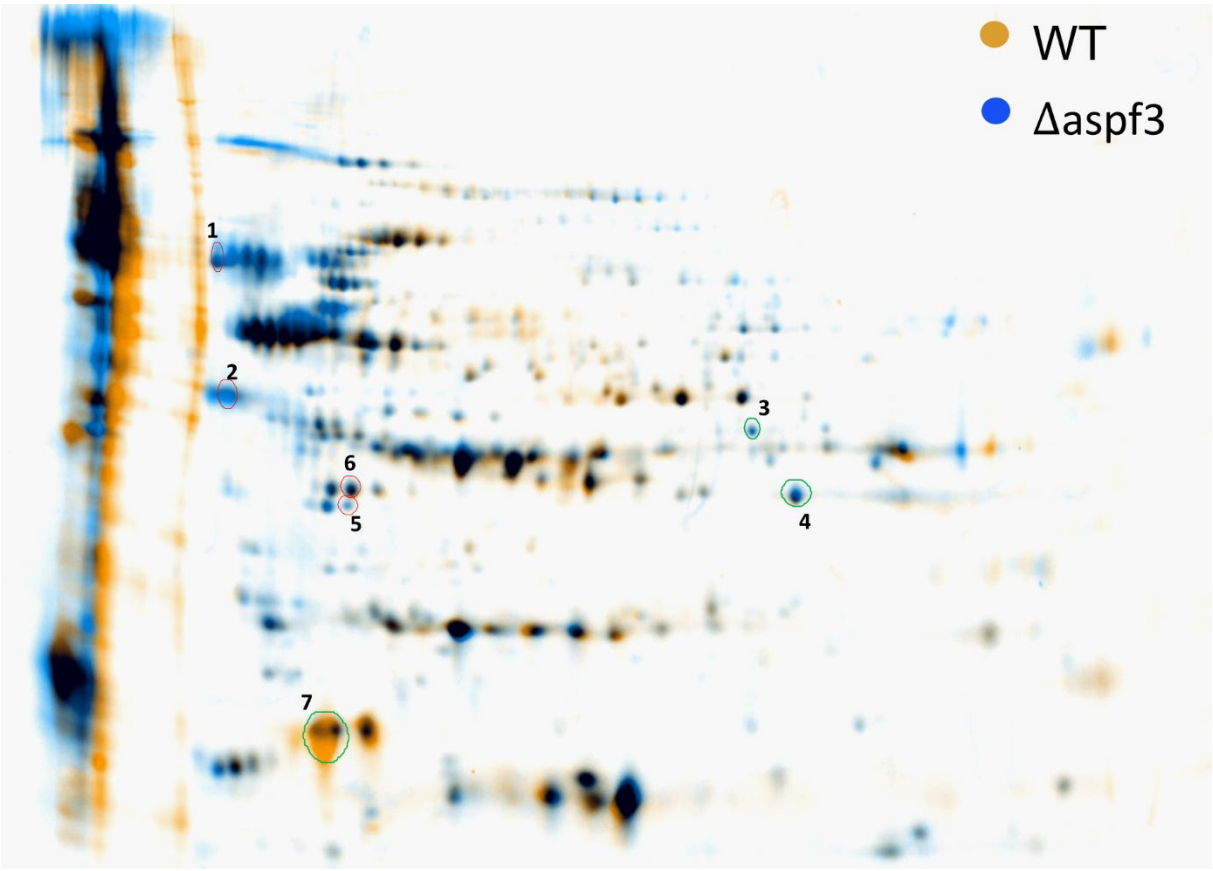

Figure 1. Merged image of 2D gel electrophoresis of protein extracts of *A. fumigatus* wild type and the Δ*asp f3* strain. *A. fumigatus* was grown in Czapek Dox medium before treatment with H_2O_2. Numbered circles indicate the protein spots picked and identified by MALDI-TOF. Potential targets were identified by the Delta2D software, which was also used to merge the images of *A. fumigatus* wild type and the Δa*sp f3* protein gels.

Table 2 Differentially oxidized and successfully identified target proteins of *A. fumigatus*.

Spot Nr.*	Gene Number	Putative function	Mascot Score (ms/msms)	Nr. of Cys	FunCat category	GO category (biological process)
1	AFUA_ 2g06150	PdiA, putative protein disulphide isomerase	134.0/-	6	electron transport	cell redox homeostasis
2	AFUA_ 3g11400	Pep2, Aspartic acid endopeptidase	68.5/ 242.4	4	lysosomal protein degradation	
3	AFUA_ 3g14490	Ketol-acid reductoisomerase (KARI)	260.0/ 262.0	2		oxidation-reduction process, branched-chain amino acid biosynthetic process, cellular amino acid biosynthetic process
4	AFUA_ 6g05210	Putative NAD-dependent malate dehydrogenase (MDH)	303.0/ 366.7	3	tricarboxylic-acid pathway, electron transport	oxidation-reduction process, malate metabolic process, cellular carbohydrate metabolic process
5	AFUA_ 7g05470	Putative electron transfer flavoprotein alpha subunit	69.9/-	1	electron transport	
6	AFUA_ 3g04170	putative pyruvate dehydrogenase E1 beta subunit PdbA	122.0/ 148.1	6	tricarboxylic-acid pathway	acetyl-CoA biosynthetic process from pyruvate, oxidation-reduction process
7	AFUA_ 6g02280	allergen Asp F3	112.0/ 169.1	2		oxidation-reduction process

*Numbers correspond to spot numbers in Figure 1

Table 3 Protein activity assay. *A. fumigatus* was grown in Czapec Dox medium before treatment with hypoxanthine and xanthine oxidase for the *in vivo* generation of reactive oxygen species. Native protein was isolated and used to measure enzyme activity of Ketol-acid reductuisomeare (KARI) and Malate dehydrogenase (MDH).

	KARI	MDH
Enzymatic reaction	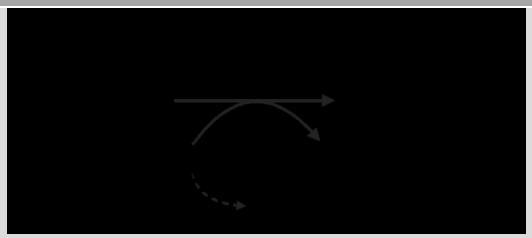	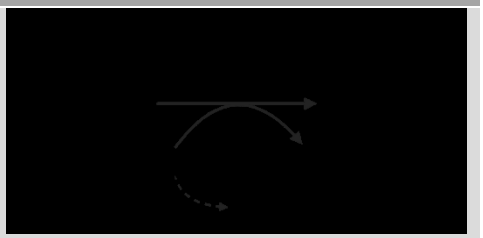
Activity WT	11.6 µM/min/mg enzyme	54.0 µM/min/mg enzyme
Activity Δ*asp f3*	17.7 µM/min/mg enzyme	57.9µM/min/mg enzyme

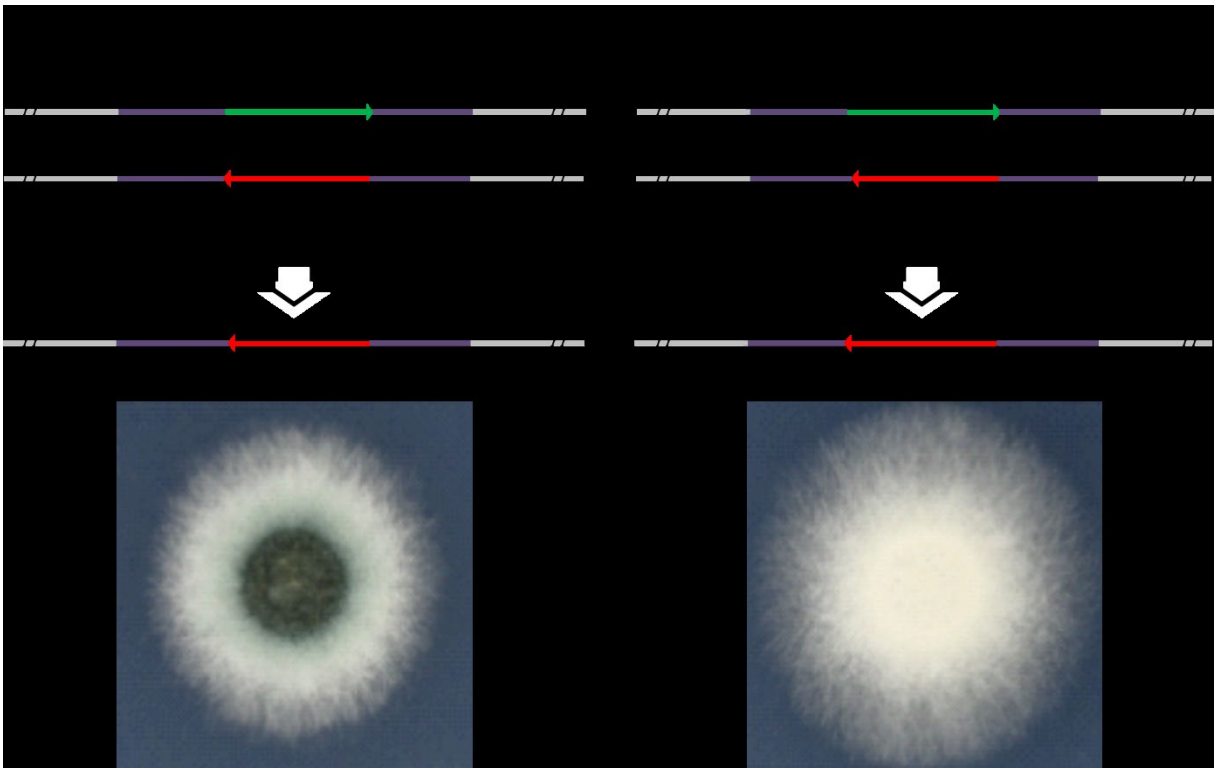

Figure 2 The deletion an reconstitution of the *pdiA* gene locus. A *pdiA* of the *A. fumigatus* wild type was exchanged against a hygromycin-resistance cassette through homologous recombination. **B** The *pdiA* gene expression was resconstituted in Δ*pdiA* through a genetic exchange of *pksP* against *pdiA* and a pyrithiamine resistance marker by homologous recombination.

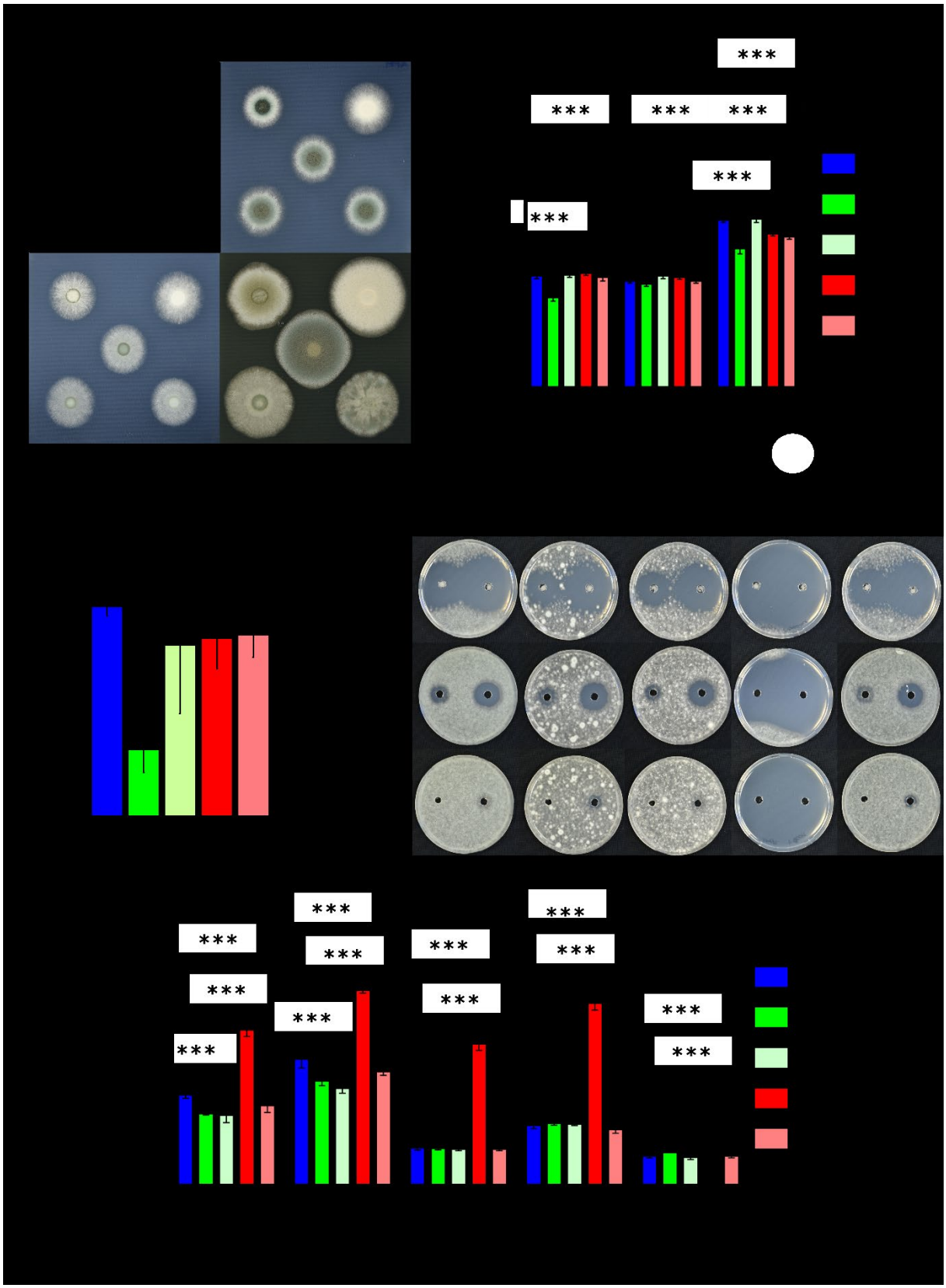

Figure 3 PdiA is involved in growth and sporulation of *A. fumigatus*. **A** *A. fumigatus* plate assay on *Aspergillus* minimal medium (AMM), Czapec Dox (CD) and malt peptone (MP). 10^5 conidia of each strain (WT D141, Δ*pdiA,* Δ*pdiA*^{C}, Δ*asp f3* and Δ*asp f3*) were applied to the plates in four biological replicates and incubated for 72 h at 37° C. **B** Columns show a graphic illustration of *A. fumigatus* growth diameter [mm] in average, error bars (n=4) indicate standard deviation. Student's t-test was performed to calculate significance with *:$p < 0.1$; **:$p < 0.05$; ***:$p < 0.01$. **C** Columns show sporulation efficiency

of *A. fumigatus* (WT D141, Δ*pdiA,* Δ*pdiA*^{C}, Δ*asp f3* and Δ*asp f3*) per cm², error bars show standard deviation (n=3). 10^5 conidia of each *A. fumigatus* strainwere seeded on AMM-Agar and incubated for 72 hours at 37°C before conidia were harvested. Total numbers of conidia were normalized to the surface area of the colonies, taking into account the slower and less extensive growth of Δ*pdiA*. Student's t-test was performed to calculate significance with *:$p < 0.1$; **:$p < 0.05$; ***:$p < 0.01$. **D** 10^5 conidia of *A. fumigatus* (WT D141, Δ*pdiA,* Δ*pdiA*^{C}, Δ*asp f3* and Δ*asp f3*) were preinoculation inside liquid agar and grown for 24 h at 37° C during agar diffusion of 75 mM (lef) and 300 mM (right) H_2O_2, 0.25 mM (left) and 1 mM (right) menadione and 30 mM *t*-bOOH with four biological replicates for each strain and each condition. **E** Columns show the size of growth inhibition zones (mm). Error bars indicate standard deviation (n=4). Student's t-test was performed to calculate significance with *, $p < 0.1$; **, $p < 0.05$; ***, $p < 0.01$.

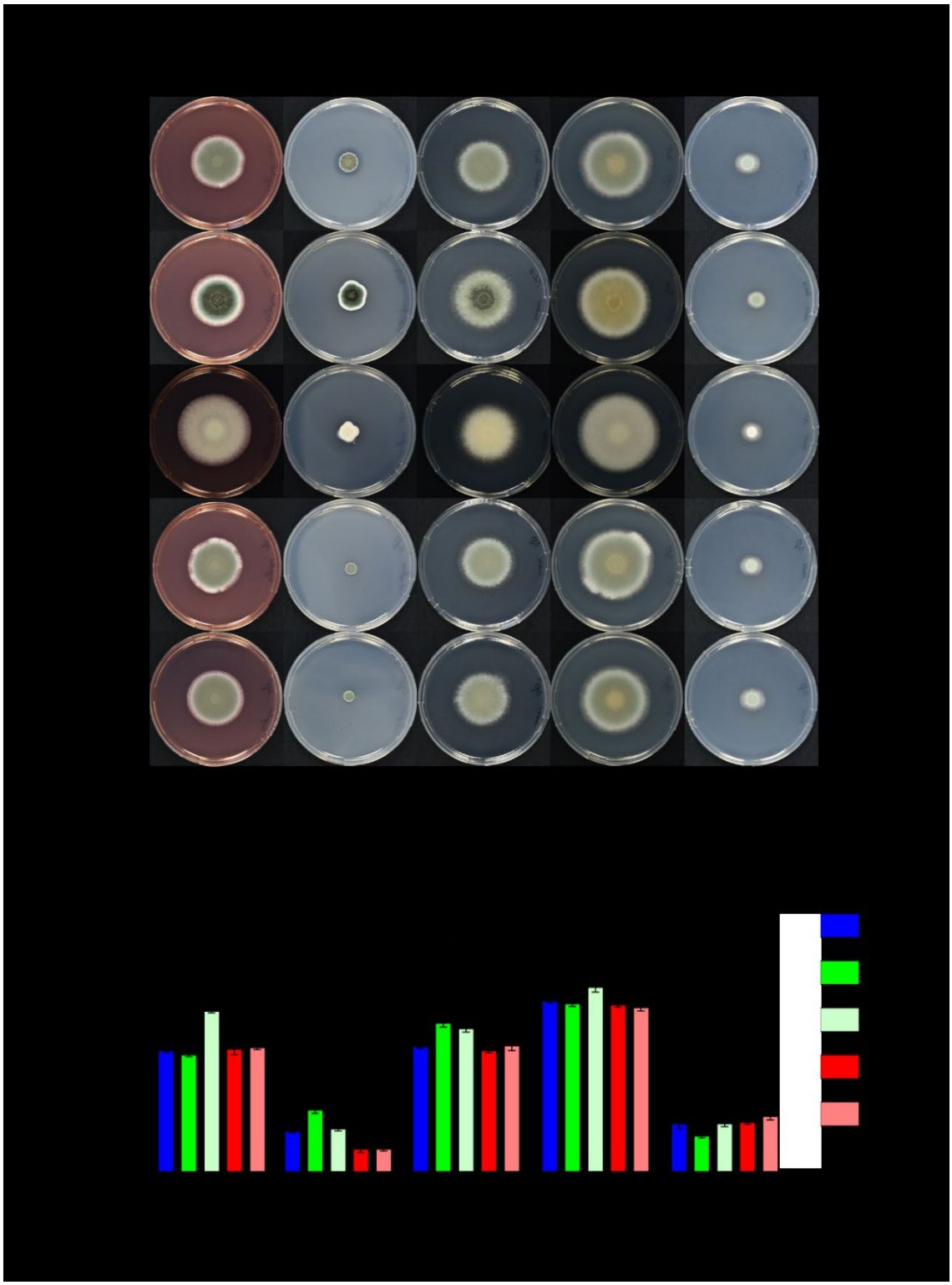

Figure 4. PdiA plays a minor role in the defence against cell wall stress . A *A. fumigastus* plate assay on *Aspergillus* minimal medium (AMM) and added stress factors as indicated (CongoRed 20 µg/mL, Calcofluor White 0.2 mg/mL, Sorbitol 1.2 M, DTT 5mM and $NaCl_2$ 1.5 M). 10^5 conidia were applied on the plate's surface in four biological replicates and incubated for 96 h at 37° C. **B** Columns show graphic illustration of *A. fumigatus* growth diameter [mm], error bars (n=4) indicate standard deviation. Student's t-test was performed to calculate significance with *:$p < 0.1$; **:$p < 0.05$; ***:$p < 0.01$.

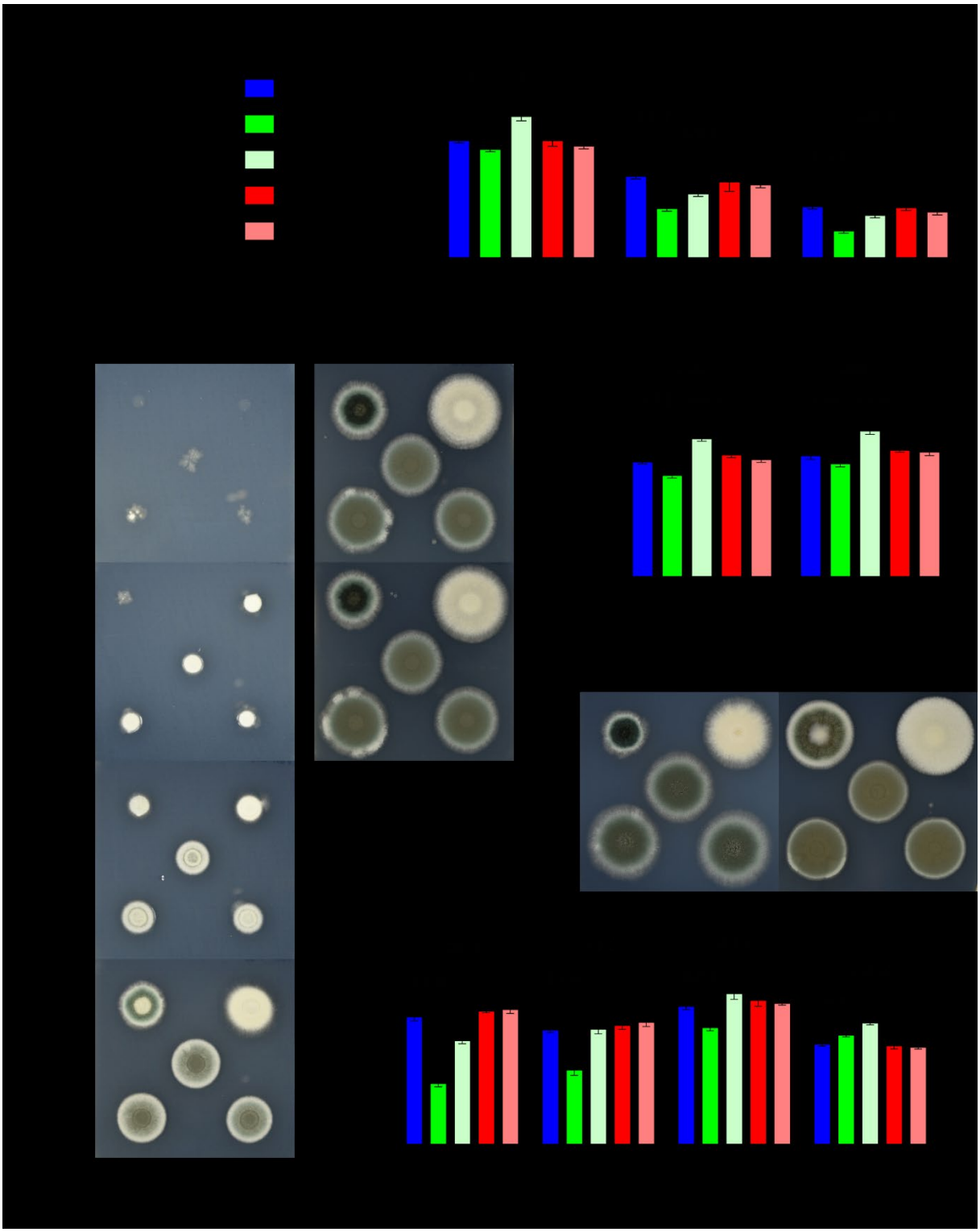

Figure 5. PdiA is involved in resistance to azoles and growth at low temperatures. A Legend for the application of fungal strains on the agar plates (**B, D, F**) and the colour code for graphic representation of growth (**C, E, G**). *A. fumigastus* plate assay on *Aspergillus* minimal medium (AMM) with different concentrations of **B** voriconazole (1 µg/mL, 0.75 µg/mL, 0.5 µg/mL and 0.25 µg/mL) and **D** itraconazol (1 µg/mL and 0.75 µg/mL). 10^5 conidia (WT D141, Δ*pdiA,* Δ*pdiA*^{C}, Δ*asp f3* and Δ*asp f3*) were applied on the agar plate surface and incubated for 72 h at 37°C Columns show a graphic illustration of *A. fumigatus* growth diameter [mm] after treatment with **C** Voriconazole and **E** Itraconazol. 1 µg/mL voriconazol was excluded from the graph since growth was too minimal in all strains to measure adequately. Error bars indicate standard deviation (n=4), student's t-test was performed to calculate

significance with *:$p < 0.1$; **:$p < 0.05$; ***:$p < 0.01$. **F** To test the influence of different temperatures *A. fumigatus* (WT D141, Δ*pdiA,* Δ*pdiA*^{C}, Δ*asp f3* and Δ*asp f3*) growth, 10^5 conidia were applied to AMM agar in four biological replicates and incubated for 96 h at 22° C, 30° C, 37° C and 45° C. The figure representatively shows 30°C and 45°C. **G** Colums show growth (mm), error bars indicate standard deviation (n=4). Student's t-test was performed to calculate significance with *:$p < 0.1$; **:$p < 0.05$; ***:$p < 0.01$.

References

Ali Khan, H. and Mutus, B., 2014. Protein disulphide isomerase a multifunctional protein with multiple physiological roles. *Frontiers in chemistry* 2, 70.

Asif, A.R., Oellerich, M., Amstrong, V.W., Riemenschneider, B., Monod, M. and Reichard, U., 2006. Proteome of conidial surface associated proteins of *Aspergillus fumigatus* reflecting potential vaccine candidates and allergens. *Journal of proteome research* 5, 954-962.

Baldin, C., Valiante, V., Kruger, T., Schafferer, L., Haas, H., Kniemeyer, O. and Brakhage, A.A., 2015. Comparative proteomics of a tor inducible *Aspergillus fumigatus* mutant reveals involvement of the Tor kinase in iron regulation. *Proteomics* 15, 2230-43.

Ballance, D. and Turner, G., 1985. Development of a high-frequency transforming vector for *Aspergillus nidulans*. *Gene* 36, 321-331.

Barker, B.M., Kroll, K., Vödisch, M., Mazurie, A., Kniemeyer, O. and Cramer, R.A., 2012. Transcriptomic and proteomic analyses of the *Aspergillus fumigatus* hypoxia response using an oxygen-controlled fermenter. *BMC genomics* 13, 1-25.

Bongomin, F., Gago, S., Oladele, R.O. and Denning, D.W., 2017. Global and Multi-National Prevalence of Fungal Diseases-Estimate Precision. *J Fungi* (Basel) 3.

Boysen, J.M., Saeed, N., Wolf, T., Panagiotou, G. and Hillmann, F., 2021. The Peroxiredoxin Asp f3 Acts as Redox Sensor in *Aspergillus fumigatus*. *Genes* 12, 668.

Bradford, M.M., 1976. A rapid and sensitive method for the quantitation of microgram quantities of protein utilizing the principle of protein-dye binding. *Analytical biochemistry* 72, 248-254.

Brakhage, A.A. and Van den Brulle, J., 1995. Use of reporter genes to identify recessive trans-acting mutations specifically involved in the regulation of *Aspergillus nidulans* penicillin biosynthesis genes. *Journal of bacteriology* 177, 2781-2788.

Brantl, V., Boysen, J.M., Yap, A., Golubtsov, E., Ruf, D., Heinekamp, T., Strassburger, M., Dichtl, K., Haas, H., Hillmann, F. and Wagener, J., 2021. Peroxiredoxin Asp f3 Is Essential for *Aspergillus fumigatus* To Overcome Iron Limitation during Infection. *mBio* 12, e0097621.

Cenis, J., 1992. Rapid extraction of fungal DNA for PCR amplification. Nucleic acids research 20, 2380.

Chunduru, S.K., Mrachko, G.T. and Calvo, K., 1989. Mechanism of ketol acid reductoisomerase. Steady-state analysis and metal ion requirement. *Biochemistry* 28, 486-493.

de Gouvêa, P.F., Soriani, F.M., Malavazi, I., Savoldi, M., de Souza Goldman, M.H., Loss, O., Bignell, E., da Silva Ferreira, M.E. and Goldman, G.H., 2008. Functional characterization of the *Aspergillus fumigatus* PHO80 homologue. *Fungal Genetics and Biology* 45, 1135-1146.

Diaz-Arevalo, D., Bagramyan, K., Hong, T.B., Ito, J.I. and Kalkum, M., 2011. CD4+ T cells mediate the protective effect of the recombinant Asp f3-based anti-aspergillosis vaccine. *Infection and immunity* 79, 2257-2266.

Durner, J., Knorzer, O.C. and Boger, P., 1993. Ketol-acid reductoisomerase from barley (Hordeum vulgare)(purification, properties, and specific inhibition). *Plant physiology* 103, 903-910.

Farquhar, R., Honey, N., Murant, S.J., Bossier, P., Schultz, L., Montgomery, D., Ellis, R.W., Freedman, R.B. and Tuite, M.F., 1991. Protein disulphide isomerase is essential for viability in *Saccharomyces cerevisiae*. *Gene* 108, 81-89.

Gavaldà, J., Meije, Y., Fortún, J., Roilides, E., Saliba, F., Lortholary, O., Muñoz, P., Grossi, P., Cuenca-Estrella, M. and Hosts, E.S.G.f.I.i.C., 2014. Invasive fungal infections in solid organ transplant recipients. *Clinical Microbiology and infection* 20, 27-48.

Goward, C.R. and Nicholls, D.J., 1994. Malate dehydrogenase: a model for structure, evolution, and catalysis. *Protein Science* 3, 1883-1888.

Grosse, C., Heinekamp, T., Kniemeyer, O., Gehrke, A. and Brakhage, A.A., 2008. Protein kinase A regulates growth, sporulation, and pigment formation in *Aspergillus fumigatus*. *Applied and environmental microbiology* 74, 4923-4933.

Hillmann, F., Bagramyan, K., Strassburger, M., Heinekamp, T., Hong, T.B., Bzymek, K.P., Williams, J.C., Brakhage, A.A. and Kalkum, M., 2016. The Crystal Structure of Peroxiredoxin Asp f3 Provides

Mechanistic Insight into Oxidative Stress Resistance and Virulence of *Aspergillus fumigatus*. *Scientific Reports* 6, 33396.

Holst, B., Tachibana, C. and Winther, J.R., 1997. Active site mutations in yeast protein disulphide isomerase cause dithiothreitol sensitivity and a reduced rate of protein folding in the endoplasmic reticulum. *The Journal of cell biology* 138, 1229-1238.

Hutner, S.H., Provasoli, L., Schatz, A. and Haskins, C., 1950. Some approaches to the study of the role of metals in the metabolism of microorganisms. *Proceedings of the American Philosophical Society* 94, 152-170.

Ito, J.I., Lyons, J.M., Hong, T.B., Tamae, D., Liu, Y.-K., Wilczynski, S.P. and Kalkum, M., 2006. Vaccinations with recombinant variants of *Aspergillus fumigatus* allergen Asp f 3 protect mice against invasive aspergillosis. *Infection and immunity* 74, 5075-5084.

Jiang, X.-M., Fitzgerald, M., Grant, C.M. and Hogg, P.J., 1999. Redox control of exofacial protein thiols/disulphides by protein disulphide isomerase. *Journal of Biological Chemistry* 274, 2416-2423.

Kniemeyer, O., Lessing, F., Scheibner, O., Hertweck, C. and Brakhage, A.A., 2006. Optimisation of a 2-D gel electrophoresis protocol for the human-pathogenic fungus *Aspergillus fumigatus*. *Current genetics* 49, 178-189.

Kroll, K., Shekhova, E., Mattern, D.J., Thywissen, A., Jacobsen, I.D., Strassburger, M., Heinekamp, T., Shelest, E., Brakhage, A.A. and Kniemeyer, O., 2016. The hypoxia-induced dehydrogenase HorA is required for coenzyme Q10 biosynthesis, azole sensitivity and virulence of *Aspergillus fumigatus*. *Molecular microbiology* 101, 92-108.

Latgé, J.-P., 1999. *Aspergillus fumigatus* and aspergillosis. *Clinical microbiology reviews* 12, 310-350.

Laurindo, F.R., Pescatore, L.A. and de Castro Fernandes, D., 2012. Protein disulphide isomerase in redox cell signaling and homeostasis. *Free Radical Biology and Medicine* 52, 1954-1969.

Lessing, F., Kniemeyer, O., Wozniok, I., Loeffler, J., Kurzai, O., Haertl, A. and Brakhage, A.A., 2007. The *Aspergillus fumigatus* transcriptional regulator AfYap1 represents the major regulator for defense against reactive oxygen intermediates but is dispensable for pathogenicity in an intranasal mouse infection model. *Eukaryotic c*ell 6, 2290-2302.

Liu, X., Wang, J., Xu, J. and Shi, J., 2014. FgIlv5 is required for branched-chain amino acid biosynthesis and full virulence in *Fusarium graminearum*. *Microbiology* 160, 692-702.

Luo, F., Zhou, H., Zhou, X., Xie, X., Li, Y., Hu, F. and Huang, B., 2020. The intermediates in branched-chain amino acid biosynthesis are indispensable for conidial germination of the insect-pathogenic fungus *Metarhizium robertsii*. *Applied and environmental microbiology* 86, e01682-20.

McCarthy, M.W. and Walsh, T.J., 2017. Special considerations for the diagnosis and treatment of invasive pulmonary aspergillosis. *Expert review of respiratory medicine* 11, 739-748.

Morya, V., Kumari, S. and Kim, E., 2011. Imperative pathway analysis to identify the potential drug target for *Aspergillus* infection. International Journal of Latest *Trends in Computing* 2, 178-182.

Morya, V.K., Kumari, S. and Kim, E.-k., 2012. Virtual screening and evaluation of Ketol-Acid Reducto-Isomerase (KARI) as a putative drug target for Aspergillosis. *Clinical proteomics* 9, 1-13.

Nigam, S., Sarma, P., Ghosh, P. and Sarma, P.U., 2001. Characterization of *Aspergillus fumigatus* protein disulphide isomerase family gene. *Gene* 281, 143-150.

Nørgaard, P., Westphal, V., Tachibana, C., Alsøe, L., Holst, B. and Winther, J.R., 2001. Functional differences in yeast protein disulphide isomerases. *The Journal of cell biology* 152, 553-562.

Reichard, U., Büttner, S., Eiffert, H., Staib, F. and Rüchel, R., 1990. Purification and characterisation of an extracellular serine proteinase from *Aspergillus fumigatus* and its detection in tissue. *Journal of medical microbiology* 33, 243-251.

Richie, D.L., Hartl, L., Aimanianda, V., Winters, M.S., Fuller, K.K., Miley, M.D., White, S., McCarthy, J.W., Latgé, J.-P. and Feldmesser, M., 2009. A role for the unfolded protein response (UPR) in virulence and antifungal susceptibility in *Aspergillus fumigatus*. PLoS pathogens 5, e1000258.

Segal, B.H., 2009. Invasive aspergillosis in chronic granulomatous disease, *Aspergillosis: from diagnosis to prevention*. Springer, pp. 527-543.

Shevchenko, A., Wilm, M., Vorm, O. and Mann, M., 1996. Mass spectrometric sequencing of proteins from silver-stained polyacrylamide gels. *Analytical chemistry* 68, 850-858.

Singh, B., Oellerich, M., Kumar, R., Kumar, M., Bhadoria, D.P., Reichard, U., Gupta, V.K., Sharma, G.L. and Asif, A.R., 2010. Immuno-reactive molecules identified from the secreted proteome of *Aspergillus fumigatus*. *Journal of proteome research* 9, 5517-5529.

Steffan, J.S. and McAlister-Henn, L., 1992. Isolation and characterization of the yeast gene encoding the MDH3 isozyme of malate dehydrogenase. *Journal of Biological Chemistry* 267, 24708-24715.

Suh, M.-J., Fedorova, N.D., Cagas, S.E., Hastings, S., Fleischmann, R.D., Peterson, S.N., Perlin, D.S., Nierman, W.C., Pieper, R. and Momany, M., 2012. Development stage-specific proteomic profiling uncovers small, lineage specific proteins most abundant in the *Aspergillus fumigatus* conidial proteome. *Proteome science* 10, 1-13.

Takahashi-Íñiguez, T., Aburto-Rodríguez, N., Vilchis-González, A.L. and Flores, M.E., 2016. Function, kinetic properties, crystallization, and regulation of microbial malate dehydrogenase. *Journal of Zhejiang University*-SCIENCE B 17, 247-261.

Tekaia, F. and Latgé, J.-P., 2005. *Aspergillus fumigatus*: saprophyte or pathogen? *Current opinion in microbiology* 8, 385-392.

Teutschbein, J., Albrecht, D., Pötsch, M., Guthke, R., Aimanianda, V., Clavaud, C., Latgé, J.-P., Brakhage, A.A. and Kniemeyer, O., 2010. Proteome profiling and functional classification of intracellular proteins from conidia of the human-pathogenic mold *Aspergillus fumigatus*. *Journal of proteome research* 9, 3427-3442.

Tilburn, J., Sarkar, S., Widdick, D., Espeso, E., Orejas, M., Mungroo, J., Penalva, M. and Arst Jr, H., 1995. The *Aspergillus* PacC zinc finger transcription factor mediates regulation of both acid-and alkaline-expressed genes by ambient pH. *The EMBO Journal* 14, 779-790.

Tyagi, R., Lee, Y.T., Guddat, L.W. and Duggleby, R.G., 2005. Probing the mechanism of the bifunctional enzyme ketol-acid reductoisomerase by site-directed mutagenesis of the active site. *FEBS* J 272, 593-602.

Vödisch, M., Albrecht, D., Leßing, F., Schmidt, A.D., Winkler, R., Guthke, R., Brakhage, A.A. and Kniemeyer, O., 2009. Two-dimensional proteome reference maps for the human pathogenic filamentous fungus *Aspergillus fumigatus*. *Proteomics* 9, 1407-1415.

Warris, A., 2014. The biology of pulmonary *Aspergillus* infections. Journal of Infection 69, S36-S41.

Wilkinson, B. and Gilbert, H.F., 2004. Protein disulphide isomerase. Biochimica et Biophysica Acta (BBA)-*Proteins and Proteomics* 1699, 35-44.

Yu, H.-H., Yang, Y.-H. and Chiang, B.-L., 2021. Chronic granulomatous disease: a comprehensive review. *Clinical reviews in allergy & immunology* 61, 101-113.

4 Discussion

The opportunistic human-pathogenic fungus *A. fumigatus* is a specialist in versatility and can adapt to a variety of environmental and stress conditions. As a major cause of mycotic infections, it can cause severe and often fatal conditions like invasive pulmonary aspergillosis. To successfully establish infection in immunocompromised patients, the fungus must overwhelm the remaining innate immune system and cope with other challenges like oxygen-limitation and low iron conditions. In general, to survive and thrive in different habitats and often-hostile environments the fungus relies on its versatile metabolism, enabling it to adapt quickly and specifically to the encountered conditions. One part of these adaptations is the biosynthesis of a vast arsenal of secondary metabolites, which are for example involved in the accumulation of scarce nutrients like iron, the evasion of predators or the inhibition of both predators and competitors. Another part is the ability to keep up a balanced cellular state, including redox or iron homeostasis even under challenging conditions (Bignell et al., 2016; Misslinger et al., 2021). To expand our knowledge about *A. fumigatus'* adaptive metabolism and the mechanism of its pathogenicity can pave the way to quicker diagnosis and thus, allow the application of proper treatment in time. Another major aim is to identify new targets for antifungal therapy.

There are numerous chemical mediators in the interaction of host and pathogen, but their impact on the physiology of *A. fumigatus*, especially in host environments, remains blurry. Several of them may also play decisive roles in fungal interaction with predators. I have reviewed this topic in Manuscript 3. One of the factors known to influence the biosynthesis of secondary metabolites is the histone acetyltransferase GcnE, which we found to have a dual function, regulating the glutamine synthetase by direct interaction. My further experimental work mainly focussed on the impact of ROS-mediated stresses on the *A. fumigatus* metabolism. By analysing changes in the transcriptome (Manuscript 2) and to a lesser extend the proteome (Manuscript 5) under oxidative stress conditions in the context of a knock-out mutant of the peroxiredoxin Asp f3, we aimed to gain a deeper understanding of the associated mechanisms driving ROS resistance. Further, we examined the role of Asp f3 in the context of iron deficiency (Manuscript 4). We also had a closer look at the protein oxidation pattern of *A. fumigatus* in the background of Δ*asp f3*. We found a strong oxidation of the protein disulphide isomerase A (PdiA), and its *in-vivo*-function was further investigated by constructing a deletion mutant of the respective gene (Manuscript 5).

4.1 The role of ROS and Asp f3 in the redox homeostasis of *A. fumigatus*

Molecular oxygen is essential for many organisms but its intermediates are highly reactive and can lead to severe cell damage when oxidizing cellular macromolecules like DNA, lipids ore proteins, which in turn might be followed by apoptosis and cell death. To avoid the toxic effects of ROS, organisms have developed elaborate mechanisms to exploit the advantages of oxygen and protect against its dangers at the same time. Thus, most organisms possess several and sometimes redundant protective mechanism for the detoxification of reactive oxygen species and even have learned to use ROS as signalling molecules to mediate cellular processes (Mittler et al., 2011). Some ROS detoxification mechanisms are always active to balance locally produced ROS, which for example originate in the mitochondria, while other systems are only engaged when higher ROS levels are sensed. A recent work by Shlezinger et al. (2017) showed an entirely new role for ROS: They may also act as host derived signal molecules that target the fungal apoptotic pathway and thus may be indirectly involved in fungal killing. How these signals are perceived in fungal cells is yet to be resolved.

A. fumigatus has several catalases and superoxide dismutases as well as peroxidases and peroxiredoxins, which are of diverse importance in the ROS detoxification process (Aguirre *et al*., 2005). Particularly since protection against *A. fumigatus* is associated with reactive oxygen species, research in this area might provide new insights into cellular mechanisms and offer new perspectives on the development of antifungal treatment. Patients with chronic granulomatous disease (CGD) are at a high risk to develop an infection with *A. fumigatus* due to a defect in their NOX complex that impairs their aptitude to produce superoxide radicals (Yu et al., 2021).

Although ROS detoxification is important for the fungus and a gene deletion of SOD4 proved fatal, several studies have shown that neither the simultaneous loss of several superoxide dismutases (SOD1-3) nor catalases (Cat1 and Cat2) led to a complete loss of virulence in a murine model of aspergillosis. The SOD1-3 triple mutant merely exhibited increased sensitivity to being killed by alveolar macrophages of immunocompetent mice (Paris *et al*., 2003; Lambou *et al*., 2010*)*. Studies in other organisms like *C. albicans* and *Cryptococcus neoformans* also show that, although contributing to virulence, inactivation of copper- and zinc containing superoxide dismutases (Cu/Zn SOD) does not lead to a loss of pathogenicity in these organisms (Hwang et al., 2002; Cox et al., 2003). Indeed, for *C. albicans* Pradhan and colleagues (2017)

could even show that whilst an overexpression of catalases does provide higher protection against oxidative stress it leads to a reduction in fitness when stress is absent, due to an increased demand in iron, thus highlighting the intricate balance of this cost-benefit-ratio.

As for peroxiredoxins, these thioredoxin-dependent peroxidases are a ubiquitous and highly diverse group of enzymes, which were not only shown to be essential to virulence in different pathogens, but often exhibit pleiotropic functions like phospholipase or chaperone holdase activity in addition to their peroxidase activity. In addition, they are proposed to be associated with the regulation of H_2O_2 signalling (Jang et al., 2004; Watanabe et al., 2014; Toledano and Huang, 2016; Rocha et al., 2018). Contrary to the dismutating enzymes like Sods and Cats, peroxiredoxins rely finally on NAD(P)H, and thus, the reductive machinery of the cell. The high functional and structural diversity featured by Prx isoforms of different organisms predestines them as potential targets for novel and custom antibiotics as well as targets for the development of diagnostic tests and vaccines (Gretes et al., 2012; Perkins et al., 2014; Perkins et al., 2015; de Oliveira et al., 2021). In *Candida glabrata*, both Tsa1 and Tsa2 (both AhpC-Prx1 subfamily) are required for survival in neutrophils, but although they share high similarity they show differences in regulation and do not compensate for each other if either enzyme is lost (Gutierrez-Escobedo et al., 2020). In contrast, Tsa1p of *C. albican*s, although crucial for oxidative stress resistance, is not involved in virulence (Urban et al., 2005). The diverse role of peroxiredoxins in inflammation, cancer, aging, protein quality control, ROS signalling and pathogenicity left them among the most intensely studied protein classes of recent years (Wood et al., 2003; Toledano and Huang, 2016).

A. fumigatus comprises six peroxiredoxins of which Asp f3 was found to be the only one to play a key role in virulence (Hillmann et al., 2016; Rocha et al., 2018). Further, Asp f3 shows a strong affinity to serum immunoglobulin (Ig)E and was proposed as a possible target for vaccine development. First tests in mice were successful und could protect against invasive aspergillosis (Asif et al., 2006; Ito et al., 2006; Diaz-Arevalo et al., 2011). This thesis aimed to elucidate the function of Asp f3 in this infection-biological context.

4.1.1 ROS induced transcriptional shift upon loss of Asp f3 implies a function as a redox sensor

A loss of Asp f3 is not only concomitant with a loss of virulence in a murine model of pulmonary aspergillosis but as we could show, also causes a strong transcriptional shift after encountering

ROS stress, solidifying the evidence that the function of Asp f3 encompasses more than simple ROS detoxification (Hillmann et al., 2016). Under standard cultivation conditions, the wild type and Δ*asp f3* strain showed hardly any differences in their transcriptome and Asp f3 is expandable during the absence of ROS. Yet, exposure to ROS stress leads to a significant shift in the transcriptomic stress response and hypersensitivity to ROS in Δ*asp f3*. Although Asp f3 is not redundant for the ROS detoxification process, higher expression levels of other available detoxification mechanisms like catalases would be expected to compensate for the absence of Asp f3, which is not the case. Instead, induction of the oxidative stress response is impaired, which can at least partly be attributed to a lack of Yap1 activation (Boysen et al., 2021).

Due to their high abundance and very high reactivity with H_2O_2, which exceeds the reactivity of other redox-regulated proteins by several orders of magnitude, peroxiredoxins have repeatedly been proposed to be the most likely group of thiol peroxidases to be involved in redox signalling. This function is mostly based on their protein thiols and their ability to switch between a reduced thiol and an oxidized disulphide state (Stocker et al., 2018; Ulrich and Jakob, 2019). Since the description of the Orp1-Yap1 redox relay, several examples have been described to serve a corresponding purpose, including a number of recently described 2-Cys peroxiredoxins from mammalian cells like Prx1 and Prx2. They facilitate the transmission of the oxidative signal to the apoptosis signalling kinase 1 (ASK1) and the transcription factor STAT3, respectively (Jarvis et al., 2012; Sobotta et al., 2015). A similar function might be performed by Asp f3, which is also a 2-Cys peroxiredoxin and likely to act in a similar manner.

It is likely that Asp f3 acts as the major or only sensor in this relay. Of the six genes comprising putative peroxiredoxin-like domains, three of them atypical 2-Cys Prx, including Asp f3, and three 1-Cys Prx of the Prx6 subfamily and not all of them have as of yet been characterized in detail (Hemmann et al., 1999; Hillmann et al., 2016; Rocha et al., 2018). While Prx1 and PrxC were shown to be regulated by Afyap1 and efficiently reduce H_2O_2, only Prx1 was required for full virulence. Although they are assumed to play a major role in H_2O_2 metabolism due to their abundance and reactivity, loss of neither Prx1, PrxB or PrxC led to as sensitive a phenotype as loss of Asp f3 (Hillmann et al., 2016; Rocha et al., 2018). Structurally Asp f3 strongly resembles peroxiredoxin Ahp1 of *S. cerevisiae* (both Prx5 subfamily), a thioredoxin-dependent peroxidase with a substrate specificity for alkyl hydroperoxides, which was shown to physically interact with thioredoxin (Vignols et al., 2005; Hillmann et al., 2016). Together with

thioredoxin (Trx2) and the thioredoxin reductase (Trr1) Ahp1 function is contingent on regulation by global regulators Yap1 and Skn7 (Lee et al., 1999b). Incidentally, activation of Yap1 in yeast is dependent upon the function of glutathione peroxidase (GPx)-like enzyme Gpx3 (Orp1), which acts as both sensor and transducer of the oxidative stress signal triggered by hydrogen peroxide. This interaction is an early eukaryotic example for a thiol-peroxidase-based thiol oxidation cascade or redox relay, which consists of a H_2O_2 based protein thiol oxidation and subsequent transfer of the oxidative equivalents to a specific target protein *via* a thiol oxidation cascade also referred to as redox relay (Delaunay et al., 2002; Stocker et al., 2018; Ulrich and Jakob, 2019). Delaunay and colleagues could show that the transfer of the oxidative equivalent from Orp1 to the transcription factor Yap1 occurs by physical interaction of the two proteins and the formation of an intermolecular disulphide. H_2O_2 directly oxidizes Orp1 Cys36 to form sulfenic acid Cys36-SOH, which in turn reacts with Yap1 Cys598. This transient intermolecular disulphide is resolved by the transposition from Orp1 Cys36 to Yap1 Cys303 in favour of forming an intramolecular disulphide and Orp1 is released. The resulting conformational change of Yap1 masks its nuclear export signal and allows retention and accumulation in the nucleus to induce the expression of the oxidative stress response (Delaunay et al., 2000; Delaunay et al., 2002).

4.1.2 ROS dependent activation of Afyap1 target genes requires Asp f3

While the Yap1 system is well conserved in yeast-fungi, filamentous fungi are far more complex and while some domains of Yap1 are highly conserved, the overall structure, number of cysteines and thus, their function might differ accordingly (Mendoza-Martinez et al., 2020). Especially the impact on virulence was shown to differ between species. While loss of respective Yap1 orthologues in *Ustilago maydis* and *Magnaporthe oryzae* lead to a loss or reduction of pathogenicity, respectively, virulence in other filamentous fungi like *Fusarium graminearum*, or *B. cinerea* is not affected by the loss (Molina and Kahmann, 2007; Temme and Tudzynski, 2009; Guo et al., 2011; Montibus et al., 2013).

For *A. fumigatus* loss of Afyap1 leads to a hypersensitivity against H_2O_2 and menadione, albeit it does not affect virulence ((Lessing et al., 2007; Qiao et al., 2008). Thus, the Δ*asp f3* phenotype with its ROS hypersensitivity and loss of virulence is far more severe. Nevertheless, insufficient function of Afyap1 might contribute to the Δ*asp f3* phenotype as our transcriptome data showed several Afyap1 target genes failing to be upregulated upon

treatment with ROS. This effect can be attributed to Afyap1 being unable to translocate to and accumulate in the nucleus after challenge with H_2O_2, indicating a missing link in the redox relay system. Though it is yet unclear whether Asp f3 is directly involved in this signalling cascade, its status as 2-Cys peroxiredoxin certainly harbours the potential to function in a capacity equalling Orp1 function in *S. cerevisiae* as described earlier. Additionally, transcription of the Orp1-orthologue Gpx3 also failed to be upregulated in Δ*asp f3* upon challenge with ROS and lower levels might delay Afyap1 activation, assuming a similar involvement in the Afyap1 related redox relay as found in yeast (Delaunay et al., 2002; Boysen et al., 2021). Yet it should be taken into account that neither Gpx3 orthologue GpxA nor peroxiredoxins TpxA and TpxB are involved in the activation of Yap1 ortholog NapA in *Aspergillus nidulans*. Instead, Asp f3 orthologue PrxA was implicated to regulate NapA (Mendoza-Martinez et al., 2017; Mendoza-Martinez et al., 2020).

The loss of *asp f3* leading to a more severe phenotype than loss of *afyap1* and overexpression of Afyap1 failing to compensate for the loss of Δ*asp f3* suggests a more complex regulatory network or at least a broader range of Asp f3 function. Thus, the strong repercussions of ROS-related stress in Δ*asp f3* are due to additional cellular effects, which might be related to iron availability. Iron plays an important role during pathogenicity and its importance is highlighted during oxidative stress. For example, in form of iron containing heme groups, iron is an important co-factor of catalases, which are responsible for the decomposition of H_2O_2. Recently, iron availability was proposed to be compromised during oxidative stress, which might signify the importance of iron-independent detoxification mechanisms like peroxiredoxins, including Asp f3, in this situation (Kurucz et al., 2018).

4.2 Asp f3 is essential during germination in iron limited environments

As an essential micronutrient, iron is involved in many aspects of life. Numerous biological processes, like respiration or oxygen transport, exploit its ability to be readily oxidized or reduced. It contributes to both structure and function of enzymes and is an important part of many prosthetic groups like heme or iron sulphur-clusters, and thus in high demand (Tuppy and Kreil, 2004; Johnson et al., 2005). But then again, while iron is essential and beneficial, cellular levels have to be tightly regulated to avoid its toxic effects. High concentration of iron facilitate the generation of reactive oxygen species, for example *via* the Fenton reaction, which can cause severe cellular damage in form of DNA damage, lipid peroxidation or

reversible and irreversible protein modifications. Thus, acquisition, storage and utilization of iron are regulated by sophisticated mechanisms (Halliwell and Gutteridge, 1985; Sies, 1986; Nevitt, 2011). During an infection, iron plays a key role in the tug of war between the pathogen and the host immune system. On one hand, the host itself needs iron to support its cellular function, including the function of immune cells. On the other hand, the host tries to limit its bioavailability and deny the pathogen access to iron (and other trace elements) in a concept coined “nutritional immunity”. Pathogens need iron for their iron-dependent antioxidant enzymes like catalases (Cat1/Cat2) or cytochrome c peroxidase (Ccp1) to contribute to the protection against ROS launched by the immune system as a defence mechanism. To overcome this barrier of “nutritional immunity” pathogens have developed multiple strategies, for example the production of siderophores, and the ability to acquire iron is a crucial virulence factor described for several (fungal) pathogens (Nevitt, 2011; Warris and Ballou, 2019; Nairz and Weiss, 2020). In *A. fumigatus*, siderophore facilitated iron scavenging is crucial for virulence and the ability to grow in human serum. Deletion of *sidA* aborts siderophore production and the mutant is no longer able to grow in human serum and was shown to be nonvirulent in a murine mouse model of IA, highlighting the importance for virulence (Hissen et al., 2004; Schrettl et al., 2004; Hissen et al., 2005).

4.2.1 Loss of Asp f3 and its homologue Af3l1 cause sensitivity to iron limitation but do not influence iron homeostasis

As an abundant protein, peroxiredoxin Asp f3 was shown to be essential for virulence, but the exact mechanism remains elusive. As discussed above we could show a transcriptional shift and a lack of Afyap1 activation, though these effects do not seem to fully explain the extent of the Δ*asp f3* phenotype. Additionally, a newly established assay for granulocyte killing activity revealed that Δ*asp f3*$_{tetOn}$ is as likely to be killed by human granulocytes as the wild type, although the mutant is considerably more sensitive to hydrogen peroxide. Thus, loss of virulence is not attributable to higher rates of granulocyte-induced killing (Ruf et al., 2018; Brantl et al., 2021). Instead, Δ*asp f3*/Δ*asp f3*$_{tetOn}$ was found to be sensitive to low-iron conditions and show a growth defect, which could be rescued by supplementing the medium with iron. The sensitivity to iron is enhanced by additional deletion of the Asp f3 homologue Af3l1 but not Af3l2 in the Δ*asp f3*$_{tetOn}$ background. This difference is most likely due to Af3l2 putatively being located in the mitochondria rather than the cytoplasm or co-localizing with peroxisomes as was shown for Asp f3 (Hillmann et al., 2016).

Although sensitivity to low iron conditions established a connection between Asp f3, iron and possibly virulence, the mechanism remains elusive. Since loss of siderophore biosynthesis (Δ*sidA*) has also been associated with loss of virulence, Δ*asp f3*$_{tetOn}$ and Δ*asp f3*$_{tetOn}$ Δ*af3l1* were analysed for siderophore production (Hissen et al., 2004; Schrettl et al., 2004; Hissen et al., 2005). Siderophore levels were not affected though, implying that neither their biosynthesis nor SreA-function, which is involved in the regulation of siderophore biosynthesis, is affected by the loss of Asp f3 or both Asp f3 and Af3l1. Furthermore, disruption of the iron regulatory network by deletion of SreA, the major repressor of iron acquisition, led to partial recuperation of the Δ*asp f3*$_{tetOn}$ Δ*af3l1* mutant phenotype in low iron conditions while the wild type did not profit from the deletion in the same manner.

Interestingly, although Δ*asp f3*$_{tetOn}$ and Δ*asp f3*$_{tetOn}$ Δ*af3l1* do not grow in low iron conditions, the conidial transcriptome does not exhibit an "iron starvation signature" as described for example in siderophore deficient mutants. The "iron starvation signature" is defined by the repression of both iron consuming pathways and the expression of iron-dependent enzymes like catalases, while mechanisms to scavenge and enhance the uptake of iron are upregulated. This includes the upregulation of the siderophore biosynthesis as well as siderophore transporters MirB, Sit1 and Sit2 or iron permease FtrA (Raymond-Bouchard et al., 2012; Haas, 2014; Park et al., 2016). In the Δ*asp f3*$_{tetOn}$ and Δ*asp f3*$_{tetOn}$ Δ*af3l1* strain, none of the analysed enzymes showed enhanced transcript levels (Wallner et al., 2009). Instead, expression of *asp f3* itself was shown to be subject to iron availability, probably in a HapX-dependent manner, and transcript levels changed after a shift from iron starvation to iron sufficiency in a short-term adaptation response. Together these results show that while Asp f3 does not regulate iron homeostasis, it is instead subject to iron dependent regulation, thus corroborating a connection of peroxiredoxins and iron homeostasis.

4.2.2 Iron supplementation fully restores virulence to Δ*asp f3* mutants

The combination of nutritional immunity by sequestering iron and exposure to oxidative stress is an often-employed strategy of host organisms to prevent infections. Kurucz and colleagues (2018) could show that the transcriptional adaptation to singular ROS and iron starvation stress and combined stress of both factors is highly specific and no simple addition of both responses. Instead, the system can change dynamically in answer to the combined stress factors. The same can be expected during virulence, when the fungus must not only adapt to

several stresses simultaneously, like low levels of both oxygen and nutrients, including micronutrients like iron, which must be scavenged from the host, but moreover must successfully prevail against attacks of the hosts immune system (Paulussen et al., 2017). Iron availability is one of the key factors for *A. fumigatus* virulence. As we could show Δ*asp f3* is unable to cope with low-iron conditions, it was thus standing to reason that the mutants' avirulence in a mouse model of pulmonary aspergillosis is attributable to the low iron conditions prevalent in the host environment. Also, under repressed conditions Δ*asp f3*$_{tetOn}$ and Δ*asp f3*$_{tetOn}$ Δ*af3l1* were strongly inhibited when confronted with lactoferrin, a mammalian protein with multifunction enzyme activity, which also facilitates the sequestration of iron in several body fluids (Travis et al., 1999; Singh et al., 2002). *In vitro* supplementation of excess iron fully restored the growth to wild type levels and indeed, the same effect could be shown *in vivo* in a murine infection model. Here, supplementation of excess iron restored full virulence of the Δ*asp f3* mutant strain of *A. fumigatus* highlighting the importance of iron for virulence.

4.2.3 Asp f3 devoid cells may have higher demand for iron

Our results conclusively link Asp f3 and its homologue Af3l1 to a possible new function of peroxiredoxins in iron homeostasis. Although such a connection was not yet shown in other fungal pathogens, even so several homologues of Asp f3 have been analysed in related filamentous fungi like *A. nidulans* (AnPrxA) and yeasts like *S. cerevisiae* (ScAhp1) or *C. albicans* (CaAhp1) (Lee et al., 1999b; Hillmann et al., 2016; Truong et al., 2016; Xia et al., 2018). They further suggest that the avirulent phenotype of Δ*asp f3* is rather due to an inability to cope with low iron conditions, than either an enhanced susceptibility to ROS associated stress or innate immune cells. However, ROS sensitivity might still play a role in that it is additionally enhanced under iron limited conditions. Furthermore, laboratory conditions do not completely equal *in vivo* conditions and might thus miss relevant factors. Nevertheless, based on our results we propose a new possible role for peroxiredoxins in iron homeostasis, which should receive further attention in the future.

The mechanism by which Asp f3 and iron homeostasis are connected is not yet unravelled. For *S. cerevisiae* it was recently shown that starvation leads to the production of reactive oxygen species as well as to the secretion of ScAhp1. The authors propose that the secreted antioxidant enzymes prolong cell survival until they can start growing again when more

favourable conditions arise (Cruz-Garcia et al., 2020). Like Asp f3, its homologue ScAhp1 is generally located intracellular and its secretion is thus unusual, especially considering the lack of a secretion signal. However, there is evidence that Asp f3 is also secreted, which should not come as a surprise giving Asp f3s early identification as a fungal allergen, making it likely to also be found outside of the cells (Singh et al., 2010; Diaz-Arevalo et al., 2011; Souza et al., 2019). Like the starving yeast cells, death is not directly imminent for Δ*asp f3*$_{tetOn}$ and Δ*asp f3*$_{tetOn}$ Δ*af3l1* under low iron conditions, but they are instead viable for several days and will kick-start growth as soon as conditions change for the better (in this case by addition of iron).

I hypothesize that Δ*asp f3* might have a higher basal requirement for iron as the *A. fumigatus* wild type, because the mutant must compensate for the loss of this abundant and efficient detoxification mechanism. In contrast to Asp f3, alternative ROS detoxification mechanisms like SODs or Cats rely heavily on metal co-factors like iron, copper or manganese and are not functional without them. With Asp f3 present, the wild type is able to cope better with the low iron stress, for Asp f3 can compensate for the iron-dependent antioxidants like cytochrome c peroxidase Ccp1 or the mycelial catalase Cat1 and catalase-peroxidase Cat2, which are downregulated during iron starvation (Figure 8). This theory also fits together with the fact that, dependent on iron availability, *cat1* and *asp f3* transcription are inversely regulated (Schrettl et al., 2008; Schrettl et al., 2010; Kurucz et al., 2018).

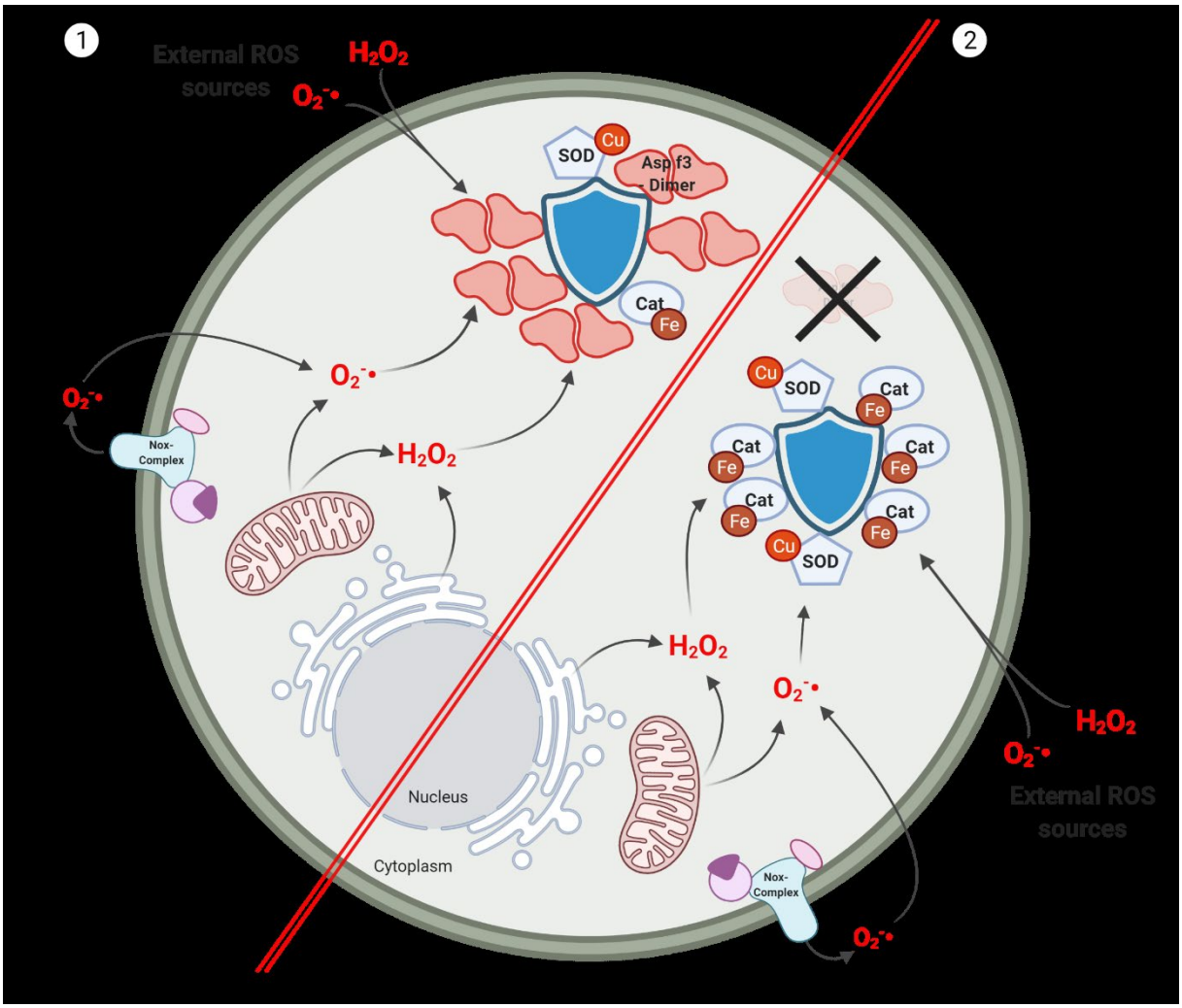

Figure 8 Absence of peroxiredoxin Asp f3 leads to increased basal requirement of iron in *A. fumigatus*. 1 The fungus must detoxify reactive oxygen species (ROS) of endogenous and external origin. Peroxiredoxin Asp f3 is an abundant protein supporting this purpose and functions independent of metal-, especially iron-, cofactors. **2** In the absence of Asp f3, the fungus must compensate its function with other proteins of the ROS detoxification machinery. Contrary to Asp f3, many of these proteins rely on iron/heme-cofactors for function, thus heightening the basal requirement for these cofactors (created with biorender.com).

4.3 Asp f3 protects from protein oxidation of major metabolic enzymes

In an early approach to elucidate potential targets of oxidative damage in the background of the Asp f3 deletion mutant, we took a proteomics approach. With a 2D-gel electrophoresis we were able to show the protein oxidation level in both the wild type and after treatment with xanthine oxidase to generate Superoxide *in vivo*. Total oxidation levels were raised in Δ*asp f3* compared to the wild type and several proteins with a distinctly stronger oxidation signal were identified and considered as potential primary protein targets of oxidative damage.

Of the identified proteins Pep2, a vacuolar proteinase, was presumed not to be involved in redox sensitivity since deletion of its homologue vacuolar proteinase K in *S. cerevisiae* did not show an obvious phenotype (Reichard et al., 1990). Two of the oxidized target genes were the malate dehydrogenase (MDH) and the ketol-acid reductoisomerase (KARI), both of which offer accessible activity assay to study their activity. As part of the citric acid cycle MDH is an important member of basic cellular processes (Goward and Nicholls, 1994). However, enzymatic activity was not impaired by protein oxidation in the enzymatic assay we performed. KARI is suitable protein target and its inactivation might potentially have severe effects as consequences of deletion of KARI homologues in other fungi like plant-pathogenic *F. graminearum* and insect-pathogenic *Metarhizium robertsii* include defects in growth and conidiation as well as virulence (Liu et al., 2014; Luo et al., 2020). As the second enzyme in the branched chain amino acid (BCAA) biosynthetic pathway KARI plays a major role in the biosynthesis of valine, leucine and isoleucine. As BCAAs are only produces in bacteria, fungi and higher plants, but not in mammals, they are a promising target for the development of new antibiotic as well as herbicidal treatment options (Wong et al., 2012; Amorim Franco and Blanchard, 2017). However, we have not found a decrease in KARI activity in our results. The most promising target at first glance is the protein disulphide isomerase (PDI) A, which we found to be strongly oxidized. Protein disulphide isomerases are enzymes that facilitate the formation of disulphide bonds as part of the protein folding machinery as well as during the unfolded protein response. Their function is diverse and reaches from thiol oxidation, reduction and isomerization of their substrate proteins to chaperone activities. Furthermore PDIs are involved in ER redox homeostasis where they are connected in a redox cycle with ER oxireductin Ero1 (Moretti and Laurindo, 2017). Here we studied the deletion of the *A. fumigatus* PdiA, which, in comparison to its homologue Pdi1 in *S. cerevisiae*, was no lethal. Despite a general impairment in growth and sporulation, Δ*pdiA* was surprisingly viable and even coped sufficiently well with several stress factors. Merely low temperatures strongly enhanced the growth defect. For human pathogenic *C. neoformans* is was shown that ER stress is involved in the adaptation to different temperatures (Glazier and Panepinto, 2014). A similar mechanism might be employed in *A. fumigatus*. In addition, different temperatures might affect the folding dynamics while protein content will change in adaptation to different temperatures, thus heightening the need for folding assistance. The general viability of Δ*pdiA* indicates the presence of other PDIs, which are able to take over at least some PdiA-functions.

Although PdiA is an important enzyme and its deletion presents a phenotype, it is unlikely to be involved in the redox sensitive phenotype of Δ*asp f3*. Neither does Δ*pdiA* show specific sensitivity to oxidative stress, nor does protein oxidation destroy PdiAs function, but rather increases the need for redox equivalents to continue PdiAs redox cycle to fold proteins and control their structural integrity and enzymatic activity.

4.4 Regulation of secondary metabolism in answer to environmental stimuli

Secondary metabolites can gain an environmental advantage for their producers, nevertheless, their biosynthesis is tightly regulated to save resources and only produce those metabolites needed at every specific time. Control is exerted on different levels from pathway-specific transcription factors, which are often part of the SM gene clusters themselves, to global regulators, which mediate a broader transcriptional response (Brakhage, 2013). The function of global regulators is based on environmental cues and initiates or prevents the biosynthesis of secondary metabolites in adaptation to specific conditions. Examples for this kind of regulators are the pH regulator PacC or the nitrogen dependent regulator AreA, which control a whole set of genes (Caddick et al., 1994; Tilburn et al., 1995). While these regulators directly affect gene transcription, there is also a higher regulatory level – the modulation of the chromatin structure, which also allows for global regulation.

4.4.1 Histone Acetyltransferase GcnE physically interacts with non-histone target proteins

Histone acetyltransferases (HATs) and histone deacetylases (HDACs), which are responsible for the attachment and removal of acetyl-groups to and from histones, respectively, play a significant role for changes in chromatin architecture. In general, acetylation is associated with euchromatin formation while deacetylation promotes heterochromatin formation and thus gene silencing. However, there are exceptions in which deacetylation led to the up regulation or activation of gene transcription (Brosch et al., 2008; Studt et al., 2013). In fungi histone acetylation and deacetylation has proven essential for the transcriptional regulation of secondary metabolism. As all genes involved in the biosynthesis of a specific secondary metabolite are generally organized in a cluster of adjacent genes, often localized in the subtelomeric region of chromosomes, they can easily be regulated together by changes in chromatin status. This was shown first for the aflatoxin gene cluster in *Aspergillus parasiticus*

(Perrin et al., 2007; Roze et al., 2007; Cichewicz, 2010; Nützmann et al., 2011; Soukup et al., 2012).

In *A. fumigatus* histone acetyltransferase GcnE is a key regulator of chromatin structure and involved in the regulation of secondary metabolism (Nützmann et al., 2013; Wang et al., 2018). Although histones are the most common targets of acetylation by HATs like GcnE, some are also able to acetylate other protein targets like transcriptional activators or structural proteins such as tubulin and are involved in different physiological processes like signal transduction or the regulation of enzymatic activity (Roth et al., 2001; Choudhary et al., 2014). GcnE for example is involved in the cell cycle by acetylation of cell-division cycle (CDC)-protein 6 in human HeLa cells (Paolinelli et al., 2009).

In manuscript Nr. 1 by Nossmann et al. (2018) we showed that GcnE does not only function by the acetylation of histones in *A. fumigatus*, but also physically interacts with other target genes like GbpA and glutamine synthetase GlnA, which was first shown in a yeast-2-hybrid approach and confirmed with bimolecular fluorescence complementation (BiFC). BiFC is a method in which a yellow fluorescent protein (YFP) is split and each half is attached to one of the two putative protein interaction partners. Their close proximity during physical interaction of the two proteins will allow reconstitution of both YFP-halves to a functional conformation, as was successfully shown in other filamentous fungi like *Neurospora crassa* and *A. nidulans* and *A. fumigatus* itself (Thön et al., 2010; Kollath-Leiss et al., 2014; Jöhnk et al., 2016). The resulting fluorescent signal does not only prove interaction of the target genes, but further allows to identify the cellular compartment in which this interaction occurs. In *C. neoformans* and *Fusarium fujikuroi* GcnE localizes to the nucleus almost exclusively, while it was shown to translocate between the cytoplasm and the nucleus in other fungi like *C. albicans* and *S. cerevisiae, which* might impact its mode of action in different species (O'Meara et al., 2010; Dastidar et al., 2012; Chang et al., 2015; Rösler et al., 2016). For *A. fumigatus* GcnE localization was observed in the cytoplasm for both the positive control and during interaction with both interaction partners, GbpA and GlnA, and for GbpA additionally in the nuclei, during BIFC (Nossmann et al., 2019). Our results indicate that interaction of GcnE and GbpA presumably impacts conidiation. Loss of *gcnE* as well as overexpression of *gbpA* both led to impaired conidiation and the GbpA acetylation pattern in Δ*gcnE* resembled the wild type. Thus, our

results imply that rather than GcnE regulating GbpA by acetylation, GbpA functions as a repressor for GcnE during physical interaction.

4.4.2 Histone Acetyltransferase GcnE controls the activity of glutamine synthetase GlnA by direct interaction

Secondary metabolite production often responds to environmental cues, including the availability and quality of nitrogen sources. For example 30 of 47 SM gene clusters of the filamentous fungi *Fusarium fujikuroi* depend on nitrogen availability (Wiemann et al., 2013; Tudzynski, 2014). Glutamine synthetase GlnA plays a major role in the nitrate assimilation as it is responsible for the final step - the condensation of glutamate and ammonia to glutamine in an ATP-dependent fashion (Liaw et al., 1995). Further, involvement of GlnA in nitrogen metabolite repression was shown for *N. crassa* and *F. fujikuroi* and a role in sensing of glutamine and ammonia was implicated for the latter (Dunn-Coleman and Garrett, 1980; Teichert et al., 2004; Wagner et al., 2013; Pfannmüller et al., 2017). Like in *F. fujikuroi*, *A. fumigatus* Δ*GlnA* leads to glutamine auxotrophy as the fungi are no longer able to metabolize other nitrogen sources, which highlights the importance of this protein (Teichert et al., 2004; Nossmann et al., 2019). Regulation of the glutamine synthetase in the actinomycete *Saccharopolyspora erythraea* was shown to depend on a reversible acetylation, its presence led to GlnA-repression. Acetylation was facilitated by a GcnE-like protein (You et al., 2016). Likewise, human glutamine synthetase was shown to carry acetylation when represses by high glutamine concentrations, which are transferred by a GcnE-like acetyl transferase(Van Nguyen et al., 2016). Since lysine acetylation was repeatedly shown to control enzyme activity we initially assumed that GlnA activity in *A. fumigatus* would also be controlled by lysine acetylation. However, GlnA activity increased in the absence of GcnE while showing no change in lysine acetylation compared to the wild type. Thus, regulation of GlnA by GcnE seems to rely on physical interaction rather than acetylation by GcnE.

4.4.3 GcnE – a connecting link between primary and secondary metabolism

Enzymes involved in chromatin remodelling are of major importance for the regulation of cellular processes from development and determination of cell fate to control of secondary metabolism. Especially in filamentous fungi, transcriptional regulation of SM gene clusters is often associated with environmental conditions and histone modulation (Nützmann et al., 2011; Brakhage, 2013; Nützmann et al., 2013). As part of the SAGA-complex histone

acetyltransferase GcnE fulfils important regulatory functions by acetylating histones, often influencing SM biosynthesis in the process. However, HATs, including GcnE homologues, were also shown to acetylate lysine residues on non-histone target proteins. Here we demonstrate that GcnE is involved in the regulation of the primary metabolism independent of lysine acetylation but instead through direct interaction with glutamine synthetase GlnA. We thus propose GcnE as a mediator between primary and secondary metabolism.

5 Conclusion

Albeit generally living a saprophytic lifestyle *A. fumigatus* is a successful opportunistic human-pathogenic. As a specialist in versatility it can efficiently counteract stress and adapt to and even thrive in a variety of environmental conditions. Being a major cause of mycotic infections, especially in immunocompromised patients, it can cause severe and often fatal conditions like invasive aspergillosis. A more sophisticated knowledge about the fungus is the basis to choose suitable targets for diagnosis and therapeutic treatments. To successfully establish infection, *A. fumigatus* has to overcome the residual immune system and adapt to challenges like oxygen- and iron limitation. This thesis mainly focused on the impact of ROS-mediated stresses on the *A. fumigatus* metabolism using an *asp f3* deletion strain that is highly sensitive to ROS and avirulent in a murine infection model.

I could show that Asp f3 is dispensable during non-stress conditions, which is reflected in the nearly identical transcriptomes of the wild type and Δ*asp f3* strain. However, *in vivo* treatment with superoxide causes a significant shift between the transcriptomes of those strains. Conspicuously, Δ*asp f3* fails to upregulate a large subset of genes typically upregulated in the wild type upon challenge with oxidative stress. Amongst those genes we identified target genes subjected to the regulation of Afyap1, an activator of the oxidative stress response. We show that absence of Asp f3 prevents the accumulation of Afyap1 in the nucleus, which thus cannot activate transcription of target genes like catalase 2. Furthermore, a collaborative work revealed that in addition to ROS sensitivity, Δ*asp f3* is strongly affected by iron limitation. Indeed, both ROS sensitivity and dependence on iron are closely connected as many ROS detoxification mechanisms rely on metal-, and especially iron-, cofactors for their catalytic activity. While Asp f3 is an iron independent peroxiredoxin, its loss might force the fungus to rely on alternative, and thus more iron consuming, mechanisms. The effect is of such magnitude that a replete supply with iron is able to restore full virulence of Δ*asp f3* in a murine model of invasive aspergillosis. Overall, the knowledge generated by our research provides valuable new insights into the regulation of redox homeostasis and virulence in *A. fumigatus*.

6 Summary

The incidence of human fungal infections has strongly increased over the last years and *Aspergillus fumigatus* causes approximately 80 % of all cases in often fatal invasive aspergillosis. *A. fumigatus* is a ubiquitous ascomycete with a generally saprophytic lifestyle but is also known as an opportunistic human pathogen for immunocompromised individuals. Options for diagnosis and treatment are limited and decline further due to antimycotic resistances. Thus, development of better diagnostic methods as well as the discovery and development of new antifungal treatment options are urgently required.

To successfully establish an infection, the fungus must adapt its metabolism to the environment of its human host. This includes adaptation to general conditions like low oxygen or iron deficiency and protection against active innate immune defence mechanisms. The aim of this thesis was to elucidate the functional role of peroxiredoxin Asp f3 in virulence and how it is involved in sensing and detoxification of ROS-associated stress in *A. fumigatus*. Asp f3 is a two-cysteine type peroxiredoxin that was first identified as a major allergen of *A. fumigatus* and later as a virulence determinant in a murine model of pulmonary aspergillosis.

Here I show that the loss of Asp f3 leads to a shift in the transcriptome upon challenge with reactive oxygen species. Amongst the affected genes are several of putative Afyap1 target genes and the research results provided in this thesis show that Asp f3 does not only have a sensing function, which is required for the full activation of the Afyap1-dependent ROS-response pathway, but is furthermore required for the fungus survival during low iron conditions. Indeed, my research showed that, although Afyap1 fails to sufficiently accumulate in the nucleus to activate ROS-detoxification mechanisms like the production of catalases, the *asp f3*-deficient strain is no more susceptible to being killed by human granulocytes than the wild type. Instead, loss of virulence is likely linked to the fungus ability to grow under low iron conditions or loss thereof in the *asp f3* deficient strain and iron supplementation even leads to a full restoration of virulence in a murine infection model.

Overall, my work showed that the peroxiredoxin Asp f3 is a key player in the defence against *A. fumigatus* reactive oxygen species by acting as a ROS sensor and enabling the activation of Afyap1 dependent ROS detoxification. Furthermore, the role of Asp f3 during virulence could be linked to its ability to overcome the nutritional immunity imposed by the host by generating low iron conditions.

7 Zusammenfassung

Die Inzidenz von Pilzinfektionen in Menschen hat in den letzten Jahren stark zugenommen, wobei *Aspergillus fumigatus* in mehr als 80 % als Erreger einer Invasiven Aspergillose nachgewiesen wurde. Der filamentöse Pilz *A. fumigatus* gehört zur Abteilung der Schlauchpilze und ist ein ubiquitär verbreiteter Saprophyt, kann jedoch auch immunsupprimierte Individuen infizieren. Die Möglichkeiten der Diagnose und Behandlung sind auf wenige Methoden und Antimykotika beschränkt, wobei letzteres zusätzlich durch aufkommende Resistenzen erschwert wird. Während der Infektion muss sich der Pilz an die Bedingungen des menschlichen Wirts adaptieren, dazu zählt auch eine Exposition gegenüber reaktiven Sauerstoffspezies (ROS) aus Zellen des angeborenen Immunsystems. Ziel dieser Arbeit war die Aufklärung der biochemischen Funktion des Peroxiredoxins Asp f3 während der Infektion. Das Protein wurde zuerst als Allergen Asp f3 identifiziert, sowie später als ein wichtiger Faktor bei der Abwehr reaktiver Sauerstoffspezies (ROS) sowie auch als ein essentieller Virulenz-Faktor im Maus-Modell für Invasive Aspergillose beschrieben.

Meine Arbeit zeigt, dass dem Asp f3 während der transkriptionellen Antwort auf eine Behandlung mit ROS eine entscheidende Bedeutung zukommt. Unter den betroffenen Genen, die zwar im Wild Typ, nicht aber in der Δ*asp f3*-Mutante, nach ROS Exposition angeschaltet werden, waren insbesondere die Ziel Gene des Afyap1, dem zentralen Regulator der oxidativen Stress-Antwort. Meine Ergebnisse zeigen, dass Asp f3 dabei eine Sensor-Funktion übernimmt und nötig ist, um eine ausreichende Akkumulation von Afyap1 im Zellkern und die damit verbundene transkriptionelle Antwort zu ermöglichen. Obwohl in der Δ*asp f3*-Mutante Afyap1 nicht in der Lage ist wichtige ROS-detoxifizierende Mechanismen, wie beispielsweise die Produktion von Katalasen, zu initiieren, ist dies nicht der Grund für den Verlust der Virulenz. Stattdessen konnte gezeigt werden, dass Asp f3 für das Auskeimen der Konidien unter Eisen-limitierenden Bedingungen am Infektionsort von essentieller Bedeutung ist.

Insgesamt zeigt meine Arbeit, dass das Peroxiredoxin Asp f3 eine Schlüsselrolle bei der Abwehr von reaktiven Sauerstoffspezies durch *A. fumigatus* spielt, indem es als ROS-Sensor fungiert und die Aktivierung der Afyap1-abhängigen ROS-Entgiftung ermöglicht. Darüber hinaus könnte die Rolle von Asp f3 während der Virulenz mit seiner Fähigkeit verbunden sein, die vom Wirt auferlegte Ernährungsimmunität, welche dieser durch eisenarme Bedingungen erzeugt, zu überwinden.

8 Bibliography

Publications and Manuscripts in preparation contain their own list of references. Thus, references listed in publications or manuscripts in preparation will not be repeated in this bibliography, unless referred to outside of them.

Agarwal, R., Chakrabarti, A., Shah, A., Gupta, D., Meis, J., Guleria, R., Moss, R., Denning, D. and Group, A.C.A.I.W., 2013. Allergic bronchopulmonary aspergillosis: review of literature and proposal of new diagnostic and classification criteria. *Clinical & Experimental Allergy*, 43, 850-873.

Aguirre, J., Ríos-Momberg, M., Hewitt, D. and Hansberg, W., 2005. Reactive oxygen species and development in microbial eukaryotes. *Trends in microbiology*, 13, 111-118.

Aimanianda, V., Bayry, J., Bozza, S., Kniemeyer, O., Perruccio, K., Elluru, S.R., Clavaud, C., Paris, S., Brakhage, A.A. and Kaveri, S.V., 2009. Surface hydrophobin prevents immune recognition of airborne fungal spores. *Nature*, 460, 1117-1121.

Alastruey-Izquierdo, A., Cadranel, J., Flick, H., Godet, C., Hennequin, C., Hoenigl, M., Kosmidis, C., Lange, C., Munteanu, O. and Page, I., 2018. Treatment of chronic pulmonary aspergillosis: current standards and future perspectives. *Respiration*, 96, 159-170.

Ali Khan, H. and Mutus, B., 2014. Protein disulfide isomerase a multifunctional protein with multiple physiological roles. *Frontiers in chemistry*, 2, 70.

Amich, J. and Bignell, E., 2016. Amino acid biosynthetic routes as drug targets for pulmonary fungal pathogens: what is known and why do we need to know more? *Current opinion in microbiology*, 32, 151-158.

Amir, A., Meshner, S., Beatus, T. and Stavans, J., 2010. Damped oscillations in the adaptive response of the iron homeostasis network of *E. coli*. *Molecular microbiology*, 76, 428-436.

Amorim Franco, T.M. and Blanchard, J.S., 2017. Bacterial branched-chain amino acid biosynthesis: structures, mechanisms, and drugability. *Biochemistry*, 56, 5849-5865.

Ashok, B.T. and Ali, R., 1999. The aging paradox: free radical theory of aging. *Experimental gerontology*, 34, 293-303.

Asif, A.R., Oellerich, M., Amstrong, V.W., Riemenschneider, B., Monod, M. and Reichard, U., 2006. Proteome of conidial surface associated proteins of *Aspergillus fumigatus* reflecting potential vaccine candidates and allergens. *Journal of proteome research*, 5, 954-962.

Askew, D.S., 2008. *Aspergillus fumigatus*: virulence genes in a street-smart mold. *Current opinion in microbiology*, 11, 331-337.

Ayala, A., Muñoz, M.F. and Argüelles, S., 2014. Lipid peroxidation: production, metabolism, and signaling mechanisms of malondialdehyde and 4-hydroxy-2-nonenal. *Oxidative medicine and cellular longevity*, 2014.

Bain, J.M., Tavanti, A., Davidson, A.D., Jacobsen, M., Shaw, D., Gow, N. and Odds, F.C., 2007. Multilocus sequence typing of the pathogenic fungus *Aspergillus fumigatus*. *Journal of clinical microbiology*, 45, 1469-1477.

Bandres, M.V. and Sharma, S., 2020. *Aspergillus fumigatus*, *StatPearls [Internet]*. StatPearls Publishing.

Bedard, K. and Krause, K.-H., 2007. The NOX family of ROS-generating NADPH oxidases: physiology and pathophysiology. *Physiological reviews*, 87, 245-313.

Benedict, K., Jackson, B.R., Chiller, T. and Beer, K.D., 2019. Estimation of direct healthcare costs of fungal diseases in the United States. *Clinical Infectious Diseases*, 68, 1791-1797.

Bignell, E., Cairns, T.C., Throckmorton, K., Nierman, W.C. and Keller, N.P., 2016. Secondary metabolite arsenal of an opportunistic pathogenic fungus. *Philosophical Transactions of the Royal Society B: Biological Sciences*, 371.

Bignell, E.M., 2012. Conservation in *Aspergillus fumigatus* of pH-signaling seven transmembrane domain and arrestin proteins, and implications for drug discovery. *Annals of the New York Academy of Sciences*, 1273, 35-43.

Blatzer, M. and Latgé, J.-P., 2017. Metal-homeostasis in the pathobiology of the opportunistic human fungal pathogen *Aspergillus fumigatus*. *Current opinion in microbiology*, 40, 152-159.

Boysen, J.M., Saeed, N., Wolf, T., Panagiotou, G. and Hillmann, F., 2021. The Peroxiredoxin Asp f3 Acts as Redox Sensor in *Aspergillus fumigatus*. *Genes*, 12, 668.

Brakhage, A.A., 2013. Regulation of fungal secondary metabolism. *Nature Reviews Microbiology*, 11, 21-32.

Brakhage, A.A. and Langfelder, K., 2002. Menacing mold: the molecular biology of *Aspergillus fumigatus*. *Annual Reviews in Microbiology*, 56, 433-455.

Brandon, M., Howard, B., Lawrence, C. and Laubenbacher, R., 2015. Iron acquisition and oxidative stress response in *Aspergillus fumigatus*. *BMC systems biology*, 9, 19.

Brantl, V., Boysen, J.M., Yap, A., Golubtsov, E., Ruf, D., Heinekamp, T., Strassburger, M., Dichtl, K., Haas, H., Hillmann, F. and Wagener, J., 2021. Peroxiredoxin Asp f3 Is Essential for *Aspergillus fumigatus* To Overcome Iron Limitation during Infection. *mBio*, 12, e0097621.

Brosch, G., Loidl, P. and Graessle, S., 2008. Histone modifications and chromatin dynamics: a focus on filamentous fungi. *FEMS microbiology reviews*, 32, 409-439.

Brown, G.D., Denning, D.W., Gow, N.A., Levitz, S.M., Netea, M.G. and White, T.C., 2012. Hidden killers: human fungal infections. *Science translational medicine*, 4, 165rv13-165rv13.

Caddick, M.X., Peters, D. and Platt, A., 1994. Nitrogen regulation in fungi. *Antonie Van Leeuwenhoek*, 65, 169-177.

Cadet, J. and Davies, K.J., 2017. Oxidative DNA damage & repair: an introduction. *Free Radical Biology and Medicine*, 107, 2-12.

Cagas, S.E., Jain, M.R., Li, H. and Perlin, D.S., 2011. The proteomic signature of *Aspergillus fumigatus* during early development. *Molecular & Cellular Proteomics*, 10.

Canton, J., Khezri, R., Glogauer, M. and Grinstein, S., 2014. Contrasting phagosome pH regulation and maturation in human M1 and M2 macrophages. *Molecular biology of the cell*, 25, 3330-3341.

Casadevall, A., 2012. Amoeba provide insight into the origin of virulence in pathogenic fungi, *Recent advances on model hosts*. Springer, pp. 1-10.

Cerqueira, G.C., Arnaud, M.B., Inglis, D.O., Skrzypek, M.S., Binkley, G., Simison, M., Miyasato, S.R., Binkley, J., Orvis, J. and Shah, P., 2014. The *Aspergillus* Genome Database: multispecies curation and incorporation of RNA-Seq data to improve structural gene annotations. *Nucleic acids research*, 42, D705-D710.

Chang, P., Fan, X. and Chen, J., 2015. Function and subcellular localization of Gcn5, a histone acetyltransferase in *Candida albicans*. *Fungal Genetics and Biology*, 81, 132-141.

Choi, H.-J., Kang, S.W., Yang, C.-H., Rhee, S.G. and Ryu, S.-E., 1998. Crystal structure of a novel human peroxidase enzyme at 2.0 Å resolution. *Nature structural biology*, 5, 400-406.

Choudhary, C., Weinert, B.T., Nishida, Y., Verdin, E. and Mann, M., 2014. The growing landscape of lysine acetylation links metabolism and cell signalling. *Nature reviews Molecular cell biology*, 15, 536-550.

Cichewicz, R.H., 2010. Epigenome manipulation as a pathway to new natural product scaffolds and their congeners. *Natural product reports*, 27, 11-22.

Couto, N., Malys, N., Gaskell, S.J. and Barber, J., 2013. Partition and turnover of glutathione reductase from *Saccharomyces cerevisiae*: a proteomic approach. *Journal of proteome research*, 12, 2885-2894.

Cox, G.M., Harrison, T.S., McDade, H.C., Taborda, C.P., Heinrich, G., Casadevall, A. and Perfect, J.R., 2003. Superoxide dismutase influences the virulence of *Cryptococcus neoformans* by affecting growth within macrophages. *Infection and immunity*, 71, 173-180.

Crameri, R. and Blaser, K., 1996. Cloning *Aspergillus fumigatus* allergens by the pJuFo filamentous phage display system. *International archives of allergy and immunology*, 110, 41-45.

Cruz-Garcia, D., Brouwers, N., Malhotra, V. and Curwin, A.J., 2020. Reactive oxygen species triggers unconventional secretion of antioxidants and Acb1. *Journal of Cell Biology*, 219.

Dalle-Donne, I., Giustarini, D., Colombo, R., Milzani, A. and Rossi, R., 2005. S-glutathionylation in human platelets by a thiol–disulfide exchange-independent mechanism. *Free Radical Biology and Medicine*, 38, 1501-1510.

Dalle-Donne, I., Aldini, G., Carini, M., Colombo, R., Rossi, R. and Milzani, A., 2006. Protein carbonylation, cellular dysfunction, and disease progression. *Journal of cellular and molecular medicine*, 10, 389-406.

Dastidar, R.G., Hooda, J., Shah, A., Cao, T.M., Henke, R.M. and Zhang, L., 2012. The nuclear localization of SWI/SNF proteins is subjected to oxygen regulation. *Cell & bioscience*, 2, 1-13.

Davies, K.J., 2016. The oxygen paradox, oxidative stress, and ageing. *Archives of biochemistry and biophysics*, 595, 28-32.

de Oliveira, M.A., Tairum, C.A., Netto, L.E.S., de Oliveira, A.L.P., Aleixo-Silva, R.L., Cabrera, V.I.M., Breyer, C.A. and Dos Santos, M.C., 2021. Relevance of peroxiredoxins in pathogenic microorganisms. *Applied Microbiology and Biotechnology*, 105, 5701-5717.

Debeaupuis, J.-P., Sarfati, J., Chazalet, V. and Latge, J.-P., 1997. Genetic diversity among clinical and environmental isolates of *Aspergillus fumigatus*. *Infection and immunity*, 65, 3080-3085.

Delaunay, A., Isnard, A.D. and Toledano, M.B., 2000. H_2O_2 sensing through oxidation of the Yap1 transcription factor. *The EMBO journal*, 19, 5157-5166.

Delaunay, A., Pflieger, D., Barrault, M.-B., Vinh, J. and Toledano, M.B., 2002. A thiol peroxidase is an H_2O_2 receptor and redox-transducer in gene activation. *Cell*, 111, 471-481.

Denning, D.W., Cadranel, J., Beigelman-Aubry, C., Ader, F., Chakrabarti, A., Blot, S., Ullmann, A.J., Dimopoulos, G. and Lange, C., 2016. Chronic pulmonary aspergillosis: rationale and clinical guidelines for diagnosis and management. *European Respiratory Journal*, 47, 45-68.

Diaz-Arevalo, D., Bagramyan, K., Hong, T.B., Ito, J.I. and Kalkum, M., 2011. CD4+ T cells mediate the protective effect of the recombinant Asp f3-based anti-aspergillosis vaccine. *Infection and immunity*, 79, 2257-2266.

Dignani, M.C., 2014. Epidemiology of invasive fungal diseases on the basis of autopsy reports. *F1000prime reports*, 6.

Dinamarco, T.M., Almeida, R.S., de Castro, P.A., Brown, N.A., dos Reis, T.F., Ramalho, L.N.Z., Savoldi, M., Goldman, M.H.S. and Goldman, G.H., 2012. Molecular characterization of the putative transcription factor SebA involved in virulence in *Aspergillus fumigatus*. *Eukaryotic cell*, 11, 518-531.

Dunn-Coleman, N.S. and Garrett, R.H., 1980. The role of glutamine synthetase and glutamine metabolism in nitrogen metabolite repression, a regulatory phenomenon in the lower eukaryote *Neurospora crassa*. *Molecular and General Genetics MGG*, 179, 25-32.

Dyer, P.S. and O'Gorman, C.M., 2012. Sexual development and cryptic sexuality in fungi: insights from *Aspergillus* species. *FEMS microbiology reviews*, 36, 165-192.

Eisendle, M., Oberegger, H., Buttinger, R., Illmer, P. and Haas, H., 2004. Biosynthesis and uptake of siderophores is controlled by the PacC-mediated ambient-pH regulatory system in *Aspergillus nidulans*. *Eukaryotic cell*, 3, 561-563.

Ellis, H.R. and Poole, L.B., 1997. Roles for the two cysteine residues of AhpC in catalysis of peroxide reduction by alkyl hydroperoxide reductase from *Salmonella typhimurium*. *Biochemistry*, 36, 13349-13356.

Ermak, G. and Davies, K.J., 2002. Calcium and oxidative stress: from cell signaling to cell death. *Molecular immunology*, 38, 713-721.

Esterbauer, H., Schaur, R.J. and Zollner, H., 1991. Chemistry and biochemistry of 4-hydroxynonenal, malonaldehyde and related aldehydes. *Free radical Biology and medicine*, 11, 81-128.

Finkel, T., 2011. Signal transduction by reactive oxygen species. *Journal of Cell Biology*, 194, 7-15.

Finkel, T. and Holbrook, N.J., 2000. Oxidants, oxidative stress and the biology of ageing. *Nature*, 408, 239-247.

Fridovich, I., 1978. The biology of oxygen radicals. *Science*, 201, 875-880.

Galaris, D., Barbouti, A. and Pantopoulos, K., 2019. Iron homeostasis and oxidative stress: An intimate relationship. *Biochimica et Biophysica Acta (BBA)-Molecular Cell Research*, 1866, 118535.

Glazier, V.E. and Panepinto, J.C., 2014. The ER stress response and host temperature adaptation in the human fungal pathogen *Cryptococcus neoformans*. *Virulence*, 5, 351-356.

Goetz, K.E., Coyle, C.M., Cheng, J.Z., O'Connor, S.E. and Panaccione, D.G., 2011. Ergot cluster-encoded catalase is required for synthesis of chanoclavine-I in *Aspergillus fumigatus*. *Current genetics*, 57, 201.

Goward, C.R. and Nicholls, D.J., 1994. Malate dehydrogenase: a model for structure, evolution, and catalysis. *Protein Science*, 3, 1883-1888.

Greenberger, P.A., 2002. Allergic bronchopulmonary aspergillosis. *Journal of Allergy and Clinical Immunology*, 110, 685-692.

Gregg, K.S. and Kauffman, C.A., 2015. Invasive aspergillosis: epidemiology, clinical aspects, and treatment, *Seminars in respiratory and critical care medicine*. Thieme Medical Publishers, pp. 662-672.

Gretes, M.C., Poole, L.B. and Karplus, P.A., 2012. Peroxiredoxins in parasites. *Antioxidants & redox signaling*, 17, 608-33.

Guo, M., Chen, Y., Du, Y., Dong, Y., Guo, W., Zhai, S., Zhang, H., Dong, S., Zhang, Z. and Wang, Y., 2011. The bZIP transcription factor MoAP1 mediates the oxidative stress response and is critical for pathogenicity of the rice blast fungus *Magnaporthe oryzae*. *PLoS pathogens*, 7, e1001302.

Gutierrez-Escobedo, G., Hernandez-Carreon, O., Morales-Rojano, B., Revuelta-Rodriguez, B., Vazquez-Franco, N., Castano, I. and De Las Penas, A., 2020. *Candida glabrata* peroxiredoxins, Tsa1 and Tsa2, and sulfiredoxin, Srx1, protect against oxidative damage and are necessary for virulence. *Fungal Genetics and Biology*, 135, 103287.

Haas, H., 2014. Fungal siderophore metabolism with a focus on *Aspergillus fumigatus*. *Natural product reports*, 31, 1266-76.

Haber, F. and Weiss, J., 1934. The catalytic decomposition of hydrogen peroxide by iron salts. *Proceedings of the Royal Society of London. Series A-Mathematical and Physical Sciences*, 147, 332-351.

Hall, A., Nelson, K., Poole, L.B. and Karplus, P.A., 2011. Structure-based insights into the catalytic power and conformational dexterity of peroxiredoxins. *Antioxidants & redox signaling*, 15, 795-815.

Hall, D.B., Holmlin, R.E. and Barton, J.K., 1996. Oxidative DNA damage through long-range electron transfer. *Nature*, 382, 731-735.

Hall, L.A. and Denning, D., 1994. Oxygen requirements of *Aspergillus* species. *Journal of medical microbiology*, 41, 311-315.

Halliwell, B. and Gutteridge, J.M., 1985. The importance of free radicals and catalytic metal ions in human diseases. *Molecular aspects of medicine*, 8, 89-193.

Halliwell, B. and Gutteridge, J.M., 2015. *Free radicals in biology and medicine*, Oxford university press, USA.

Han, D., Antunes, F., Canali, R., Rettori, D. and Cadenas, E., 2003. Voltage-dependent anion channels control the release of the superoxide anion from mitochondria to cytosol. *Journal of Biological Chemistry*, 278, 5557-5563.

Hartmann, T., Sasse, C., Schedler, A., Hasenberg, M., Gunzer, M. and Krappmann, S., 2011. Shaping the fungal adaptome–stress responses of *Aspergillus fumigatus*. *International Journal of Medical Microbiology*, 301, 408-416.

Heinekamp, T., Thywißen, A., Macheleidt, J., Keller, S., Valiante, V. and Brakhage, A.A., 2013. *Aspergillus fumigatus* melanins: interference with the host endocytosis pathway and impact on virulence. *Frontiers in microbiology*, 3, 440.

Hemmann, S., Menz, G., Ismail, C., Blaser, K. and Crameri, R., 1999. Skin test reactivity to 2 recombinant *Aspergillus fumigatus* allergens in A *fumigatus*–sensitized asthmatic subjects allows diagnostic separation of allergic bronchopulmonary aspergillosis from fungal sensitization. *Journal of allergy and clinical immunology*, 104, 601-607.

Hemmann, S., Nikolaizik, W.H., Schöni, M.H., Blaser, K. and Crameri, R., 1998. Differential IgE recognition of recombinant *Aspergillus fumigatus* allergens by cystic fibrosis patients with allergic bronchopulmonary aspergillosis or *Aspergillus* allergy. *European journal of immunology*, 28, 1155-1160.

Hemnani, T. and Parihar, M., 1998. Reactive oxygen species and oxidative DNA damage. *Indian journal of physiology and pharmacology*, 42, 440-452.

Henriet, S., Verweij, P.E., Holland, S.M. and Warris, A., 2013. Invasive fungal infections in patients with chronic granulomatous disease, *Hot Topics in Infection and Immunity in Children IX*. Springer, pp. 27-55.

Hillmann, F., Bagramyan, K., Strassburger, M., Heinekamp, T., Hong, T.B., Bzymek, K.P., Williams, J.C., Brakhage, A.A. and Kalkum, M., 2016. The Crystal Structure of Peroxiredoxin Asp f3 Provides Mechanistic Insight into Oxidative Stress Resistance and Virulence of *Aspergillus fumigatus*. *Scientific Reports*, 6, 33396.

Hissen, A.H., Chow, J.M., Pinto, L.J. and Moore, M.M., 2004. Survival of *Aspergillus fumigatus* in serum involves removal of iron from transferrin: the role of siderophores. *Infection and immunity*, 72, 1402-8.

Hissen, A.H., Wan, A.N., Warwas, M.L., Pinto, L.J. and Moore, M.M., 2005. The *Aspergillus fumigatus* siderophore biosynthetic gene sidA, encoding L-ornithine N5-oxygenase, is required for virulence. *Infection and immunity*, 73, 5493-5503.

Hwang, C.-S., Rhie, G.-e., Oh, J.-H., Huh, W.-K., Yim, H.-S. and Kang, S.-O., 2002. Copper-and zinc-containing superoxide dismutase (Cu/ZnSOD) is required for the protection of *Candida albicans* against oxidative stresses and the expression of its full virulence. *Microbiology*, 148, 3705-3713.

Isoyama, T., Murayama, A., Nomoto, A. and Kuge, S., 2001. Nuclear import of the yeast AP-1-like transcription factor Yap1p is mediated by transport receptor Pse1p, and this import step is not affected by oxidative stress. *Journal of Biological Chemistry*, 276, 21863-21869.

Ito, J.I., Lyons, J.M., Hong, T.B., Tamae, D., Liu, Y.-K., Wilczynski, S.P. and Kalkum, M., 2006. Vaccinations with recombinant variants of *Aspergillus fumigatus* allergen Asp f 3 protect mice against invasive aspergillosis. *Infection and immunity*, 74, 5075-5084.

Jahn, B., Koch, A., Schmidt, A., Wanner, G., Gehringer, H., Bhakdi, S. and Brakhage, A.A., 1997. Isolation and characterization of a pigmentless-conidium mutant of *Aspergillus fumigatus* with altered conidial surface and reduced virulence. *Infection and immunity*, 65, 5110-5117.

Jang, H.H., Lee, K.O., Chi, Y.H., Jung, B.G., Park, S.K., Park, J.H., Lee, J.R., Lee, S.S., Moon, J.C. and Yun, J.W., 2004. Two enzymes in one: two yeast peroxiredoxins display oxidative stress-dependent switching from a peroxidase to a molecular chaperone function. *Cell*, 117, 625-635.

Jarvis, R.M., Hughes, S.M. and Ledgerwood, E.C., 2012. Peroxiredoxin 1 functions as a signal peroxidase to receive, transduce, and transmit peroxide signals in mammalian cells. *Free Radical Biology and Medicine*, 53, 1522-30.

Jöhnk, B., Bayram, Ö., Abelmann, A., Heinekamp, T., Mattern, D.J., Brakhage, A.A., Jacobsen, I.D., Valerius, O. and Braus, G.H., 2016. SCF ubiquitin ligase F-box protein Fbx15 controls nuclear co-repressor localization, stress response and virulence of the human pathogen *Aspergillus fumigatus*. *PLoS pathogens*, 12, e1005899.

Johnson, D.C., Dean, D.R., Smith, A.D. and Johnson, M.K., 2005. Structure, function, and formation of biological iron-sulfur clusters. *Annual Review of Biochemistry*, 74, 247-281.

Keller, N.P., 2019. Fungal secondary metabolism: regulation, function and drug discovery. *Nature Reviews Microbiology*, 17, 167-180.

Kerr, S.C., Fischer, G.J., Sinha, M., McCabe, O., Palmer, J.M., Choera, T., Yun Lim, F., Wimmerova, M., Carrington, S.D. and Yuan, S., 2016. FleA expression in *Aspergillus fumigatus* is recognized by fucosylated structures on mucins and macrophages to prevent lung infection. *PLoS pathogens*, 12, e1005555.

Kim, S., Sideris, D.P., Sevier, C.S. and Kaiser, C.A., 2012. Balanced Ero1 activation and inactivation establishes ER redox homeostasis. *Journal of Cell Biology*, 196, 713-725.

Knox, B.P., Blachowicz, A., Palmer, J.M., Romsdahl, J., Huttenlocher, A., Wang, C.C., Keller, N.P. and Venkateswaran, K., 2016. Characterization of *Aspergillus fumigatus* isolates from air and surfaces of the International Space Station. *Msphere*, 1.

Knutsen, A.P. and Slavin, R.G., 2011. Allergic bronchopulmonary aspergillosis in asthma and cystic fibrosis. *Clinical and developmental immunology*, 2011.

Kollath-Leiss, K., Bonniger, C., Sardar, P. and Kempken, F., 2014. BEM46 shows eisosomal localization and association with tryptophan-derived auxin pathway in *Neurospora crassa*. *Eukaryot Cell*, 13, 1051-63.

Koshland Jr, D.E., 1994. Molecule of the year: the DNA repair enzyme. *Science*, 266, 1925-1926.

Kowalski, C.H., Beattie, S.R., Fuller, K.K., McGurk, E.A., Tang, Y.-W., Hohl, T.M., Obar, J.J. and Cramer, R.A., 2016. Heterogeneity among isolates reveals that fitness in low oxygen correlates with *Aspergillus fumigatus* virulence. *mBio*, 7.

Kuge, S., Arita, M., Murayama, A., Maeta, K., Izawa, S., Inoue, Y. and Nomoto, A., 2001. Regulation of the yeast Yap1p nuclear export signal is mediated by redox signal-induced reversible disulfide bond formation. *Mol Cell Biol*, 21, 6139-50.

Kurucz, V., Kruger, T., Antal, K., Dietl, A.M., Haas, H., Pocsi, I., Kniemeyer, O. and Emri, T., 2018. Additional oxidative stress reroutes the global response of *Aspergillus fumigatus* to iron depletion. *BMC Genomics*, 19, 357.

Kussmaul, L. and Hirst, J., 2006. The mechanism of superoxide production by NADH: ubiquinone oxidoreductase (complex I) from bovine heart mitochondria. *Proceedings of the National Academy of Sciences*, 103, 7607-7612.

Kwon-Chung, K.J. and Sugui, J.A., 2013. *Aspergillus fumigatus*—what makes the species a ubiquitous human fungal pathogen? *PLoS pathogens*, 9, e1003743.

Lamarre, C., Ibrahim-Granet, O., Du, C., Calderone, R. and Latgé, J.-P., 2007. Characterization of the SKN7 ortholog of *Aspergillus fumigatus*. *Fungal Genetics and Biology*, 44, 682-690.

Langfelder, K., Jahn, B., Gehringer, H., Schmidt, A., Wanner, G. and Brakhage, A.A., 1998. Identification of a polyketide synthase gene (pksP) of *Aspergillus fumigatus* involved in conidial pigment biosynthesis and virulence. *Medical microbiology and immunology*, 187, 79-89.

Latgé, J.-P., 1999. *Aspergillus fumigatus* and aspergillosis. *Clinical microbiology reviews*, 12, 310-350.

Latgé, J.-P., 2001. The pathobiology of *Aspergillus fumigatus*. *Trends in microbiology*, 9, 382-389.

Latge, J.-P. and Chamilos, G., 2019. *Aspergillus fumigatus* and aspergillosis in 2019. *Clinical microbiology reviews*, 33.

Laurindo, F.R., Pescatore, L.A. and de Castro Fernandes, D., 2012. Protein disulfide isomerase in redox cell signaling and homeostasis. *Free Radical Biology and Medicine*, 52, 1954-1969.

Lee, J., Godon, C., Lagniel, G., Spector, D., Garin, J., Labarre, J. and Toledano, M.B., 1999a. Yap1 and Skn7 control two specialized oxidative stress response regulons in yeast. *Journal of Biological Chemistry*, 274, 16040-16046.

Lee, J., Spector, D., Godon, C., Labarre, J. and Toledano, M.B., 1999b. A new antioxidant with alkyl hydroperoxide defense properties in yeast. *Journal of Biological Chemistry*, 274, 4537-4544.

Lessing, F., Kniemeyer, O., Wozniok, I., Loeffler, J., Kurzai, O., Haertl, A. and Brakhage, A.A., 2007. The *Aspergillus fumigatus* transcriptional regulator AfYap1 represents the major regulator for defense against reactive oxygen intermediates but is dispensable for pathogenicity in an intranasal mouse infection model. *Eukaryotic cell*, 6, 2290-2302.

Levine, R.L., Moskovitz, J. and Stadtman, E.R., 2000. Oxidation of methionine in proteins: roles in antioxidant defense and cellular regulation. *IUBMB life*, 50, 301-307.

Liaw, S.H., Kuo, I. and Eisenberg, D., 1995. Discovery of the ammonium substrate site on glutamine synthetase, a third cation binding site. *Protein Science*, 4, 2358-2365.

Liu, X., Wang, J., Xu, J. and Shi, J., 2014. FgIlv5 is required for branched-chain amino acid biosynthesis and full virulence in *Fusarium graminearum*. *Microbiology*, 160, 692-702.

Loussert, C., Schmitt, C., Prevost, M.C., Balloy, V., Fadel, E., Philippe, B., Kauffmann-Lacroix, C., Latgé, J.P. and Beauvais, A., 2010. In vivo biofilm composition of *Aspergillus fumigatus*. *Cellular microbiology*, 12, 405-410.

Luo, F., Zhou, H., Zhou, X., Xie, X., Li, Y., Hu, F. and Huang, B., 2020. The intermediates in branched-chain amino acid biosynthesis are indispensable for conidial germination of the insect-pathogenic fungus *Metarhizium robertsii*. *Applied and environmental microbiology*, 86, e01682-20.

Ma, Y., Qiao, J., Liu, W., Wan, Z., Wang, X., Calderone, R. and Li, R., 2008. The sho1 sensor regulates growth, morphology, and oxidant adaptation in *Aspergillus fumigatus* but is not essential for development of invasive pulmonary aspergillosis. *Infection and immunity*, 76, 1695-1701.

Mannervik, B., 1985. [60] Glutathione peroxidase, *Methods in enzymology*. Elsevier, pp. 490-495.

Maschmeyer, G., Haas, A. and Cornely, O.A., 2007. Invasive aspergillosis. *Drugs*, 67, 1567-1601.

McDonagh, A., Fedorova, N.D., Crabtree, J., Yu, Y., Kim, S., Chen, D., Loss, O., Cairns, T., Goldman, G. and Armstrong-James, D., 2008. Sub-telomere directed gene expression during initiation of invasive aspergillosis. *PLoS pathogens*, 4, e1000154.

McNaught, K.S.P. and Olanow, C.W., 2006. Protein aggregation in the pathogenesis of familial and sporadic Parkinson's disease. *Neurobiology of aging*, 27, 530-545.

Mendoza-Martinez, A.E., Cano-Dominguez, N. and Aguirre, J., 2020. Yap1 homologs mediate more than the redox regulation of the antioxidant response in filamentous fungi. *Fungal biology*, 124, 253-262.

Mendoza-Martinez, A.E., Lara-Rojas, F., Sanchez, O. and Aguirre, J., 2017. NapA Mediates a Redox Regulation of the Antioxidant Response, Carbon Utilization and Development in *Aspergillus nidulans*. *Frontiers in microbiology*, 8, 516.

Misslinger, M., Hortschansky, P., Brakhage, A.A. and Haas, H., 2021. Fungal iron homeostasis with a focus on *Aspergillus fumigatus*. *Biochimica et Biophysica Acta (BBA)-Molecular Cell Research*, 1868, 118885.

Mittler, R., Vanderauwera, S., Suzuki, N., Miller, G., Tognetti, V.B., Vandepoele, K., Gollery, M., Shulaev, V. and Van Breusegem, F., 2011. ROS signaling: the new wave? *Trends in plant science*, 16, 300-309.

Moldovan, L. and Moldovan, N.I., 2004. Oxygen free radicals and redox biology of organelles. *Histochemistry and cell biology*, 122, 395-412.

Molina, L. and Kahmann, R., 2007. An *Ustilago maydis* gene involved in H_2O_2 detoxification is required for virulence. *The Plant Cell*, 19, 2293-2309.

Montibus, M., Ducos, C., Bonnin-Verdal, M.-N., Bormann, J., Ponts, N., Richard-Forget, F. and Barreau, C., 2013. The bZIP transcription factor Fgap1 mediates oxidative stress response and trichothecene biosynthesis but not virulence in *Fusarium graminearum*. *PLoS One*, 8, e83377.

Moretti, A.I.S. and Laurindo, F.R.M., 2017. Protein disulfide isomerases: Redox connections in and out of the endoplasmic reticulum. *Archives of biochemistry and biophysics*, 617, 106-119.

Morgan, B.A., Banks, G.R., Toone, W.M., Raitt, D., Kuge, S. and Johnston, L.H., 1997. The Skn7 response regulator controls gene expression in the oxidative stress response of the budding yeast *Saccharomyces cerevisiae*. *The EMBO Journal*, 16, 1035-1044.

Muller, F.L., Liu, Y. and Van Remmen, H., 2004. Complex III releases superoxide to both sides of the inner mitochondrial membrane. *Journal of Biological Chemistry*, 279, 49064-49073.

Mullins, J., Harvey, R. and Seaton, A., 1976. Sources and incidence of airborne *Aspergillus fumigatus* (Fres). *Clinical & Experimental Allergy*, 6, 209-217.

Murphy, M.P., 2009. How mitochondria produce reactive oxygen species. *Biochemical journal*, 417, 1-13.

Nairz, M. and Weiss, G., 2020. Iron in infection and immunity. *Molecular Aspects of Medicine*, 75, 100864.

Nathan, C. and Cunningham-Bussel, A., 2013. Beyond oxidative stress: an immunologist's guide to reactive oxygen species. *Nature Reviews Immunology*, 13, 349-361.

Nevitt, T., 2011. War-Fe-re: iron at the core of fungal virulence and host immunity. *Biometals*, 24, 547-58.

Nierman, W.C., Pain, A., Anderson, M.J., Wortman, J.R., Kim, H.S., Arroyo, J., Berriman, M., Abe, K., Archer, D.B., Bermejo, C., Bennett, J., Bowyer, P., Chen, D., Collins, M., Coulsen, R., Davies, R., Dyer, P.S., Farman, M., Fedorova, N., Fedorova, N., Feldblyum, T.V., Fischer, R., Fosker, N., Fraser, A., Garcia, J.L., Garcia, M.J., Goble, A., Goldman, G.H., Gomi, K., Griffith-Jones, S., Gwilliam, R., Haas, B., Haas, H., Harris, D., Horiuchi, H., Huang, J., Humphray, S., Jimenez, J., Keller, N., Khouri, H., Kitamoto, K., Kobayashi, T., Konzack, S., Kulkarni, R., Kumagai, T., Lafon, A., Latge, J.P., Li, W., Lord, A., Lu, C., Majoros, W.H., May, G.S., Miller, B.L., Mohamoud, Y., Molina, M., Monod, M., Mouyna, I., Mulligan, S., Murphy, L., O'Neil, S., Paulsen, I., Penalva, M.A., Pertea, M., Price, C., Pritchard, B.L., Quail, M.A., Rabbinowitsch, E., Rawlins, N., Rajandream, M.A., Reichard, U., Renauld, H., Robson, G.D., Rodriguez de Cordoba, S., Rodriguez-Pena, J.M., Ronning, C.M., Rutter, S., Salzberg, S.L., Sanchez, M., Sanchez-Ferrero, J.C., Saunders, D., Seeger, K., Squares, R., Squares, S., Takeuchi, M., Tekaia, F., Turner, G., Vazquez de Aldana, C.R., Weidman, J., White, O., Woodward, J., Yu, J.H., Fraser, C., Galagan, J.E., Asai, K., Machida, M., Hall, N., Barrell, B. and Denning, D.W., 2005. Genomic sequence of the pathogenic and allergenic filamentous fungus *Aspergillus fumigatus*. *Nature*, 438, 1151-6.

Nigam, S., Sarma, P., Ghosh, P. and Sarma, P.U., 2001. Characterization of *Aspergillus fumigatus* protein disulfide isomerase family gene. *Gene*, 281, 143-150.

Nonell, S. and Flors, C., 2016. *Singlet Oxygen: Applications in Biosciences and Nanosciences, Volume 1*, Royal Society of Chemistry.

Noßmann, M., 2018. Identifizierung von Protein-Protein-Interaktionen des humanpathogenen Pilzes *Aspergillus fumigatus* unter Verwendung eines Arginin-tRNA-adaptierten *Saccharomyces cerevisiae* Stammes. Friedrich-Schiller-Universität Jena.

Nossmann, M., Boysen, J.M., Kruger, T., Konig, C.C., Hillmann, F., Munder, T. and Brakhage, A.A., 2019. Yeast two-hybrid screening reveals a dual function for the histone acetyltransferase GcnE by controlling glutamine synthesis and development in *Aspergillus fumigatus*. *Current Genetics*, 65, 523-538.

Novohradska, S., Ferling, I. and Hillmann, F., 2017. Exploring Virulence Determinants of Filamentous Fungal Pathogens through Interactions with Soil Amoebae. *Frontiers in cellular and infection microbiology*, 7, 497.

Nützmann, H.-W., Fischer, J., Scherlach, K., Hertweck, C. and Brakhage, A.A., 2013. Distinct amino acids of histone H3 control secondary metabolism in *Aspergillus nidulans*. *Applied and environmental microbiology*, 79, 6102-6109.

Nützmann, H.-W., Reyes-Dominguez, Y., Scherlach, K., Schroeckh, V., Horn, F., Gacek, A., Schümann, J., Hertweck, C., Strauss, J. and Brakhage, A.A., 2011. Bacteria-induced natural product formation in the fungus *Aspergillus nidulans* requires Saga/Ada-mediated histone acetylation. *Proceedings of the National Academy of Sciences*, 108, 14282-14287.

O'Meara, T.R., Hay, C., Price, M.S., Giles, S. and Alspaugh, J.A., 2010. *Cryptococcus neoformans* histone acetyltransferase Gcn5 regulates fungal adaptation to the host. *Eukaryotic cell*, 9, 1193-1202.

O'Gorman, C.M., Fuller, H.T. and Dyer, P.S., 2009. Discovery of a sexual cycle in the opportunistic fungal pathogen *Aspergillus fumigatus*. *Nature*, 457, 471-474.

Paoletti, M., Rydholm, C., Schwier, E.U., Anderson, M.J., Szakacs, G., Lutzoni, F., Debeaupuis, J.-P., Latgé, J.-P., Denning, D.W. and Dyer, P.S., 2005. Evidence for sexuality in the opportunistic fungal pathogen *Aspergillus fumigatus*. *Current Biology*, 15, 1242-1248.

Paolinelli, R., Mendoza-Maldonado, R., Cereseto, A. and Giacca, M., 2009. Acetylation by GCN5 regulates CDC6 phosphorylation in the S phase of the cell cycle. *Nature structural & molecular biology*, 16, 412-420.

Paris, S., Wysong, D., Debeaupuis, J.-P., Shibuya, K., Philippe, B., Diamond, R.D. and Latgé, J.-P., 2003. Catalases of *Aspergillus fumigatus*. *Infection and immunity*, 71, 3551-3562.

Park, Y.S., Kim, J.Y. and Yun, C.W., 2016. Identification of ferrichrome- and ferrioxamine B-mediated iron uptake by *Aspergillus fumigatus*. *Biochemical Journal*, 473, 1203-13.

Patterson, T.F., Thompson III, G.R., Denning, D.W., Fishman, J.A., Hadley, S., Herbrecht, R., Kontoyiannis, D.P., Marr, K.A., Morrison, V.A. and Nguyen, M.H., 2016. Practice guidelines for the diagnosis and management of aspergillosis: 2016 update by the Infectious Diseases Society of America. *Clinical Infectious Diseases*, 63, e1-e60.

Paulussen, C., Hallsworth, J.E., Alvarez-Perez, S., Nierman, W.C., Hamill, P.G., Blain, D., Rediers, H. and Lievens, B., 2017. Ecology of aspergillosis: insights into the pathogenic potency of *Aspergillus fumigatus* and some other *Aspergillus* species. *Microbial biotechnology*, 10, 296-322.

Perkins, A., Nelson, K.J., Parsonage, D., Poole, L.B. and Karplus, P.A., 2015. Peroxiredoxins: guardians against oxidative stress and modulators of peroxide signaling. *Trends in biochemical sciences*, 40, 435-445.

Perkins, A., Poole, L.B. and Karplus, P.A., 2014. Tuning of peroxiredoxin catalysis for various physiological roles. *Biochemistry*, 53, 7693-705.

Perrin, R.M., Fedorova, N.D., Bok, J.W., Cramer Jr, R.A., Wortman, J.R., Kim, H.S., Nierman, W.C. and Keller, N.P., 2007. Transcriptional regulation of chemical diversity in *Aspergillus fumigatus* by LaeA. *PLoS pathogens*, 3, e50.

Pfannmüller, A., Boysen, J.M. and Tudzynski, B., 2017. Nitrate assimilation in *Fusarium fujikuroi* is controlled by multiple levels of regulation. *Frontiers in microbiology*, 8, 381.

Pradhan, A., Herrero-de-Dios, C., Belmonte, R., Budge, S., Lopez Garcia, A., Kolmogorova, A., Lee, K.K., Martin, B.D., Ribeiro, A. and Bebes, A., 2017. Elevated catalase expression in a fungal pathogen is a double-edged sword of iron. *PLoS pathogens*, 13, e1006405.

Qiao, J., Kontoyiannis, D.P., Calderone, R., Li, D., Ma, Y., Wan, Z., Li, R. and Liu, W., 2008. Af yap1, encoding a bZip transcriptional factor of *Aspergillus fumigatus*, contributes to oxidative stress response but is not essential to the virulence of this pathogen in mice

immunosuppressed by cyclophosphamide and triamcinolone. *Sabouraudia*, 46, 773-782.

Raymond-Bouchard, I., Carroll, C.S., Nesbitt, J.R., Henry, K.A., Pinto, L.J., Moinzadeh, M., Scott, J.K. and Moore, M.M., 2012. Structural requirements for the activity of the MirB ferrisiderophore transporter of *Aspergillus fumigatus*. *Eukaryot Cell*, 11, 1333-44.

Reichard, U., Büttner, S., Eiffert, H., Staib, F. and Rüchel, R., 1990. Purification and characterisation of an extracellular serine proteinase from *Aspergillus fumigatus* and its detection in tissue. *Journal of medical microbiology*, 33, 243-251.

Rhodes, J.C., 2006. *Aspergillus fumigatus*: growth and virulence. *Medical mycology*, 44, S77-S81.

Richter, C., Park, J.-W. and Ames, B.N., 1988. Normal oxidative damage to mitochondrial and nuclear DNA is extensive. *Proceedings of the National Academy of Sciences*, 85, 6465-6467.

Rocha, M.C., de Godoy, K.F., Bannitz-Fernandes, R., Fabri, J., Barbosa, M.M.F., de Castro, P.A., Almeida, F., Goldman, G.H., da Cunha, A.F., Netto, L.E.S., de Oliveira, M.A. and Malavazi, I., 2018. Analyses of the three 1-Cys Peroxiredoxins from *Aspergillus fumigatus* reveal that cytosolic Prx1 is central to H_2O_2 metabolism and virulence. *Scientific reports*, 8, 12314.

Romani, L., 2011. Immunity to fungal infections. *Nature Reviews Immunology*, 11, 275-288.

Rösler, S.M., Kramer, K., Finkemeier, I., Humpf, H.U. and Tudzynski, B., 2016. The SAGA complex in the rice pathogen *Fusarium fujikuroi*: structure and functional characterization. *Molecular microbiology*, 102, 951-974.

Roth, S.Y., Denu, J.M. and Allis, C.D., 2001. Histone acetyltransferases. *Annual review of biochemistry*, 70, 81-120.

Roze, L.V., Arthur, A.E., Hong, S.Y., Chanda, A. and Linz, J.E., 2007. The initiation and pattern of spread of histone H4 acetylation parallel the order of transcriptional activation of genes in the aflatoxin cluster. *Molecular microbiology*, 66, 713-726.

Ruf, D., Brantl, V. and Wagener, J., 2018. Mitochondrial Fragmentation in *Aspergillus fumigatus* as Early Marker of Granulocyte Killing Activity. *Frontiers in Cellular and Infection Microbiology*, 8.

Samson, R.A., 1999. The genus *Aspergillus* with special regard to the *Aspergillus fumigatus* group. *Contributions to microbiology*, 2, 5-20.

Sazanov, L.A., 2015. A giant molecular proton pump: structure and mechanism of respiratory complex I. *Nature Reviews Molecular Cell Biology*, 16, 375-388.

Schmidt, A., 1998. Georg Fresenius und die Spezies *Aspergillus fumigatus*: Georg Fresenius and the species *Aspergillus fumigatus*. *Mycoses*, 41, 89-91.

Schrettl, M., Beckmann, N., Varga, J., Heinekamp, T., Jacobsen, I.D., Jöchl, C., Moussa, T.A., Wang, S., Gsaller, F. and Blatzer, M., 2010. HapX-mediated adaption to iron starvation is crucial for virulence of *Aspergillus fumigatus*. *PLoS pathogens*, 6, e1001124.

Schrettl, M., Bignell, E., Kragl, C., Joechl, C., Rogers, T., Arst Jr, H.N., Haynes, K. and Haas, H., 2004. Siderophore biosynthesis but not reductive iron assimilation is essential for *Aspergillus fumigatus* virulence. *The Journal of experimental medicine*, 200, 1213-1219.

Schrettl, M., Bignell, E., Kragl, C., Sabiha, Y., Loss, O., Eisendle, M., Wallner, A., Arst, H.N., Jr., Haynes, K. and Haas, H., 2007. Distinct roles for intra- and extracellular siderophores during *Aspergillus fumigatus* infection. *PLoS pathogens*, 3, 1195-207.

Schrettl, M., Kim, H.S., Eisendle, M., Kragl, C., Nierman, W.C., Heinekamp, T., Werner, E.R., Jacobsen, I., Illmer, P., Yi, H., Brakhage, A.A. and Haas, H., 2008. SreA-mediated iron regulation in *Aspergillus fumigatus*. *Molecular microbiology*, 70, 27-43.

Segal, B.H., 2009. Invasive aspergillosis in chronic granulomatous disease, *Aspergillosis: from diagnosis to prevention*. Springer, pp. 527-543.

Sevier, C.S. and Kaiser, C.A., 2008. Ero1 and redox homeostasis in the endoplasmic reticulum. *Biochimica et Biophysica Acta (BBA)-Molecular Cell Research*, 1783, 549-556.

Shepardson, K.M., Jhingran, A., Caffrey, A., Obar, J.J., Suratt, B.T., Berwin, B.L., Hohl, T.M. and Cramer, R.A., 2014. Myeloid derived hypoxia inducible factor 1-alpha is required for protection against pulmonary *Aspergillus fumigatus* infection. *PLoS pathogens*, 10, e1004378.

Sheppard, D.C., Doedt, T., Chiang, L.Y., Kim, H.S., Chen, D., Nierman, W.C. and Filler, S.G., 2005. The *Aspergillus fumigatus* StuA protein governs the up-regulation of a discrete transcriptional program during the acquisition of developmental competence. *Molecular biology of the cell*, 16, 5866-5879.

Shlezinger, N., Irmer, H., Dhingra, S., Beattie, S.R., Cramer, R.A., Braus, G.H., Sharon, A. and Hohl, T.M., 2017. Sterilizing immunity in the lung relies on targeting fungal apoptosis-like programmed cell death. *Science*, 357, 1037-1041.

Sies, H., 1986. Biochemistry of oxidative stress. *Angewandte Chemie International Edition in English*, 25, 1058-1071.

Sies, H., 1994. Strategies of antioxidant defense. *EJB Reviews 1993*, 101-107.

Sies, H., 2000. What is oxidative stress?, *Oxidative stress and vascular disease*. Springer, pp. 1-8.

Singh, B., Oellerich, M., Kumar, R., Kumar, M., Bhadoria, D.P., Reichard, U., Gupta, V.K., Sharma, G.L. and Asif, A.R., 2010. Immuno-reactive molecules identified from the secreted proteome of *Aspergillus fumigatus*. *Journal of proteome research*, 9, 5517-5529.

Singh, P.K., Parsek, M.R., Greenberg, E.P. and Welsh, M.J., 2002. A component of innate immunity prevents bacterial biofilm development. *Nature*, 417, 552-555.

Sobotta, M.C., Liou, W., Stocker, S., Talwar, D., Oehler, M., Ruppert, T., Scharf, A.N. and Dick, T.P., 2015. Peroxiredoxin-2 and STAT3 form a redox relay for H_2O_2 signaling. *Nature chemical biology*, 11, 64-70.

Soukup, A.A., Chiang, Y.M., Bok, J.W., Reyes-Dominguez, Y., Oakley, B.R., Wang, C.C., Strauss, J. and Keller, N.P., 2012. Overexpression of the *Aspergillus nidulans* histone 4 acetyltransferase EsaA increases activation of secondary metabolite production. *Molecular microbiology*, 86, 314-330.

Souza, J.A.M., Baltazar, L.d.M., Carregal, V.M., Gouveia-Eufrasio, L., de Oliveira, A.G., Dias, W.G., Campos Rocha, M., Rocha de Miranda, K., Malavazi, I. and Santos, D.d.A., 2019. Characterization of *Aspergillus fumigatus* extracellular vesicles and their effects on macrophages and neutrophils functions. *Frontiers in microbiology*, 10, 2008.

Stocker, S., Maurer, M., Ruppert, T. and Dick, T.P., 2018. A role for 2-Cys peroxiredoxins in facilitating cytosolic protein thiol oxidation. *Nature chemical biology*, 14, 148-155.

Studt, L., Schmidt, F., Jahn, L., Sieber, C., Connolly, L., Niehaus, E.-M., Freitag, M., Humpf, H.-U. and Tudzynski, B., 2013. Two histone deacetylases, FfHda1 and FfHda2, are important for secondary metabolism and virulence in *Fusarium fujikuroi*. *Applied and Environmental Microbiology*.

Su, T., Si, M., Zhao, Y., Liu, Y., Yao, S., Che, C. and Chen, C., 2018. A thioredoxin-dependent peroxiredoxin Q from *Corynebacterium glutamicum* plays an important role in defense against oxidative stress. *PLoS One*, 13, e0192674.

Teichert, S., Schönig, B., Richter, S. and Tudzynski, B., 2004. Deletion of the *Gibberella fujikuroi* glutamine synthetase gene has significant impact on transcriptional control of primary and secondary metabolism. *Molecular microbiology*, 53, 1661-1675.

Tekaia, F. and Latgé, J.-P., 2005. *Aspergillus fumigatus*: saprophyte or pathogen? *Current opinion in microbiology*, 8, 385-392.

Temme, N. and Tudzynski, P., 2009. Does *Botrytis cinerea* ignore H_2O_2-induced oxidative stress during infection? Characterization of *Botrytis* activator protein 1. *Molecular plant-microbe interactions*, 22, 987-998.

Thannickal, V.J. and Fanburg, B.L., 2000. Reactive oxygen species in cell signaling. *American Journal of Physiology-Lung Cellular and Molecular Physiology*, 279, L1005-L1028.

Thön, M., Al Abdallah, Q., Hortschansky, P., Scharf, D.H., Eisendle, M., Haas, H. and Brakhage, A.A., 2010. The CCAAT-binding complex coordinates the oxidative stress response in eukaryotes. *Nucleic acids research*, 38, 1098-1113.

Tilburn, J., Sarkar, S., Widdick, D., Espeso, E., Orejas, M., Mungroo, J., Penalva, M. and Arst Jr, H., 1995. The *Aspergillus* PacC zinc finger transcription factor mediates regulation of both acid-and alkaline-expressed genes by ambient pH. *The EMBO Journal*, 14, 779-790.

Toledano, M.B. and Huang, B., 2016. Microbial 2-Cys Peroxiredoxins: Insights into Their Complex Physiological Roles. *Molecules and cells*, 39, 31-9.

Travis, S.M., Conway, B.-A.D., Zabner, J., Smith, J.J., Anderson, N.N., Singh, P.K., Peter Greenberg, E. and Welsh, M.J., 1999. Activity of abundant antimicrobials of the human airway. *American journal of respiratory cell and molecular biology*, 20, 872-879.

Truong, T., Zeng, G., Qingsong, L., Kwang, L.T., Tong, C., Chan, F.Y., Wang, Y. and Seneviratne, C.J., 2016. Comparative ploidy proteomics of *Candida albicans* biofilms unraveled the role of the AHP1 gene in the biofilm persistence against amphotericin B. *Molecular & Cellular Proteomics*, 15, 3488-3500.

Tu, B.P. and Weissman, J.S., 2002. The FAD-and O2-dependent reaction cycle of Ero1-mediated oxidative protein folding in the endoplasmic reticulum. *Molecular cell*, 10, 983-994.

Tudzynski, B., 2014. Nitrogen regulation of fungal secondary metabolism in fungi. *Frontiers in microbiology*, 5, 656.

Tudzynski, P., Heller, J. and Siegmund, U., 2012. Reactive oxygen species generation in fungal development and pathogenesis. *Current opinion in microbiology*, 15, 653-659.

Tuppy, H. and Kreil, G., 2004. Cytochrome c.

Turrens, J.F., 1997. Superoxide production by the mitochondrial respiratory chain. *Bioscience reports*, 17, 3-8.

Turrens, J.F., 2003. Mitochondrial formation of reactive oxygen species. *The Journal of physiology*, 552, 335-344.

Ulrich, K. and Jakob, U., 2019. The role of thiols in antioxidant systems. *Free Radical Biology and Medicine*, 140, 14-27.

Urban, C., Xiong, X., Sohn, K., Schroppel, K., Brunner, H. and Rupp, S., 2005. The moonlighting protein Tsa1p is implicated in oxidative stress response and in cell wall biogenesis in *Candida albicans*. *Molecular microbiology*, 57, 1318-41.

van de Veerdonk, F.L., Gresnigt, M.S., Romani, L., Netea, M.G. and Latge, J.P., 2017. *Aspergillus fumigatus* morphology and dynamic host interactions. *Nature Reviews Microbiology*, 15, 661-674.

Van Nguyen, T., Lee, J.E., Sweredoski, M.J., Yang, S.-J., Jeon, S.-J., Harrison, J.S., Yim, J.-H., Lee, S.G., Handa, H. and Kuhlman, B., 2016. Glutamine triggers acetylation-dependent degradation of glutamine synthetase via the thalidomide receptor cereblon. *Molecular cell*, 61, 809-820.

Vignols, F., Bréhélin, C., Surdin-Kerjan, Y., Thomas, D. and Meyer, Y., 2005. A yeast two-hybrid knockout strain to explore thioredoxin-interacting proteins in vivo. *Proceedings of the National Academy of Sciences*, 102, 16729-16734.

Wagner, D., Wiemann, P., Huß, K., Brandt, U., Fleißner, A. and Tudzynski, B., 2013. A sensing role of the glutamine synthetase in the nitrogen regulation network in *Fusarium fujikuroi*. *PLoS One*, 8, e80740.

Walling, C., 1998. Intermediates in the reactions of Fenton type reagents. *Accounts of Chemical Research*, 31, 155-157.

Wallner, A., Blatzer, M., Schrettl, M., Sarg, B., Lindner, H. and Haas, H., 2009. Ferricrocin, a Siderophore Involved in Intra- and Transcellular Iron Distribution in *Aspergillus fumigatus*. *Applied and Environmental Microbiology*, 75, 4194-4196.

Wang, B., Li, X., Yu, D., Chen, X., Tabudravu, J., Deng, H. and Pan, L., 2018. Deletion of the epigenetic regulator GcnE in *Aspergillus* niger FGSC A1279 activates the production of multiple polyketide metabolites. *Microbiological research*, 217, 101-107.

Warris, A. and Ballou, E.R., 2019. Oxidative responses and fungal infection biology, *Seminars in cell & developmental biology*. Elsevier, pp. 34-46.

Watanabe, T., Irokawa, H., Ogasawara, A., Iwai, K. and Kuge, S., 2014. Requirement of peroxiredoxin on the stationary phase of yeast cell growth. *The Journal of toxicological sciences*, 39, 51-58.

Wiemann, P., Sieber, C.M., Von Bargen, K.W., Studt, L., Niehaus, E.-M., Espino, J.J., Huss, K., Michielse, C.B., Albermann, S. and Wagner, D., 2013. Deciphering the cryptic genome: genome-wide analyses of the rice pathogen *Fusarium fujikuroi* reveal complex regulation of secondary metabolism and novel metabolites. *PLoS pathogens*, 9, e1003475.

Wilkinson, B. and Gilbert, H.F., 2004. Protein disulfide isomerase. *Biochimica et Biophysica Acta (BBA)-Proteins and Proteomics*, 1699, 35-44.

Winterbourn, C.C., 2008. Reconciling the chemistry and biology of reactive oxygen species. *Nature chemical biology*, 4, 278-286.

Winterbourn, C.C., Hampton, M.B., Livesey, J.H. and Kettle, A.J., 2006. Modeling the reactions of superoxide and myeloperoxidase in the neutrophil phagosome implications for microbial killing. *Journal of Biological Chemistry*, 281, 39860-39869.

Winters, B., Custer, J., Galvagno, S.M., Colantuoni, E., Kapoor, S.G., Lee, H., Goode, V., Robinson, K., Nakhasi, A. and Pronovost, P., 2012. Diagnostic errors in the intensive care unit: a systematic review of autopsy studies. *BMJ quality & safety*, 21, 894-902.

Wong, C.M., Wong, K.H. and Chen, X.D., 2008. Glucose oxidase: natural occurrence, function, properties and industrial applications. *Applied microbiology and biotechnology*, 78, 927-938.

Wong, S.-H., Lonhienne, T.G., Winzor, D.J., Schenk, G. and Guddat, L.W., 2012. Bacterial and plant ketol-acid reductoisomerases have different mechanisms of induced fit during the catalytic cycle. *Journal of molecular biology*, 424, 168-179.

Wood, M.J., Storz, G. and Tjandra, N., 2004. Structural basis for redox regulation of Yap1 transcription factor localization. *Nature*, 430, 917-921.

Wood, Z.A., Schröder, E., Harris, J.R. and Poole, L.B., 2003. Structure, mechanism and regulation of peroxiredoxins. *Trends in biochemical sciences*, 28, 32-40.

Xia, Y., Yu, H., Zhou, Z., Takaya, N., Zhou, S. and Wang, P., 2018. Peroxiredoxin System of *Aspergillus nidulans* Resists Inactivation by High Concentration of Hydrogen Peroxide-Mediated Oxidative Stress. *Journal of microbiology and biotechnology*, 28, 145-156.

Yan, C., Lee, L.H. and Davis, L.I., 1998. Crm1p mediates regulated nuclear export of a yeast AP-1-like transcription factor. *The EMBO journal*, 17, 7416-7429.

Yasmin, S., Abt, B., Schrettl, M., Moussa, T.A., Werner, E.R. and Haas, H., 2009. The interplay between iron and zinc metabolism in *Aspergillus fumigatus*. *Fungal Genetics and Biology*, 46, 707-713.

You, D., Yin, B.-C., Li, Z.-H., Zhou, Y., Yu, W.-B., Zuo, P. and Ye, B.-C., 2016. Sirtuin-dependent reversible lysine acetylation of glutamine synthetases reveals an autofeedback loop in nitrogen metabolism. *Proceedings of the National Academy of Sciences*, 113, 6653-6658.

Yu, H.-H., Yang, Y.-H. and Chiang, B.-L., 2021. Chronic granulomatous disease: a comprehensive review. *Clinical reviews in allergy & immunology*, 61, 101-113.

Zito, E., 2015. ERO1: A protein disulfide oxidase and H_2O_2 producer. *Free Radical Biology and Medicine*, 83, 299-304.

9 List of scientific publications and conference contributions

9.1 List of scientific publications

Pfannmüller, A., **Boysen, J. M.**, & Tudzynski, B. (2017). Nitrate assimilation in *Fusarium fujikuroi* is controlled by multiple levels of regulation. *Frontiers in microbiology*, *8*, 381. https://doi.org/10.3389/fmicb.2017.00381

Nossmann, M., **Boysen, J. M.**, Krüger, T., König, C. C., Hillmann, F., Munder, T., & Brakhage, A. A. (2019). Yeast two-hybrid screening reveals a dual function for the histone acetyltransferase GcnE by controlling glutamine synthesis and development in *Aspergillus fumigatus*. *Current genetics*, *65*(2), 523-538. https://doi.org/10.1007/s00294-018-0891-z

Boysen, J. M., Saeed, N., Wolf, T., Panagiotou, G., & Hillmann, F. (2021). The Peroxiredoxin Asp f3 Acts as Redox Sensor in *Aspergillus fumigatus*. Genes, 12(5), 668. https://doi.org/10.3390/genes12050668

Boysen, J. M., Saeed, N., & Hillmann, F. (2021). Natural products in the predatory defence of the filamentous fungal pathogen *Aspergillus fumigatus*. Beilstein Journal of Organic Chemistry, 17(1), 1814-1827. https://doi.org/10.3762/bjoc.17.124

Brantl V, **Boysen J. M.**, Yap A, Golubtsov E, Ruf D, Heinekamp T, Straßburger M, Dichtl K, Haas H, Hillmann F, Wagener J. (2021). Peroxiredoxin Asp f3 is essential for *Aspergillus fumigatus* to overcome iron limitation during infection. mBio 12:e00976-21. https://doi.org/10.1128/mBio.00976-21.

9.2 List of conference contributions

Jana M. Boysen, Bettina Bardl, Falk Hillmann

The peroxiredoxin Asp f3 protects *Aspergillus fumigatus* against external superoxide

69th DGHM Jahrestagung; Jahrestagung VAAM; 5th Gemeinsame Tagung von DGHM und VAMM, Würzburg, March 2017, poster presentation

Jana M. Boysen, Bettina Bardl, Falk Hillmann

The peroxiredoxin Asp f3 protects *Aspergillus fumigatus* against external superoxide

6th International Conference on Microbial Communication for Young Scientists (MiCom), Jena, March 2017, poster presentation

Jana M. Boysen, Elena Shekhova, Olaf Kniemeyer, Falk Hillmann

The peroxiredoxin Asp f3 protects *Aspergillus fumigatus* against external superoxide

12th Symposium of the VAAM Special Group Biology and Biotechnology of Fungi, Jena, September 2017, poster presentation

Jana M. Boysen, Elena Shekhova, Olaf Kniemeyer, Falk Hillmann

The peroxiredoxin Asp f3 protects *Aspergillus fumigatus* against reactive oxygen species

70. DGHM Annual Meeting, Bochum, February 2018, poster presentation, **awarded as best poster presentation**

Jana M. Boysen, Bettina Bardl, Falk Hillmann

The peroxiredoxin Asp f3 protects *Aspergillus fumigatus* against external superoxide

7th International Conference on Microbial Communication for Young Scientists (MiCom), Jena, March 2018, poster presentation

Jana M. Boysen, Elena Shekhova, Olaf Kniemeyer, Falk Hillmann

The fungal peroxiredoxin Asp f3 is essential for virulence of *Aspergillus fumigatus* and protects against protein oxidation by reactive oxygen species

VAAM Annual Meeting, Wolfsburg, April 2018, poster presentation

Jana M. Boysen, Thomas Wolf, Elena Shekhova, Olaf Kniemeyer, Falk Hillmann

The fungal peroxiredoxin Asp f3 of *Aspergillus fumigatus* is essential for redox homeostasis during exposure to external reactive oxygen species

71st DGHM Annual Meeting, Göttingen, February 2019, poster presentation

Jana M. Boysen, Nauman Saeed, Elena Shekova, Thomas Wolf, Gianni Panagiotou, Peter Hortschansky, Axel A. Brakhage, Olaf Kniemeyer, Falk Hillmann

The peroxiredoxin Asp f3 is crucial for redox balance, sensing of reactive oxygen species and virulence in *Aspergillus fumigatus*

13th Symposium of the VAAM Special Group Biology and Biotechnology of Fungi; 1st joint meeting with the GeneAG "Fungal Genetics" of the German Genetics Society, Göttingen, September 2019, poster presentation

Jana M. Boysen, Nauman Saeed, Elena Shekhova, Thomas Wolf, Gianni Panagiotou, Olaf Kniemeyer, Falk Hillmann

The peroxiredoxin Asp f3 is crucial for redox balance, sensing of reactive oxygen species and virulence in *Aspergillus fumigatus*

72nd DGHM Annual Meeting; VAAM Annual Meeting; 6th Joint Conference of DGHM und VAMM, Leipzig, March 2020, poster presentation

Jana M. Boysen, Nauman Saeed, Elena Shekhova, Thomas Wolf, Gianni Panagiotou, Olaf Kniemeyer, Falk Hillmann

The peroxiredoxin Asp f3 is crucial for redox balance, sensing of reactive oxygen species and virulence in *Aspergillus fumigatus*

DMykG 2020, 54. Wissenschaftliche Tagung der Deutschsprachigen Mykologischen Gesellschaft e.V. / 3rd International Symposium of the CRC/Transregio FungiNet, online, September 2020, poster presentation

10 Curriculum Vitae

Personal data

Name	Jana Marie Boysen
Date and place of birth	15th February 1990 in Neumünster, Germany

Education

Since 05/2016	PhD project, Leibniz Institute for Natural Product Research and Infection Biology – Hans Knöll Institute (HKI), Jena, Junior Research Group Evolution of Microbial Interactions, Supervisor Dr. Falk Hillmann, Topic: "The Role of Peroxiredoxin Asp f3 in Redox Homeostasis of the Human Fungal Pathogen *Aspergillus fumigatus*"
10/2013 – 03/2016	M.Sc. (Biotechnology), Westfälische Wilhelms-Universität Münster Topic: "The Regulation of Secondary Metabolism in *Fusarium fujikuroi*: the Impact of Nitrogen and Pathway specific Transcription Factors",
10/2010 – 09/2013	B.Sc Science (Biosciences), Westfälische Wilhelms-Universität Münster Topic: „ Various aspects for the induction of silent secondary metabolite gene clusters in *Fusarium fujikuroi*"
08/2000 – 06/2009	A-levels ("Abitur") Integrierte Gesamtschule Neumünster (Brachenfeld)

Practical training

07/2014 – 12/2014	Optional internship, BASF SE, Ludwigshafen Fermentation Products Research, Group Prof. O. Zelder; Lab Dr. B. Hoff Establishment of a new molecular biological method for application in production organisms.

11 Ehrenwörtliche Erklärung

Die geltende Promotionsordnung der Fakultät für Biowissenschaften der Friedrich-Schiller-Universität Jena ist mir bekannt. Die vorliegende Dissertation habe ich selbständig verfasst und dabei weder Textabschnitte von dritten oder aus einer eigenen Prüfungsarbeit ohne Kennzeichnung übernommen. Es wurden ausschließlich die von mir angegebenen Quellen, Hilfsmittel und persönliche Mitteilungen verwendet. Ich versichere, dass die aufgelisteten Publikationen und Manuskripte, ausschließlich auf Ergebnissen beruhen, die während meiner Promotion generiert wurden.

Alle Personen, dich mich bei der Auswahl und Auswertung des Materials, wie auch bei der Herstellung der Manuskripte unterstützt haben, sind in der Danksagung meiner Dissertation genannt. Alle Personen, die bei der Anfertigung der Publikationen und Manuskripte beteiligt waren, sowie deren Eigenanteil sind gekennzeichnet.

Ein Promotionshelfer/berater wurde nicht konsultiert und Dritte haben weder unmittelbar noch mittelbar geldwerte Leistungen, die im Zusammenhang mit dem Inhalt der vorliegenden Dissertation stehen, erhalten. Die vorliegende Dissertation wurde noch nicht als Prüfungsarbeit für eine staatliche oder andere wissenschaftliche Prüfung eingereicht. Ferner wurde weder diese Arbeit oder eine in wesentlichen Teilen ähnliche noch eine andere Abhandlung bei einer anderen Hochschule als Dissertation eingereicht.

Jena, den _____

_____

Jana Marie Boysen

12 Attachements

FORMULAR 2

Manuskript Nr. 1

Kurzreferenz: Noßmann *et al*., (2019), *Current genetics*

Beitrag der Doktorandin:

Jana M. Boysen contributed to this manuscript by construction and cloning of vectors for the creation of YFP-strains of *A. fumigatus* needed for *in vivo* confirmation of protein interaction *via* BiFC. Also, Jana M. Boysen cultured the fungal strains and processed the samples for LC-MS analysis of acetylated peptides. Sample preparation included generation of protein extracts from cultured strains, enrichment of StrepII-tagged GlnA and further sample processing. Further Jana M. Boysen conducted all enzyme activity assays of glutamine synthetase and was significantly involved in the writing and editing process of the manuscript.

Manuskript Nr. 2

Kurzreferenz: Boysen *et al*., (2021a), *Genes*

Beitrag der Doktorandin

Jana M. Boysen performed all experiments included in the manuscript except microscopy, RNA sequencing and bioinformatic analysis of RNAseq data. Further, she processed the RNAseq data provided by the bioinformaticians. As main author, she wrote the manuscript, created most figures and was essentially involved in the revision and editing process.

Manuskript Nr. 3

Kurzreferenz: Boysen *et al*., (2021b), *Beilstein Journal of Organic Chemistry*

Beitrag der Doktorandin:

Jana M. Boysen wrote the abstract, the introduction and a major part of the conclusion as well as the parts “Natural products of *Aspergillus fumigatus*”, “DHN-melanin”, “Fumigaclavines” and “Fumitremorgins”. Furthermore, she designed all figures and tables and was responsible for the complete list of references and a major part of the editing process.

Manuskript Nr. 4

Kurzreferenz: Brantl *et al*., (2021), *Mbio*

Beitrag der Doktorandin:

Jana M. Boysen performed preliminary experiments and was essential in the preparations, post processing and data analysis of the murine infection experiment. Furthermore, she took part in the writing and editing process of the manuscript.

Manuskript Nr. 5

Kurzreferenz: Boysen *et al.*, in Vorbereitung

Beitrag der Doktorandin

Jana M. Boysen performed all experimental work with the exclusion of the MALDI/TOF-TOF analysis and identification of identified protein fragments. For the performance of the 2D-gel electrophoresis and subsequent spot analysis she was supported by Elena Shekhova to learn the method. Further Jana M. Boysen wrote the manuscript and designed all Tables and Figures.

13 Acknowledgements

First, I want to thank my supervisor Dr. Falk Hillmann who offered me this position and enabled me to follow my scientific interest in fungi. Your research group provided the environment I needed to grow and tackle new challenges. Thank you for the scientific discussions and your open door.

I also thank Prof. Dr. Axel Brakhage, who served as an official supervisor and is a constant source of inspiration with his vast experience and scientific know how, especially on the wonderful world of fungi and secondary metabolites. You inspired my move to Jena and I certainly do not regret it.

Following this, I also have to thank Professors Bettina and Paul Tudzynski for awakening my interest in fungi in the first place. I am sorry I did not get a chance to stick with my lovely *Fusarium fujikuroi*, but I also appreciate everything I learned with *Aspergillus*. It was a great possibility to broaden my horizon.

I thank Marcel for the good science we shared in the lab and the fun times we shared out of the Lab with our special golden guest and his best friends - orange and cinnamon. I missed your company after you finished.

Big Thanks go to the whole “Kaffeerunde” consisting of Annica, Marcel and Tom. You were my caffeine fix in the afternoon that was sometimes very urgently needed.

My stomach gives an extra thanks to Annica who supplied me regularly with the most delicious Bentos. The food was delicious and tasted all the better for the pretty optics.

Thank you to Christin, Lisa and Nauman for sharing the office. I think we had a really fun time together and I appreciated freezing together during Corona and all the nice talks we shared.

Dear Nauman, tanks for being my Master student. You did great and will become a wonderful scientist. I am very honoured to be a part of your scientific career.

I would also like to thank Lisa in her function as our technical assistant. You were a great help and I appreciate all the work you did for us. In the same breath, big thanks go to Silke Steinbach, the good soul of our corridor. I am sure you saved me lots of time running around

like a headless hen in search of things. You were always able to help and nobody can tame the copy machine like you.

Further, thanks to everybody who helped my work and was part of my research in some way. I especially would like to mention Thomas Krüger, Till Kindl, Elena Shekhova, Olaf Kniemeyer, Maria Straßburger, Thomas Wolf, Gianni Panagiotou and Sascha Schäuble.

In addition, I thank the whole EMI group for support. I especially enjoyed our times outside of the lab together and it was good to work with you.

Last but not least, I have to mention the people of my private life. I thank all my friends for understanding that I did not have time to visit often and am not very good at answering quickly to your messages. You know how it is when life gets the better of you.

I also like to thank my parents, especially my father, for always supporting me and my decisions, even if you never really understood what I am actually doing. I wish both of you were still here to finally see me accomplishing the goal that kept me away from home too often. I also thank my baby brother Nils. You are the best brother I could ever wish for and I am grateful that we stayed close in all those years and supported one another when needed.

Finally, I thank my boyfriend Peter who always supported me and never complained about our four-year distant relationship. I am so sorry it took me so long to reach the finish line. I know you would have liked me closer more often and I am happy to start the next part of this adventure called life together.

THANK YOU